Magnetism & Exotic Superconductivy

Y. Sidis

Laboratoire Léon Brillouin, CEA-CNRS

Cargèse-2022

Conventional superconductivity

Key properties of a superconductor

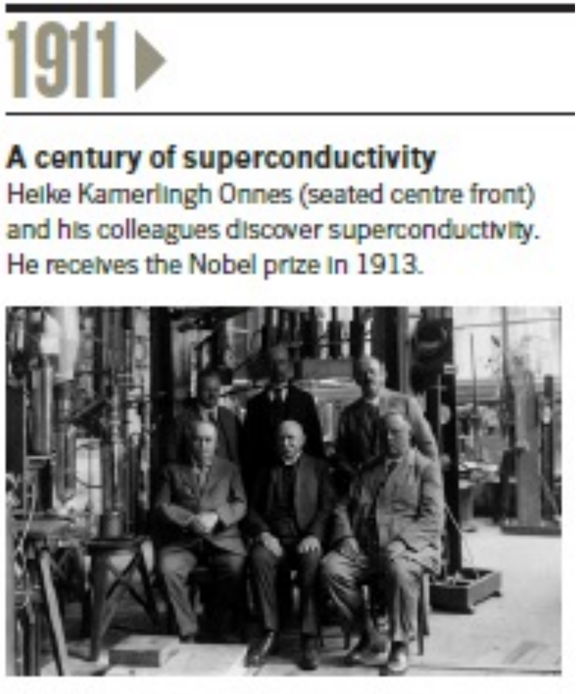

1911

A century of superconductivity
Heike Kamerlingh Onnes (seated centre front) and his colleagues discover superconductivity. He receives the Nobel prize in 1913.

No electrical resistivity (T< Tc)

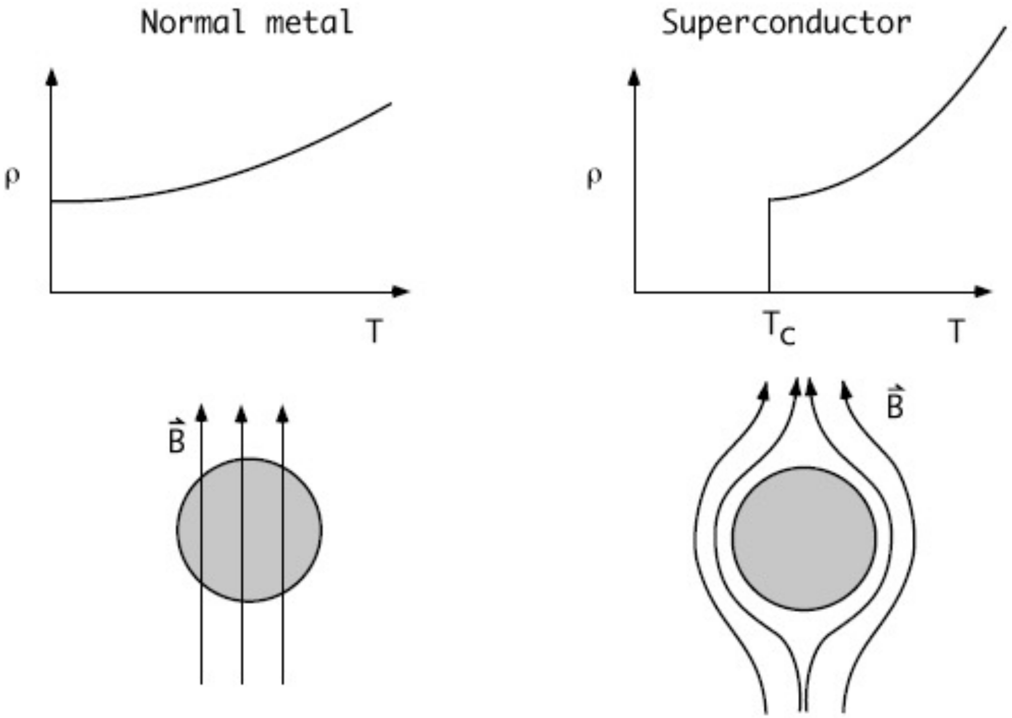

It expels a weak magnetic field (Meissner effect)

Conventional superconductivity

1957

John Bardeen, Leon Cooper and Robert Schrieffer (left to right) publish a theory of superconductivity that predicts a maximum transition temperature of 30 K. They are awarded the Nobel prize in 1972.

Conventional superconductors & BCS theory

Role of electron-ion interactions

- Ion , Heavy (masse M), electric charge +
- Electron, Light , electric charge -

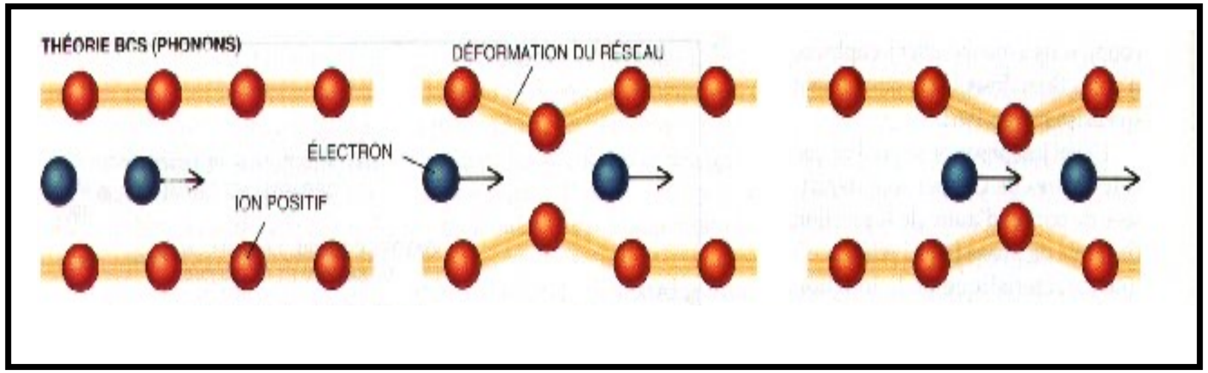

Isotope effect : $T_c \sim 1/(M)^{1/2}$ -> leading of the electron-ion interaction

Cooper pairs : attractive interaction between 2 electrons mediated by the distortion or vibration of the ionic lattice (phonons)

BCS Superconductivity: macroscopic quantum state, made of the coherent superposition of Cooper pairs

Superconducting materials

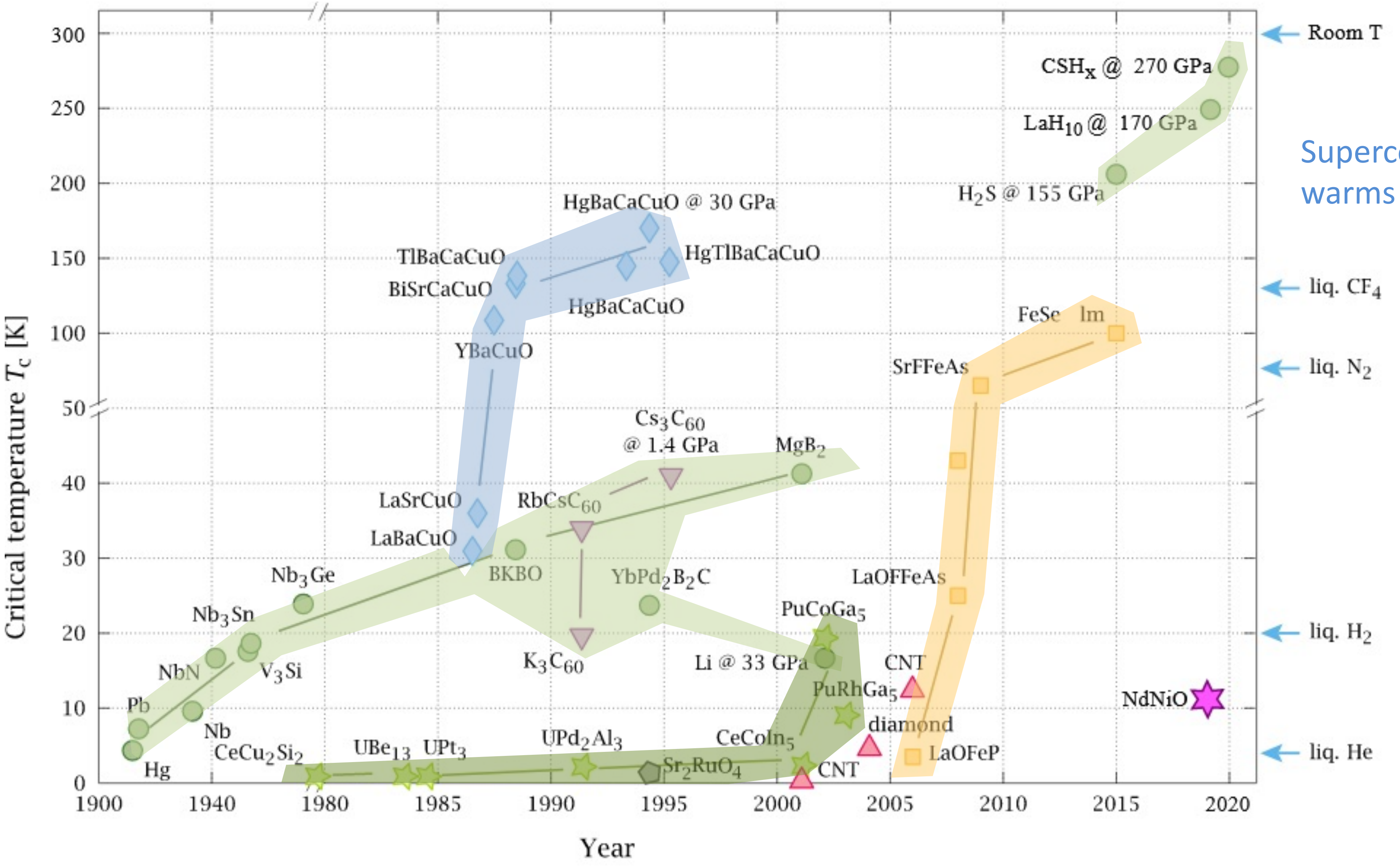

Superconductivity warms up

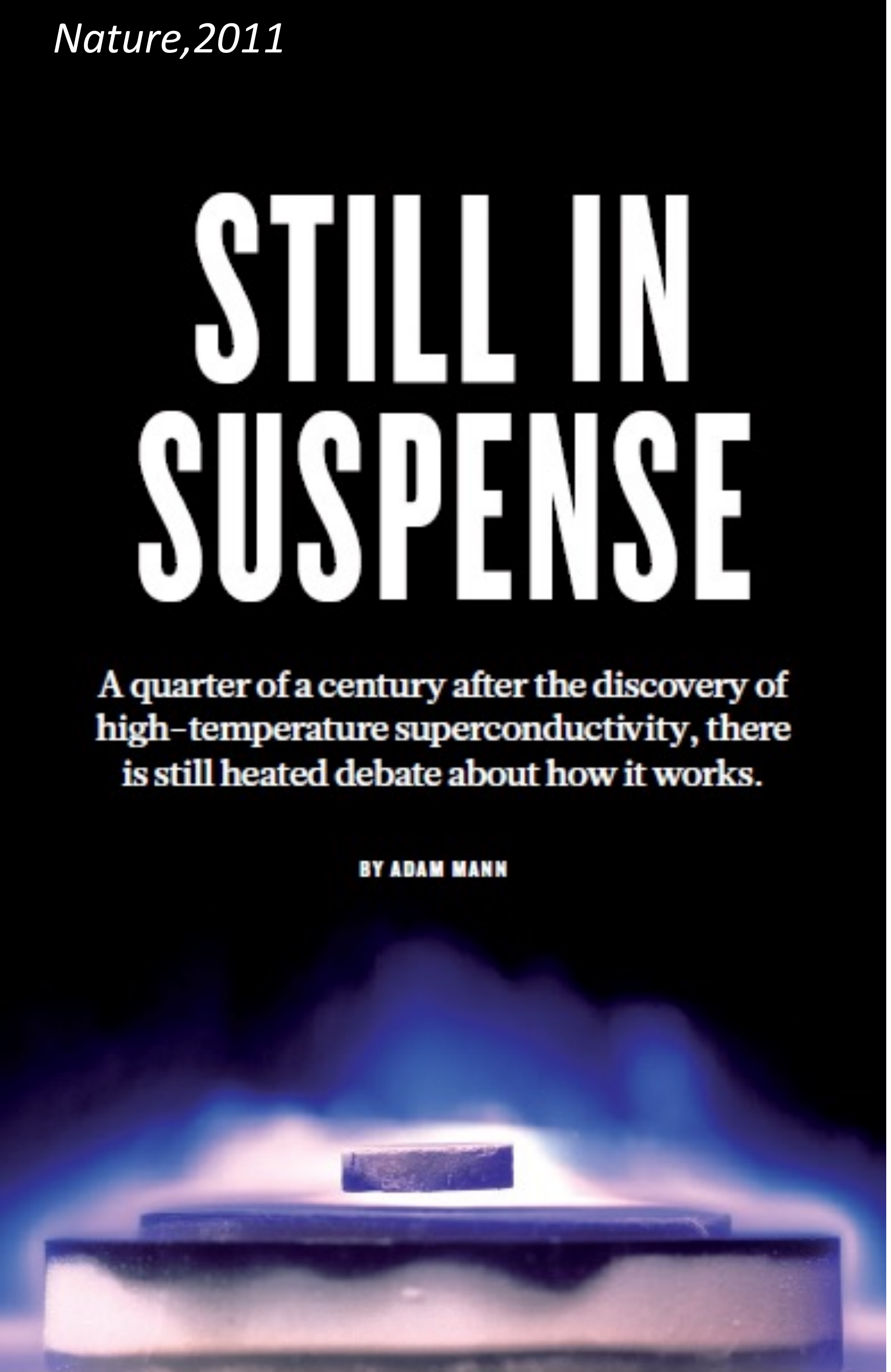

The Challenge of Unconventional Superconductivity

During the past few decades, several new classes of superconductors have been discovered that do not appear to be related to traditional superconductors.

The source of the superconductivity of these materials is likely different from the electron-ion interactions that are at the heart of conventional superconductivity.

Developing a rigorous theory for any of these classes of materials has proven to be a difficult challenge and will remain one of the major problems in physics in the decades to come.

Science, 2011

Superconductivity without phonons

P. Monthoux[1,2], D. Pines[3,4] & G. G. Lonzarich[5]

The idea of superconductivity without the mediating role of lattice vibrations (phonons) has a long history. It was realized soon after the publication of the Bardeen–Cooper–Schrieffer (BCS) theory of superconductivity 50 years ago that a full treatment of both the charge and spin degrees of freedom of the electron predicts the existence of attractive components of the effective interaction between electrons even in the absence of lattice vibrations—a particular example is the effective interaction that depends on the relative spins of the electrons. Such attraction without phonons can lead to electronic pairing and to unconventional forms of superconductivity that can be much more sensitive than traditional (BCS) superconductivity to the precise details of the crystal structure and to the electronic and magnetic properties of a material.

Review Nature 2007

Electromagnetic interaction :
an electron creates an electric or magnetic polarization of the other electrons with which it couples

$$-e[g_n\, n(\mathbf{r},t)] - \mathbf{s}\bullet[g_m\, \mathbf{m}(\mathbf{r},t)]$$

$$\mathbf{m}(\mathbf{r},t) = g_m \mathbf{s}' \chi_m(\mathbf{r},t)$$

Effective interaction

$$V_{\text{ind}}(\mathbf{r},t) = -e\,e' g_n{}^2\, \chi_n(\mathbf{r},\, t) - \mathbf{s}\bullet\mathbf{s}'\, g_m{}^2\, \chi_m(\mathbf{r},t)$$

Superconductivity without phonons

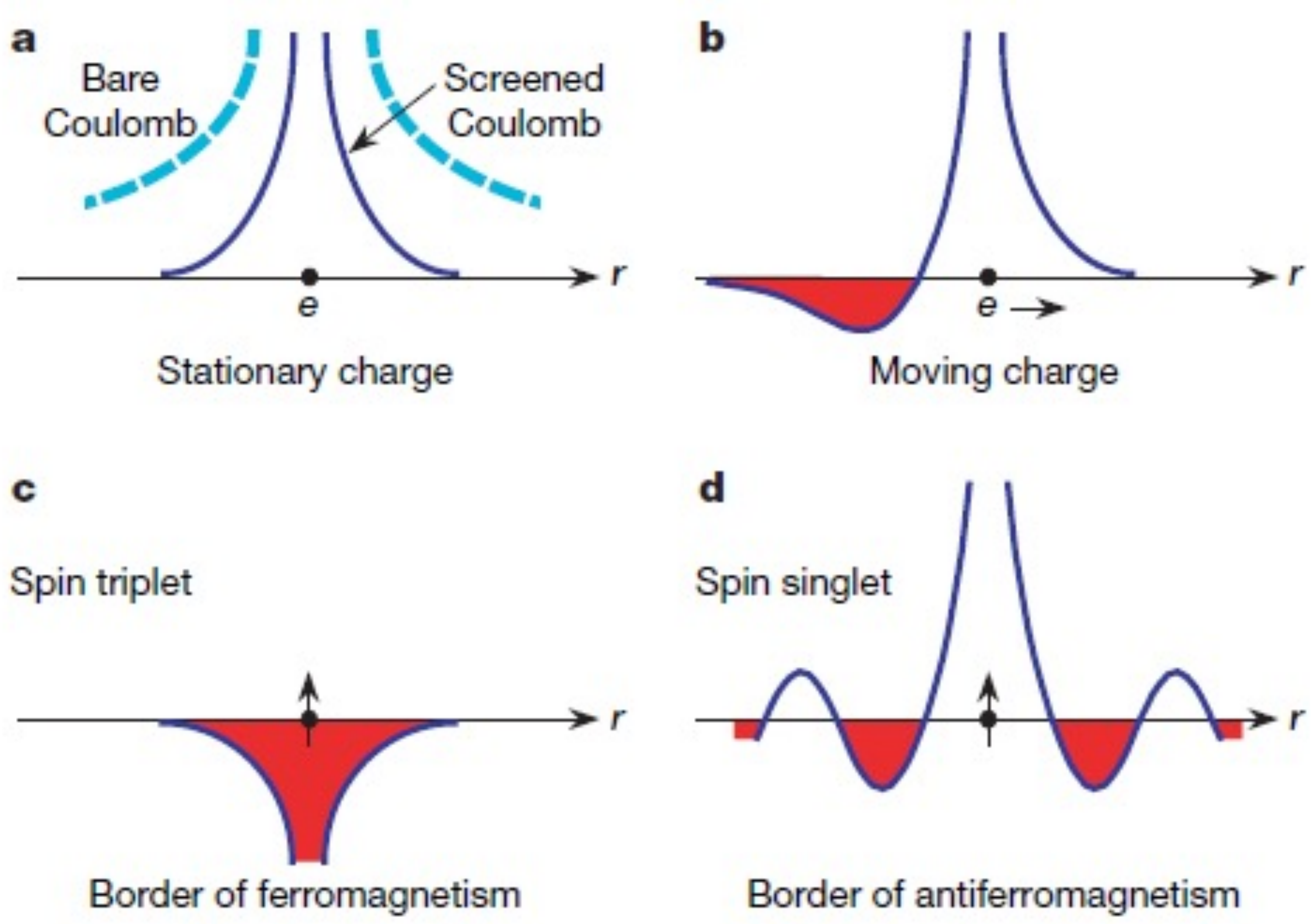

At t=0, the interaction is repulsive, but at t> 0, the electron creates an electric polarization in its wake

For a magnetic system, the product **s.s' controls the attractive** or repulsive character of the interaction

It can generate triplet (FM) or singlet (AF) pairs

Symmetry of the wave function

The symmetry of a 2-electron wave function is imposed by the PAULI principle: the wave function must be antisymmetric when the two electrons are exchanged

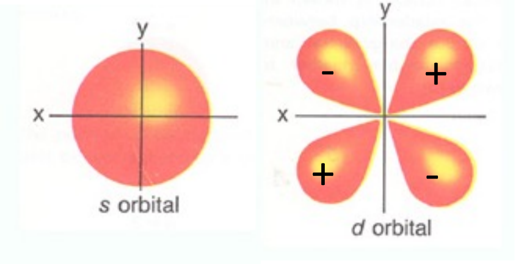

Spin singlet..... Orbital part of even symmetry : s, d, ... $\Rightarrow$ $|\psi\rangle = \Delta_0(|\uparrow\downarrow\rangle - |\downarrow\uparrow\rangle)$

Spin triplet ..... Odd symmetry orbital part : p, f, ... $\Rightarrow$ $|\psi\rangle = \Delta_{\uparrow\uparrow}|\uparrow\uparrow\rangle + \Delta_{\downarrow\downarrow}|\downarrow\downarrow\rangle + \Delta_0(|\uparrow\downarrow\rangle + |\downarrow\uparrow\rangle)$

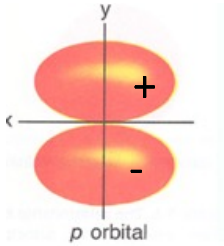

warning: *the spin must be a good quantum number....*

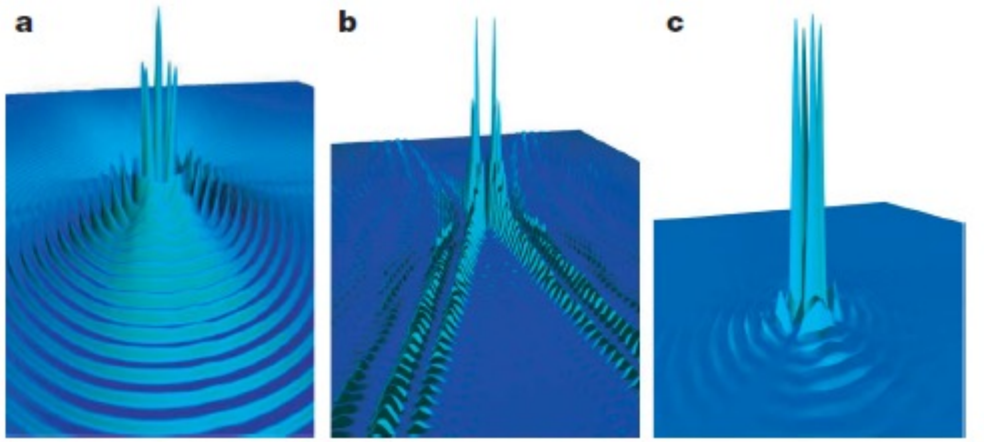

s- singlet *p- triplet* *d- singlet*

Probability of finding the second electron of a pair when the first is at the origin

Instability of the Fermi see

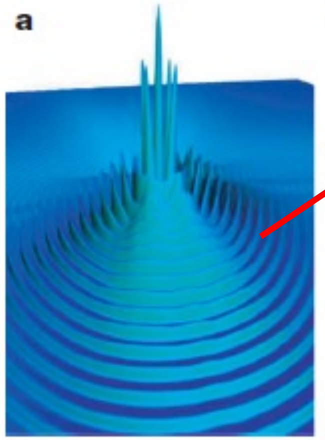

s- singlet

Why are there oscillations?
Why does the function decrease?

In the BCS theory, superconductivity results from an instability of the Fermi surface. Only the electrons in the vicinity of the Fermi surface will fully benefit from the attractive interaction.

Cooper's are formed in reciprocal space: $<c^{+}_{k,\sigma}\, c^{+}_{-k,-\sigma}>$.
The oscillations come from the electronic states in the vicinity of $\mathbf{k}_f$ that benefit optimally from the attractive interaction.

The fewer these states are, the greater the coherence length is

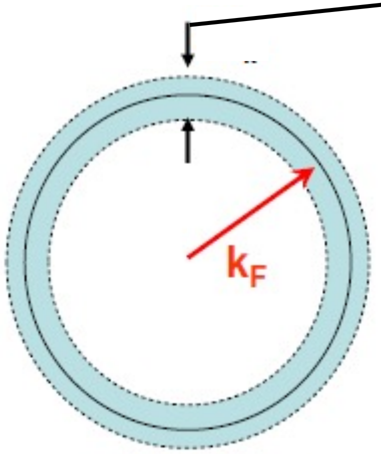

Sphère de Fermi

$$\frac{\Delta k}{k_F} \sim \frac{\hbar\omega_D}{\varepsilon_F} \sim \frac{100\mathrm{K}}{100000\mathrm{K}} = 10^{-3}$$

pairing interaction without phonons

Linearized gap equation

$$\lambda_\mu \Delta_{\mu,l,m}(\mathbf{k},\omega_n) = -\frac{T}{N}\sum_{k',\omega_j}\sum_{l',m'} V^{(2)}_{\mu,l,m}(\mathbf{k}-\mathbf{k}',\omega_n-\omega_j)\, G_{ll'}(\mathbf{k}',\omega_j)\; G_{mm'}(-\mathbf{k}',-\omega_j)\,\Delta_{\mu,l',m'}(\mathbf{k}',\omega_j).$$

Singlet pairing

$$V_s^{(2)} = \frac{1}{2}V_{\mathrm{sp}}^{zz} + V_{\mathrm{sp}}^{+-} - \frac{1}{2}V_{\mathrm{ch}}.$$

Triplet pairing S_z=+/-1

$$V_{\mathrm{tr1}}^{(2)} = -\frac{1}{2}V_{\mathrm{sp}}^{zz} - \frac{1}{2}V_{\mathrm{ch}}$$

Triplet pairing S_z=0

$$V_{\mathrm{tr0}}^{(2)} = \frac{1}{2}V_{\mathrm{sp}}^{zz} - V_{\mathrm{sp}}^{+-} - \frac{1}{2}V_{\mathrm{ch}}$$

$$V^{\mathrm{sp},zz} = U^2\frac{\chi_0^{\mathrm{sp},zz}}{1-U\chi_0^{\mathrm{sp},zz}}, \qquad V^{\mathrm{sp},+-} = U^2\frac{\chi_0^{\mathrm{sp},+-}}{1-U\chi_0^{\mathrm{sp},+-}}$$

Spin fluctuations

$$V^{\mathrm{ch}} = U^2\frac{\chi_0^{\mathrm{ch}}}{1+U\chi_0^{\mathrm{ch}}}$$

Charge fluctuations

$\chi_0^{\mathrm{ch}}, \chi_0^{\mathrm{sp},+-}$ are the irreducible part of the charge and spin susceptibilities

$$\chi_0^{\mathrm{ch}}(\mathbf{q}) = \frac{1}{N}\sum_{,} G(\mathbf{k}+\mathbf{q})G(\mathbf{k}) = \chi_0^{\mathrm{sp},+-}$$

If there is no magnetic anisotropy (for instance spin-orbite coupling effects)

d-wave singlet superconductivity and antiferromagnetic susceptibility

BCS gap equation

$$\Delta_k = -\sum_q V_{\mathbf{q}} \frac{\Delta_{\mathbf{k-q}}}{2E_{\mathbf{k-q}}}$$

Relation dispersion of quasiparticle

$$E_{\mathbf{k}} = \sqrt{\xi_{\mathbf{k}^2} + \Delta_{\mathbf{k}}}.$$

$V_{\mathbf{q}}$: Interaction potential

The structure in phase-space of the interaction potential affects the symmetry of the SC gap.

In the BCS theory, V_q ~ -V_o when the energy of the quasiparticles around the fermi level is lower than the Debbye energy of the phonons and zero otherwise.

Spherical Fermi surface -> "s" symmetry supra

The pairing potential based on the exchange of spin fluctuations reads:

Magnetic susceptibility

$$V_{\mathbf{q}} \simeq \frac{3}{2} U^2 \chi(\mathbf{q}, \omega)$$

On-site Coulomb repulsion

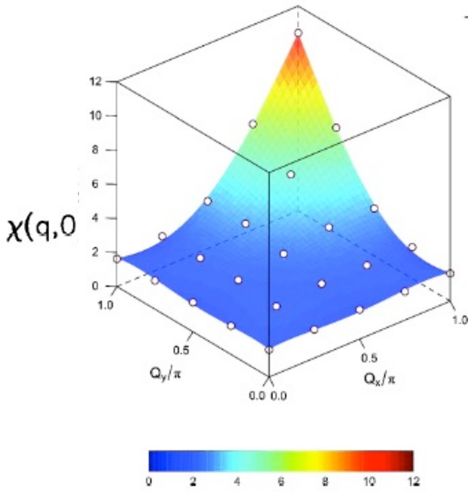

Let us consider AF $\chi(q,0)$ peaked at the AF wave vector $q_o = (\pi,\pi)$

The gap equation has a solution if Δ_k and Δ_{k-q} have opposite signs

$$\Delta_{\mathbf{k}} = \Delta_m (cos(k_x) - cos(k_y))/2$$

d-wave versus s+- superconductivities – multiband case

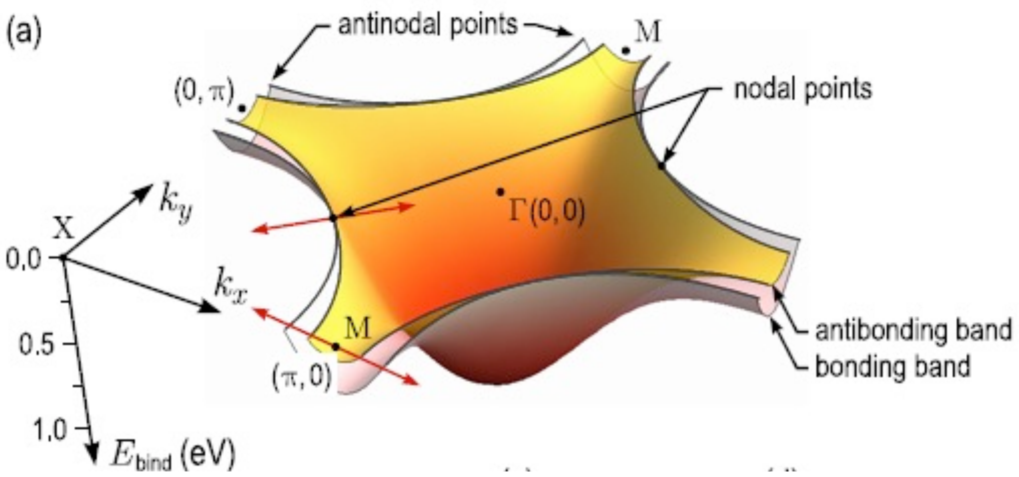

Bilayer structure

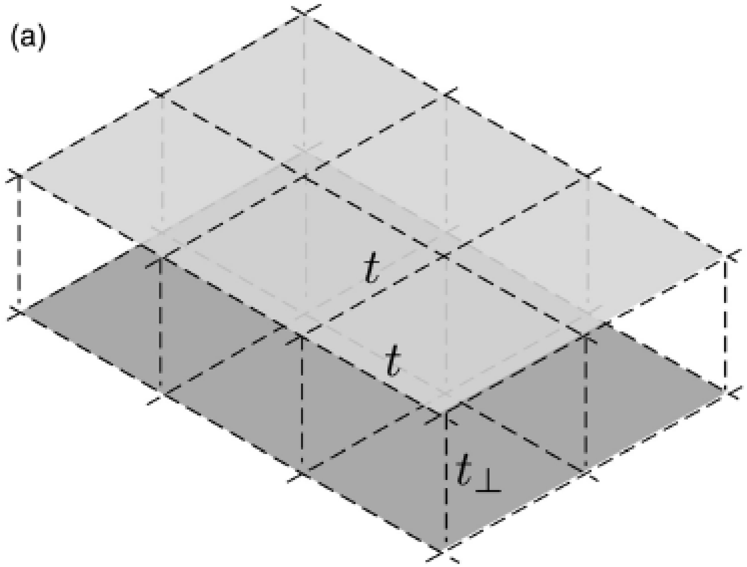

The interlayer hopping lifts the degeneracy of the 2 bands, yieldind: the bonding and antibonding bands

$$\Delta_{x^2-y^2} = \frac{1}{\sqrt{N}}\sum_k (\cos k_x - \cos k_y) c^\dagger_{k\uparrow} c^\dagger_{-k\downarrow}$$

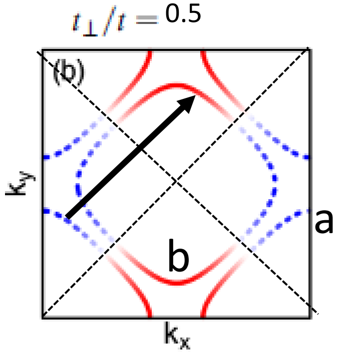

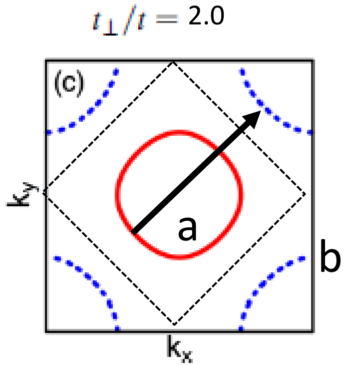

$$\Delta_{s^\pm} = \frac{1}{\sqrt{N}}\sum_k \cos k_z c^\dagger_{k\uparrow} c^\dagger_{-k\downarrow}.$$

$\chi_{aa}+\chi_{bb} \sim \chi_{ab}+\chi_{ba}$

The planar AF correlations are important

$\chi_{aa}+\chi_{bb} \ll \chi_{ab}+\chi_{ba}$

The out-of-plane AF correlations become important

where should we look for ?

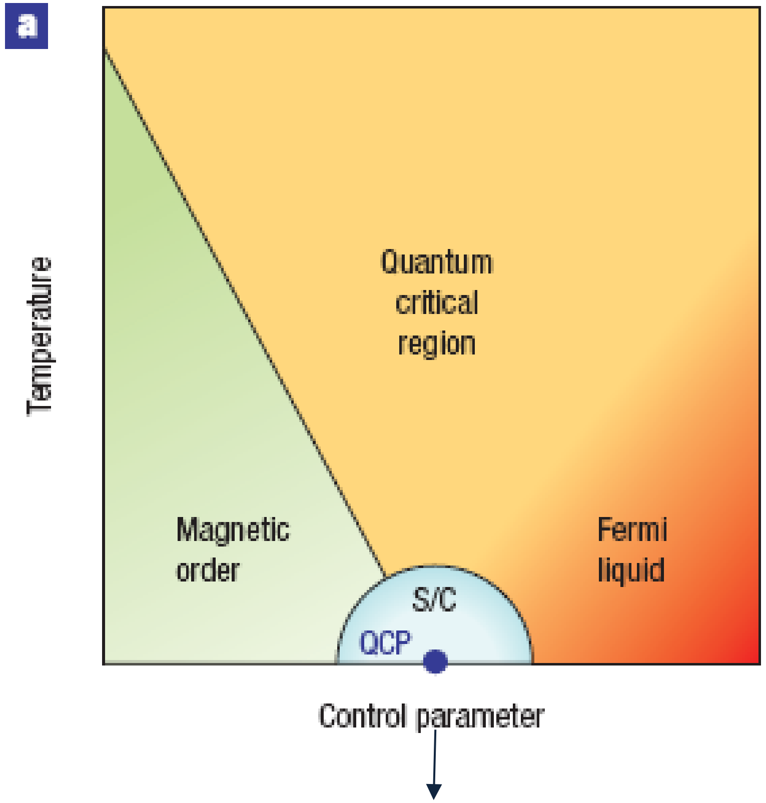

SC could develop close to QCP where spin fluctuations are very strong !

various magnetic states exist

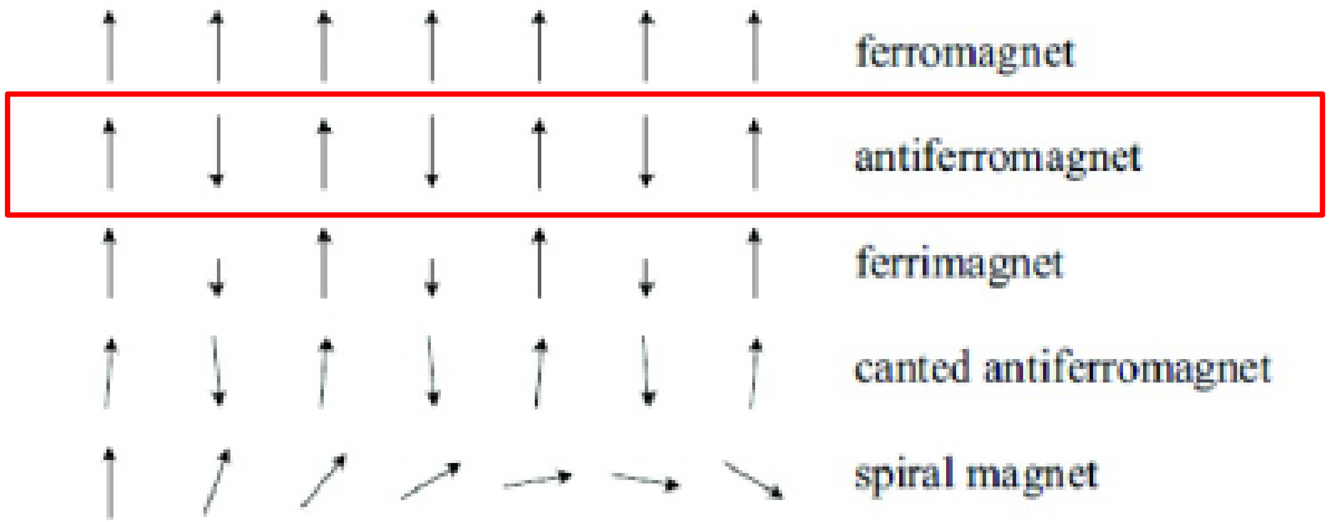

$\mathbf{S}(\mathbf{r}) = \mathbf{m}_1 \cos(\mathbf{Q}_1 \cdot \mathbf{r}) + \mathbf{m}_2 \cos(\mathbf{Q}_2 \cdot \mathbf{r})$ $\quad \mathbf{Q}_1 = (\pi, 0)$ and $\mathbf{Q}_2 = (0, \pi)$

one $\mathbf{m}_a$ being non-zero $\quad \mathbf{m}_1 \parallel \mathbf{m}_2 \neq 0 \quad \mathbf{m}_1 \perp \mathbf{m}_2 \neq 0$.

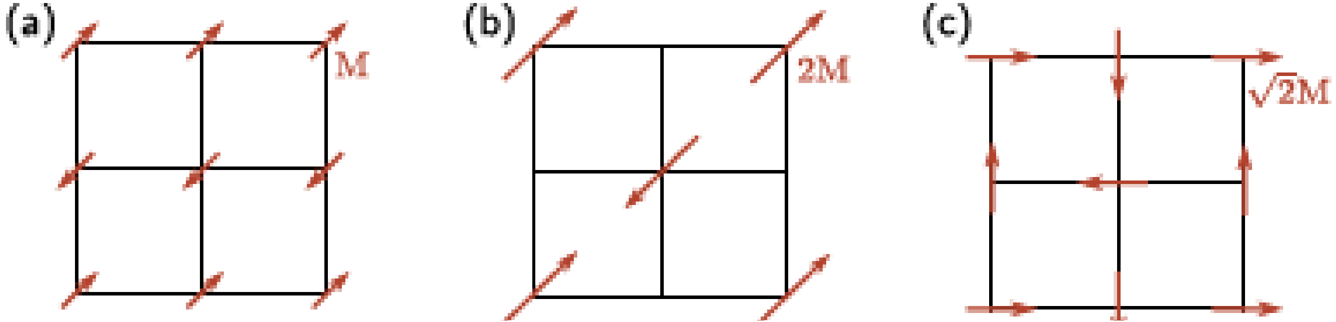

example

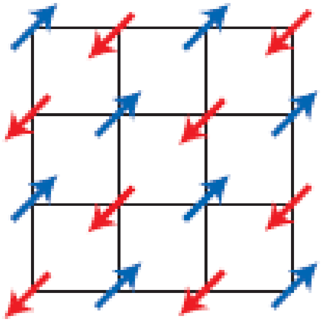

quasi-2D antiferromagnet

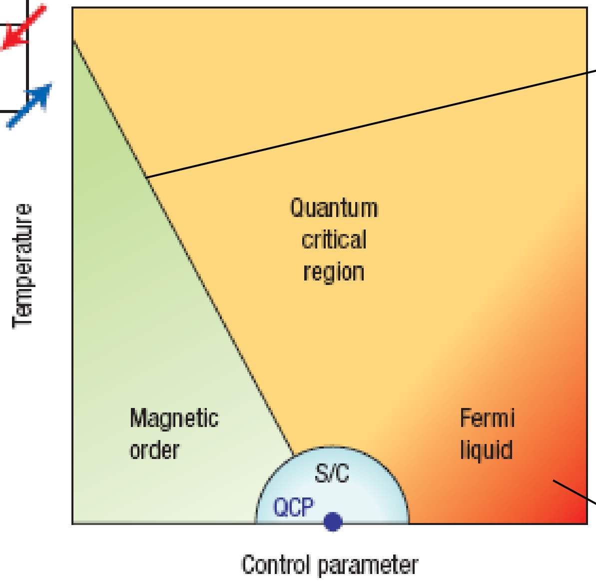

at QCP, spin fluctuations display a ω/T scaling behavior

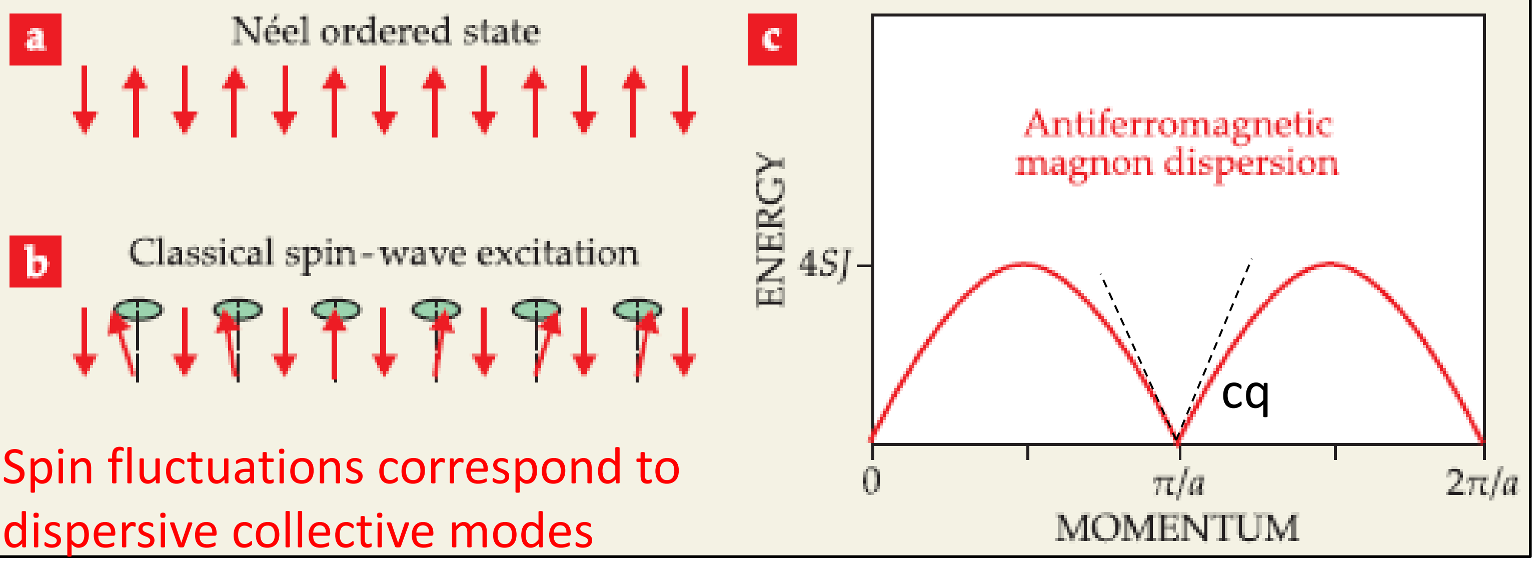

Spin fluctuations correspond to dispersive collective modes

Nearly antiferromagnetic metal

Spin fluctuation are of relaxational type

$$\chi''(q,\omega) = \frac{\chi}{1+(\xi q)^2}\cdot\frac{\omega\Gamma_q}{\omega^2+\Gamma_q^2}$$

$$\Gamma_q = \Gamma_0\left(1+\xi^2(q-q_0)^2\right)$$

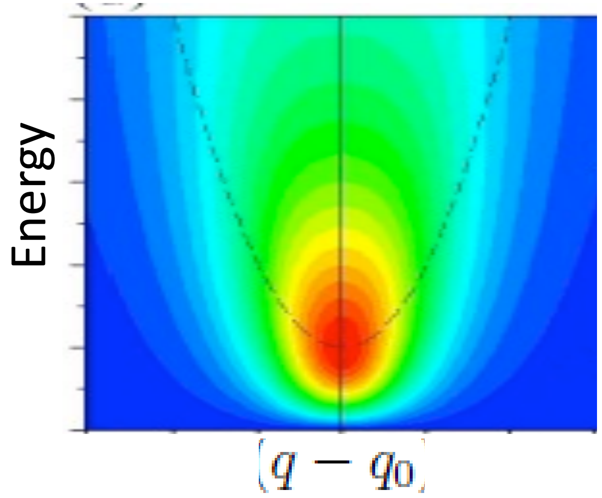

collective modes vs Contunuum of elementary excitations

dispersive collective mode

*** Ordered state**
Néel state
Spin fluctuations correspond to « magnons »

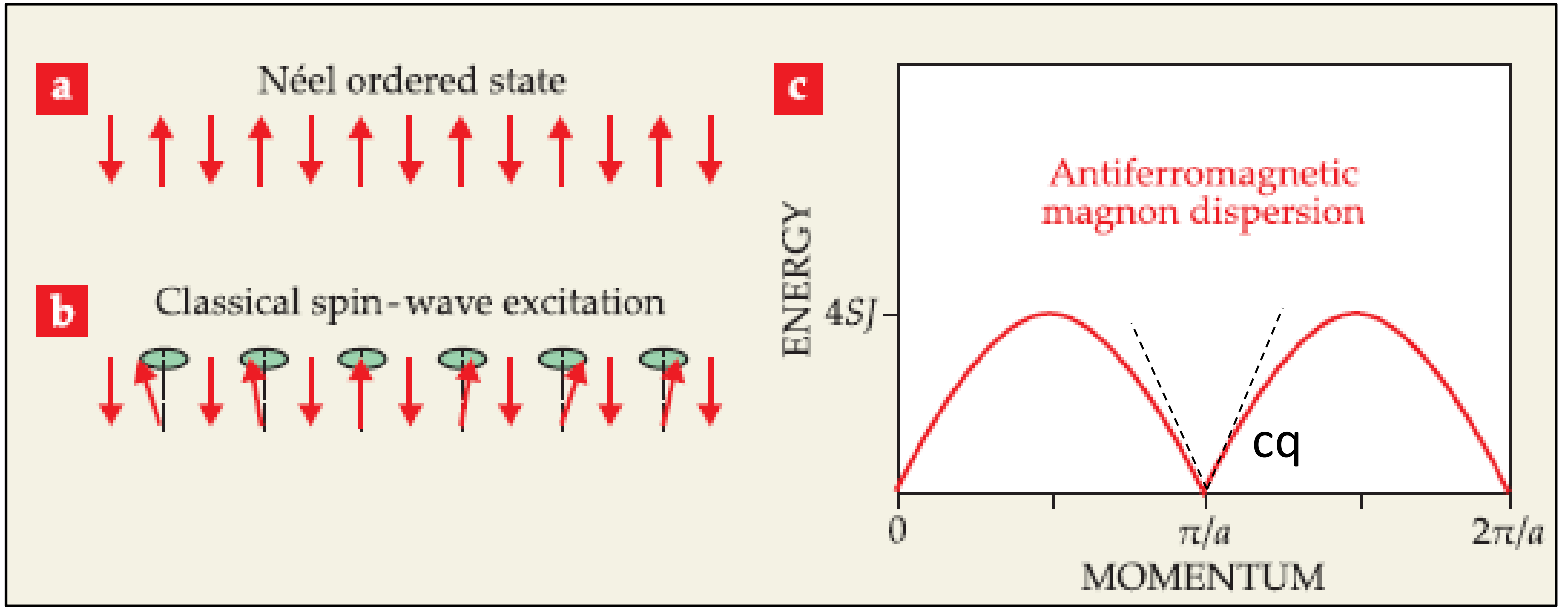

continuum of excitation

*** Quantum disordered state**
Spin liquid
Spin fluctuations correspond to pair of (S=1/2) spinons

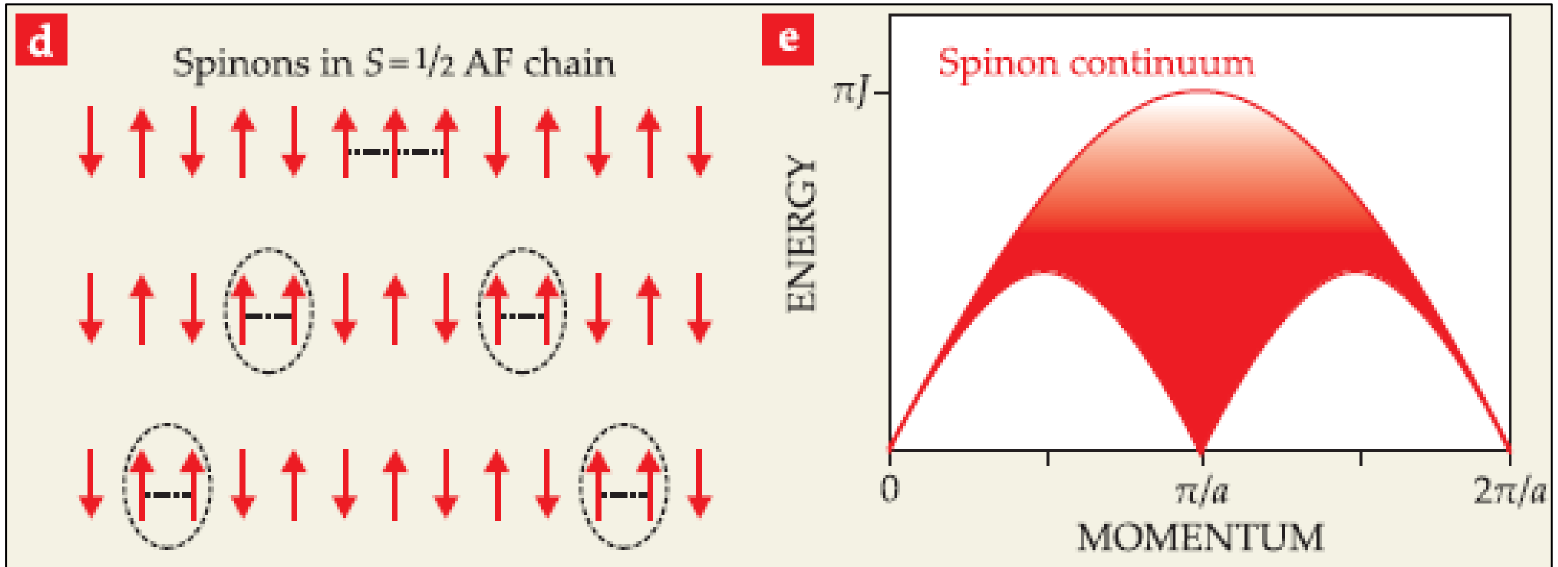

Itinerant magnetism

In a metal, spin excitation correspond to electron-hole excitations

$$S_q = \frac{1}{N}\sum_{k,\sigma,\sigma'} c^{+}_{k+q,\sigma'}\bar{\sigma}c_{k,\sigma'}$$

$$S^z_q = \frac{1}{N}\frac{1}{2}\sum_{k} c^{+}_{k+q,\uparrow}c_{k,\uparrow} - c^{+}_{k+q,\downarrow}c_{k,\downarrow}$$

$$S^+_q = S^x_q + iS^y_q = \frac{1}{N}\sum_{k} c^{+}_{k+q,\uparrow}c_{k,\downarrow}$$

$$S^-_q = S^x_q + iS^y_q = \frac{1}{N}\sum_{k} c^{+}_{k+q,\downarrow}c_{k,\uparrow}$$

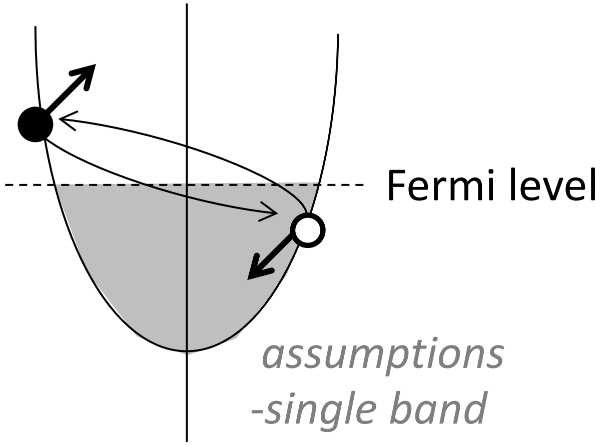

assumptions
-single band
-non SOC

Stoner continuum

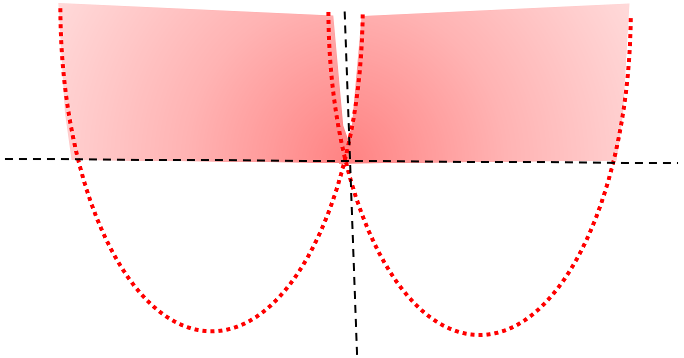

Non interaction spin susceptibility: Lindhard function

Hamiltonian: $$H = \sum_{k,\sigma}\xi_{k,\sigma} c^{+}_{k,\sigma}\, c_{k,\sigma} - g\mu_B \sum_q S^z_q H_{-q}$$

Equation of motion: $$i\frac{dc^{+}_{k+q,\sigma}c_{k,\sigma}}{dt} = [c^{+}_{k+q,\sigma}c_{k,\sigma}, H]$$

$$M^z_q = \chi^{zz}_q H_{-q} \longrightarrow M^z_q = \boxed{\frac{(\frac{1}{2}g\mu_B)^2}{N}\sum_{k,\sigma}\frac{n^F(\xi_{k,\sigma}) - n^F(\xi_{k+q,\sigma})}{\omega + \xi_{k,\sigma} - \xi_{k+q,\sigma} + i\epsilon}} H_{-q}$$

χ^{zz}
Lindhard susceptibility

fermiology

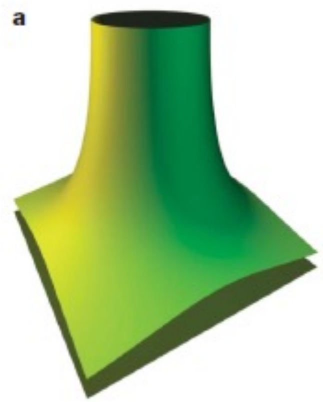

Free electron gas

In a free electron gas (jellium model), the occupied electrons are distributed on spherical equi-energetics. The magnetic susceptibility without interaction has no particular structure in the phase space.

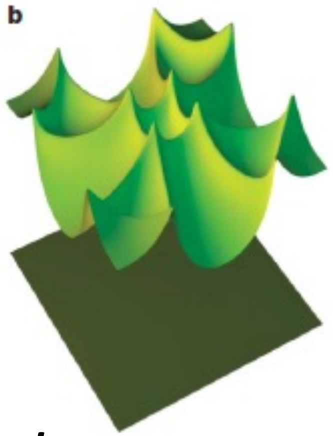

Electron on a square lattice

In a real metal, electrons move on a crystal lattice by jumping from one site to another....
The equi-energetics acquire a particular shape or topology. For the same wave vector and the same amount of energy, the system can then make a large number of excitations.
The susceptibility without interaction will be structured in the phase space

$2k_f$ processes

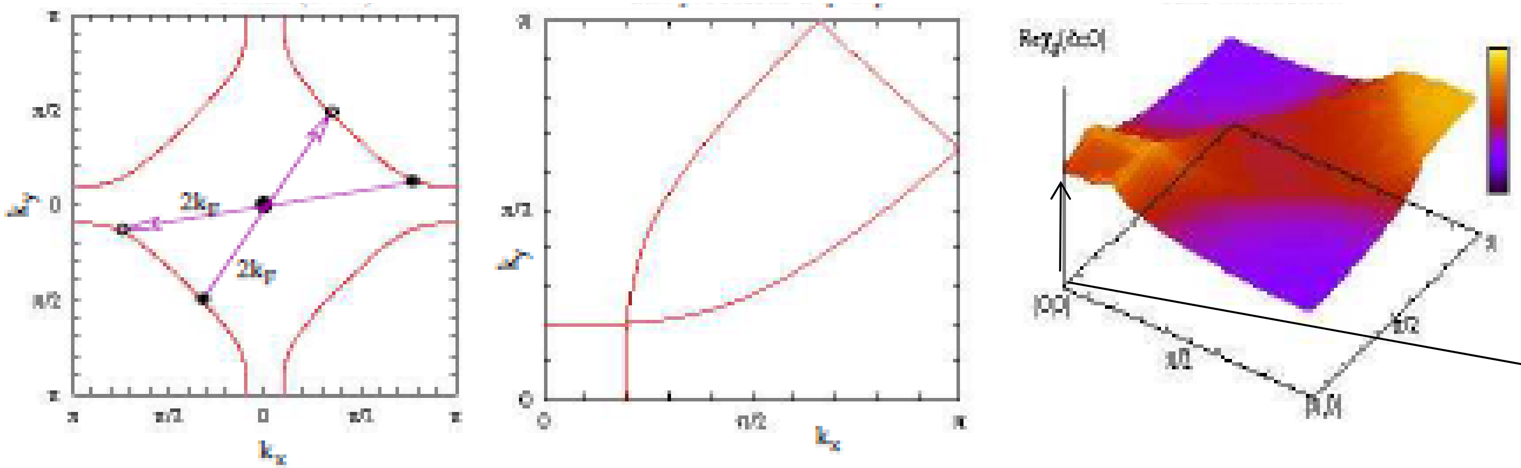

The non interacting uniform magnetic susceptitility, is called the Pauli susceptibility and is proportional the density of state a the Fermi level

$$\chi_P = \mu_0 \mu_B^2 \rho(E_F)$$

what enhances χ ?

The order of magnitude of the non interaction magnetic susceptibility is of a few μ_B^2. eV^{-1}
The threshold of experimental detection is a few tenths of μ_B^2. eV^{-1}

Causes of enhancement of χ

Toplogical properties of the Fermi:

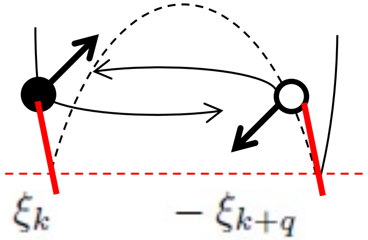

* **nesting** proprerties: for a large number of |k> states, one gets : $\xi_k = -\xi_{k+q}$

* saddle point: **Van Hove singularity** which triggers a divergence in the density of states

Interactions

Electron creates a magnetic polarization, so that each electron feels an effective field : $H_{\text{eff}} = H + \frac{U}{\mu_0\mu_B^2}M$
With $M = \chi H$

One obtains :$\chi = \frac{\partial M}{\partial H} = \chi_P(1 + \frac{U}{\mu_0\mu_B^2}\chi)$ or $\chi = \dfrac{\chi_P}{1 - \frac{U}{\mu_0\mu_B^2}\chi_P}$

in random phase approximation (RPA); the **interacting susceptibility** reads:
I stands for an effective interaction. z

$$\chi(\vec{q},\omega) = \frac{\chi_0(\vec{q},\omega)}{1 - \frac{I}{\mu_0(g\mu_B)^2}\chi_0(\vec{q},\omega)}$$

Itinerant magnetism : SC state

BCS wave function: $\Psi = \prod_{\mathbf{k}} \left(u_{\mathbf{k}} + v_{\mathbf{k}} c^{+}_{\mathbf{k}\uparrow} c^{+}_{-\mathbf{k}\downarrow} \right) |0\rangle$

The pair is absent *The pair is present*

$$u_k^2 = \frac{1}{2}\left(1 + \frac{\xi_k}{E_k}\right)$$
$$v_k^2 = \frac{1}{2}\left(1 - \frac{\xi_k}{E_k}\right)$$
$$u_k v_k = \frac{1}{2}\frac{\Delta_k}{E_k}$$

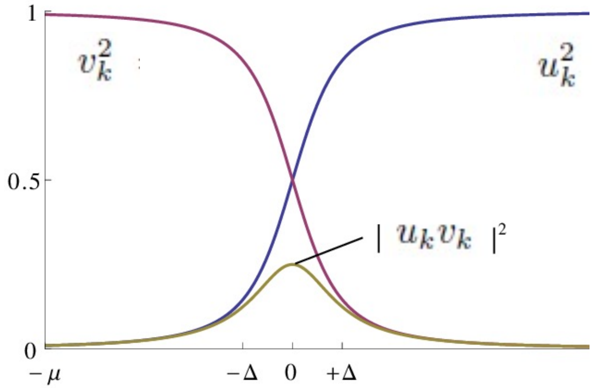

At zero temperature, the one-particle states are empty.
To be able to make electron-hole excitations, it is necessary to break the Cooper pairs. So there is a minimum energy to provide.

The quasiparticles in the superconducting state, appear as a combination of a hole and an electron.

Bogoliubov transformation: $\gamma_{-\mathbf{k}} = u_{\mathbf{k}} c_{-\mathbf{k}} + v_{\mathbf{k}} c^{+}{}_{\mathbf{k}}$ $\quad E_{\mathbf{k}} = \sqrt{\xi_{\mathbf{k}}^2 + \Delta_{\mathbf{k}}^2}$

the Lindhard function transfoms into the BCS function

BCS spin susceptibility: coherence factor & interference effect

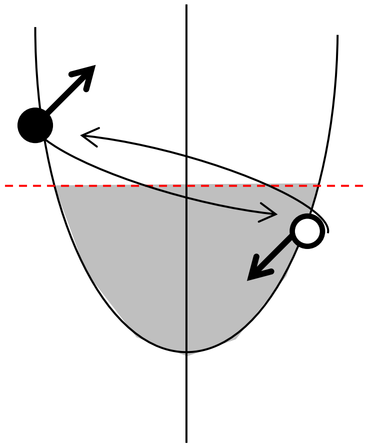

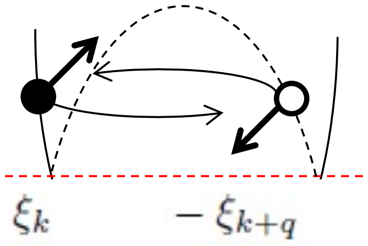

Electron or hole

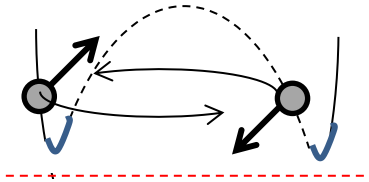

$$\gamma_{-\mathbf{k}} = u_{\mathbf{k}} c_{-\mathbf{k}} + v_{\mathbf{k}} c^{+}_{\mathbf{k}} \qquad E_{\mathbf{k}} = \sqrt{\xi_{\mathbf{k}}^2 + \Delta_{\mathbf{k}}}.$$

Mixed = electron & hole

$$\chi_o(\mathbf{q},\omega) = \frac{1}{N}\sum_k \frac{n_F(\xi_k) - n_F(\xi_{k+q})}{\omega + \xi_k - \xi_{k+q} + i\epsilon}$$

$$\chi_0^{BCS}(\mathbf{q},\omega) = \frac{1}{N}\sum_k \sum_{\alpha,\beta=\pm} M_{qk}^{\alpha\beta} \frac{n^F(\alpha E_k) - n^F(\beta E_{k+q})}{\omega + \alpha E_k - \beta E_{k+q} \cdot i\epsilon}$$

Coherence factor

$$M_{qk}^{\alpha\beta} = \frac{1}{4}\left(1 + \alpha\beta \frac{\xi_{k+q}\xi_k + \Delta_{k+q}\Delta_k}{E_{k+q}E_k}\right)$$

As T-> 0, close $\xi_k \sim \xi_{k+q} \sim 0$

$$M_{qk}^{\alpha\beta} = \frac{1}{4}\left(1 + \alpha\beta \frac{\Delta_{k+q}\Delta_k}{|\Delta_{k+q}\Delta_k|}\right)$$

The coherence factor probes the sign changes of Δ_k

BCS susceptibility

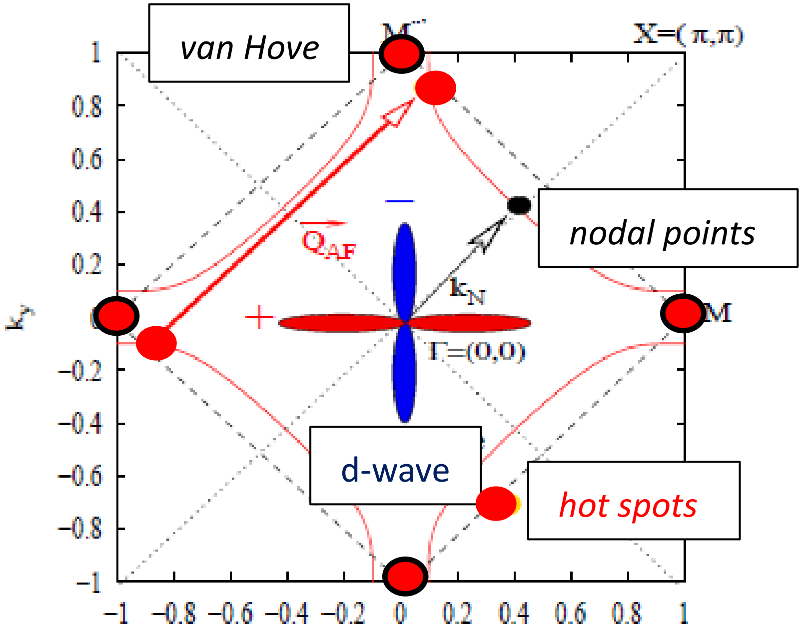

$$\epsilon_{\vec{k}} = -2t_0(cos(k_x) + cos(k_y)) - 4t_1 cos(k_x)cos(k_y) + \ldots$$

8 hot spots
4 van Hove singularities
4 modal points

The Stoner continuum is gapped
The threshold of the continuum reads:

$$\omega_c(\vec{q}) = Min(E_{\vec{k}+\vec{q}} + E_{\vec{k}})$$

Around $\mathbf{Q}_{AF}$, the SC order parameter changes its sign and the coherence factor is non-zero !!!!

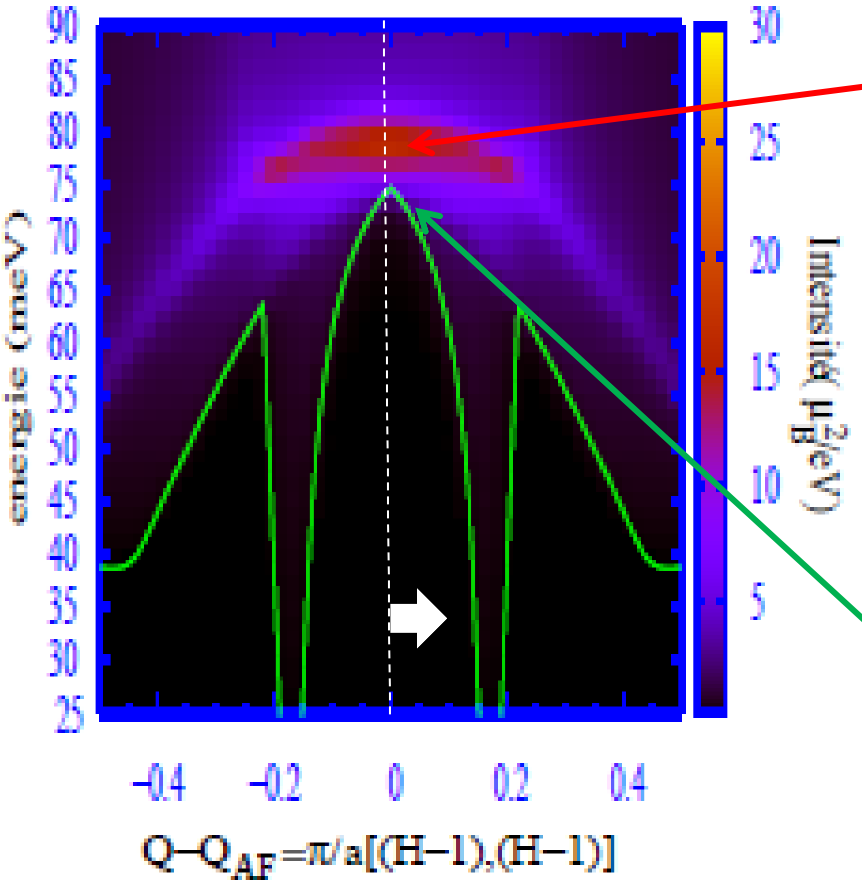

Contribution of the van Hove singularities

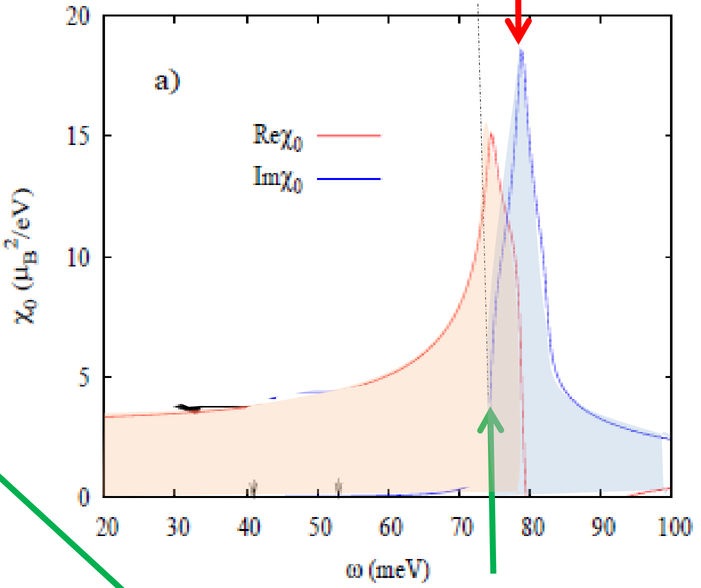

ω_c, $Re\chi(q, \omega_c)$ diverges

The spin exciton scenario

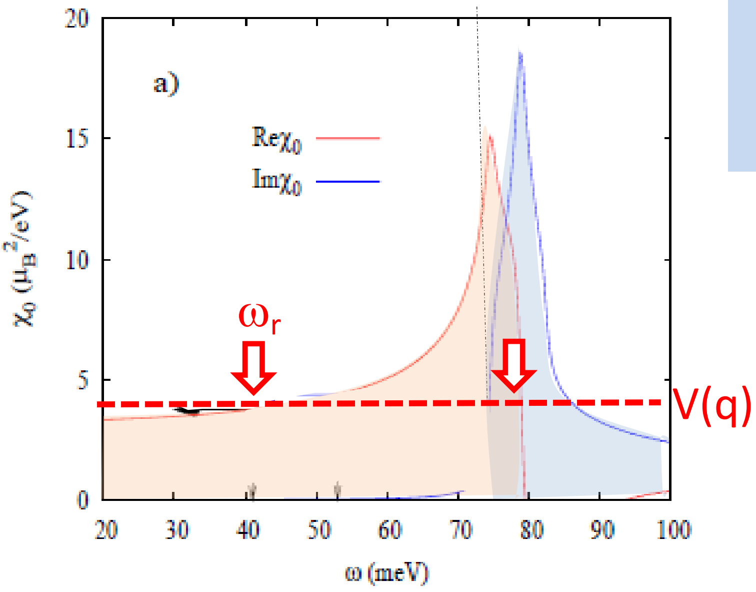

$$\chi(\vec{q},\omega)_{RPA} = \frac{\chi_0(\vec{q},\omega)}{1 - V(\vec{q})\chi_0(\vec{q},\omega)}$$

pole at $\omega_r(\vec{q})$: $\overline{1 - V(\vec{q})\chi_0(\vec{q},\omega)}$ =0

$$Im\chi(\vec{q},\omega)_{RPA} \sim Z(\vec{q})\delta(\hbar\omega - \hbar\omega_r(\vec{q}))$$

$Z(\vec{q})$: Spectral weight

A collective mode is pushed below the continuum by interaction

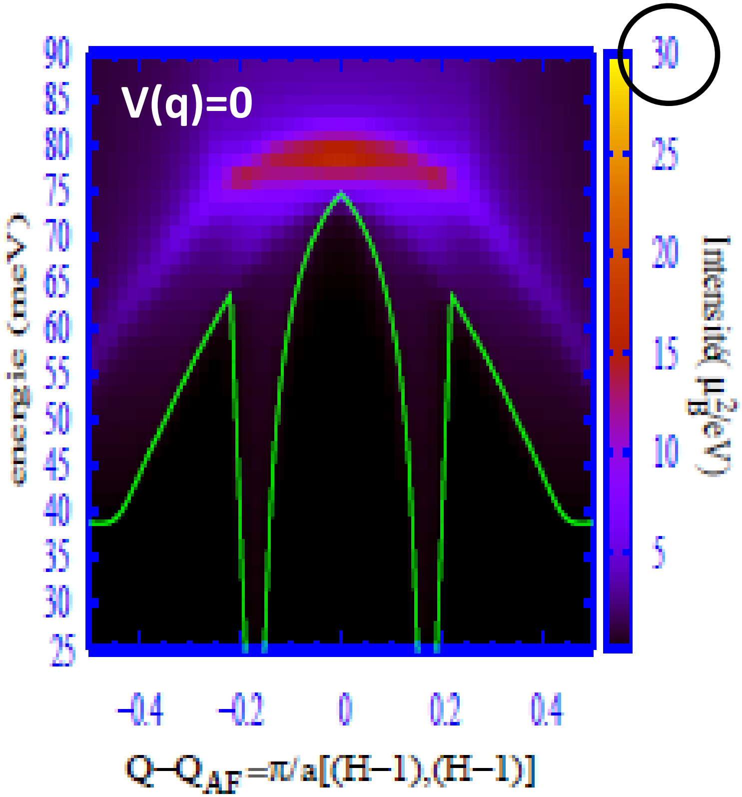

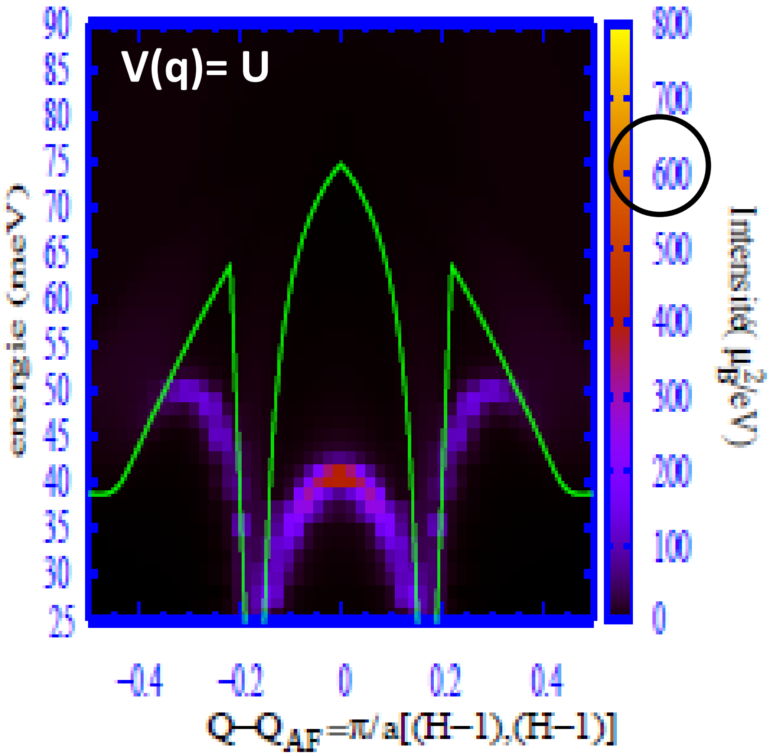

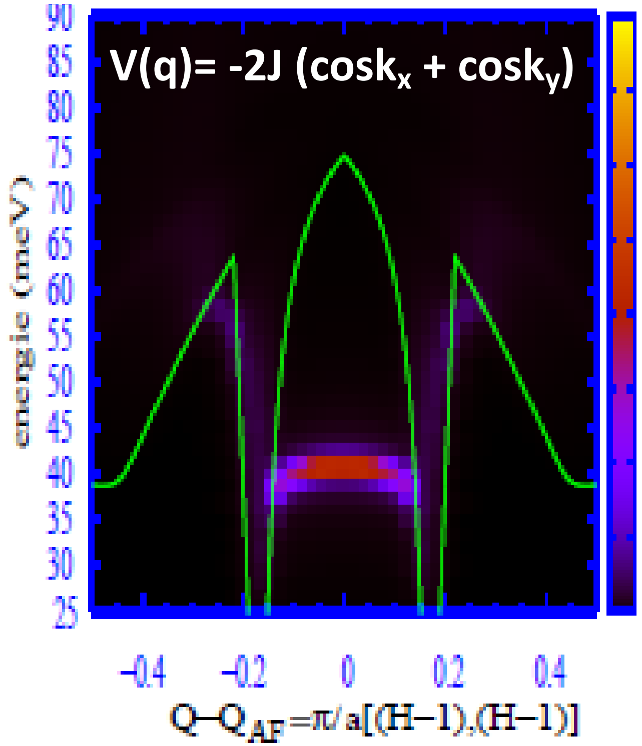

The spin exciton scenario

$$Im\chi(\vec{q},\omega)_{RPA} \sim \; Z(\vec{q})\delta(\hbar\omega - \hbar\omega_r(\vec{q}))$$

Binding energy

Spectral weight: $$Z(\vec{q}) = \frac{\pi\hbar}{V(\vec{q})^2}\left[\frac{\partial}{\partial\omega}Re\chi^0(\vec{q},\omega)\right]^{-1}_{\omega=\omega_r} \sim (\omega_c - \omega_r)$$

Damped excitation
Within the continuum

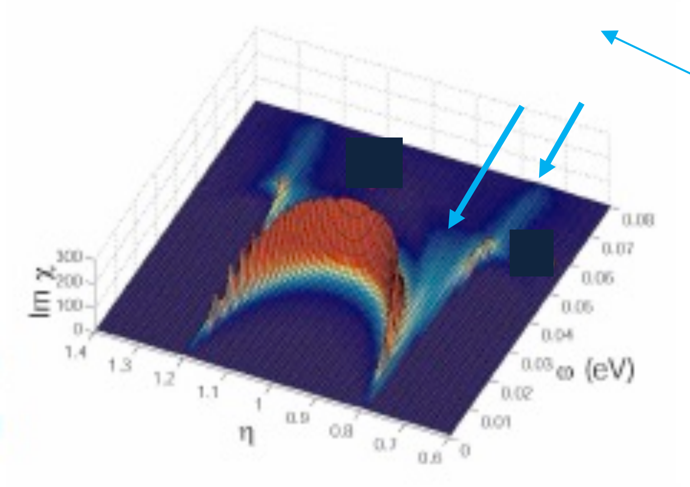

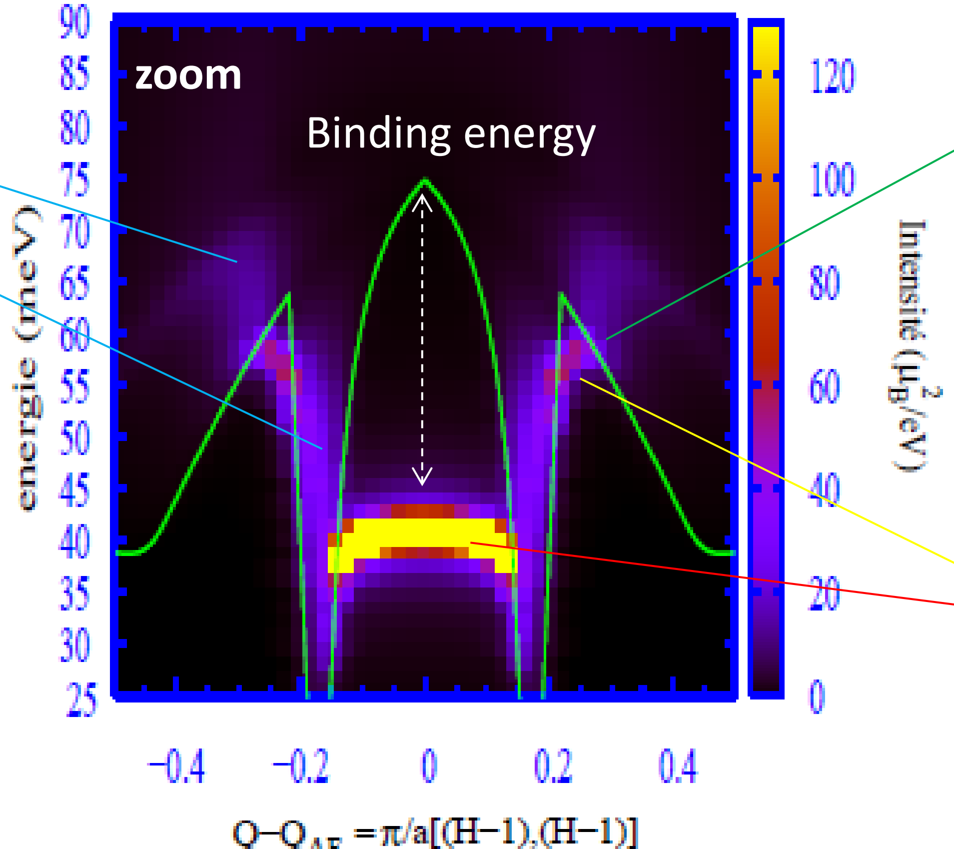

Laundau damping of the collective mode upon entering the continuum

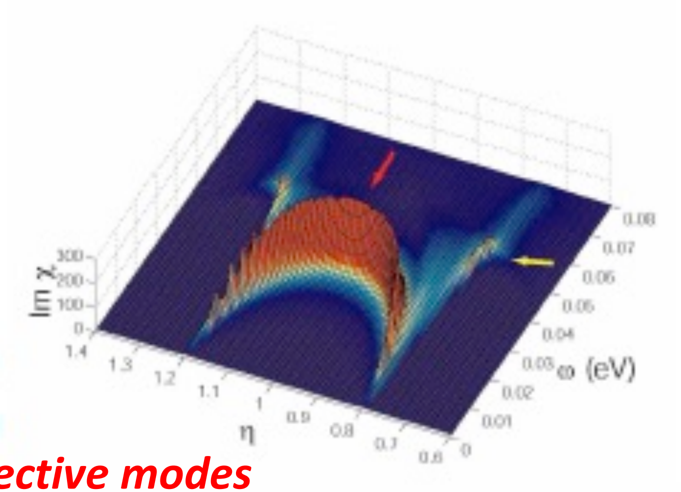

Collective modes below the threshold of the continuum

Itinerant magnetism & unconventional superconductivity
Interaction effects

The RPA approximation is generally used in the limit where the interactions are weak and can be treated as perturbations.

$$\chi(q,\omega) = \frac{\chi_o(q,\omega)}{1 - U\chi_o(q,\omega)}$$

The approximation is not suitable for treating:

- Systems in the vicinity of a magnetic transition and a quantum critical point.
- Strong correlations (U larger than the electronic bandwidth)

Effect of correlations:

1/ magnetic instability: denominator cancels at zero energy, $1 - U \,\mathrm{Re}\, \chi_o(\mathbf{q},0)=0$ (Stoner criterion)
The susceptibility diverges: a SDW develops with the propagation vector **q**

2/ superconducting instability: the pairing depends on the ability of electrons to polarize other electrons.

For a singlet superconductivity, the interaction potential depends on U and on the interaction susceptibility (RPA)

$$V_{\mathbf{q}} \simeq \frac{3}{2} U^2 \chi(\mathbf{q},\omega)$$

The strong coupling limit

When the electron-boson coupling (phonons, exc. Mag., etc) is strong, it is necessary to treat the BCS model dynamically and use the Eliashberg equations.

Green's function of quasiparticles (G) and Cooper pairs (F)

$$
\begin{aligned}
G(k,\omega) &= \frac{u_k^2}{\omega - E_k + i\epsilon} + \frac{v_k^2}{\omega + E_k + i\epsilon} \\
F(k,\omega) &= -u_k v_k \left(\frac{1}{\omega - E_k + i\epsilon} - \frac{1}{\omega + E_k + i\epsilon}\right)
\end{aligned}
$$

Owing to a strong electron-boson coupling, ξ_k et Δ_k are strongly renormalized

$$
\begin{aligned}
\xi_k &\rightarrow \bar{\xi}_{\mathbf{k},\omega} = \xi_k + \Sigma_{k,\omega} \\
\Delta_k &\rightarrow \bar{\Delta}_{k,\omega} = \Delta_k + \Phi_{k,\omega}
\end{aligned}
$$

$$
\begin{aligned}
\Sigma(k,\omega) &= \frac{1}{\pi^2}\frac{1}{N}\sum_q \int_{-\infty}^{\infty} d\Omega d\nu\, Im\chi(q,\Omega) ImG(k+q,\nu)\; V_{qk}^2 \left\{\frac{n_B(\Omega)+n_F(\nu)}{\omega+\Omega-\nu+i\epsilon}\right\} \\
\Phi(k,\omega) &= \frac{1}{\pi^2}\frac{1}{N}\sum \int_{-\infty}^{\infty} d\Omega d\nu\, Im\chi(q,\Omega) ImF(k+q,\nu)\; V_{qk}^2 \left\{\frac{n_B(\Omega)+n_F(\nu)}{\omega+\Omega-\nu+i\epsilon}\right\}
\end{aligned}
$$

The hallmark of a strong e-ph coupling

Example: in lead, the density of electronic states (measured by tunnel junction) shows anomalies at characteristic energies corresponding to maxima in the phonon density (measured by neutron scattering).

dN(E)/dE

N(E)

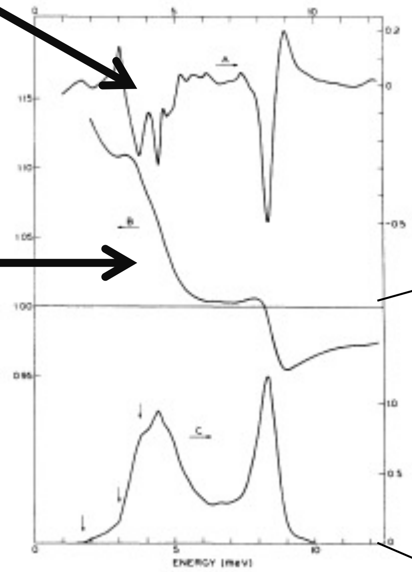

Mc Millan PRL 65

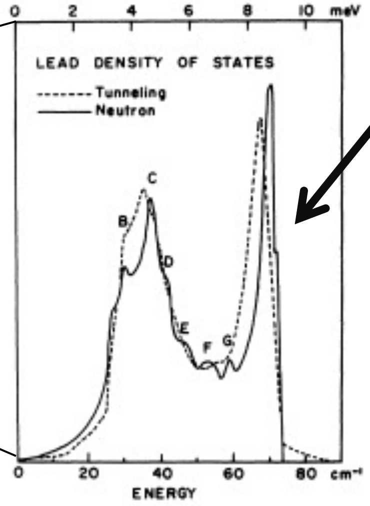

phonon density (as measured by inelastic neutron scattering)

Stedman Phys. Rev 67

Self-energy and electron-boson coupling

Particles are coupled with a single boson ω_q

$$H = \sum_{\mathbf{k}} \varepsilon_{\mathbf{k}}\, c^\dagger_{\mathbf{k}} c_{\mathbf{k}} + \sum_{\mathbf{q}} \omega_{\mathbf{q}} \left(b^\dagger_{\mathbf{q}} b_{\mathbf{q}} + \frac{1}{2} \right) + \sum_{\mathbf{kq}} g_{\mathbf{k},\mathbf{q}}\, c^\dagger_{\mathbf{k}+\mathbf{q}} c_{\mathbf{k}} \left(b_{\mathbf{q}} + b^\dagger_{-\mathbf{q}} \right) .$$

the single boson ω_q : (i) a phonon, (ii) a magnon, (iii) a CEF exciton, and so on …

* Bare Green functions

$$G_0(k, i\omega_n) = \frac{1}{i\omega_n - \varepsilon_k}$$

$$D_0(q, i\nu_m) = \frac{1}{i\nu_m - \omega_q} - \frac{1}{i\nu_m + \omega_q} .$$

* Renormalized green function

$$G(k, i\omega_n)^{-1} = G_0(k, i\omega_n)^{-1} - \Sigma(k, i\omega_n)$$

$$D(q, i\nu_m)^{-1} = D_0(q, i\nu_m)^{-1} - \Pi(q, i\nu_m) ,$$

$$\Sigma_{ep}(k, i\omega_n) = \frac{1}{N_q} \sum_{k',q} |g^q_{k',k}|^2 \left(\frac{b(\omega_q) + f(\varepsilon_{k'})}{i\omega_n + \omega_q - \varepsilon_{k'}} + \frac{b(\omega_q) + 1 - f(\varepsilon_{k'})}{i\omega_n - \omega_q - \varepsilon_{k'}} \right) .$$

$$\Pi_q(i\nu_m) = \frac{1}{N_k} \sum_{k',k} |g^q_{k',k}|^2 \frac{f(\varepsilon_k) - f(\varepsilon_{k'})}{i\nu_m + \varepsilon_k - \varepsilon_{k'}} ,$$

for constant « g » , one gets the non interactiong susceptibility

Self-energy and electron-boson coupling

$$\mathcal{D}_0(i\omega_n) \equiv \;\; = -2\Omega/(\omega_n^2+\Omega^2)$$

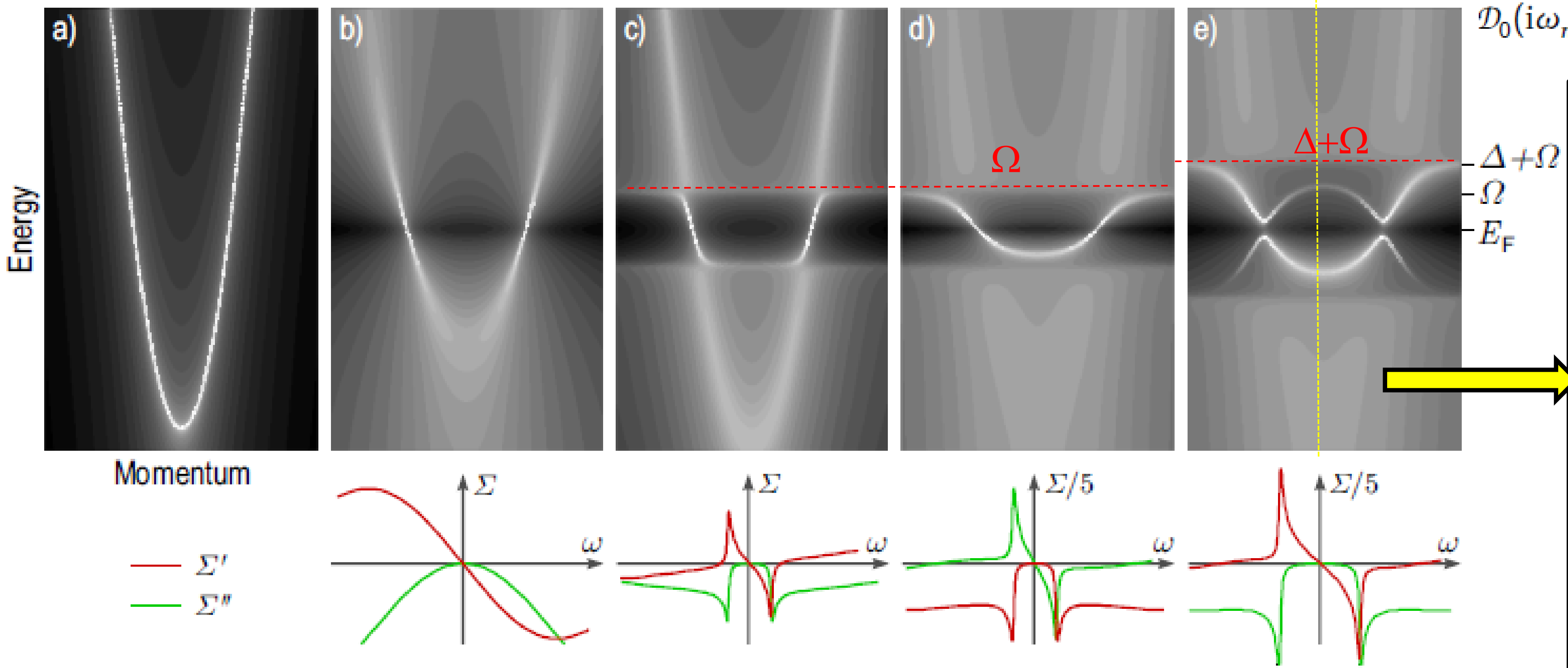

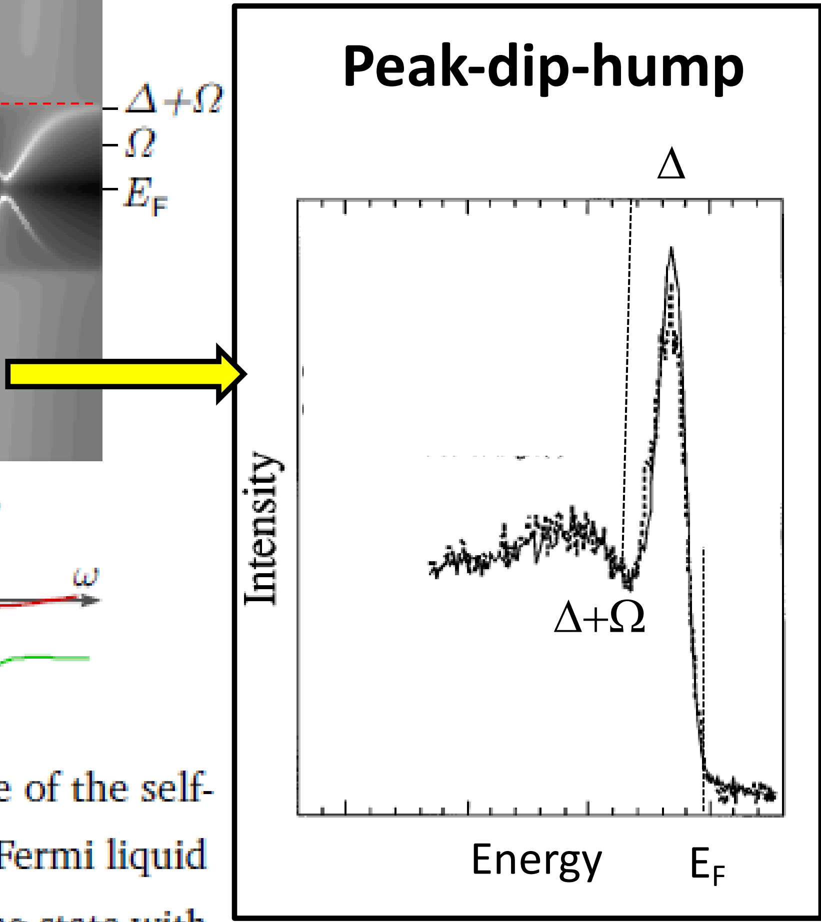

Spectral function plotted in logarithmic color scale assuming (a) no ω-dependence of the self-energy; (b) Fermi-liquid-like scattering rate; (c) weak coupling to a bosonic mode Ω; (d) both Fermi liquid contribution and strong coupling to a bosonic mode; (e) the same as (d) but in the superconducting state with a k-independent gap Δ. The real and imaginary parts of the corresponding self-energies are schematically shown below each image.

The hallmark of a strong electron-boson coupling

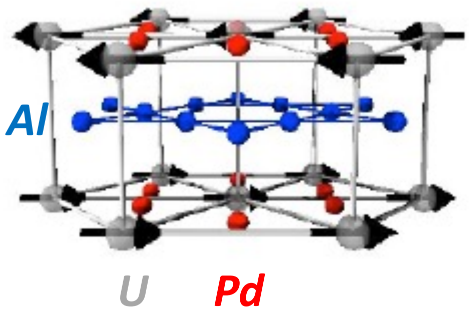

CEF excitons

$$D = \frac{D_0}{1 - D_0\Pi_0} = -\frac{2\omega_{\mathbf{q}}}{\omega^2 - \omega_{\mathbf{q}}^2 + 2\omega_{\mathbf{q}}\Pi_0}$$

$$\Pi_0(\mathrm{q}, i\omega_n) = g^2 \cdot \chi_0(\mathrm{q}, i\omega_n)$$

BCS susceptibility

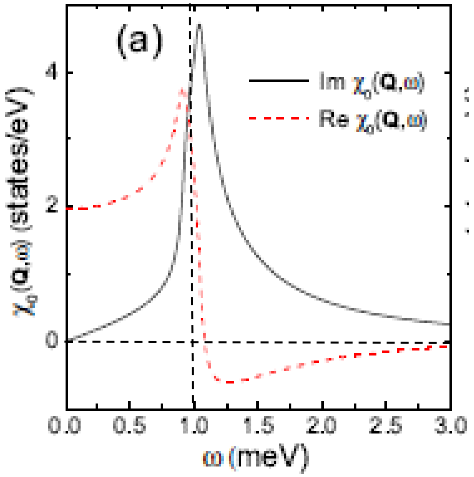

SC state

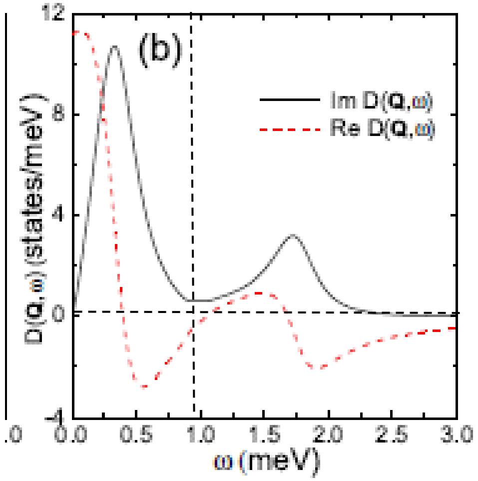

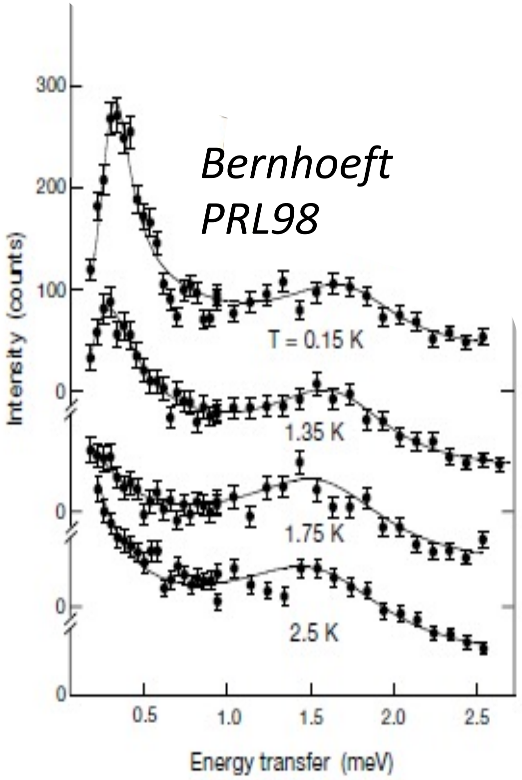

Bernhoeft PRL98

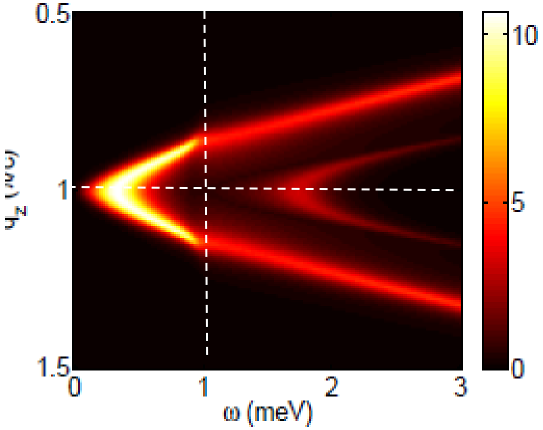

Example: UAl_2Pd_3
- Localized 4f electrons
- Itinerant d electrons

The hallmark of a strong electron-boson coupling

Magnetic excitation
(inelastic neutron scattering)

Bernhoeft
PRL98

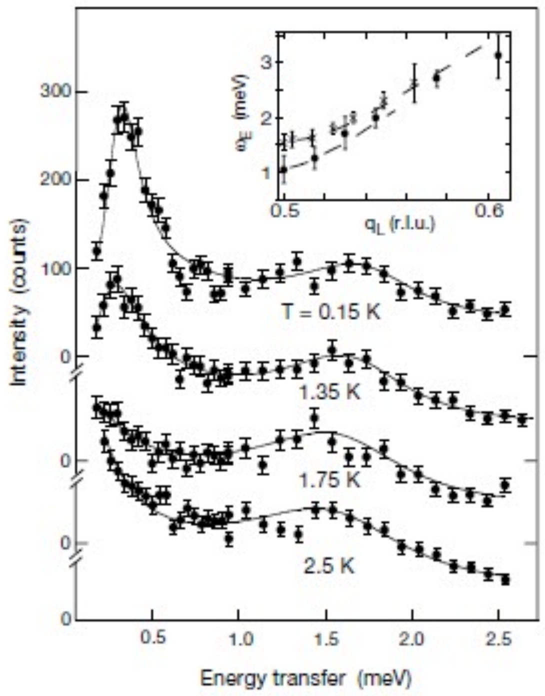

+

Differential conductivity
(tunneling junction)

Jourdan
Nature 99

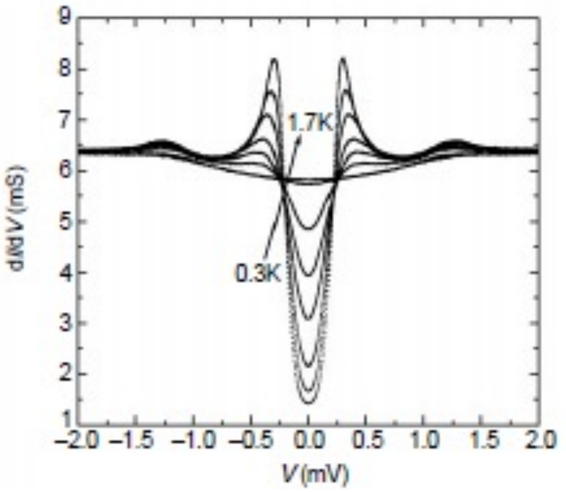

Figure 3 Differential conductivity of a UPd_2Al_3–AlO_x–Pb tunnel junction at various temperatures. (Temperatures $T = 0.3$ K, 0.5 K, 0.7 K, …, 1.7 K.) Superconductivity of Pb is suppressed in a magnetic field of $\mu_0 H = 0.3$ T.

=

Theory
(Eliashberg equation)

Sato,
Nature 01

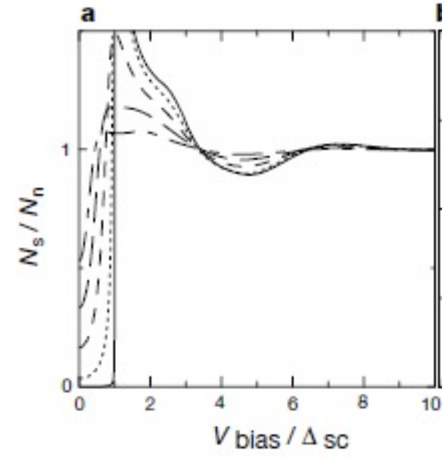

Figure 3 Tunnelling density of states calculated as function of the applied voltage V_{bias} for various temperatures. N_s/N_n is obtained from the analytic continuation of the gap function $\Phi_0(i\omega_n)$ which is the solution of the first Eliashberg equation:

$$\Phi_0(i\omega_n) = -T\sum_{\mathbf{k}'}\sum_m V_0(i\omega_n - i\omega_m)\frac{d_0^2(\mathbf{k}')\Phi_0(i\omega_m)}{\xi_{\mathbf{k}'}^2 + \omega^2(\mathbf{k}', i\omega_m) + \Phi^2(\mathbf{k}', i\omega_m)}$$

Here $d_0(\mathbf{k})$ is the $\mathbf{k}$-dependent form factor of the anisotropic gap function in equation (3), V_0 is the amplitude of the corresponding pair potential, $\Phi(\mathbf{k}, i\omega_m) = d_0(\mathbf{k})\Phi_0(i\omega_m)$ and $\omega(\mathbf{k}, i\omega_n)$ is determined by a s... equation. We solve the equation for

Magnetic neutron scattering

Y. Sidis
Laboratoire Léon Brillouin, CEA-CNRS

Cargèse-2022

Neutron scattering

Neutron:

no charge	spin ½	plane wave	energy	state
		$\psi_k(\vec{r}) = \frac{1}{\sqrt{V}} e^{i\vec{k}\vec{r}}$	$E_k = \frac{\hbar^2 k^2}{2M}$	$\vert k, \sigma >$

Target: energy E_λ state $|\lambda >$

Scattering: initial state $|k\sigma\lambda >$ $\Rightarrow$ final state $|k'\sigma'\lambda' >$

Kinematic constraints

$$
\begin{aligned}
E_\lambda + E_k &= E_{\lambda'} + E_{k'} \\
\hbar\vec{Q} &= \hbar(\vec{k} - \vec{k}')
\end{aligned}
$$

Cross-section

Probability to be scattered in a sold angle dΩ with a final energy state between E' dan E'+dE'

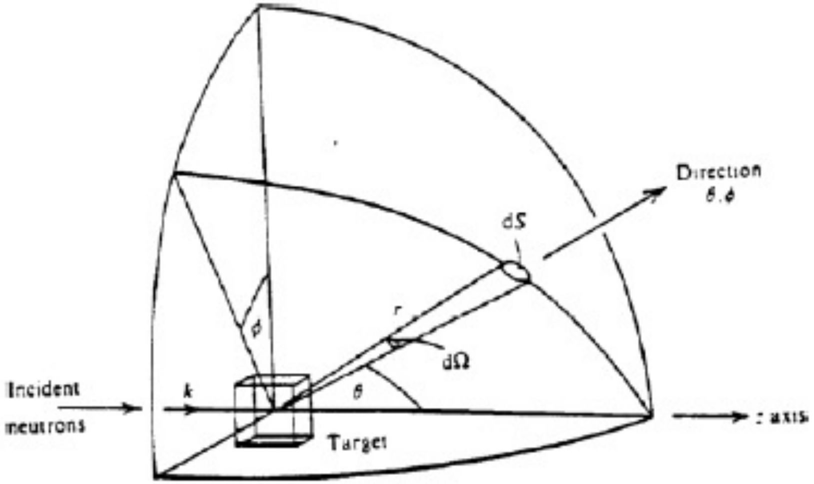

$$d\Omega = sin(\theta)d\theta d\Phi.$$

Probability for the incident neutron to be in the spin state |σ>

Density of accessible states k'

$$d\sigma = [\frac{1}{F}].\sum_{\sigma,\sigma'} p_\sigma \sum_{\lambda,\lambda'} p_\lambda [W].[D]$$

$$\begin{aligned} D &= \frac{V}{(2\pi)^3}\,\partial\vec{k}_f \\ &= \frac{V}{(2\pi)^3}\,\partial\Omega\, k_f^2\, \partial k_f \\ &= \frac{V}{(2\pi)^3}\, k_f\, \frac{m_n}{\hbar^2}\, \partial\Omega\, \partial E_f \end{aligned}$$

Probability for the target to be in the initial state |λ>

$$p_\lambda = \frac{e^{-\beta E_\lambda}}{\sum_\lambda e^{-\beta E_\lambda}}$$

Neutron flux

$$F = \frac{1}{V}\frac{\hbar k}{M}$$

Partial differential cross-section

$$d\sigma = [\frac{1}{F}].\sum_{\sigma,\sigma'} p_\sigma \sum_{\lambda,\lambda'} p_\lambda [W].[D]$$

□ W corresponds to the probability of a transition from $|k\sigma\lambda>$ to $|k'\sigma'\lambda'>$

This probability is given by the fermi's golden rule:

$$W = \frac{2\pi}{\hbar} \underbrace{| < k'\sigma'\lambda'|\hat{V}(\vec{r})|k\sigma\lambda > |^2}_{\text{Scattering potential}} \delta(E_\lambda + E_k - E_{\lambda'} - E_{k'})$$

Partial differential scattering cross-section

$$\boxed{\frac{d\sigma}{d\Omega dE'} = \frac{k}{k'}(V\frac{M}{2\pi\hbar^2})^2 \sum_{\sigma,\sigma'} p_\sigma \sum_{\lambda,\lambda'} p_\lambda | < k'\sigma'\lambda'|\hat{V}(\vec{r})|k\sigma\lambda > |^2 \delta(\hbar\omega + E_\lambda - E_{\lambda'})}$$

Nuclear scattering potential

Interaction with nuclei

$$\hat{V}_n(\vec{r}) = \frac{2\pi\hbar^2}{M} b\delta(\vec{r} - \vec{R}).$$

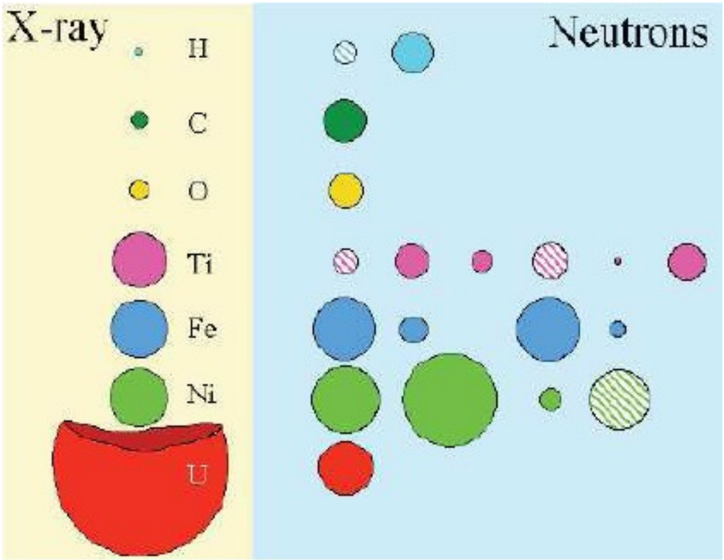

b = scattering length

Positive or negative depending on the isotope

$$\boxed{\frac{\partial^2\sigma}{\partial\Omega\partial E'} = \frac{k_f}{k_i}\sum_{i,j} b_i\, b_j \int_{-\infty}^{+\infty} dt\, \langle e^{iQ\ R_i}\, e^{-iQ\ R_j(t)}\rangle\, e^{-i\omega t}}$$

Nuclear scattering cross section

$$\frac{d\sigma}{d\Omega dE'} = \left(\frac{d\sigma}{d\Omega dE'}\right)_{elas} + \left(\frac{d\sigma}{d\Omega dE'}\right)_{inelas}$$

Elastic

$$\left(\frac{d\sigma}{d\Omega dE'}\right)_{elas} = \underbrace{\frac{k'}{k}}_{=1} N\frac{(2\pi)^3}{v_0}\sum_{\vec{\tau}}\delta(\vec{Q}-\vec{\tau}-\vec{q})\left| F_s(Q)\right|^2 \delta(\omega)$$

Static structure factor: $\boxed{F(Q) = \sum_{\ell} b_\ell \, e^{iQ\, r_\ell} e^{-W_\ell}}$

Inelastic

$$\left(\frac{d\sigma}{d\Omega dE'}\right)_{inelas} = \frac{k'}{k} N\frac{(2\pi)^3}{v_0}\sum_{\vec{\tau}}\delta(\vec{Q}-\vec{\tau}-\vec{q})\left| F_s(Q)\right|^2$$

$$\times \underbrace{\left((1+n_B(\omega_{\vec{q}}^s))\delta(\omega-\omega_{\vec{q}}^s)\right.}_{\text{Phonon creation}} + \underbrace{\left. n_B(\omega_{\vec{q}}^s)\delta(\omega+\omega_{\vec{q}}^s)\right)}_{\text{Phonon anihilation}}$$

$n_B(\omega) = \frac{1}{e^{\beta\hbar\omega}-1}$ the Bose-Einstein distribution

Phonon polarization

dynamical structure factor: $\boxed{F_s(Q) = \sum_{\ell} b_\ell \, e^{iQ\, r_\ell} \, e^{-W_\ell} \, \frac{1}{\sqrt{M_\ell \omega_{q,s}}} \left(\vec{Q}.\vec{e}_{q,\ell}\right)}$

Magnetic scattering potentials

Scattering potential:

$$E_{ne} = -\mu_n . B_e$$

<u>Neutron:</u> magnetic moment operator

$$\hat{\mu} = \gamma \mu_N \hat{\sigma}$$

$$B_e(R) = \frac{\mu_o}{4\pi}\left(\mathrm{rot}(\frac{\mu_e \times R}{R^3}) - e\, v_e \times \frac{R}{R^3}\right)$$

<u>Target</u>: distribution of internal magnetic fields

(1) Spins of unpaired electrons
(2) Electronic orbital moments

(1) spin-only scattering: Dipolar interaction with electronic spins

$$B_e(R) = \frac{\mu_o}{4\pi}\left(\mathrm{rot}(\frac{\mu_e \times R}{R^3})\right)$$

(2) *unpolarized neutron beam:*

$$\sum_\sigma p_\sigma < \sigma|\sigma_\alpha \sigma_\beta|\sigma >= \delta_{\alpha,\beta}$$

$$\boxed{\frac{\partial^2\sigma}{\partial\Omega\partial E'} = \frac{k_f}{k_i}(\gamma r_o)^2 \sum_{i,j}\int_{-\infty}^{+\infty} dt\, \langle \vec{S}_{\perp,i}\, \vec{S}_{\perp,j}(t)\, e^{iQ\ R_i}\, e^{-iQ\ R_j(t)}\rangle\, e^{-i\omega t}}$$

probes the F.T. of the spin-spin correlation function in space and time

Magnetic scattering cross section

N is the number of unit cells

Debye-Waller factor

$$\frac{d^2\sigma}{d\Omega dE} = \frac{N}{\hbar}\frac{k_f}{k_i} p\ e^{-2W} \sum_{\alpha,\beta} (\delta_{\alpha,\beta} - \tilde{Q}_\alpha \tilde{Q}_\beta) S^{\alpha\beta}(\mathbf{Q},\omega)$$

$\mathbf{Q} = \mathbf{k}_i - \mathbf{k}_f$

$E = \hbar\omega = E_i - E_f$

$E_i = \hbar^2 k_i^2/2m$

$E_f = \hbar^2 k_f^2/2m$

Magnetic structure factor

Orientation factor

$$p = (\gamma r_0/2)^2 g^2 f(\mathbf{Q})^2$$

$\gamma r_0/2 = 0.2695 \times 10^{-12}$ cm

$g \approx 2$ is the Landé factor

$f(\mathbf{Q})$ is the magnetic form factor

$\tilde{Q}_\alpha$, $\tilde{Q}_\beta$ are the projections of the unit wave $\tilde{Q}$ onto the Cartesian axes

Cartesian coordinates

fluctuation-dissipation theorem & sum rule

$S^{\alpha\beta}(\mathbf{Q},\omega)$ is the dynamic spin correlation function.

its is related to the imaginary part of the the dynamic spin susceptibility $\chi''_{\alpha\beta}(\mathbf{Q},\omega)$

<u>Fluctuation-dissipation theorem:</u>

$$\boxed{S^{\alpha\beta}(\mathbf{Q},\omega) = \frac{\hbar}{\pi}\frac{1}{(1-e^{-\hbar\omega/k_BT})}\frac{\chi''_{\alpha\beta}(\mathbf{Q},\omega)}{g^2\mu_B^2}}$$

Unit: $\mu_B^2 . eV^{-1}$

with $\chi''(\mathbf{Q},\omega) = (1/3)\mathrm{tr}(\chi''_{\alpha\beta}(\mathbf{Q},\omega))$

<u>Local spin susceptibility</u> $\chi''(\omega) = \int \chi''(\mathbf{Q},\omega) d\mathbf{Q} / \int d\mathbf{Q}$

<u>Local fluctuating moment</u> $\langle \mathbf{m}^2 \rangle = \frac{3\hbar}{\pi}\int_{-\infty}^{\infty} \frac{\chi''(\omega) d\omega}{1-\exp(-\hbar\omega/k_BT)}$

<u>Global sum rule</u> $M^2 + \langle \mathbf{m}^2 \rangle = g^2 S(S+1)$ M is the static ordered moment (if any)

note: one measures $M_\perp$ the magnetic component perpendicular to **Q**

Polarized neutron beam : « full » polarization analysis

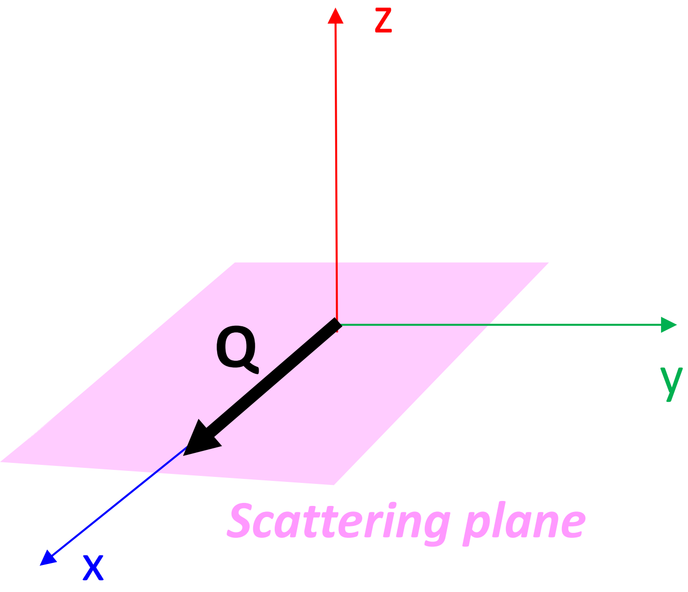

x || Q
y ⊥ Q
z ⊥ scattering plane

$$
\begin{aligned}
I_x^{++} &\propto |N|^2 \\
I_x^{--} &\propto |N|^2 \\
I_x^{+-} &\propto |M_\perp|^2 - M_{ch} \\
I_x^{-+} &\propto |M_\perp|^2 + M_{ch} \\
I_y^{++} &\propto |N|^2 + |M_\perp^y|^2 + R_y \\
I_y^{--} &\propto |N|^2 + |M_\perp^y|^2 - R_y \\
I_y^{+-} &\propto |M_\perp^z|^2 \\
I_y^{-+} &\propto |M_\perp^z|^2 \\
I_z^{++} &\propto |N|^2 + |M_\perp^z|^2 + R_z \\
I_z^{--} &\propto |N|^2 + |M_\perp^z|^2 - R_z \\
I_z^{+-} &\propto |M_\perp^y|^2 \\
I_z^{-+} &\propto |M_\perp^y|^2
\end{aligned}
$$

$|N|^2$ nuclear scattering

$|M_\perp|^2$ full magnetic scattering

$|M_\perp|^2 = |M^z_\perp|^2 + |M^y_\perp|^2$

Chiral terms

$$M_{ch} = i\,(M_\perp^{z*} M_\perp^y - M_\perp^{y*} M_\perp^z)$$

Interference terms

$$R_y = N\ M_\perp^{y*} + N^*\ M_\perp^y$$
$$R_z = N\ M_\perp^{z*} + N^*\ M_\perp^z$$

Polarized neutron beam : « basic » polarization analysis

(++)=(--) NSF
(+-)=(-+) SF
No chirality
No N-M interference

The of neutron is polarized.
R is the flipping ratio, which defines the quality of the polarization
The scattering processes are spin-flip (SF) or non-spin-flip (NSF)

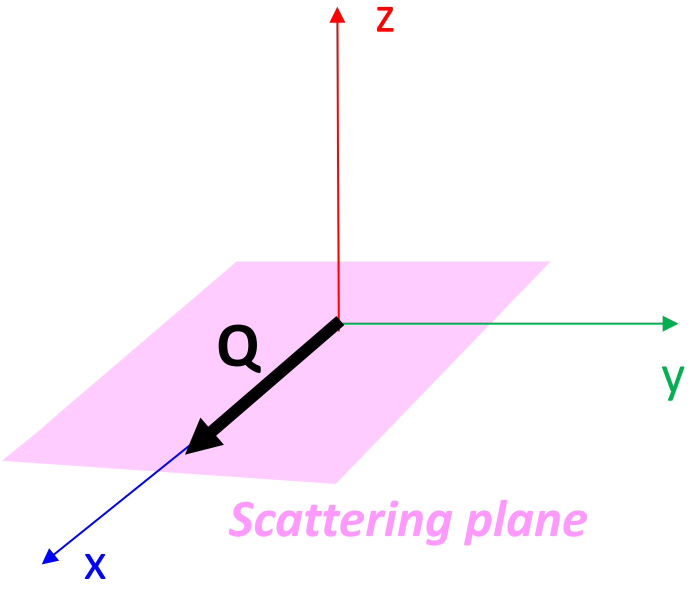

x || Q
y ⊥ Q
z ⊥ scattering plane

$$\begin{array}{c} \\ \text{SF} \\ \\ \\ \text{NSF} \\ \\ \end{array} \begin{pmatrix} \sigma_x^{\mathrm{SF}} \\ \sigma_y^{\mathrm{SF}} \\ \sigma_z^{\mathrm{SF}} \\ \sigma_x^{\mathrm{NSF}} \\ \sigma_y^{\mathrm{NSF}} \\ \sigma_z^{\mathrm{NSF}} \end{pmatrix} = \frac{1}{(R+1)} \begin{pmatrix} R & R & 1 & 2R/3+1/3 & (R+1) \\ 1 & R & 1 & 2R/3+1/3 & (R+1) \\ R & 1 & 1 & 2R/3+1/3 & (R+1) \\ 1 & 1 & R & R/3+2/3 & (R+1) \\ R & 1 & R & R/3+2/3 & (R+1) \\ 1 & R & R & R/3+2/3 & (R+1) \end{pmatrix} \begin{pmatrix} M_y \\ M_z \\ N \\ \mathrm{NSI} \\ B \end{pmatrix}$$

B is a background term
NSI is the nuclear spin incoherent scattering
$\longrightarrow$ moments within the nuclei of the isotopes

Polarized neutron beam : example

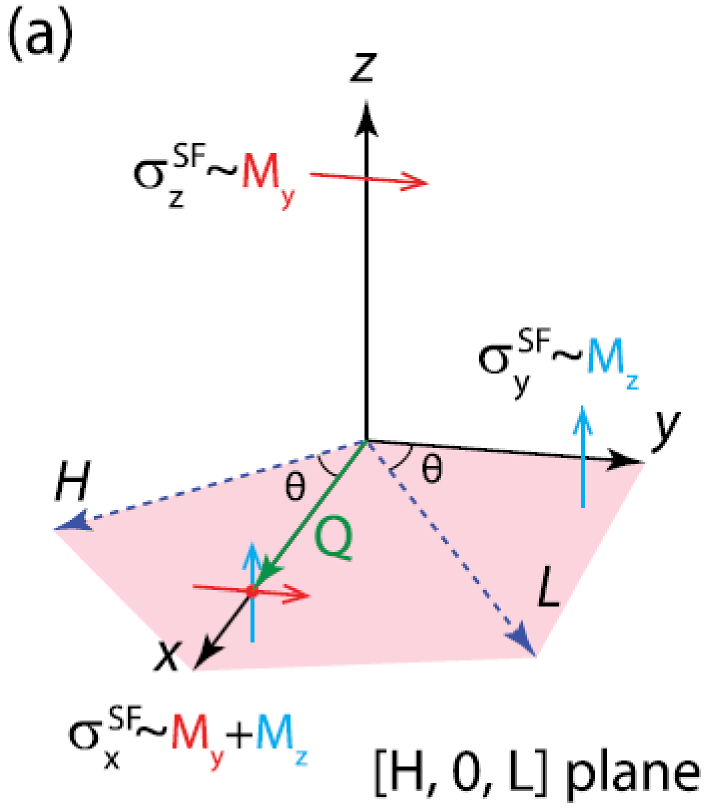

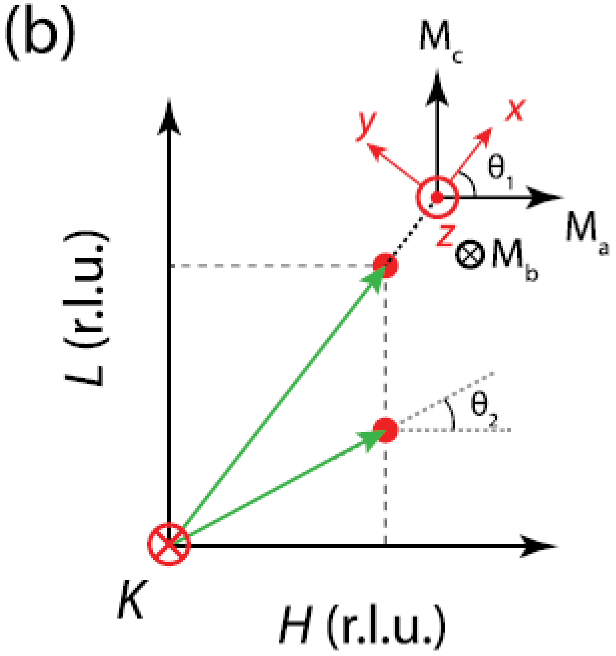

M_y and M_z are magnitudes of spin excitations along the y and z directions

<u>Polarization sum rule</u>

$$\sigma_x^{SF} \sim M_y + M_z$$
$$\sigma_y^{SF} \sim M_z$$
$$\sigma_z^{SF} \sim M_y$$

SF: σ_x ~ $(L/Q)^2$ M_a + M_b + $\{1-(L/Q)^2\}$ M_c

SF: σ_y ~ M_b

SF: σ_z ~ $(L/Q)^2$ M_a + $\{1-(L/Q)^2\}$ M_c

I_{mag} ~ $\{1-(H/Q)^2\}$ M_a + $\{1-(K/Q)^2\}$ M_b+ $\{1-(L/Q)^2\}$ M_c

Instrumental resolution

Measured intensity proportional to $\underbrace{S(\vec{Q},\omega) \otimes R(\vec{Q},\omega)}$

The Fourier transform of the theoretical structure factor convoluted by the instrumental resolution function

$R(\vec{Q},\omega)$ ⇨ Gaussian function (4 dimensions)

Resolution ellipsoid

Simplified description (Cooper, Nathans,1967…)

The resolution function reads : $R_0 \exp(-X^t \mathbf{A} X)$

X stands for a 4D vector : $(Q-Q_0, w-w_0)$

with $$R_0 = V_i V_f \sqrt{\det(A)} \, {}^{1}\!/_{\pi^2}$$

$V_i = p_m k_i^3 \cot(q_m)$ et $V_f = p_a k_f^3 \cot(q_a)$

Ex: focussing effect

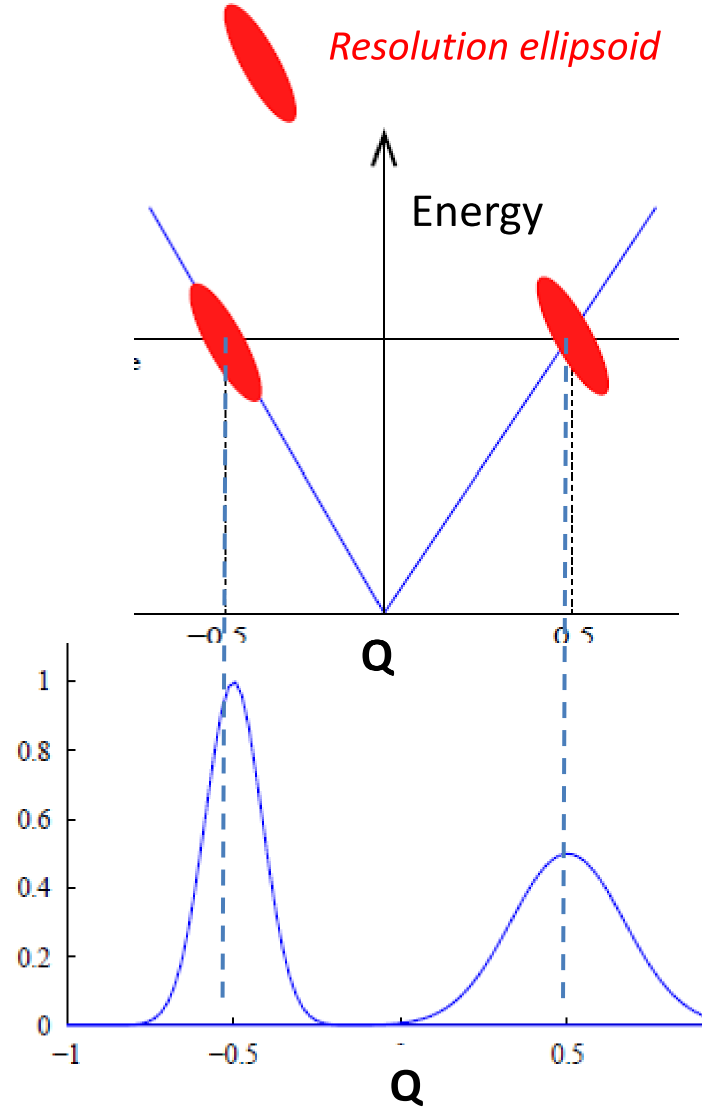

INS: triple axis spectrometer (TAS)

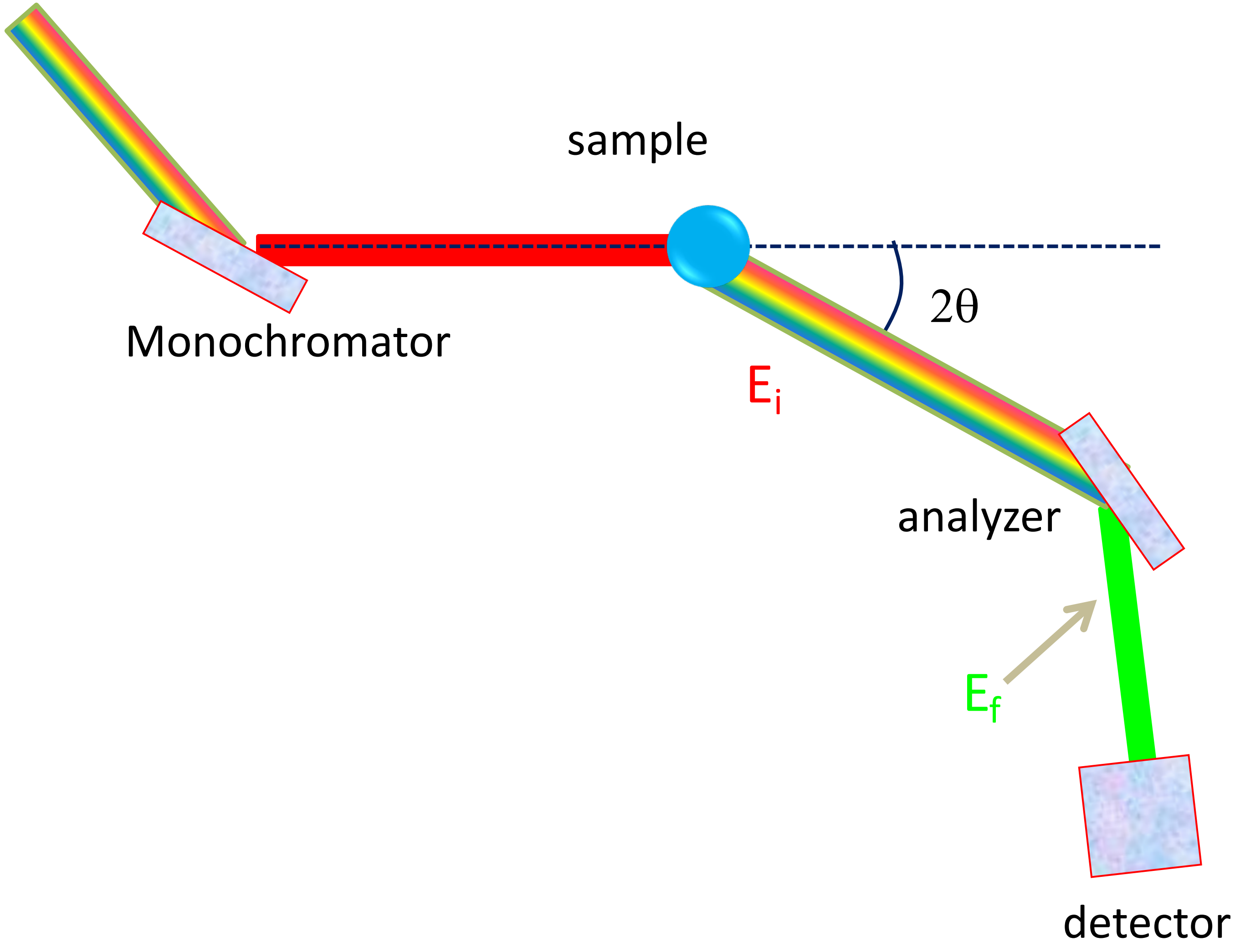

Triple Axis Spectrometeur [TAS]
(IN8, IN20, IN12, IN22 @ ILL)

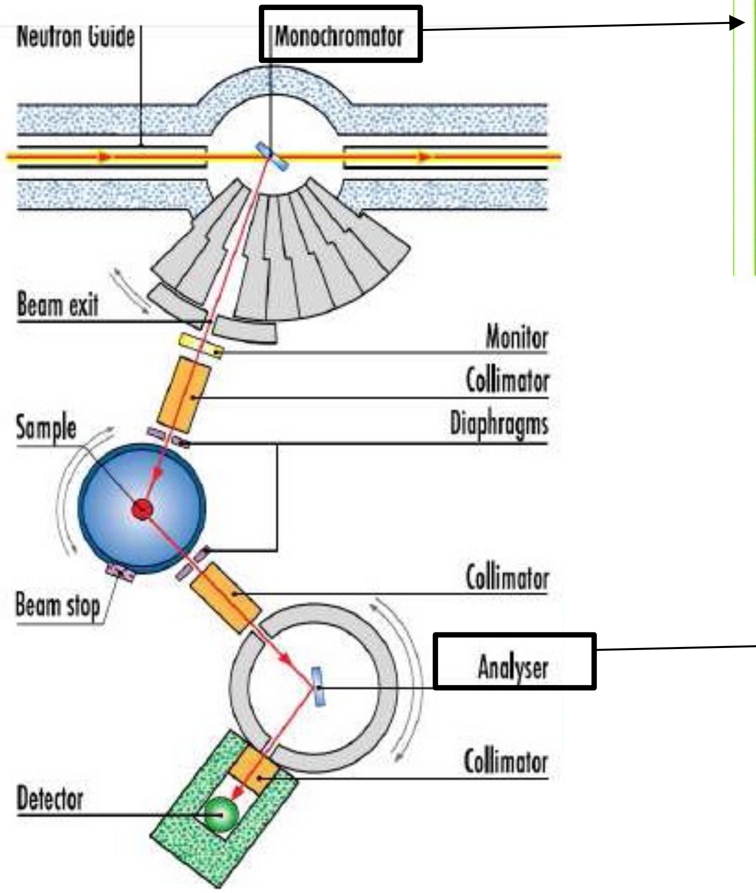

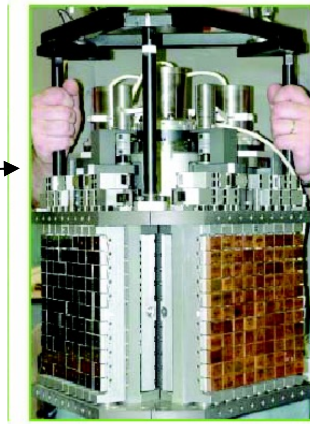

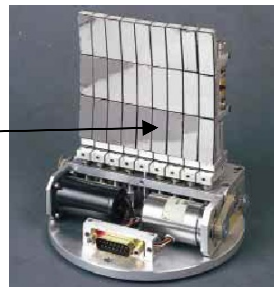

INS: time of fligth spectrometer (ToF)

$$t = \frac{d}{\sqrt{2E_f/m_n}}$$

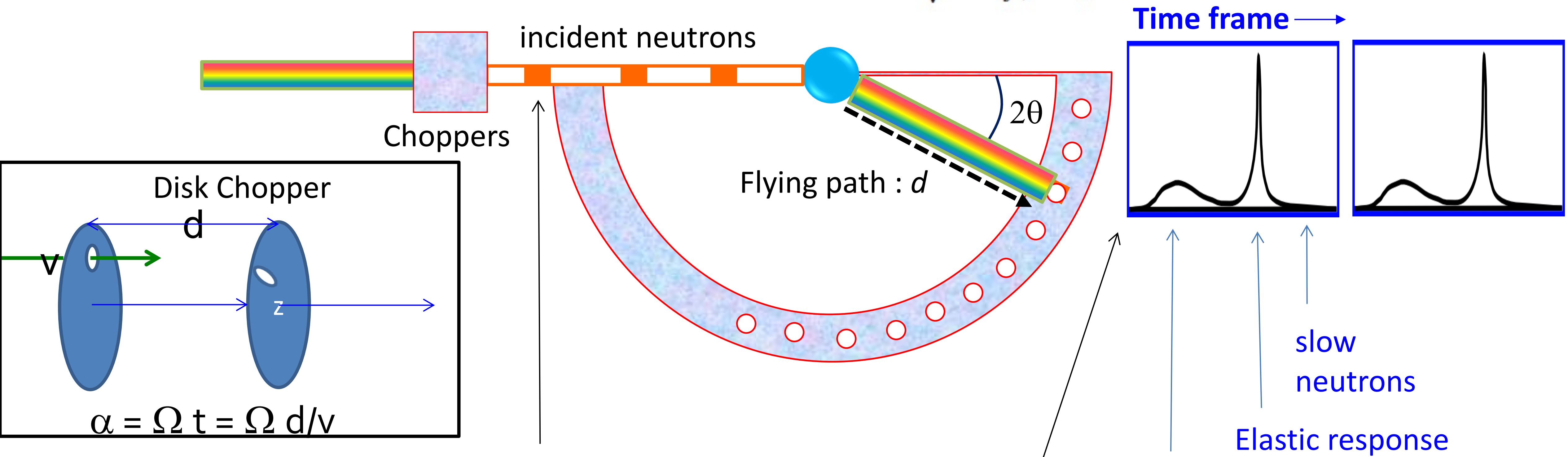

One chops the neutron beam to prepare **neutrons packets** of a certain time frame, with a repetition time that allows the superposition of information in the detectors

INS: time of fligth spectrometer (ToF)

Time of Flight (ToF) spectrometer
IN4-Panther, IN5, IN6-Sharp @ ILL
FOCUS @ PSI
…

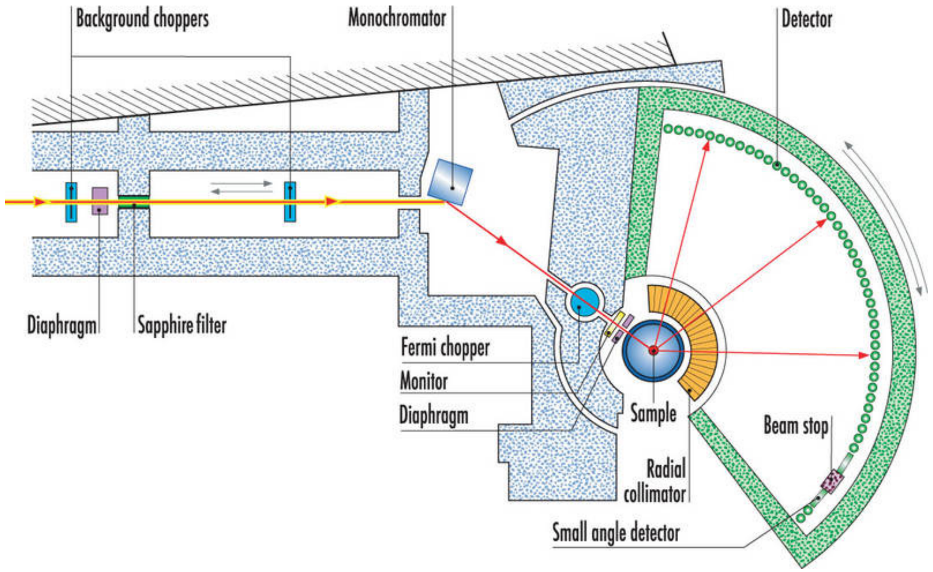

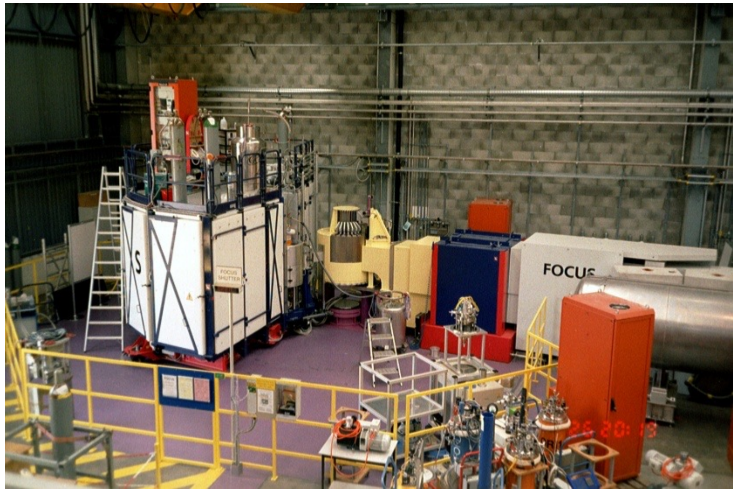

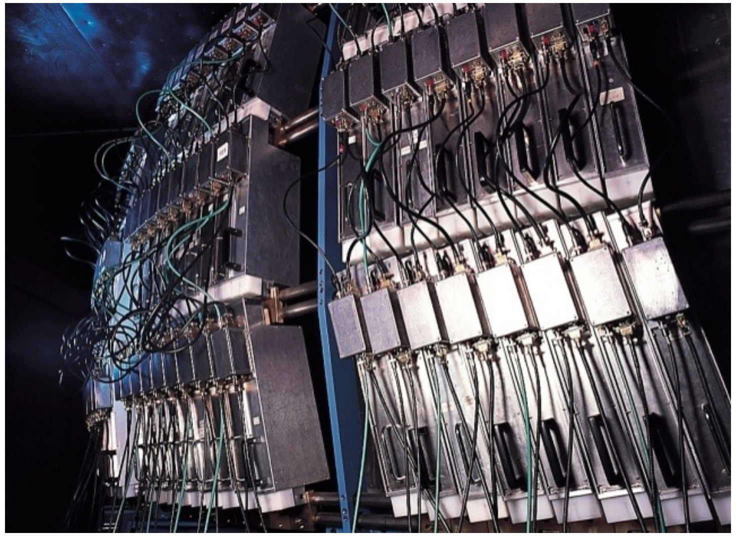

Time scale

Neutron spectroscopy can be used to probe the nuclear and magnetic structures of a sample and the related nuclear and magnetic excitations. This is a <u>bulk</u> and <u>non destructive</u> measurement.

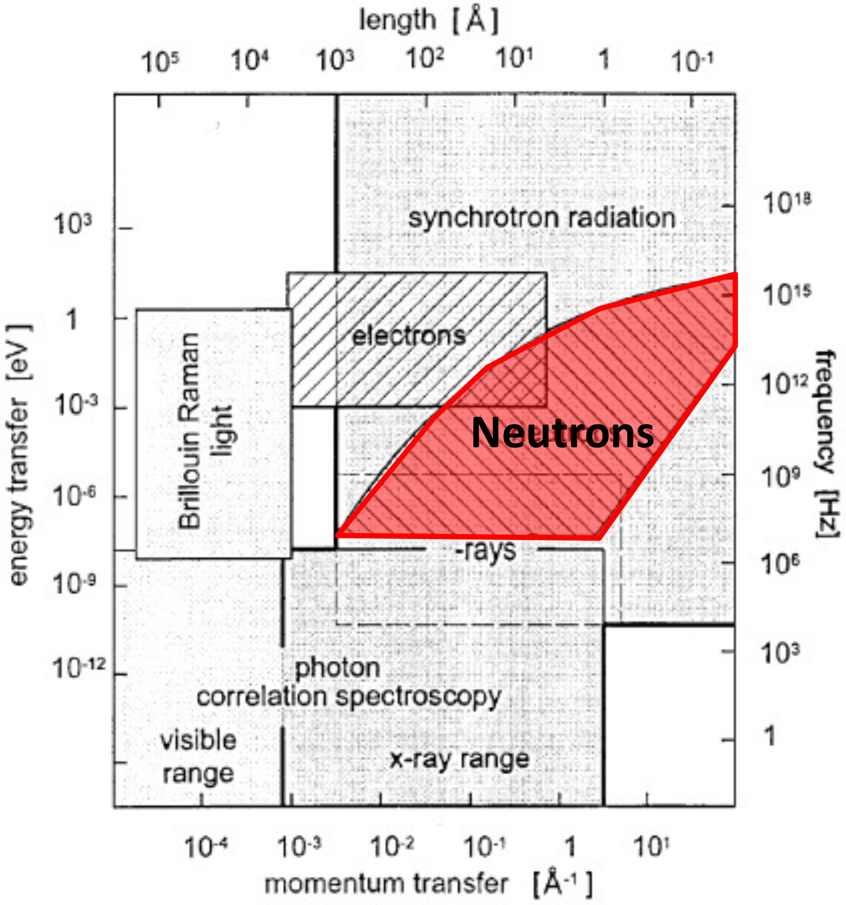

Neutron scatering vs. Other inelastic probes

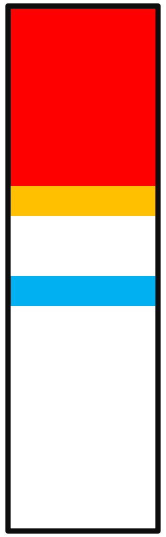

Neutrons (10^{-12} s)

μSR, MossBauer spectroscopy

(10^{-9} s)

NMR

(10^{-6} s)

Local probes

Technics

INS and RIXS : $\chi(q, \omega)$

$$S_{\alpha\beta}(\mathbf{Q},\omega) = \frac{1}{\pi}\frac{Im\chi_{\alpha\beta}(\mathbf{q},\omega)}{1-exp(-\hbar\omega/k_BT)}$$

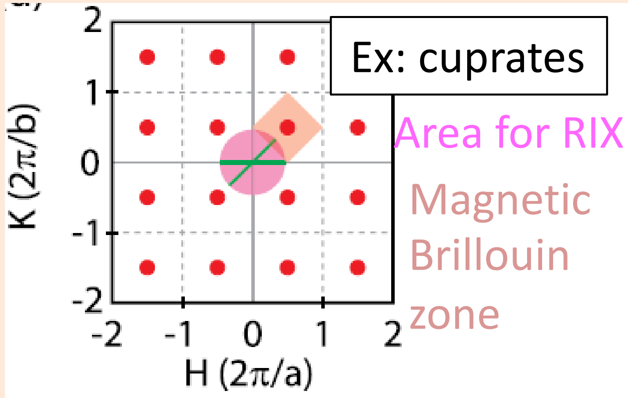

Area for RIX

Magnetic Brillouin zone

NMR local: χ_q, $\omega \to 0$

spin lattice relataxion $1/T_1$

$$(1/T_1T) \simeq \frac{k_B\gamma_n^2}{(g\mu_B)^2}\sum_q |A(\mathbf{q})|^2 \left.\frac{Im\chi(\mathbf{q},\omega)}{\omega}\right|_{\omega\to 0}$$

Hyperfine factor

Magnetic neutron scattering : examples of states & excitations

q=0 states in e-h channel [intra-unit-cell instabilities]

	Ferromagnetic	**Nematic (d-wave)** charge	**Nematic (d-wave)** spin	**Loop current**

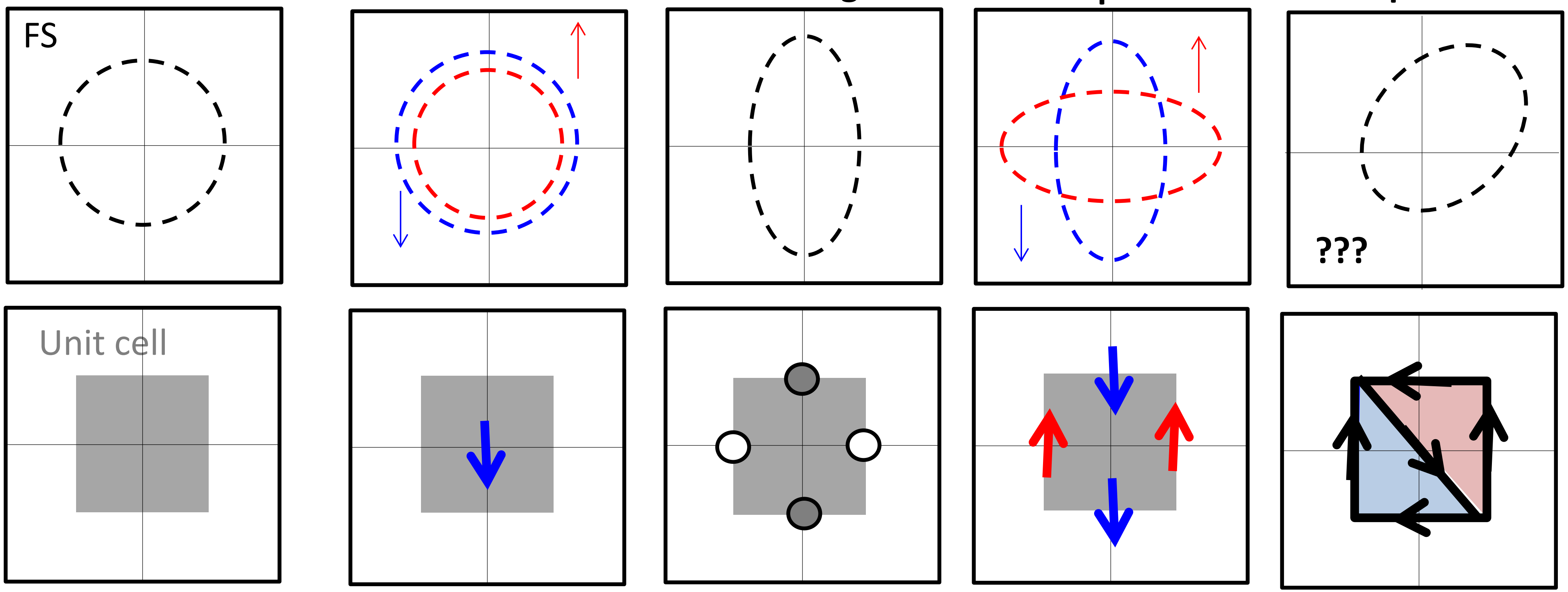

magnetic structure factor	**m**	**0**	**m** 2{cos(πH) – cos(πK)}	**m** 2i sin(2π x_o(H+K))

Magnetic neutron scattering : examples of states & excitations

q≠0 , density wave states in e-h channel
[breaking of lattice translation symmetry]

q≠0 , density wave states in Cooper channel
[breaking of lattice translation symmetry]

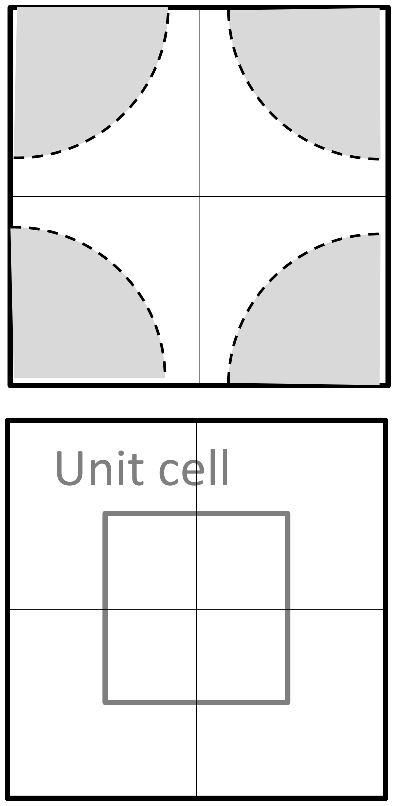

SpinDW q(1/2,1/2)
s-wave,

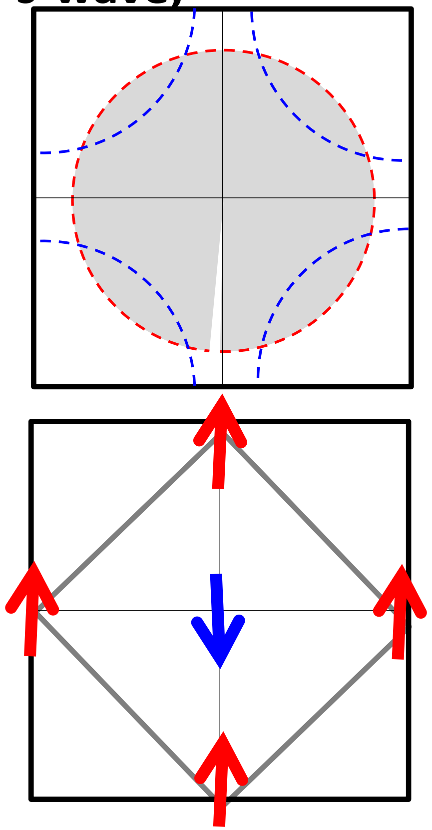

CurrentDW q(1/2,1/2)
d-wave

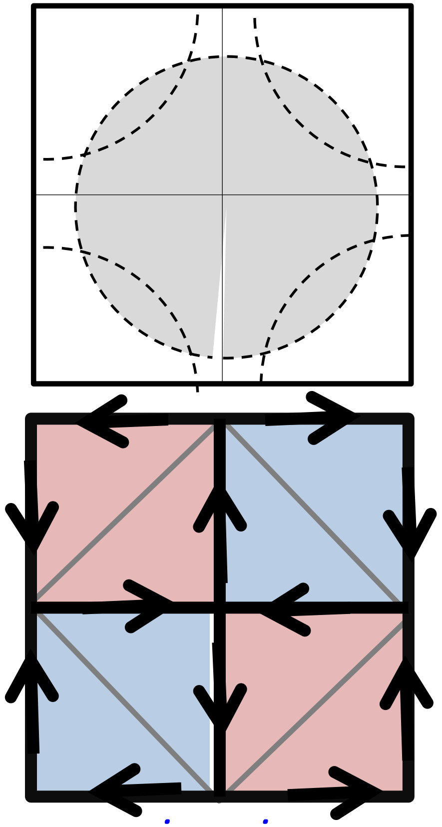

pure imaginary order parameter

PairDW q(1/2,1/2)
?-wave , S=1

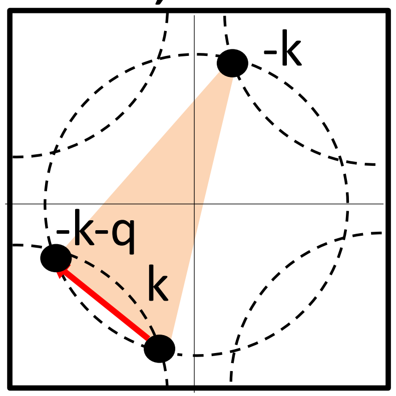

Spin dynamics in HTc supercondicting cuprates

Y. Sidis
Laboratoire Léon Brillouin, CEA-CNRS

Cargèse-2022

Crystal structure

Layered materials, made of stacking of one or several CuO_2 layers per unit cell, separated by other atomic layers playing the role of charge reservoirs

Building block: CuO_2 square plaquette

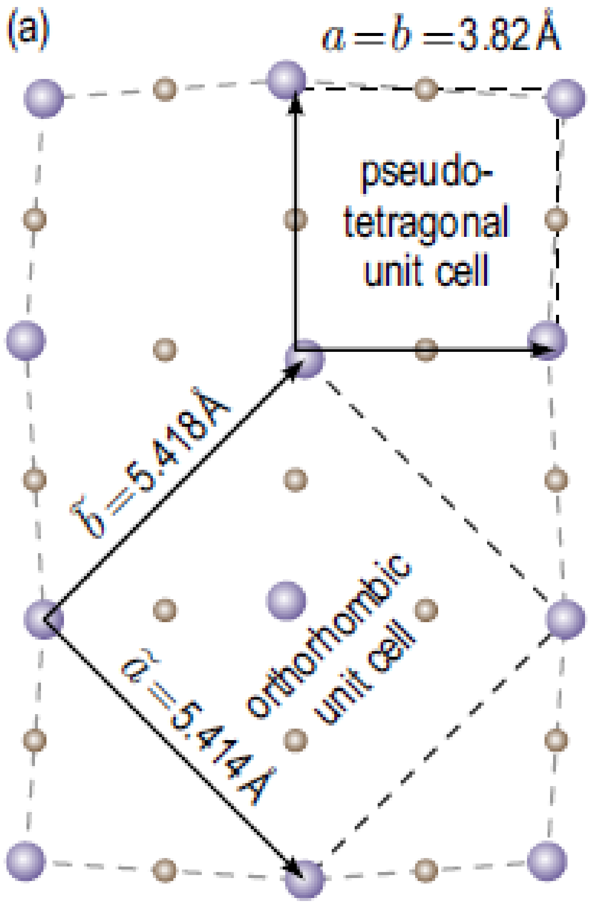

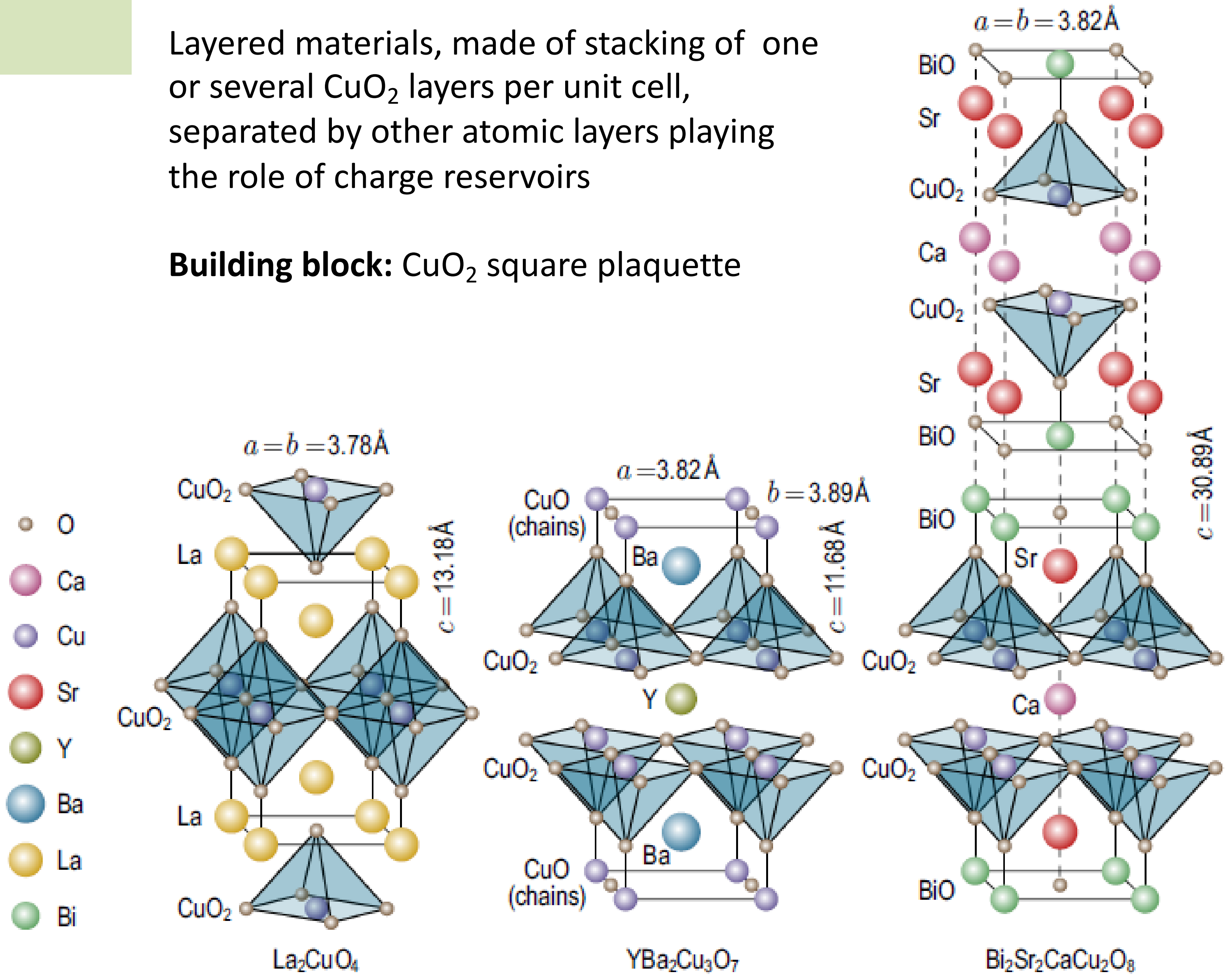

Minimum model

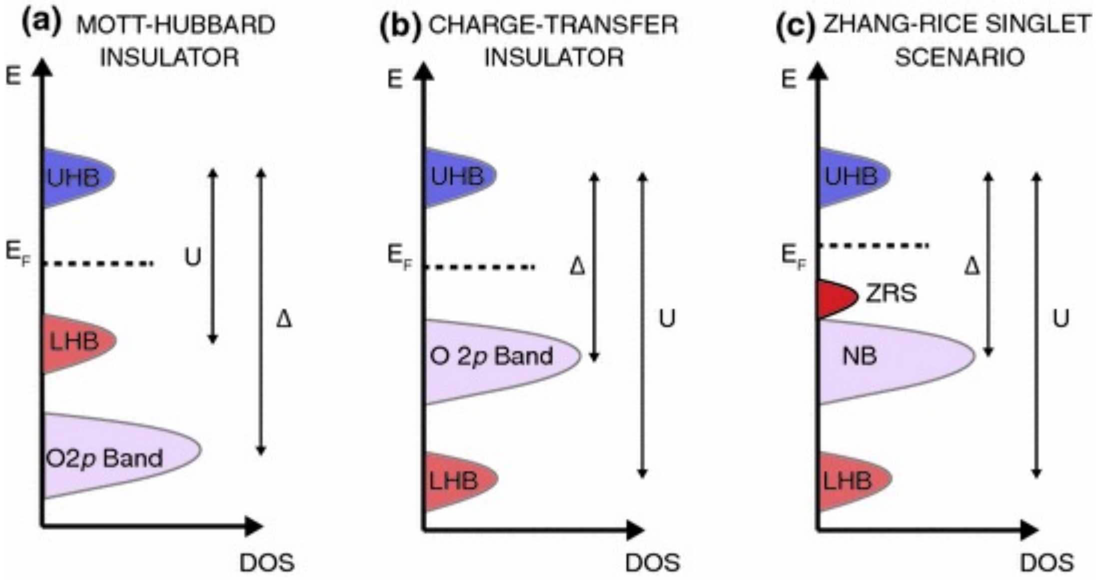

At zero doping, cuprates are charge transfert insulators.

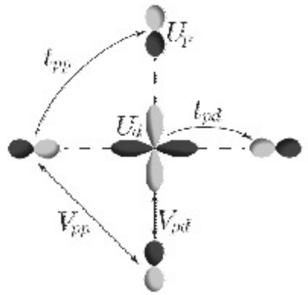

In the CuO_2 plaquettes:

*** 3- band model**

$$H = \sum_{\sigma,<ij>} t_{ij}\left(d^\dagger_{i\sigma}p_{j\sigma} + H.c.\right) + \sum_{\sigma,<jj'>} \bar{t}_{jj'}\left(p^\dagger_{j\sigma}p_{j'\sigma} + H.c.\right) + (\epsilon_d - \mu)\sum_{\sigma,i} n^d_{i\sigma} + (\epsilon_d - \mu)\sum_{\sigma,j} n^p_{j\sigma} + U_{dd}\sum_i n^d_{i\uparrow}n^d_{i\downarrow} + U_{pp}\sum_i n^p_{i\uparrow}n^p_{i\downarrow} + U_{pd}\sum_{\sigma\sigma',<ij>} n^d_{i\sigma}n^p_{j\sigma'}$$

the $O2p^5$ and Cu $3d^9$ orbitals hybridize into the so-called **Zhang-Rice singlet** state

$$J = \frac{4t^4_{pd}}{(E_d - E_p)^3}$$

Effective single band model

*** Hubbard model**

$$H = -\sum_{<i,j>\sigma} t_{ij}c^\dagger_{i\sigma}c_{j\sigma} + U\sum_i n_{i\uparrow}n_{i\downarrow}$$

$$n_{i\sigma} = c^\dagger_{i\sigma}c_{i\sigma},$$

2nd order perturbation theory

$$J = 4t^2/U$$

Effective single band model

*** t-J model**

$$H = P\left[\sum_{<ij>,\sigma} t_{ij}c^\dagger_{i\sigma}c_{j\sigma} + J\sum_{<ij>}\left(\boldsymbol{S}_i\cdot\boldsymbol{S}_j - \frac{1}{4}n_i n_j\right)\right]P.$$

projection operator excludes doubly occupied states

$$\boldsymbol{S}_i = \tfrac{1}{2}c^\dagger_{i\alpha}\boldsymbol{\sigma}_{\alpha\beta}c_{i\beta}$$

Generic phase diagram

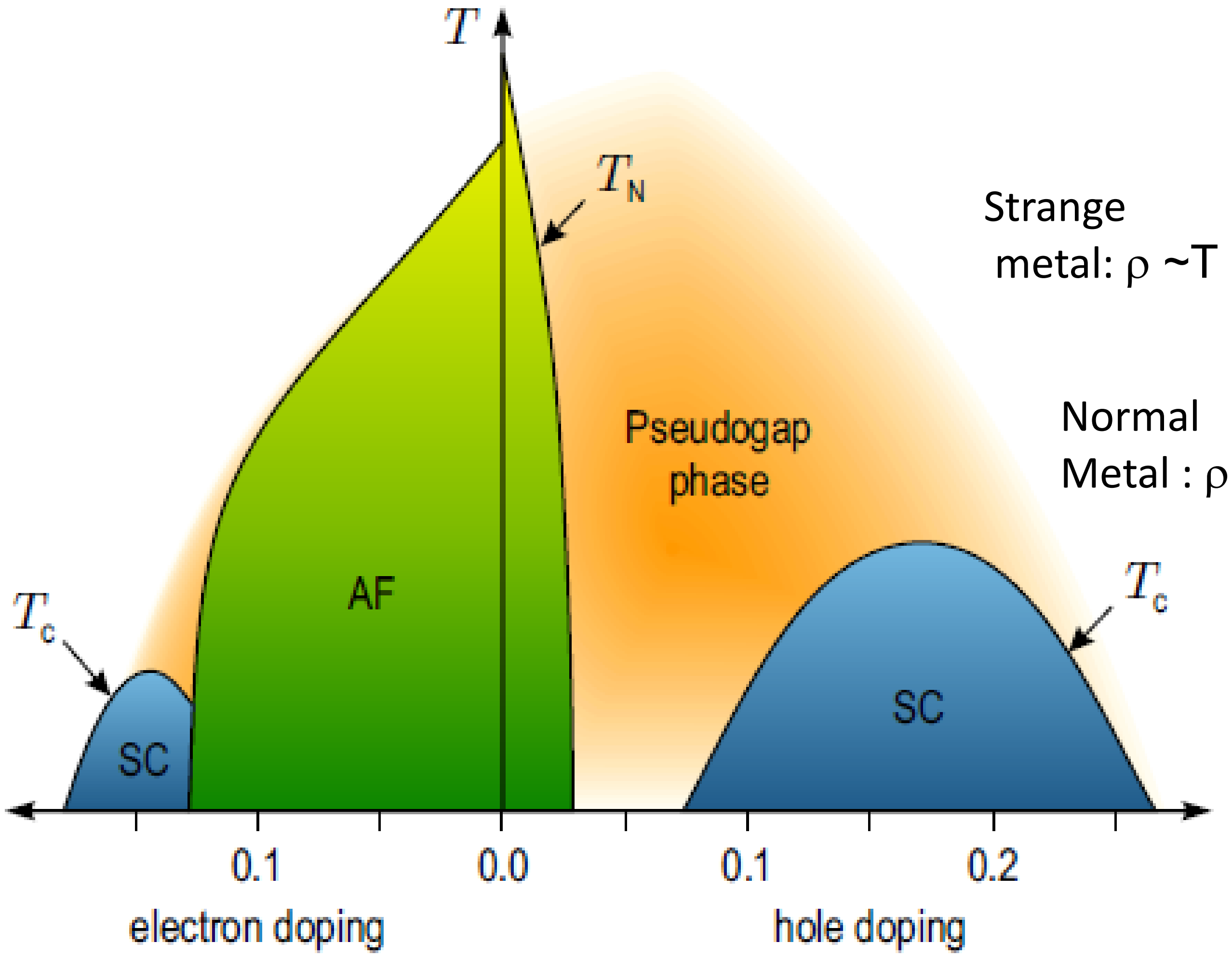

Strange metal: $\rho \sim T$

Normal Metal : $\rho \sim T^2$

Schematic doping phase diagram of electron- and hole- doped High-T_c superconductors, showing:

- The AF phase
- The d-wave SC state
- The so-called pseudogap state

Heisenberg AF state

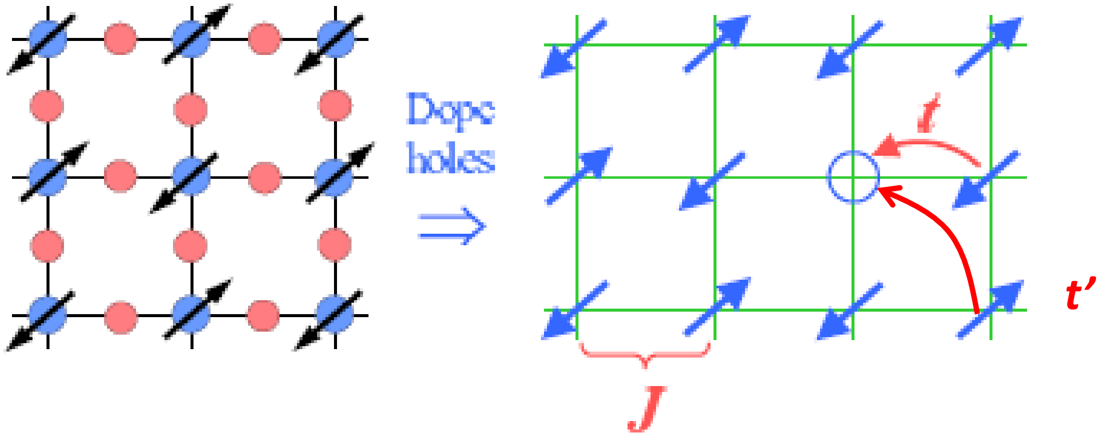

Generic phase diagram

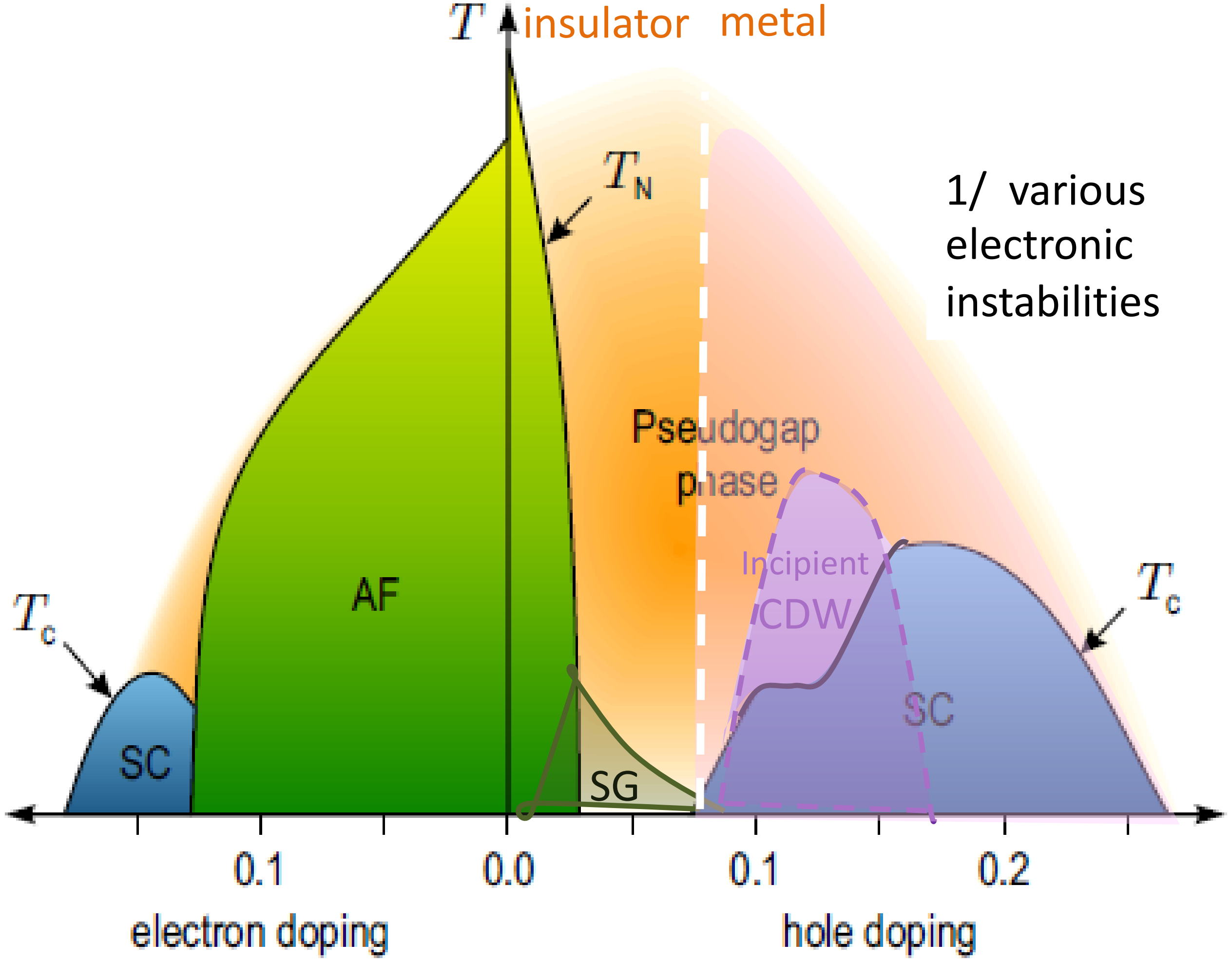

1/ various electronic instabilities

2/ various pictures

crossover

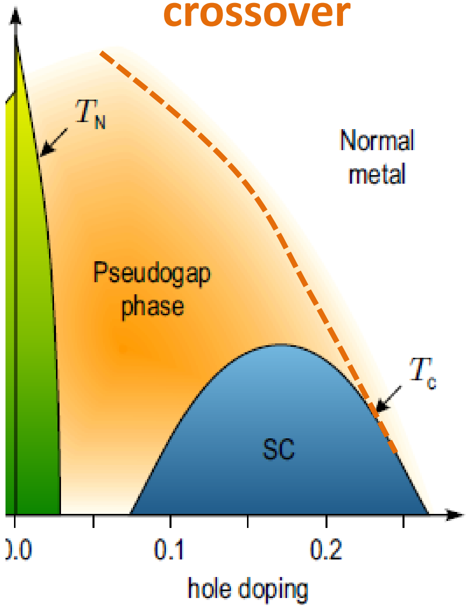

true symmetry breaking state

(i) which ordre parameter?

(ii) role of fluctuations associated with the broken symmetry

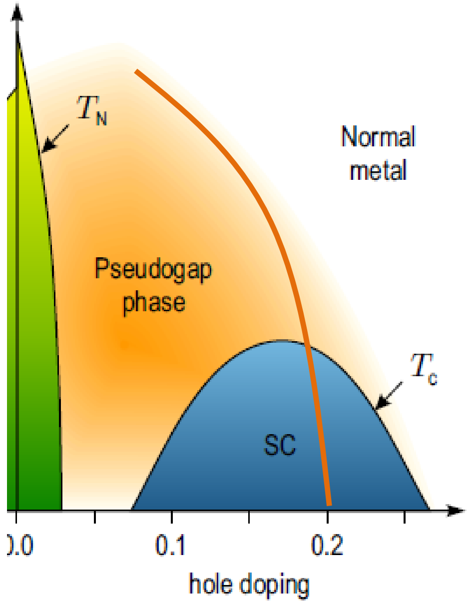

Generic phase diagram – AF spin susceptibility

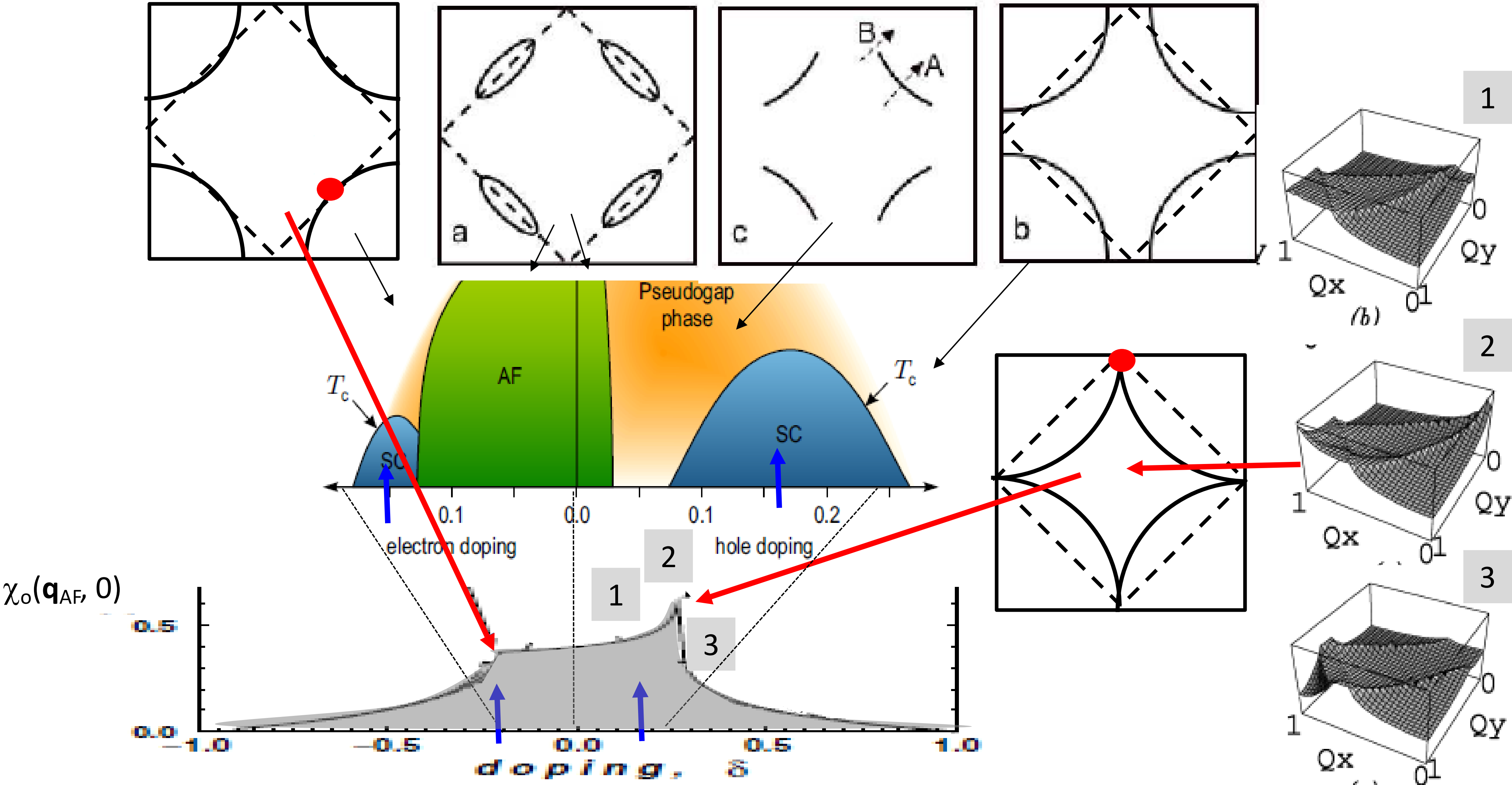

AF state

La_2CuO_4

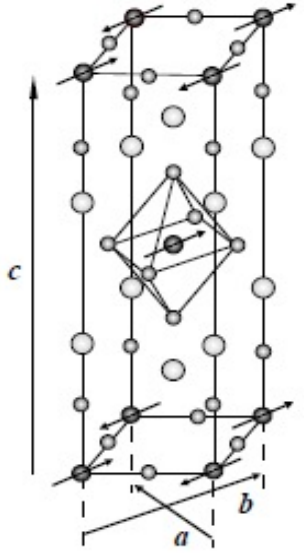

B. Keimer et al, PRB 1992

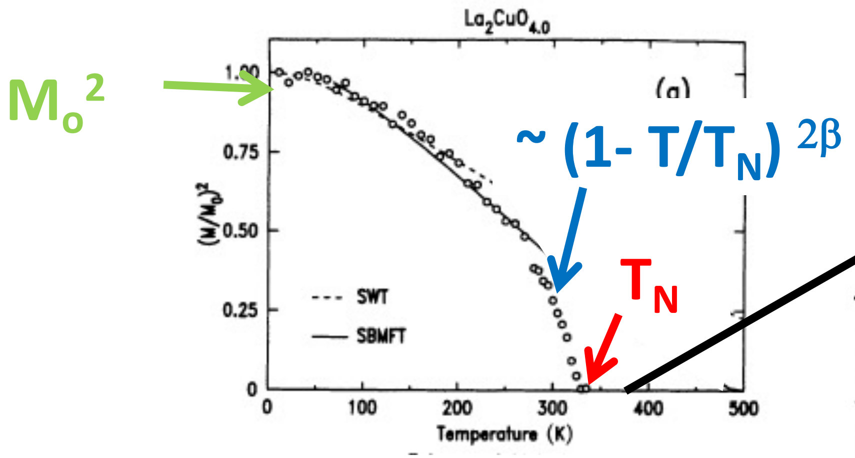

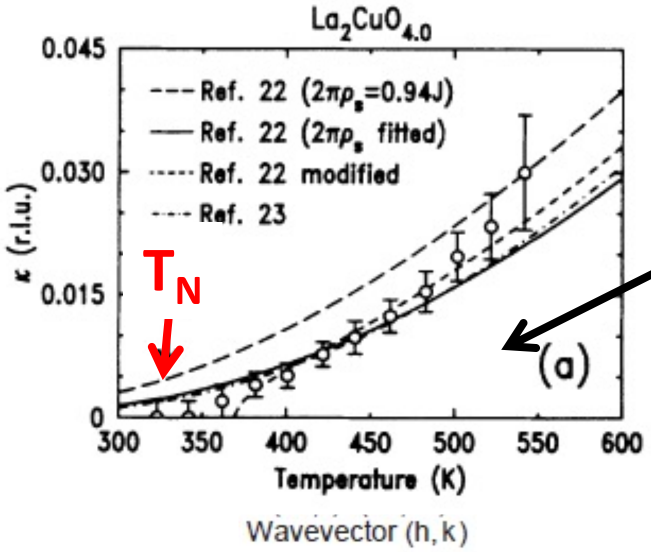

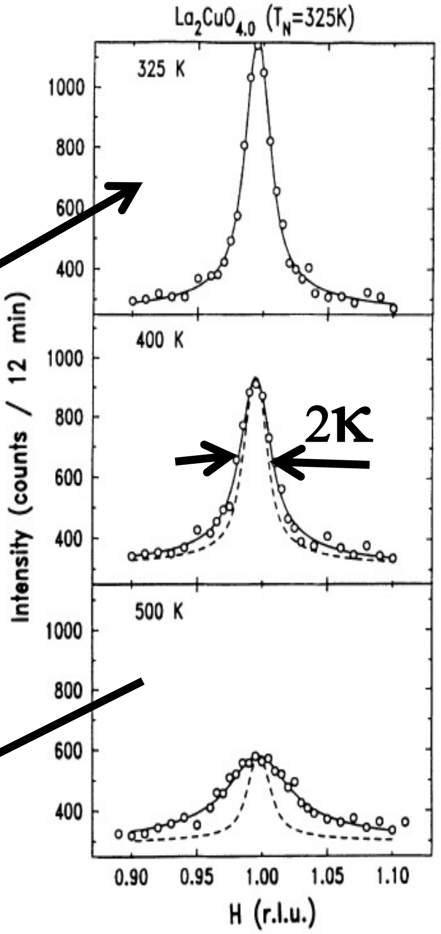

$\kappa^{-1} = \xi$

Correlation length:
S=1/2 Heisenberg AF
(quantum non-linear σ model)

$$\boxed{\xi = 0.24 \frac{c}{2\pi\rho_s} \exp\left[\frac{2\pi\rho_s}{T}\right]}$$

$$c = 850 \text{ meV Å}$$
$$2\pi\rho_s = 0.94J$$
$$J \sim 135 \text{ meV}$$

Chakravarty, Halperin & Nelson, PRB 1989

AF state

$La_{2-x}Sr_xCuO_4$

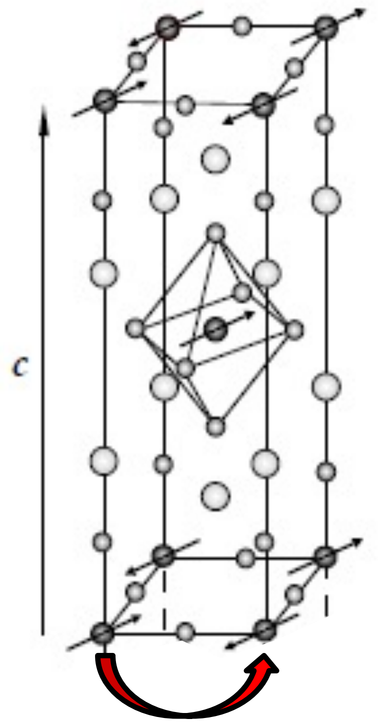

J : super-exchange

$$H = J \sum_{\langle i,j \rangle} \mathbf{S}_i \cdot \mathbf{S}_j$$

Linear spin wave theory

at low energy $\omega = c\, q$

$$c = \sqrt{8} S Z_c J a/\hbar,$$

$$Z_c \approx 1.18$$

Compound	T_N (K)	m_{Cu} (μ_B)	J (meV)	Crystal Symmetry	Layers per cell	Refs.
La_2CuO_4	325(2)	0.60(5)	146(4)	O	1	[65, 64, 68]
$Sr_2CuO_2Cl_2$	256(2)	0.34(4)	125(6)	T	1	[69, 70, 71]
$Ca_2CuO_2Cl_2$	247(5)	0.25(10)		T	1	[72]
Nd_2CuO_4	276(1)	0.46(5)	155(3)	T	1	[73, 74, 75, 76]
Pr_2CuO_4	284(1)	0.40(2)	130(13)	T	1	[77, 73]
$YBa_2Cu_3O_{6.1}$	410(1)	0.55(3)	106(7)	T	2	[78, 32]
$TlBa_2YCu_2O_7$	> 350	0.52(8)		T	2	[79]
$Ca_{0.85}Sr_{0.15}CuO_2$	537(5)	0.51(5)		T	∞	[80]

corrections (ring exchange)

super-exchange

anisotropy gap

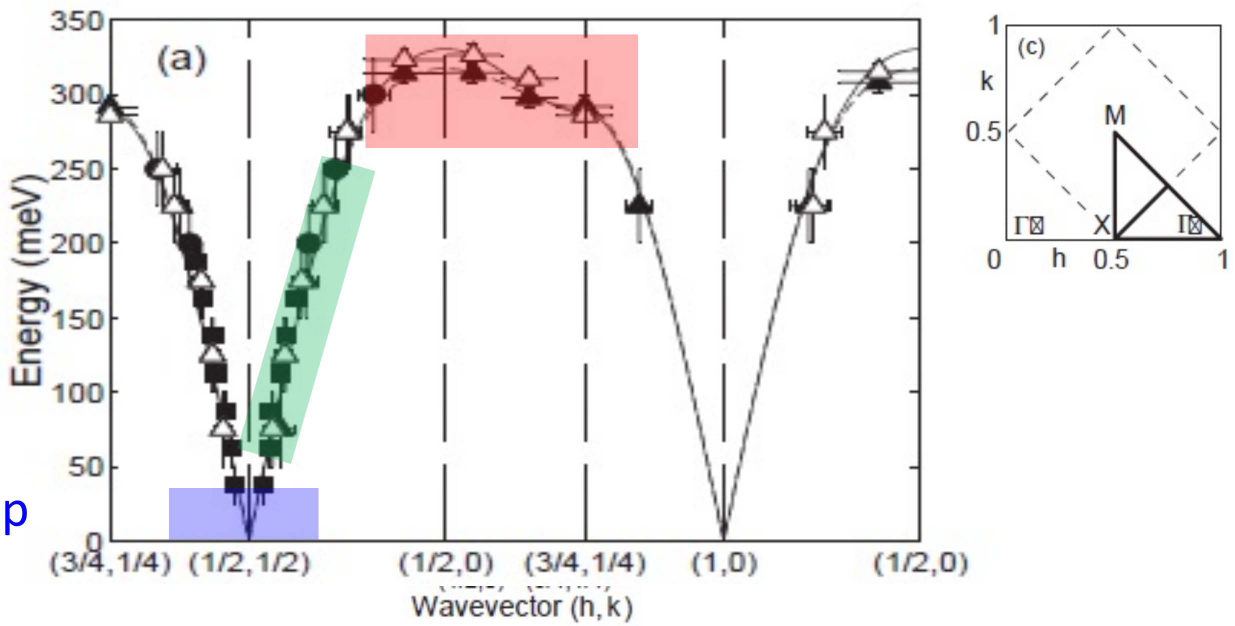

R. Coldea et al., PRL 2001
N. S Headings et al., PRL 2010

Lightly doped state

$La_{2-x}Sr_xCuO_4$ (p<0.05)

* <u>perturbation:</u>
Magnetic correlation lengths are blocked by doped holes:

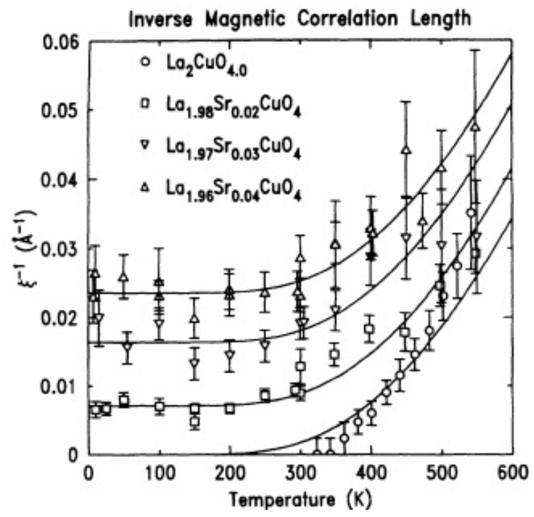

$$\frac{1}{\xi(x,T)} = \frac{1}{\xi(x,0)} + \frac{1}{\xi(0,T)},$$

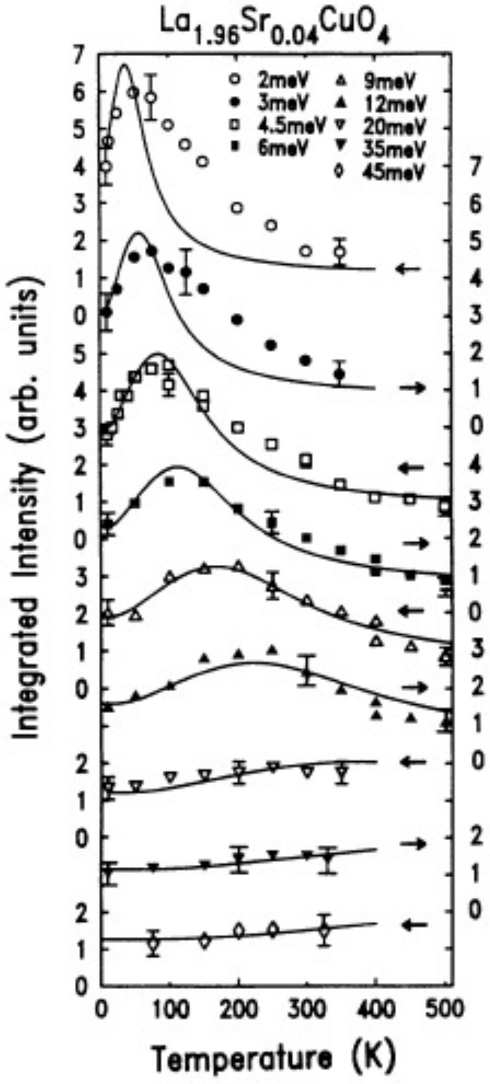

* <u>perturbation:</u>
Low energy spin fluctation do not look like damped spin wave, but display a singular ω/T sacling behavior

$$\int d^2Q\chi''(\mathbf{Q},\omega) = I(|\omega|,0)\arctan\left[a_1\frac{\omega}{T}+a_3\left[\frac{\omega}{T}\right]^3\right].$$

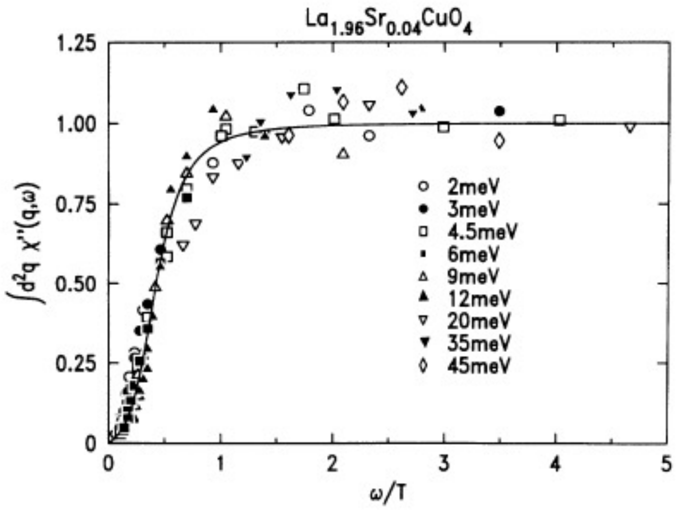

B. Keimer et al., PRL 1992

S. Sachdev et al., PRL 1992
A. Chubukov et al., PRB 1994

Lightly doped state

* <u>perturbation:</u> Doped holes frustate the AF correlations and modify the spin texture
The AF ground state is destroyed

(i) charge segregation

(ii) twisted spin texture

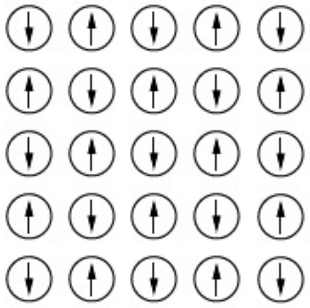

diagonal stripes

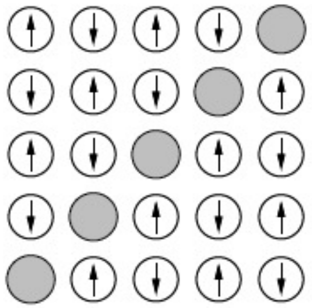

Vertical stripes

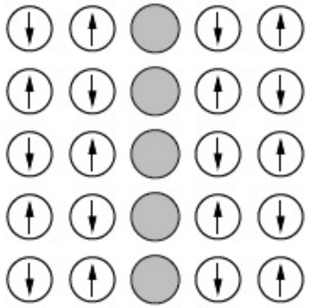

Spiral AF state

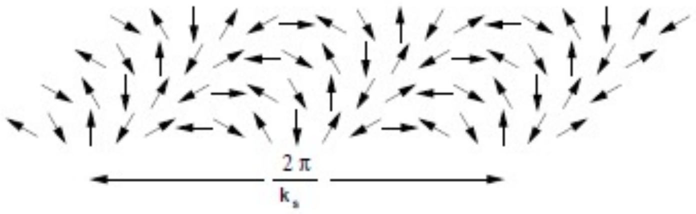

H

0.5

AF

K

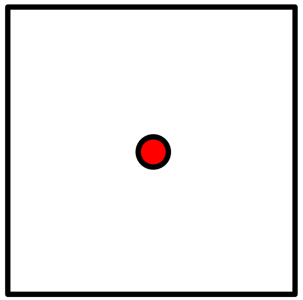

0.5

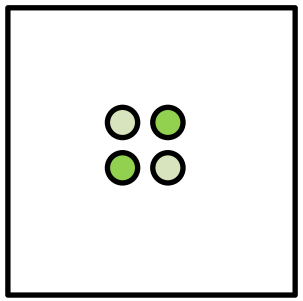

Incommensurate
spin response

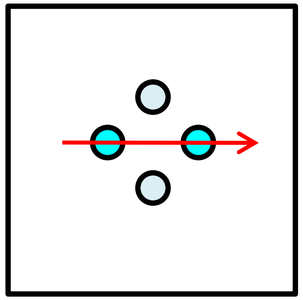

Lightly doped state: spin glass state & nematicity

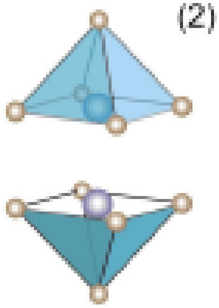

$YBa_2Cu_3O_{6.45}$
($p=0.08$ $T_c=35$ K)

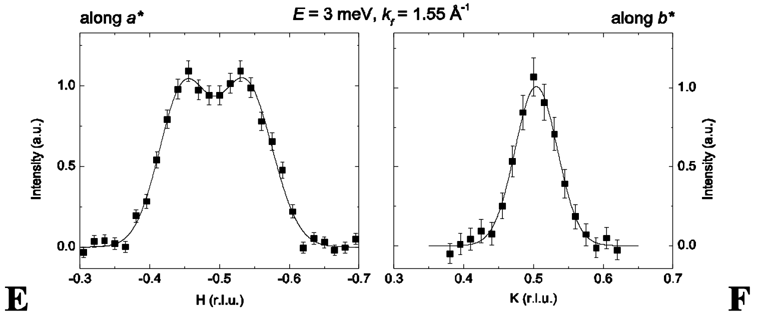

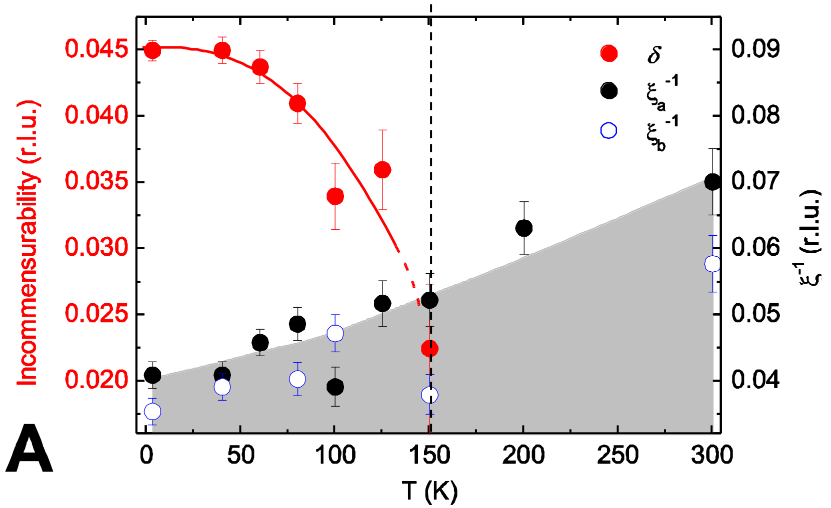

Spontaneous onset of
incommensurability at ~150 K

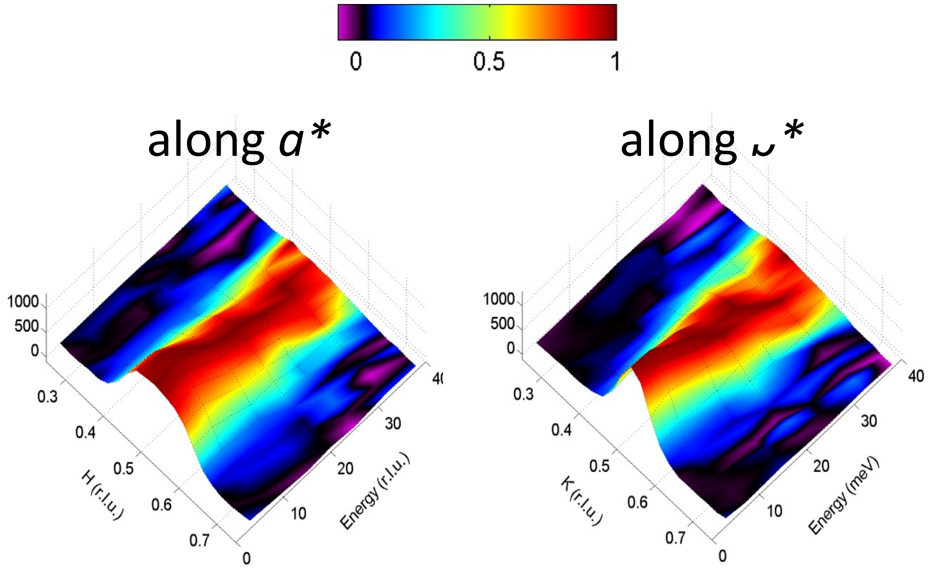

ω /T scaling

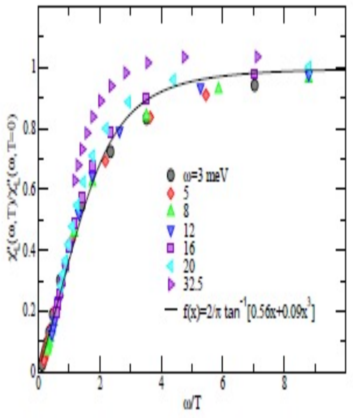

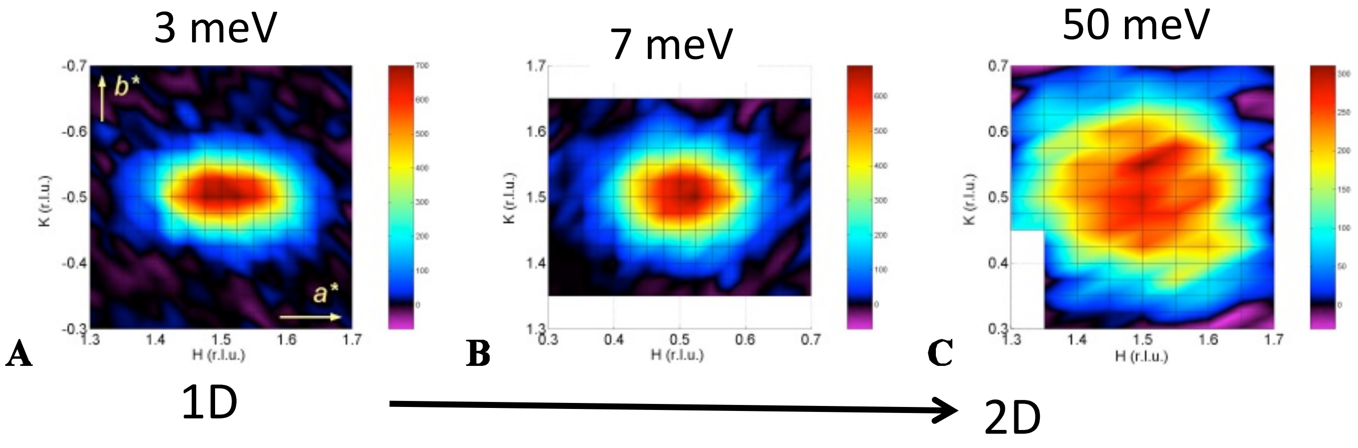

V. Hinkov et al., Science 2008
V. Hinkov et al, PHD 2008

Spin dynamics in $YBa_2Cu_3O_{6+x}$
($x = 0.6$ $p \sim 0.12$ $T_c = 63$ K)

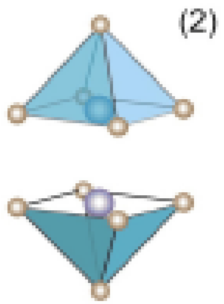

P. Dai et al., PRL 1996

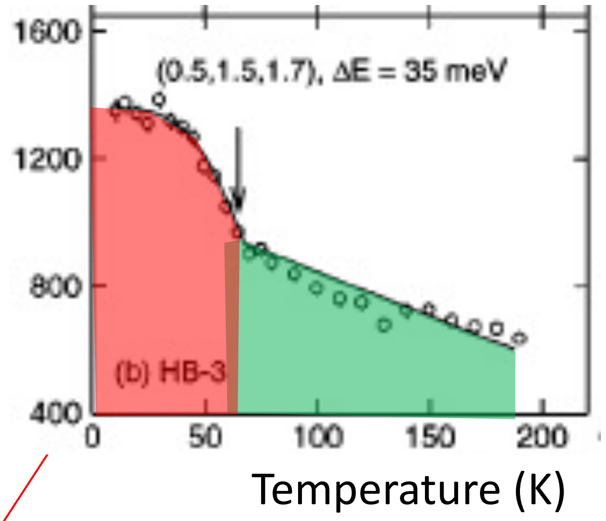

P. Dai et al., Science 1999
H.F. Fong et al., PRB 2000
C. Stock et al., PRB 2005

Resonance peak
$E_r \sim 5\, k_B T_c$

Spin gap for p>0.09

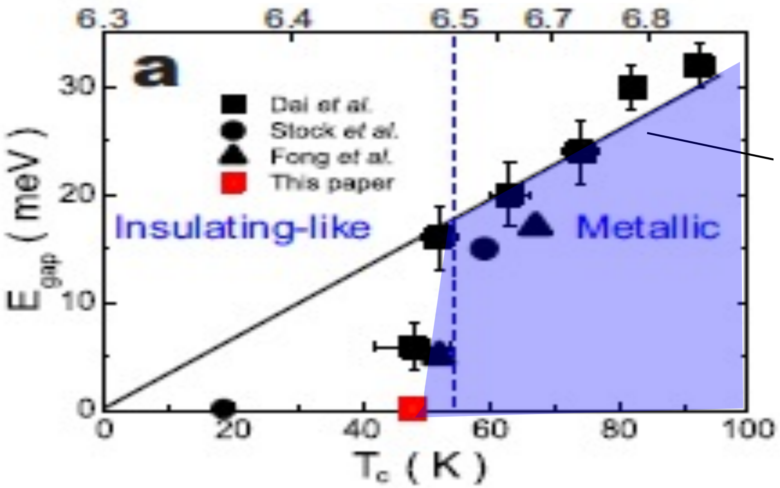

Spin gap

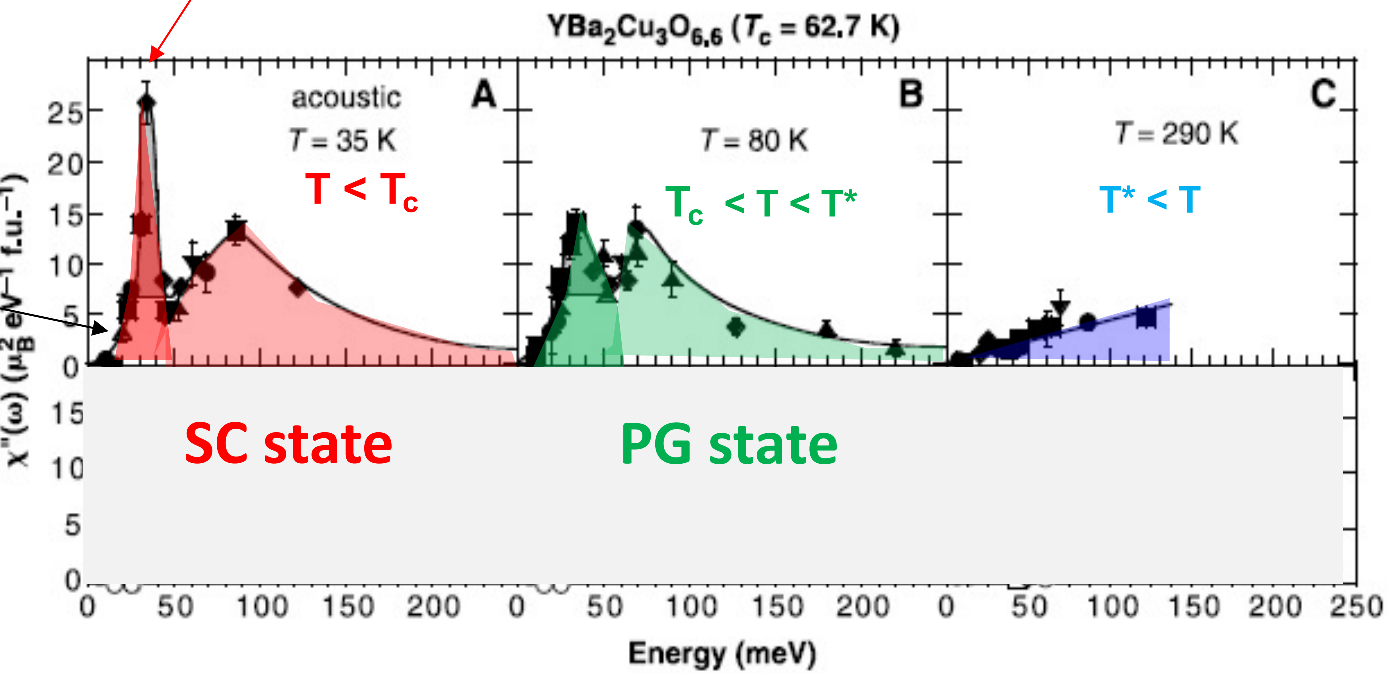

J. Rossat-Mignot et al., Physica B 1992
Li et al., PRB 2008

X-Y Dispersion in $YBa_2Cu_3O_{6+x}$
($x = 0.6$ $p \sim 0.12$ $T_c = 63$ K)

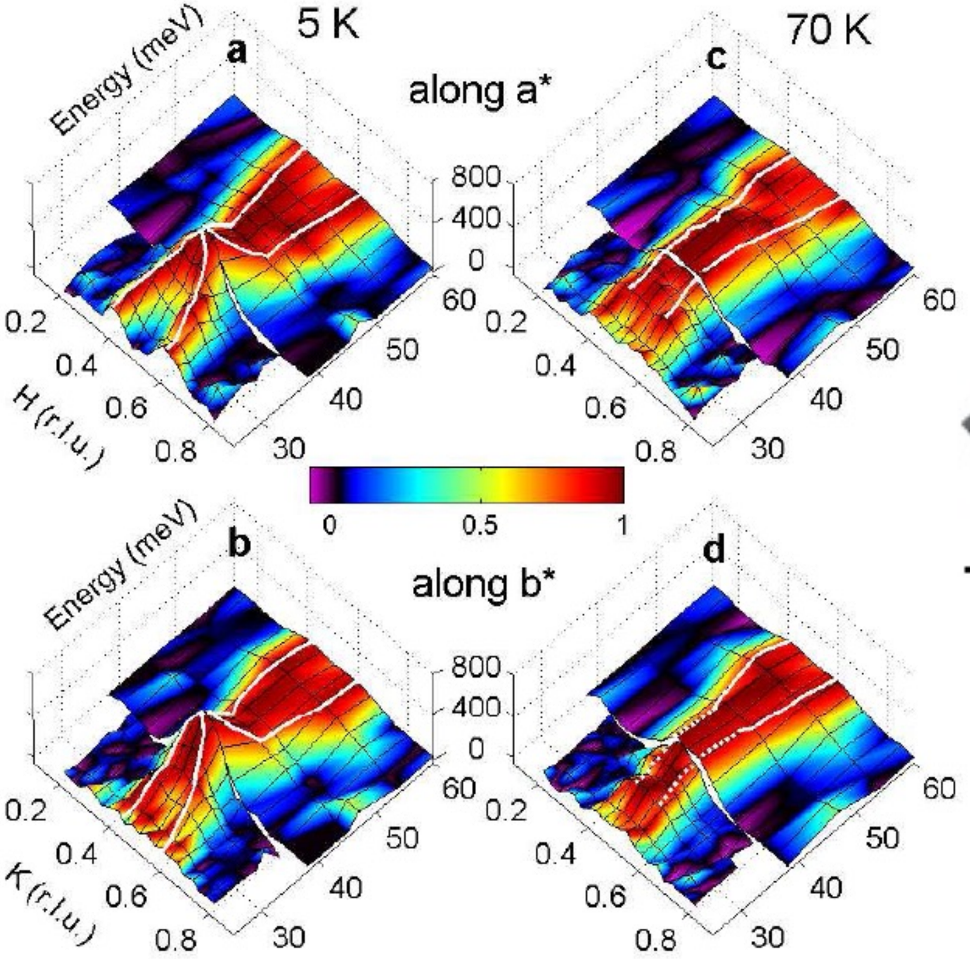

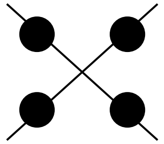

High energy
2D

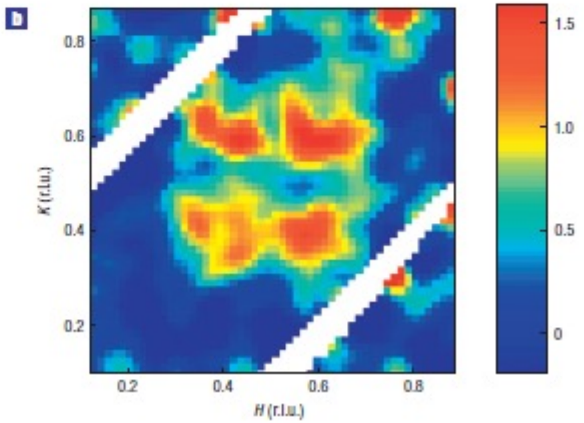

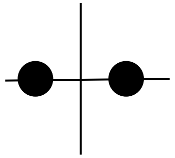

low energy
Quasi-1D

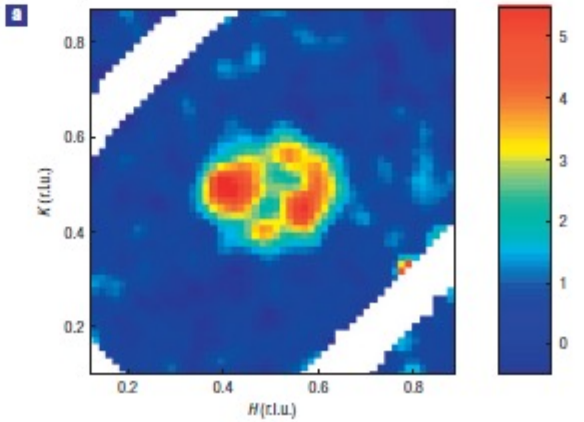

V. Hinkov et al., Nat.Phys. 2007
S. Hayden et al., Nature 2004

YBCO:Zn : Comparison between INS and $1/T_1T$ NMR

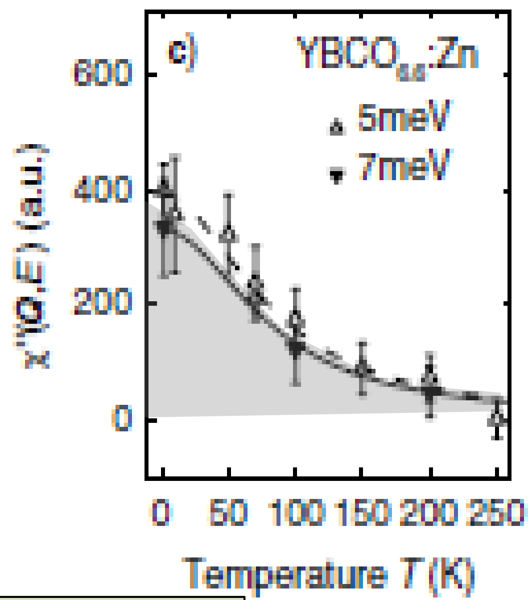

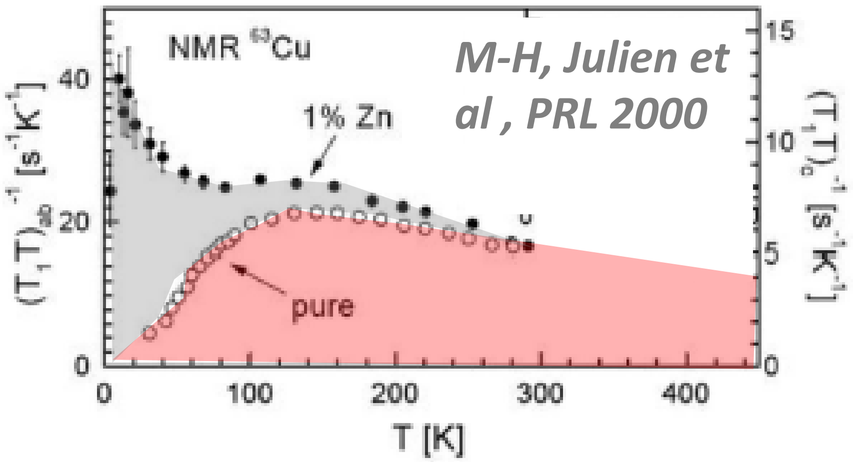

M-H, Julien et al , PRL 2000

nucleation around a point defect

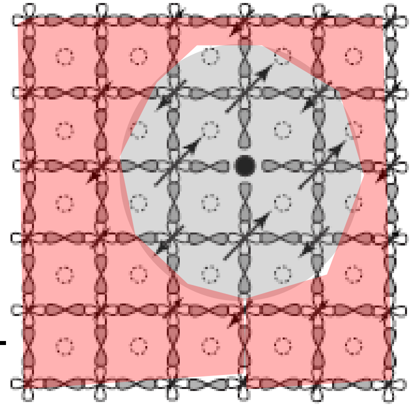

V. Hinkov et al , Nat. Phys. 2007

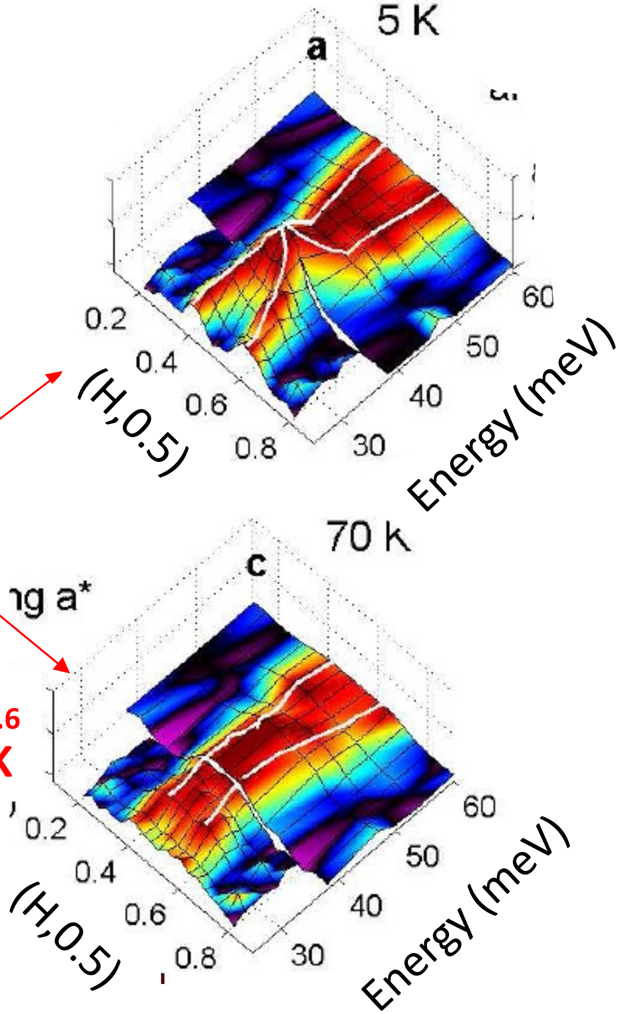

$YBCO_{6.6}$:Zn
T_c=30 K

Non magnetic impuruity that reduces Tc songly and introduces a finite DOS at the fermi level

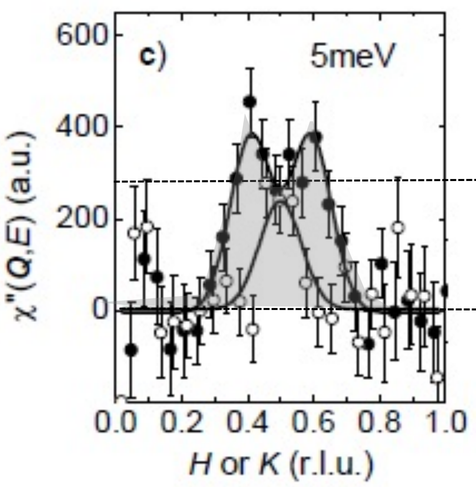

A. Suchaneck et al , PRL 2010

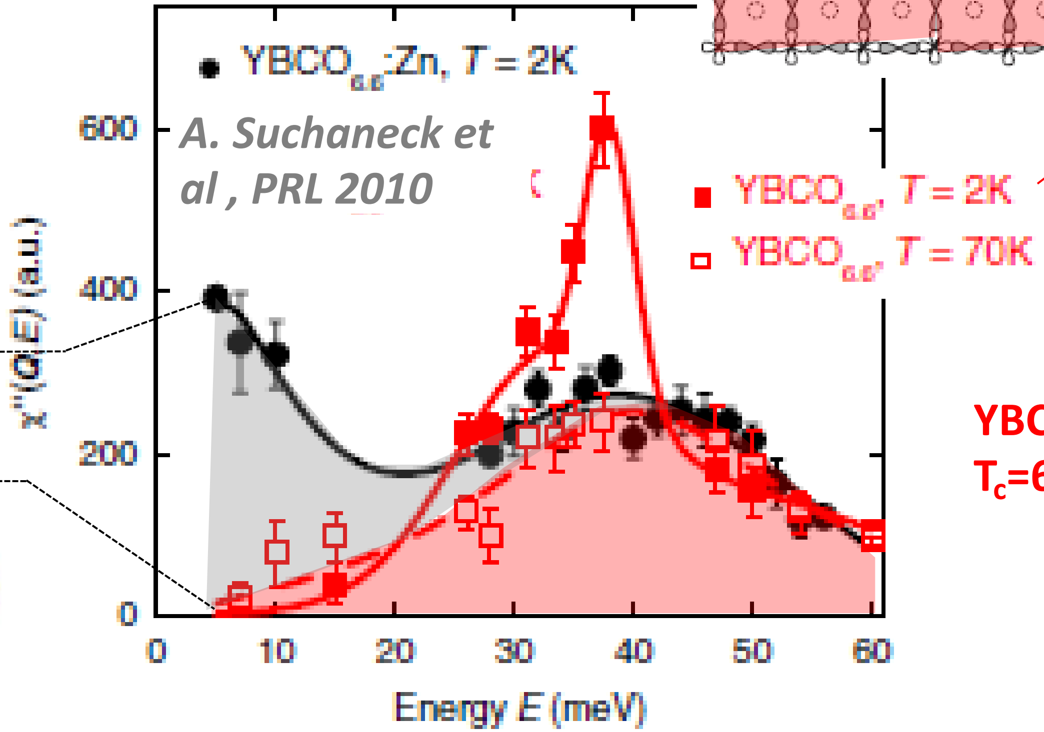

$YBCO_{6.6}$
T_c=63 K

Dispersion of AF spin fluctuations

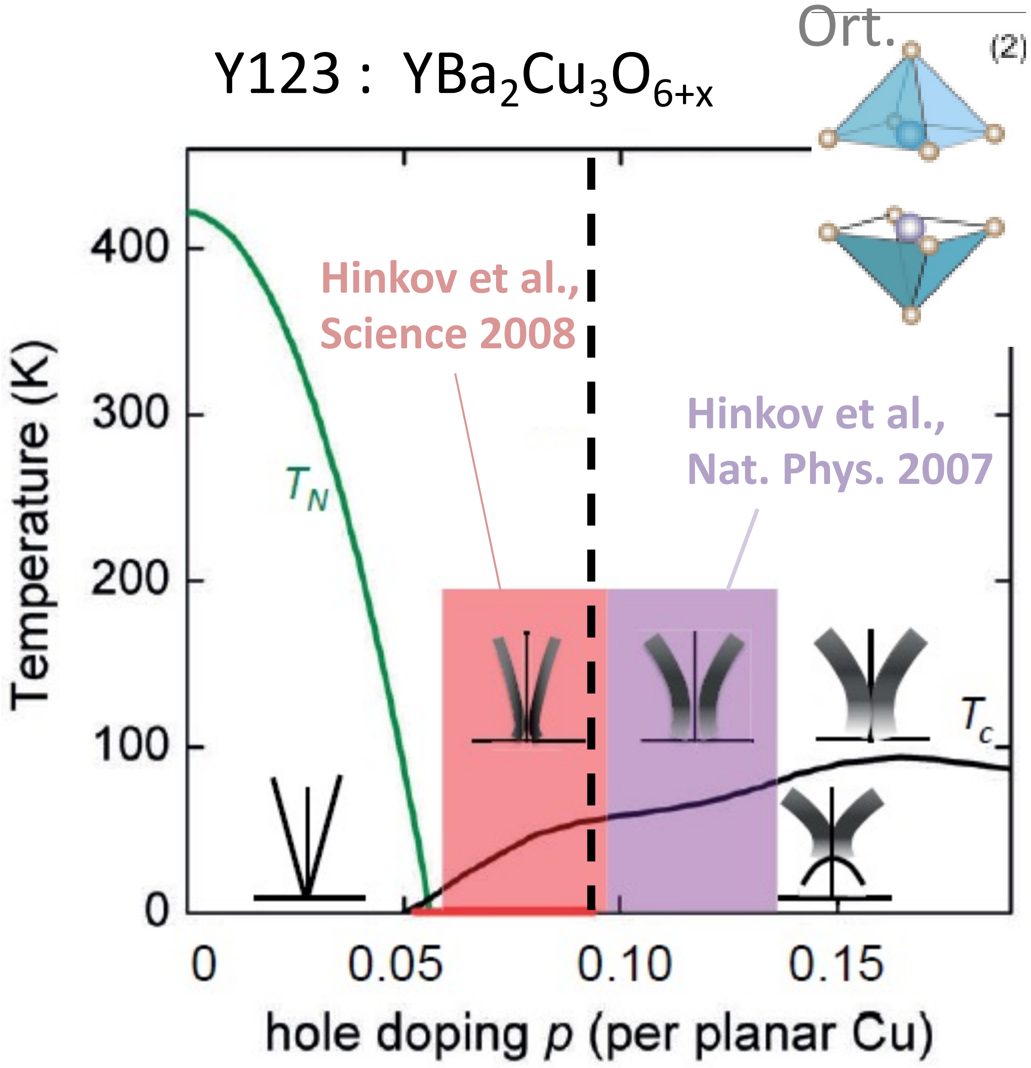

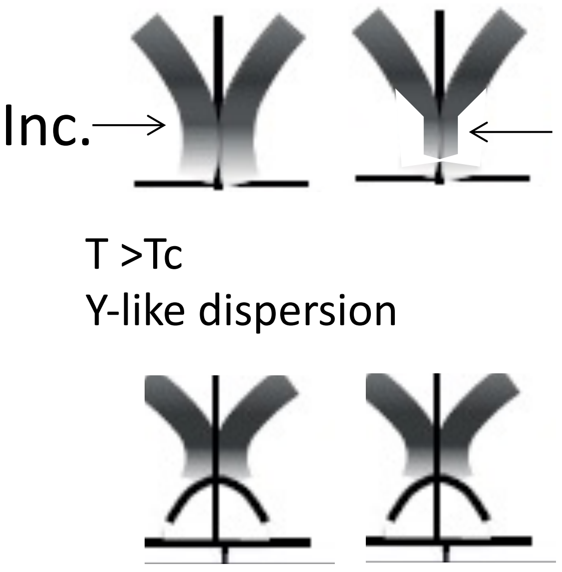

T >Tc

Y-like dispersion

T <Tc

X-like dispersion

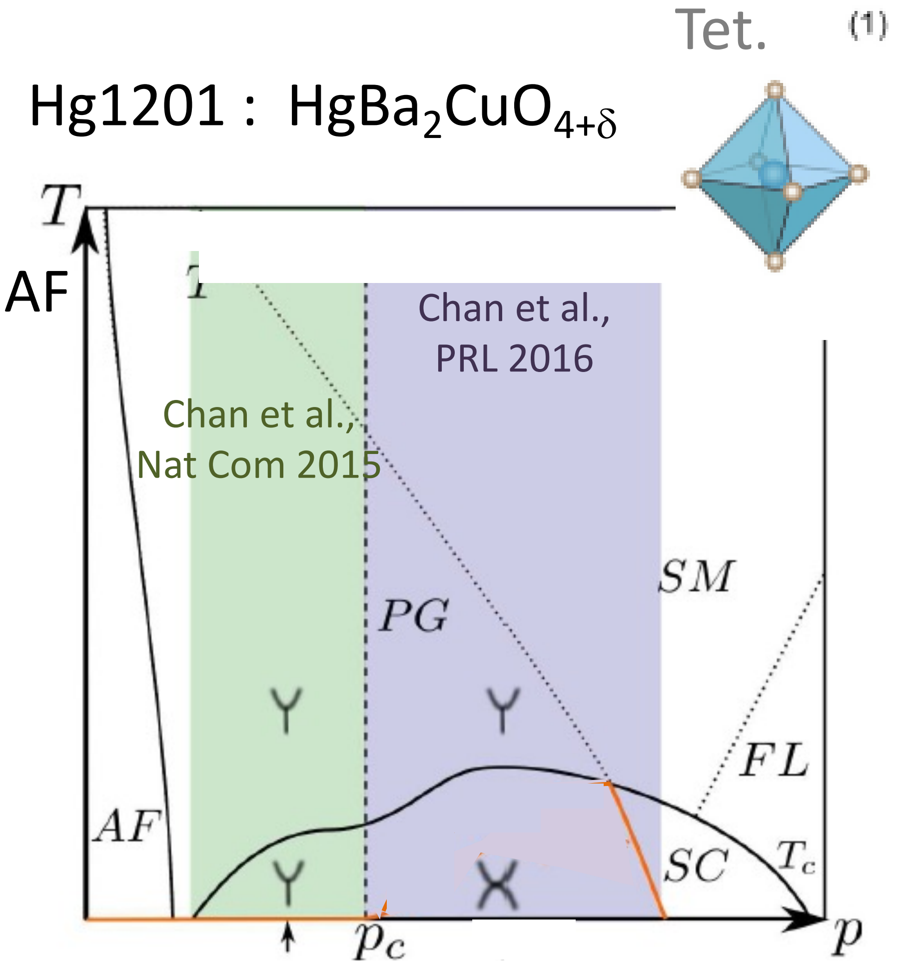

Keimer, Recent Advances in Experimental Research on High-Temperature Superconductivity in Emergent phenomena in Correlated Matter Modeling and Simulation, 2013, Vol. 3, p. 91.

Commensurate AF excitations as a signature of the PG state in Hg1201

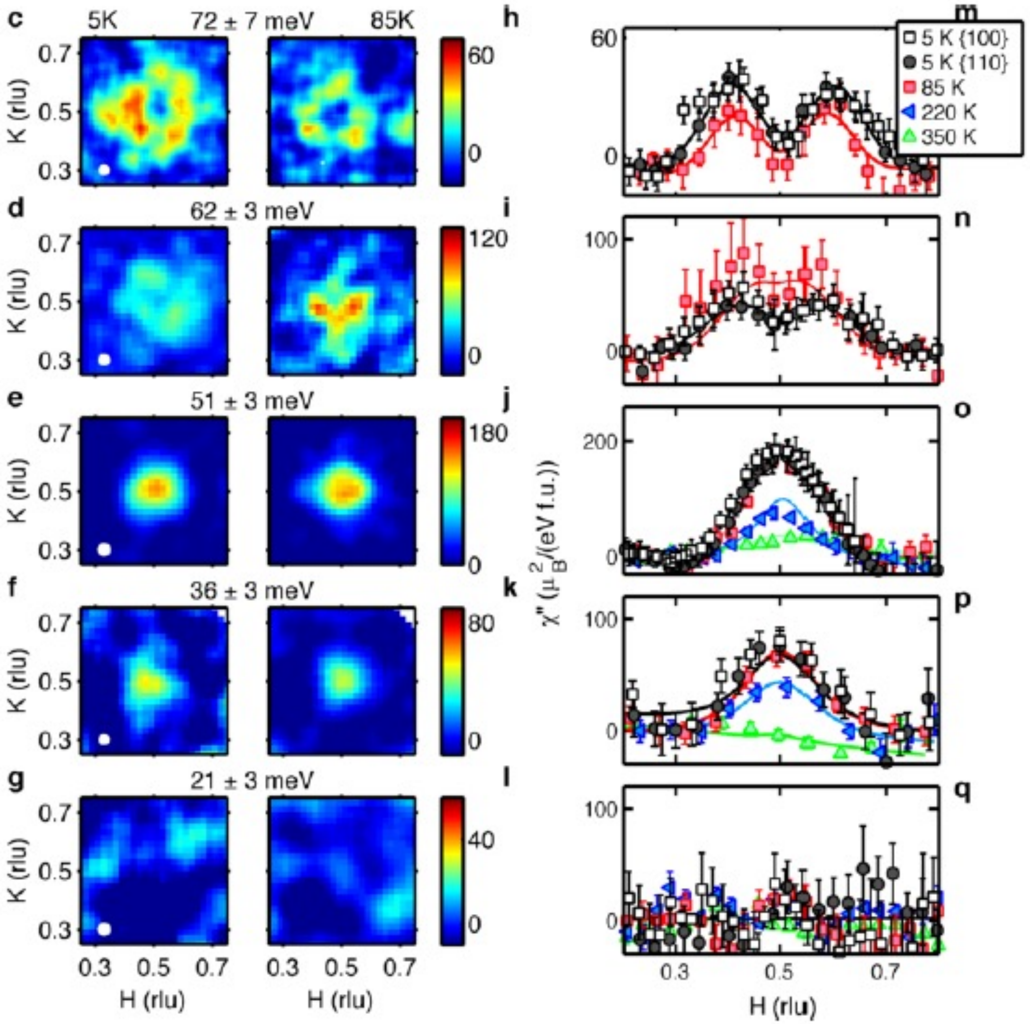

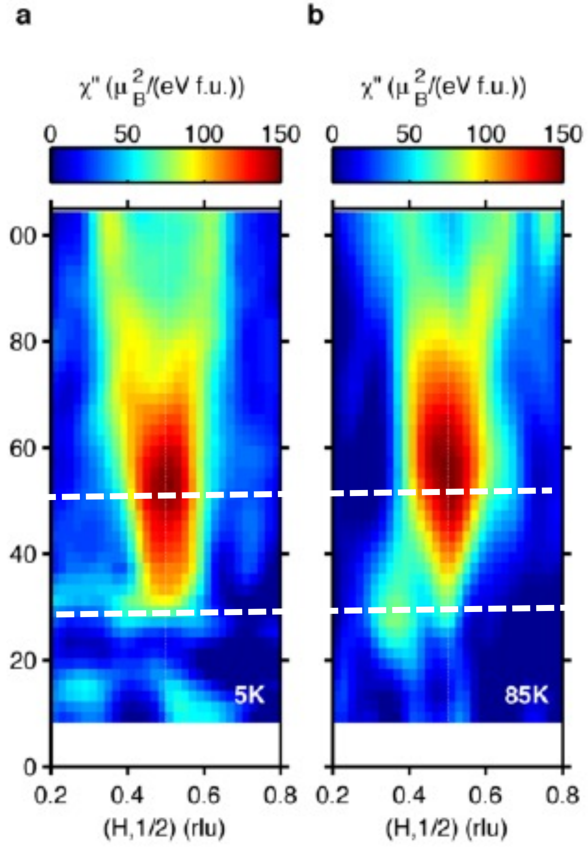

PG state & SC

(T<T*)

Max

51 meV

Gap

24 meV

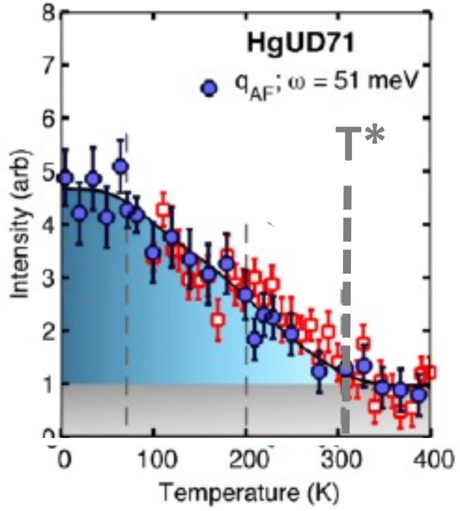

HgUD71 (T_c=71 K)

M.K. Chan et al, Nat. Com. 2015

HgUD88 – X-Y dispersion of magnetic excitations

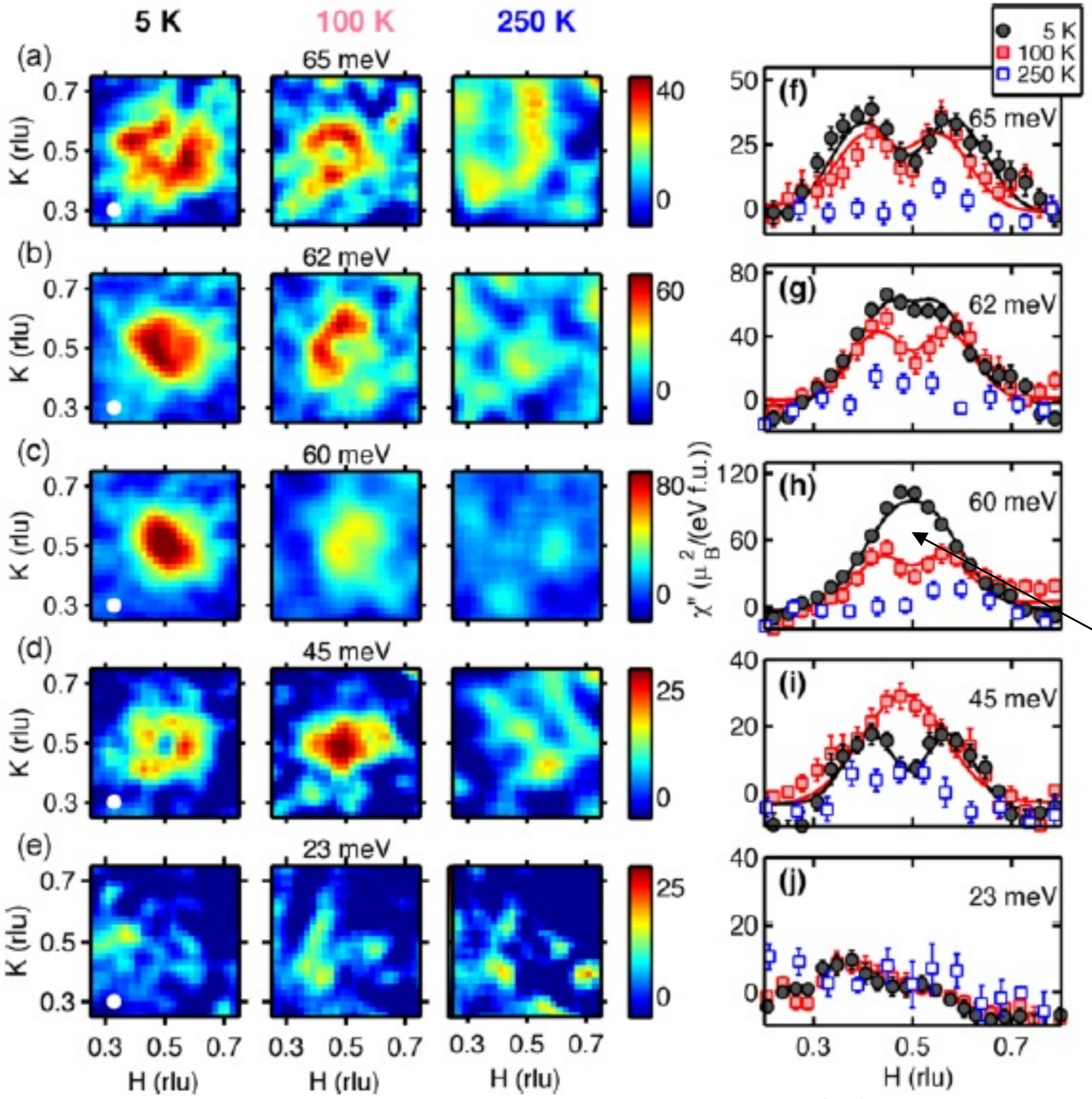

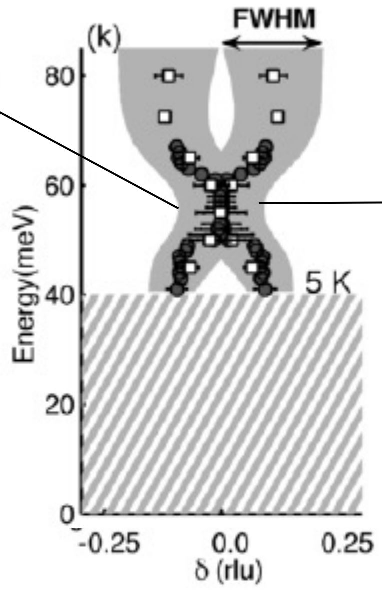

SC state

(T<T_c)

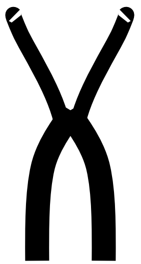

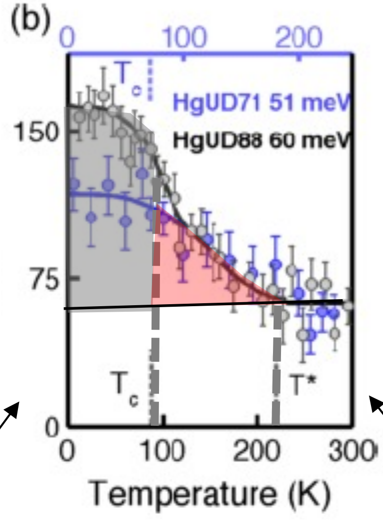

Magnetic resonance peak at Q_{AF}

ω_r=59(1) meV

$\Delta\omega$=5meV (FWHM)

spin gap ~30 meV

PG state

(T_c<T<T*)

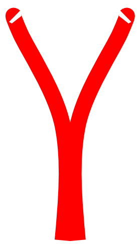

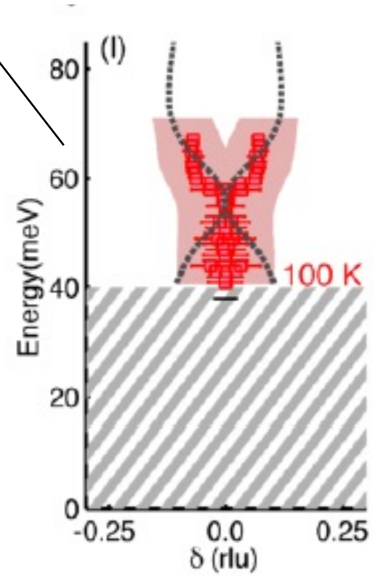

HgUD88 (T_c=88 K, T*~220 K)

SC coherence : Electronic Raman Scattering

ERS –B_{1g} : SC coherence effect at antinodes

ERS –B_{2g} : SC coherence effects at nodes

Hg1201 : $HgBa_2CuO_{4+\delta}$

HgUD71 p~0.09

HgUD88 p~0,13

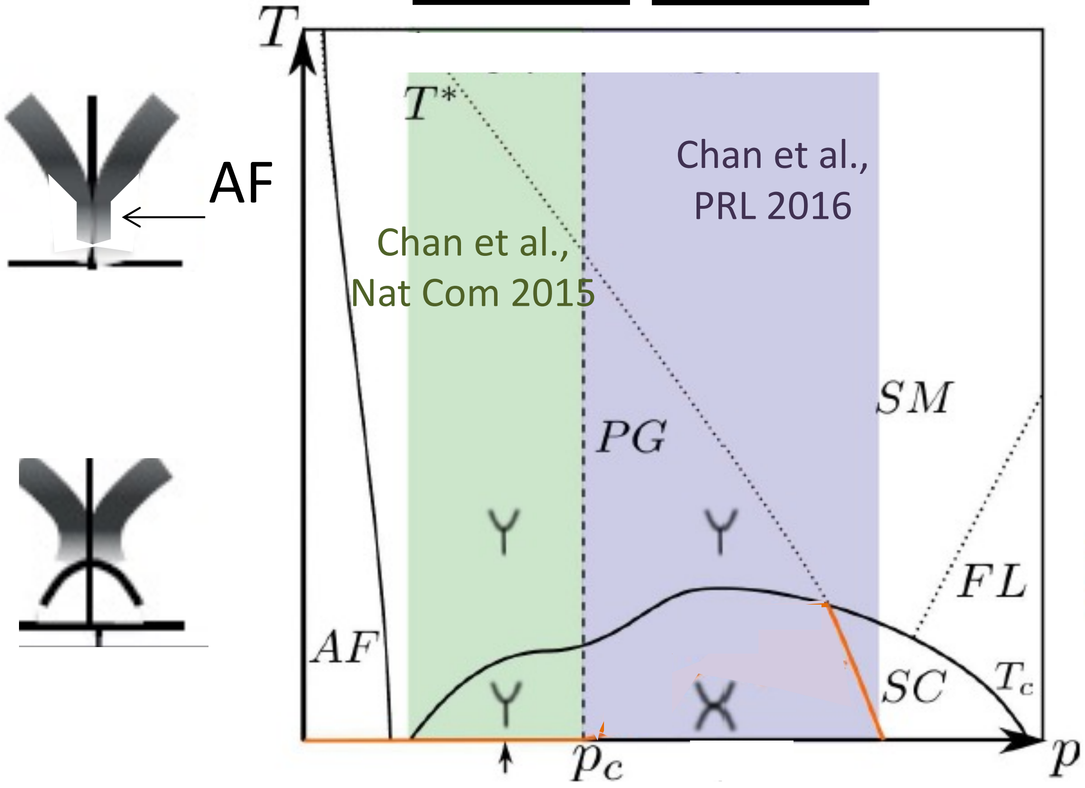

HgUD71 p~0.09

HgUD88 p~0,13

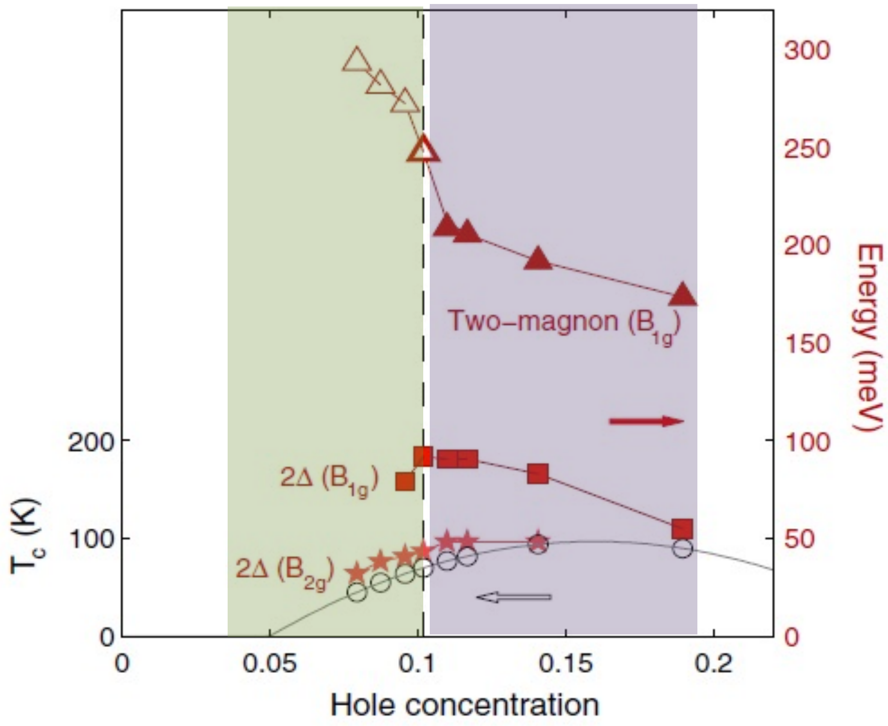

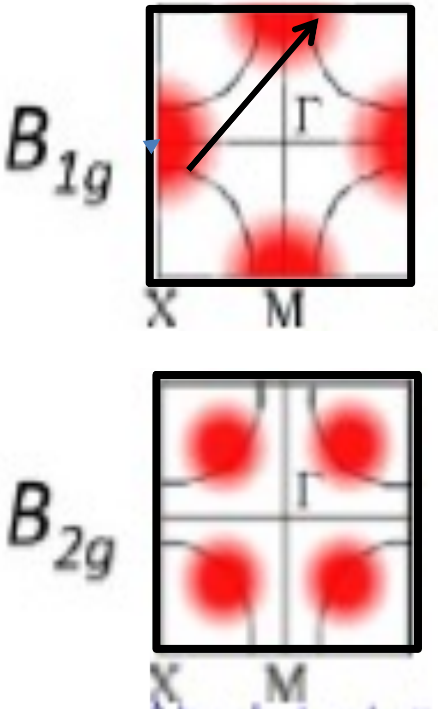

Y. Li et al., PRL 2013

Underlying nematicity

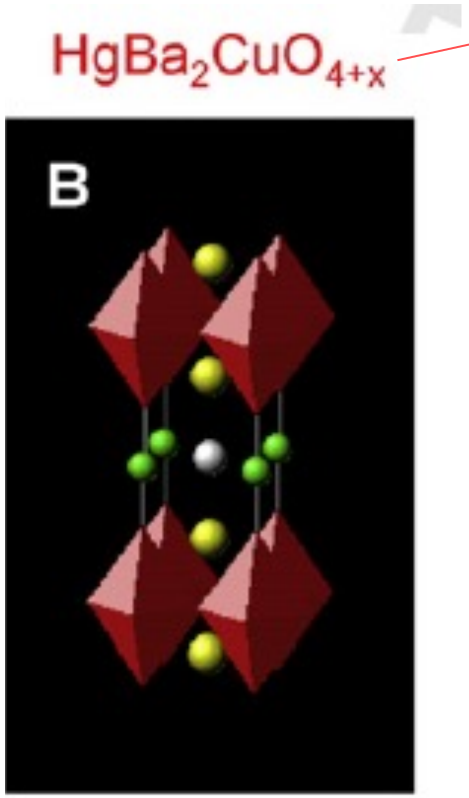

no spontaneous nematic order, but a large χ_{nem}

A natural disturbance of the tetragonal symmetry is provided by the *CuO chains*

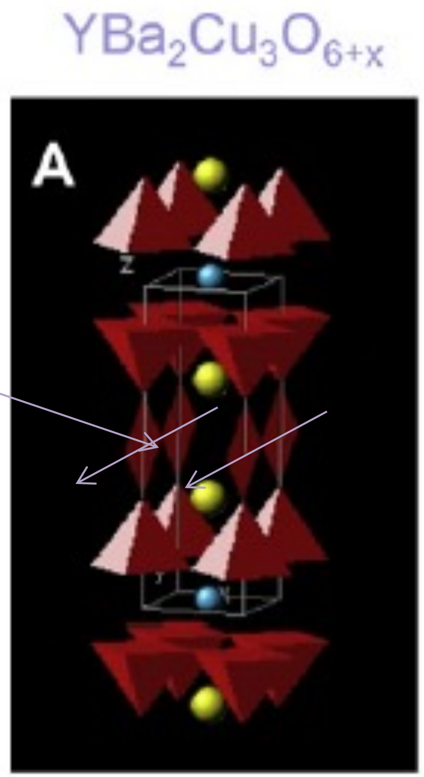

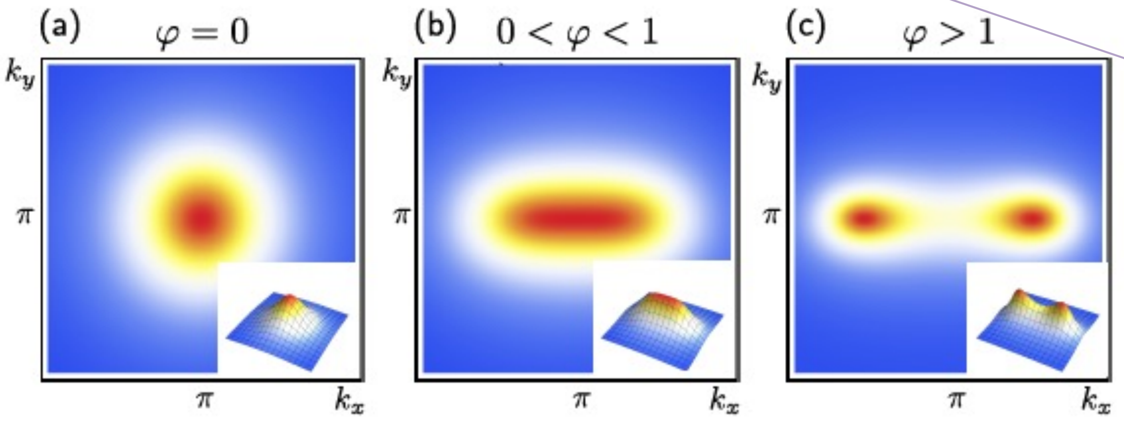

Incommensurate transition induced by an induced nematic order φ on the inelastic neutron scattering cross-section :

$$\chi_{\mathrm{AFM}}\left(\mathbf{Q}+\mathbf{q},\omega\right)=\frac{1}{\xi^{-2}+\mathbf{q}^2-\varphi\left(q_x^2-q_y^2\right)+f\left(\omega_n\right)}$$

Orth et al., arXiv: 1703.02210

Magnetic resonance peak

Generic feature observed in almost all cuprates

Bi2212 (Tc=91 K - Bilayer)
H.F. Fong et al, Nature 1999
G. Xu et al, Nat. Phys. 2009
Tl2201 (Tc=90 K – Mono-layer)
H. He et al, Science 2002
Bi2223 (Tc=110 K – Tri Layer)
S. Bayrakci et al, unpublished 2003
Hg1201 (Tc=95 K – monlayer)
G. Yu et al, PRB 2010
PLCCO (Tc=24 K - monlayer)
S. D. Wilson et al, Nature 2006
NCCO (Tc=25 K - monolayer)
G. Yu et al, PRB 2012

Universal excitation in unconventional superconductors
review : Y. Yu et al, Nat. Phys. 2009

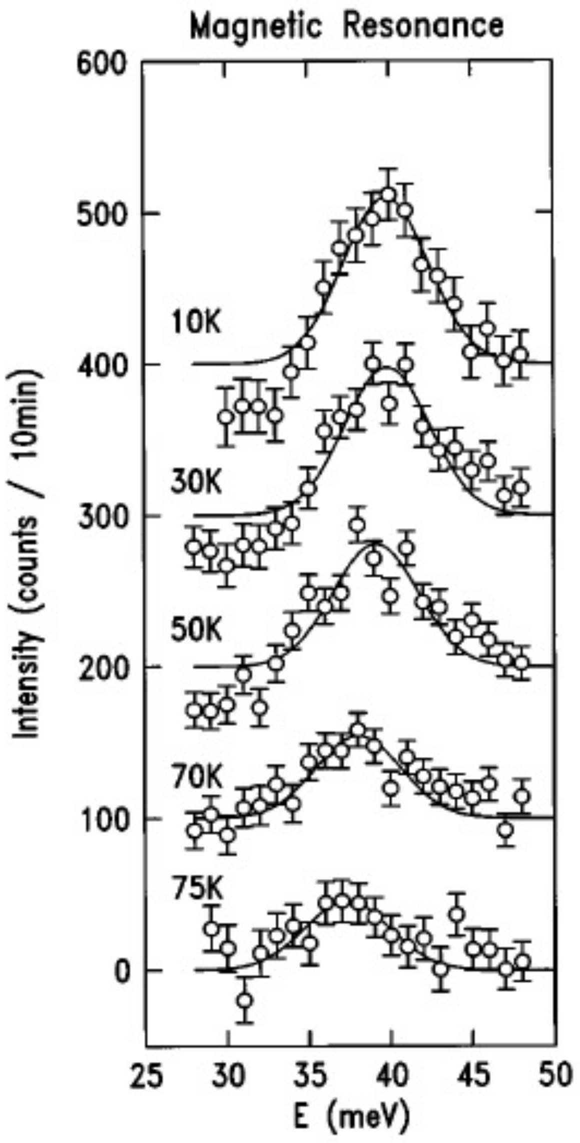

$YBa_2Cu_3O_{7-\delta}$
(p ~ 0.16 T_c=92.7 K)

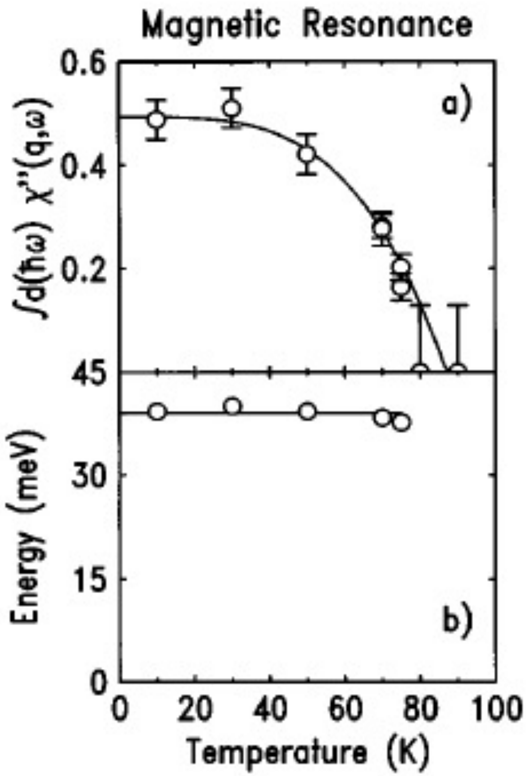

J. Rossat-Mignot et al., Physica C 1991
P. Bourges et al, PRB 1996
H.F. Fong et al, , PRB 1996
N. S. Headings et al, PRB 2011

The spin exciton scenario

Dispersion in $YBa_2Cu_3O_{6+x}$
($x = 0.85$ $p \sim 0.15$ $T_c = 89$ K)

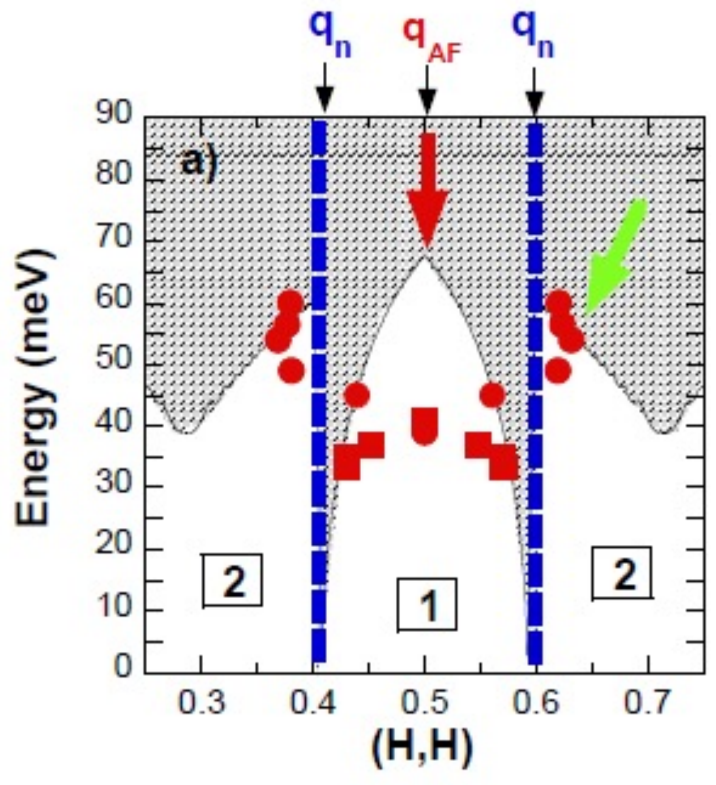

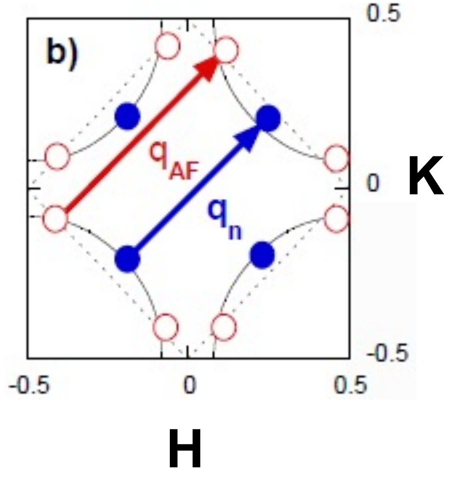

S=1 collective mode below the Stoner continuum in the SC state

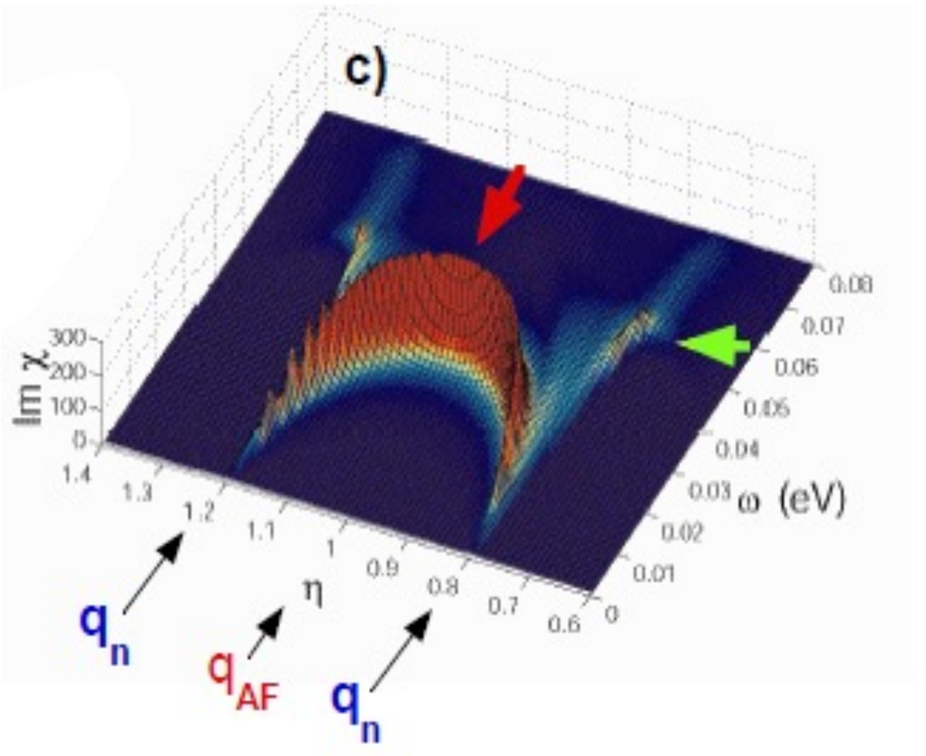

P. Bourges et al, Science 2000
S. Pailhès et al, PRL 2004
D. Reznik et al, PRL 2004

A. Chubukov et al, PRB 2001
F. Onufrieva et al., PRB 2002
I. Eremin et al, PRL 2005

Spin-fermion coupling: the feedback effect

review :
M. Eschrig, Advances in physics 2006

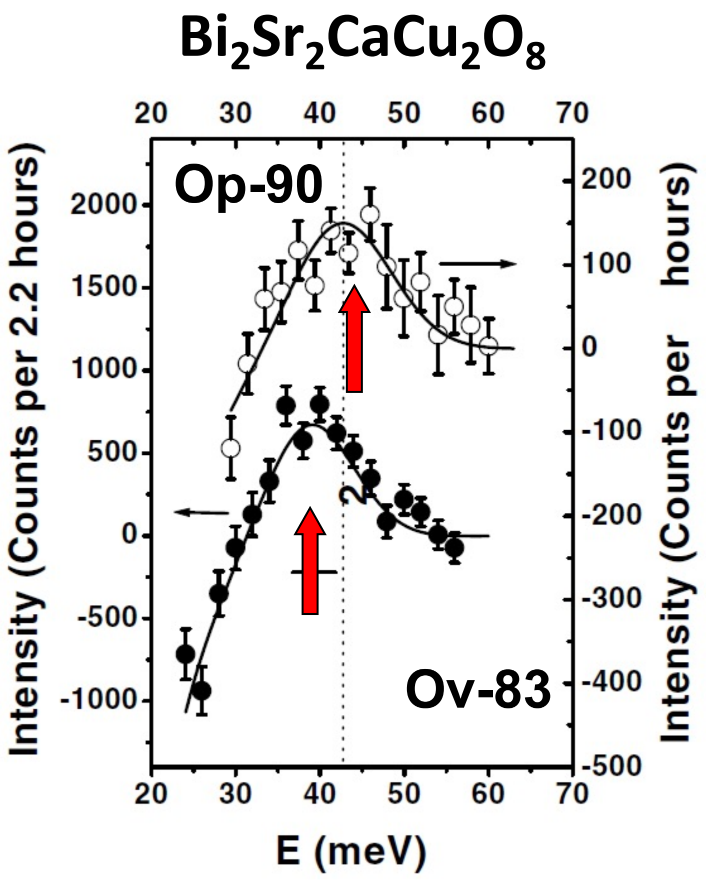

H. He et al., PRL 2001
B. Fauque et al., PRB 2007
L. Capogna et al., PRB 2007

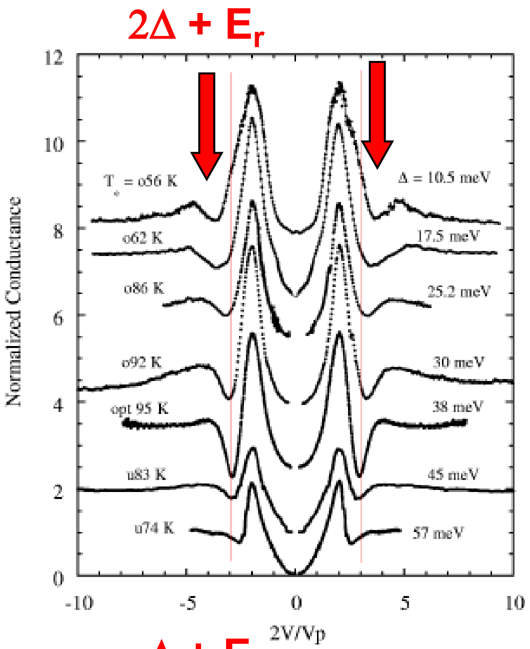

STM
(SIS junction)

Zasadsinski et al., PRL (2001)

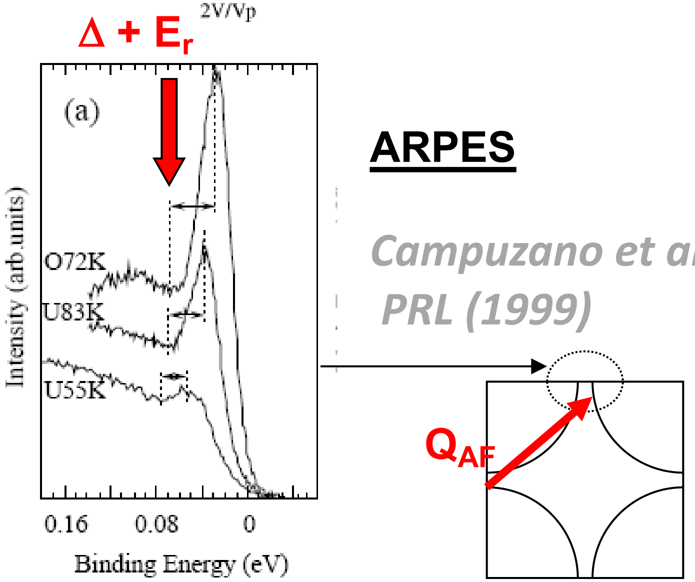

ARPES

Campuzano et al, PRL (1999)

Spin-fermion coupling: the feedback effect

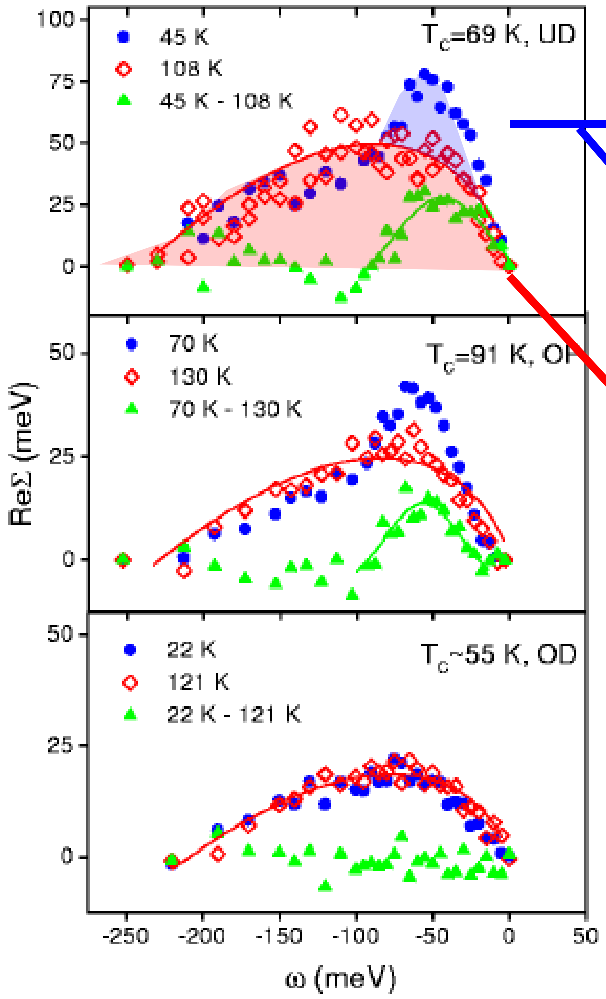

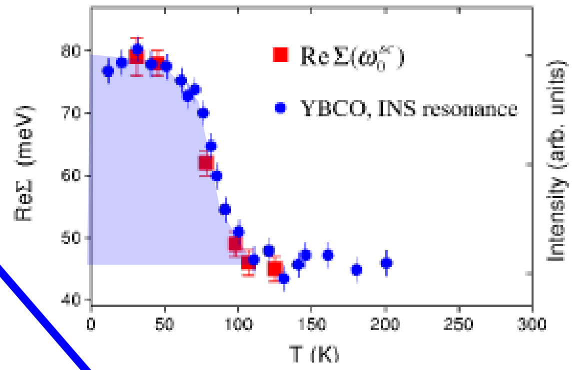

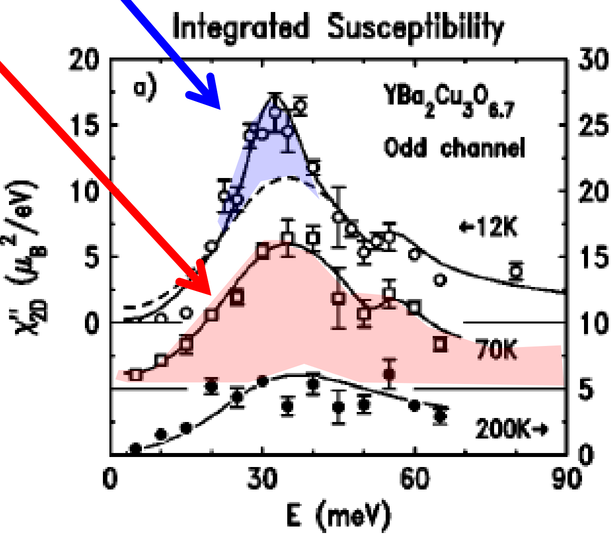

Real part of the quasiparticle self-energy measured by ARPES ($Bi_2Sr_2CaCu_2O_{8+\delta}$)

* ***Johnson et al., PRL (2001)***

Local AF spin fluctuations measured by INS ($YBa_2Cu_3O_{6+x}$)

* ***Fong et al., PRB (2000)***

Strength of the spin-fluctuation-mediated pairing interaction in a high-temperature superconductor

INS

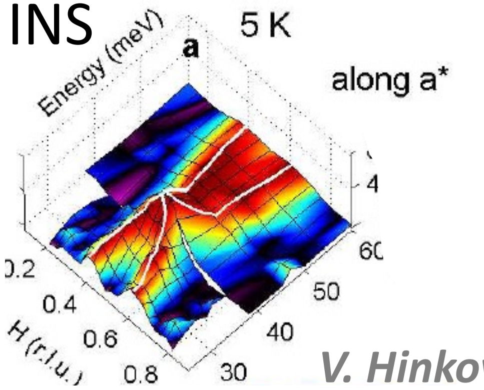

V. Hinkov et al., Nat.Phys. 2007

Linearized gap equation

$$\lambda_d \,\mathrm{Im}\,\phi_{A,B}(\mathbf{k},\omega) = \frac{1}{\pi N}\sum_{\mathbf{k}'}\int_{-\infty}^{\infty} d\omega' [n(\omega-\omega')+f(-\omega')]$$

$$\mathrm{Im}\,V_{\mathrm{eff}}(\mathbf{k}-\mathbf{k}',\omega-\omega')\,\mathrm{Im}\left\{\frac{\phi_{B,A}(\mathbf{k}',\omega')}{(\omega' Z_{B,A})^2-(\tilde{\epsilon}_{\mathbf{k}'}^{B,A})^2}\right\}$$

$$\lambda_d = 1.49.$$

$$V_{\mathrm{eff}}(\mathbf{Q},\Omega) = \frac{3}{2}\,\bar{U}^2\,\chi(\mathbf{Q},\Omega),$$

Parametrization of the spin dynamics along (H,H)

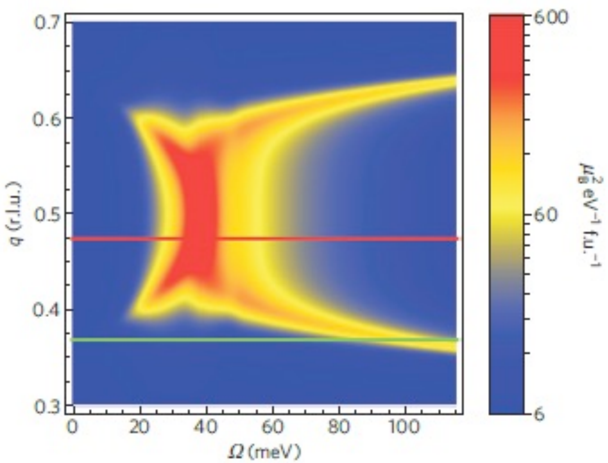

T Dahm, et al., Nat. Phys. 2009

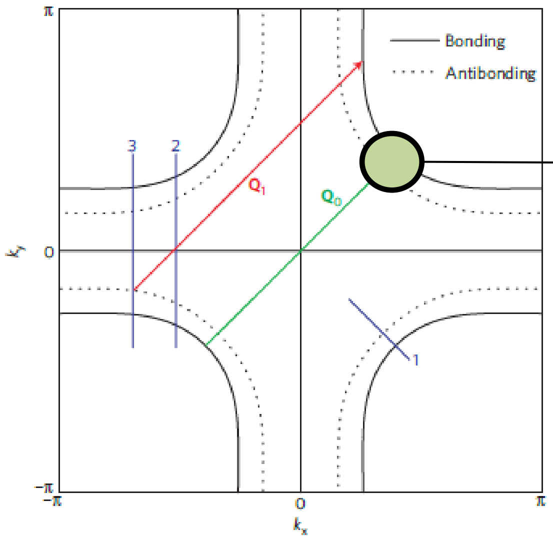

Renormalization of the quasiparticle dispersion along the nodal direction: kink at 80 meV

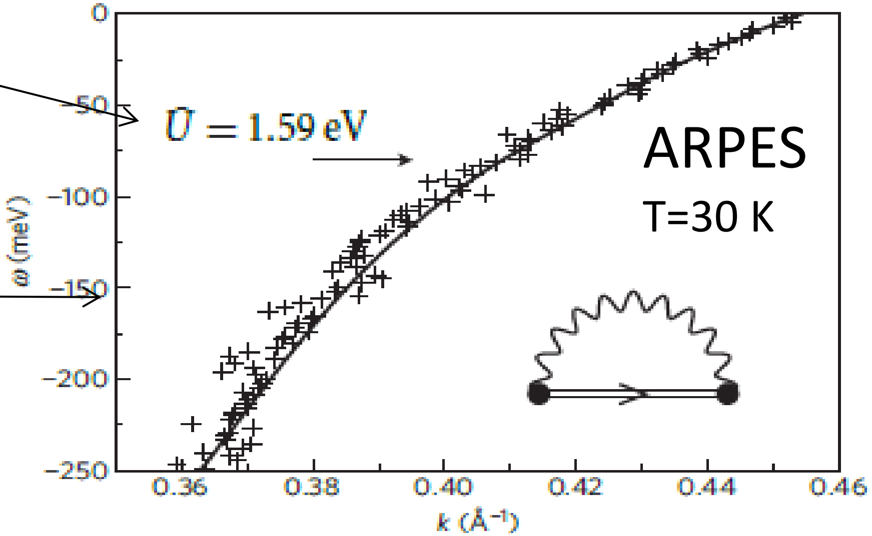

$$\mathrm{Im}\,\Sigma_{A,B}(\mathbf{k},\omega) = \frac{1}{\pi N}\sum_{\mathbf{Q}}\int_{-\infty}^{\infty} d\Omega [n(\Omega)+f(\Omega-\omega)]$$

$$\times\,\mathrm{Im}\,V_{\mathrm{eff}}(\mathbf{Q},\Omega)\,\mathrm{Im}\,G_{B,A}(\mathbf{k}-\mathbf{Q},\omega-\Omega).$$

Spin fluctuation spectral weight

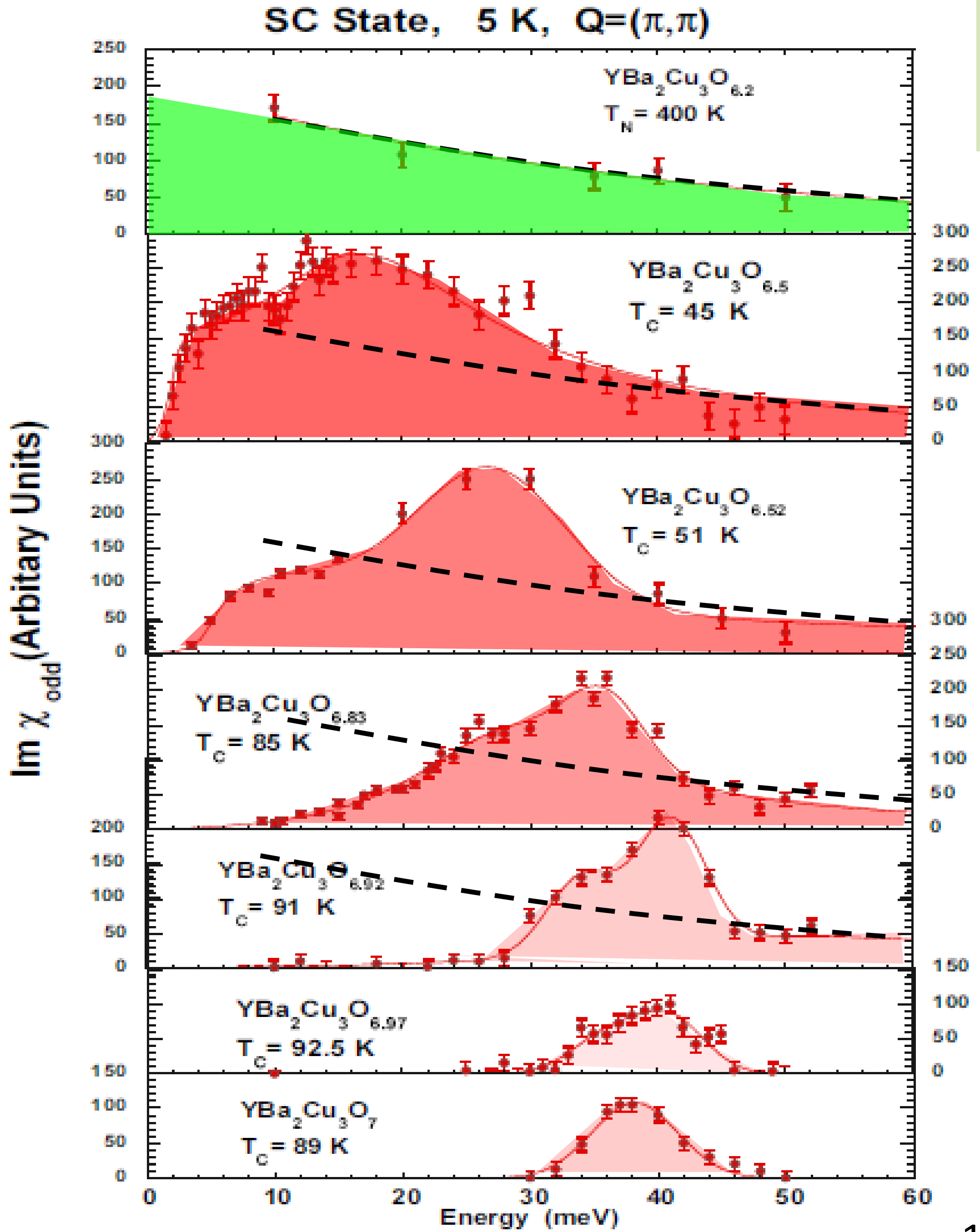

Spin susceptibility
at Q_{AF} in $YBa_2Cu_3O_{6+x}$

100 cnts -> 350 μ_B^2/ eV

cuprates	$\int d^3Q d\omega\, Im\chi(Q,\omega)\ (\mu_B^2)$ $\pm$ 30 %	$\int d\omega\, Im\chi(Q,\omega)\ (\mu_B^2)$ $\pm$ 30 %
$YBCO_{6.5}$	0.8	25
$YBCO_{6.7}$	0.6	15
$YBCO_{6.92}$	0.4	10
$YBCO_7$	0.043	1.6

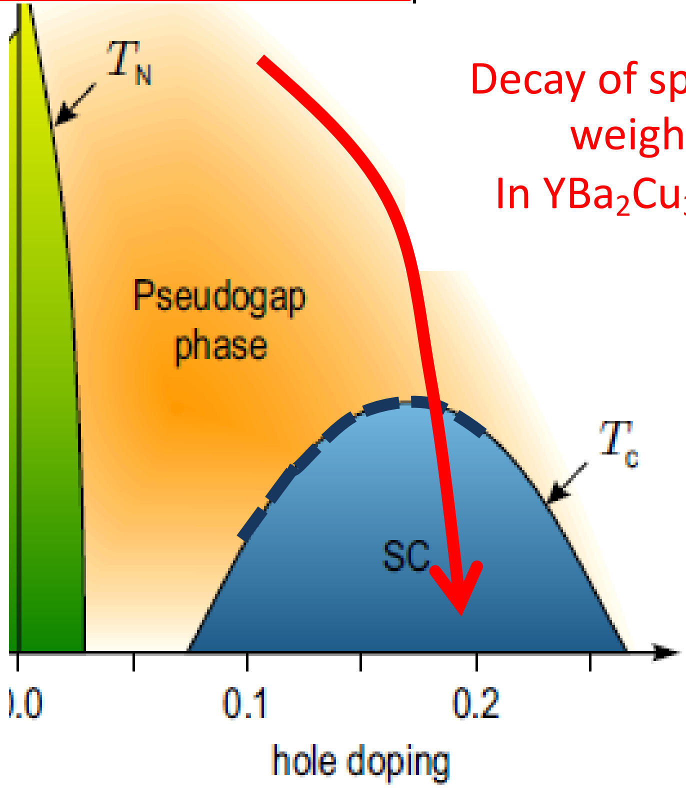

Decay of spectral weight
In $YBa_2Cu_3O_{6+x}$

Superconductivity mediated by direct interaction(s)

In the <u>strong coupling limit</u>, the **t-J model** can be formulated in terms of Hubbard operators

$$X_i^{\lambda\mu} = |\lambda\rangle\langle\mu|.$$

3 states per CuO_2 plaquette: |0> for a doped hole, |1>or |-1> for a spin S=1/2 on Cu site

$$H = H_0 + H_t + H_J,$$

$$H_t = \sum_{ij} t_{ij}\{X_i^{01}X_j^{10} + X_i^{0-1}X_j^{-10}\},$$

$$H_J = \sum_{ij} J_{ij}\{X_i^{1-1}X_j^{-11} - X_i^{11}X_j^{-1-1}\},$$

$$H_0 = \sum_i E_0 X_i^{00} + E_\sigma(X_i^{-1-1} + X_i^{11}) - \frac{h}{2}(X_i^{11} - X_i^{-1-1}).$$

F. Onufrieva et al., PRB 1996

<u>Mean field gap equation:</u>

Direct pairing

$$\Delta_{\mathbf{k}} = \frac{1+\delta}{2}\frac{1}{N}\sum_{\mathbf{q}} \frac{J_{\mathbf{k}-\mathbf{q}} - t_{\mathbf{q}}}{E_{\mathbf{q}\sigma}} \Delta_{\mathbf{q}} \tanh\left(\frac{E_{\mathbf{q}\sigma}}{2T}\right),$$

$-t_q$: kinematic pairing due to the simple motion of doped holes in a correlated system

$-J_{k-q}$: super-exchange induces a direct pairing

<u>Dual character of spin fluctuations</u>

The spin susceptibility is made of itinerant and localized components , which are self-consistently coupled

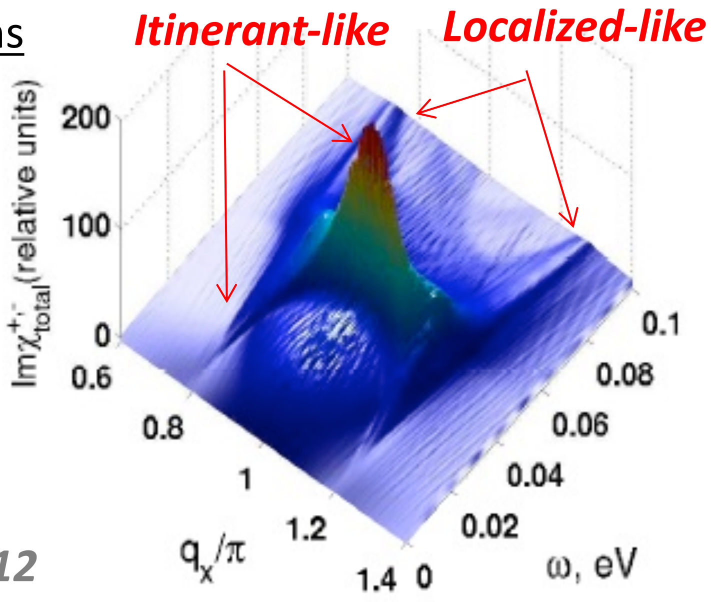

I Eremin et al., EPJ 2012

Unstable superconductivity

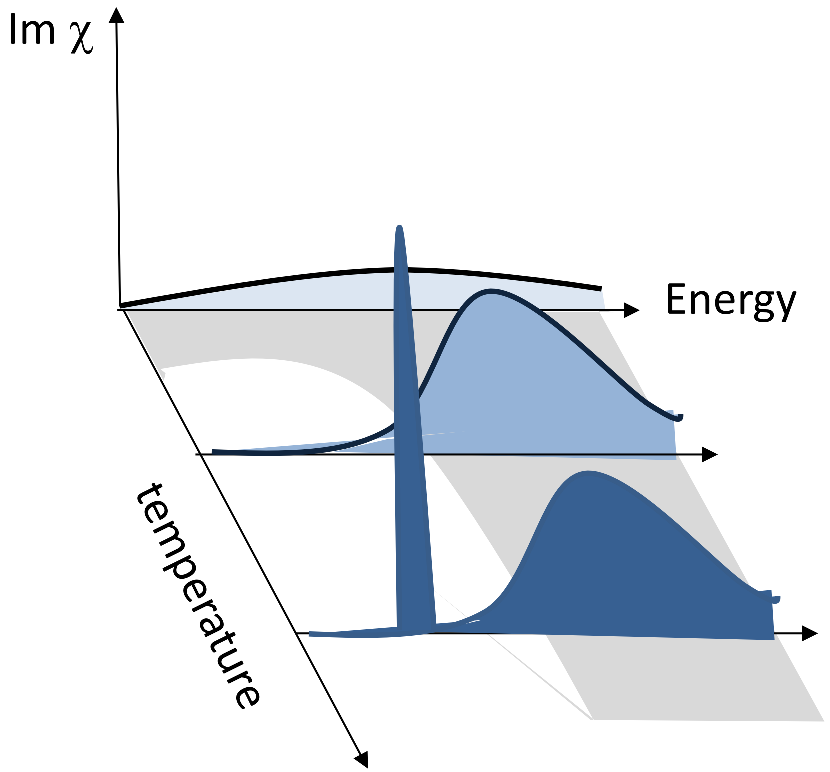

Spin-charge seperation	Fluctuating SC or prefomed pairs	Vectorial order parameter	Competing order
normal	normal	normal	normal
Spinon Pairing (S=0)	Fluctuating SC (D<3)	Fluctuating SC + other state 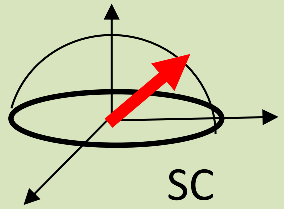	Competing state
Spinon Pairing + Holon condensation	SC coherence	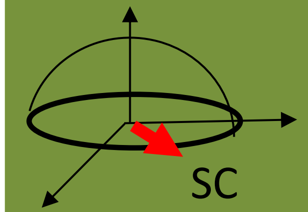	SC

The spin exciton scenario : competing state... X-Y dispersion

Example of DDW

Ismer et al, PRB 2006

$$E_{\mathbf{k}}^{\pm} = \varepsilon_{\mathbf{k}}^{+} \pm \sqrt{(\varepsilon_{\mathbf{k}}^{-})^2 + W_{\mathbf{k}}^2},$$

$$\varepsilon_{\mathbf{k}}^{\pm} = (\varepsilon_{\mathbf{k}} \pm \varepsilon_{\mathbf{k+Q}})/2$$

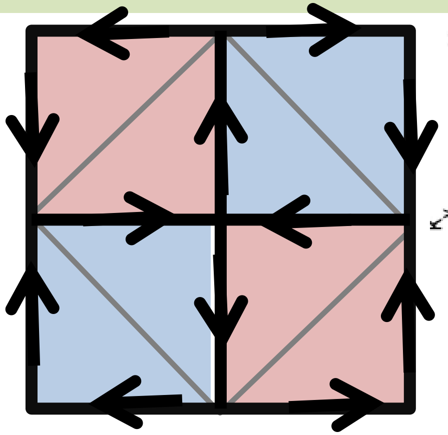

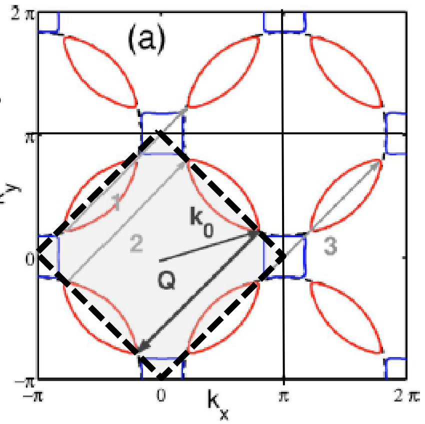

$$\chi_0(\mathbf{q},\omega) = \frac{1}{8}\sum_{\mathbf{k}} \left(1 + \frac{\varepsilon_{\mathbf{k}}^{-}\varepsilon_{\mathbf{k+q}}^{-} + W_{\mathbf{k}}W_{\mathbf{k+q}}}{\sqrt{(\varepsilon_{\mathbf{k}}^{-})^2 + W_{\mathbf{k}}^2}\sqrt{(\varepsilon_{\mathbf{k+q}}^{-})^2 + W_{\mathbf{k+q}}^2}}\right)$$
$$\times \left(\frac{f(E_{\mathbf{k+q}}^{+}) - f(E_{\mathbf{k}}^{+})}{\omega + i0^{+} - E_{\mathbf{k+q}}^{+} + E_{\mathbf{k}}^{+}} + \frac{f(E_{\mathbf{k+q}}^{-}) - f(E_{\mathbf{k}}^{-})}{\omega + i0^{+} - E_{\mathbf{k+q}}^{-} + E_{\mathbf{k}}^{-}}\right)$$
$$+ \left(1 - \frac{\varepsilon_{\mathbf{k}}^{-}\varepsilon_{\mathbf{k+q}}^{-} + W_{\mathbf{k}}W_{\mathbf{k+q}}}{\sqrt{(\varepsilon_{\mathbf{k}}^{-})^2 + W_{\mathbf{k}}^2}\sqrt{(\varepsilon_{\mathbf{k+q}}^{-})^2 + W_{\mathbf{k+q}}^2}}\right)$$
$$\times \left(\frac{f(E_{\mathbf{k+q}}^{-}) - f(E_{\mathbf{k}}^{+})}{\omega + i0^{+} - E_{\mathbf{k+q}}^{-} + E_{\mathbf{k}}^{+}} + \frac{f(E_{\mathbf{k+q}}^{+}) - f(E_{\mathbf{k}}^{-})}{\omega + i0^{+} - E_{\mathbf{k+q}}^{+} + E_{\mathbf{k}}^{-}}\right)$$

$$\boxed{\chi_{RPA}(\mathbf{q},\omega) = \frac{\chi_0(\mathbf{q},\omega)}{1 - U\chi_0(\mathbf{q},\omega)}}$$

SC state

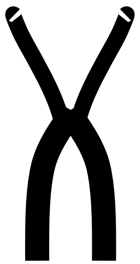

dispersing S=1 mode

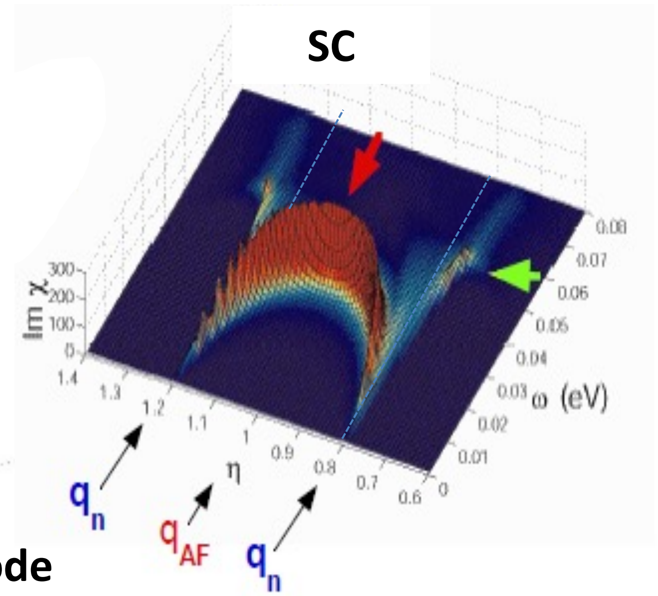

narrow S=1 mode
DDW

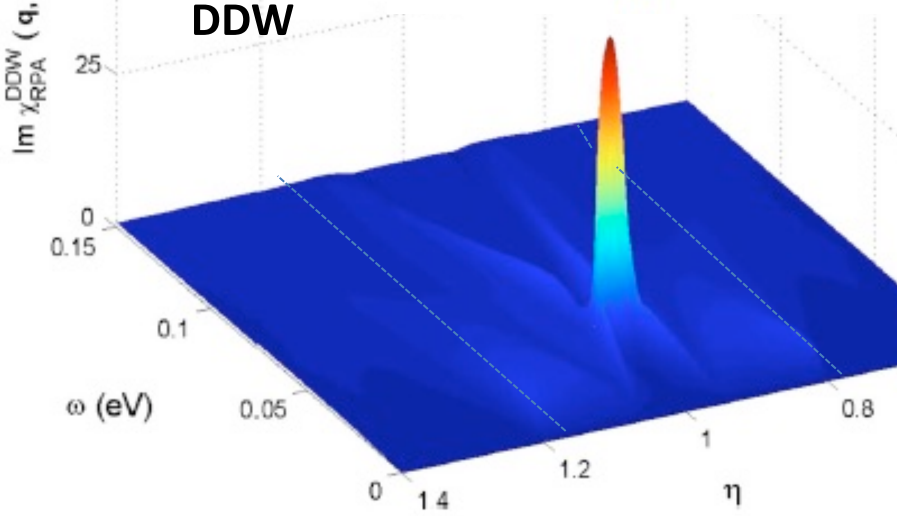

DDW

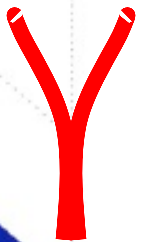

The spin exciton scenario : vectorial order parameter SC+CDW

Example of Resonant Excitonic State (RES) *Montiel et al, PRB 2017*

$$W_{\pm,\mathbf{k}} = \tfrac{1}{2}\left(\xi_{\mathbf{k}} + \xi_{\mathbf{k}+2\mathbf{p}_F(\mathbf{k})} \pm \sqrt{(\xi_{\mathbf{k}} - \xi_{\mathbf{k}+2\mathbf{p}_F(\mathbf{k})})^2 + 4\Delta^2_{\mathrm{RES},\mathbf{k}}}\right)$$

$$\begin{aligned}
\chi^0_{S,\mathrm{RES}}(\omega,\mathbf{q}) = \sum_{\mathbf{k}} \Bigg[& \frac{1}{4}\left(1 + \frac{(\xi_{\mathbf{k}} - \xi_{\mathbf{k}+2\mathbf{p}_F(\mathbf{k})})(\xi_{\mathbf{k}+\mathbf{q}} - \xi_{\mathbf{k}+\mathbf{q}+2\mathbf{p}_F(\mathbf{k}+\mathbf{q})}) + 4\Delta_{\mathrm{RES},\mathbf{k}}\Delta_{\mathrm{RES},\mathbf{k}+\mathbf{q}} f(\mathbf{q})}{(W_{+,\mathbf{k}} - W_{-,\mathbf{k}})(W_{+,\mathbf{k}+\mathbf{q}} - W_{-,\mathbf{k}+\mathbf{q}})}\right) \\
& \times \left(\frac{n_F(W_{-,\mathbf{k}}) - n_F(W_{-,\mathbf{k}+\mathbf{q}})}{\omega + i\eta + W_{-,\mathbf{k}} - W_{-,\mathbf{k}+\mathbf{q}}} + \frac{n_F(W_{+,\mathbf{k}}) - n_F(W_{+,\mathbf{k}+\mathbf{q}})}{\omega + i\eta + W_{+,\mathbf{k}} - W_{+,\mathbf{k}+\mathbf{q}}}\right) \\
& + \frac{1}{4}\left(1 - \frac{(\xi_{\mathbf{k}} - \xi_{\mathbf{k}+2\mathbf{p}_F(\mathbf{k})})(\xi_{\mathbf{k}+\mathbf{q}} - \xi_{\mathbf{k}+\mathbf{q}+2\mathbf{p}_F(\mathbf{k}+\mathbf{q})}) + 4\Delta_{\mathrm{RES},\mathbf{k}}\Delta_{\mathrm{RES},\mathbf{k}+\mathbf{q}} f(\mathbf{q})}{(W_{+,\mathbf{k}} - W_{-,\mathbf{k}})(W_{+,\mathbf{k}+\mathbf{q}} - W_{-,\mathbf{k}+\mathbf{q}})}\right) \\
& \times \left(\frac{n_F(W_{-,\mathbf{k}}) - n_F(W_{+,\mathbf{k}+\mathbf{q}})}{\omega + i\eta + W_{-,\mathbf{k}} - W_{+,\mathbf{k}+\mathbf{q}}} + \frac{n_F(W_{+,\mathbf{k}}) - n_F(W_{-,\mathbf{k}+\mathbf{q}})}{\omega + i\eta + W_{+,\mathbf{k}} - W_{-,\mathbf{k}+\mathbf{q}}}\right)\Bigg],
\end{aligned}$$

$$\boxed{\chi_S(\omega,\mathbf{q}) = \frac{\chi^0_S(\omega,\mathbf{q})}{1 + J(\mathbf{q})\chi^0_S(\omega,\mathbf{q})}}$$

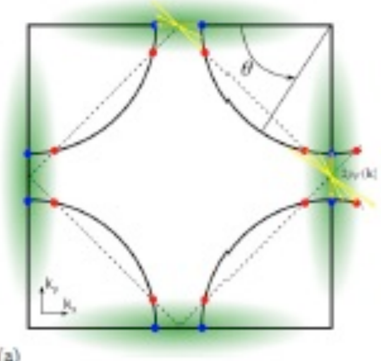

dispersing S=1 mode

SC

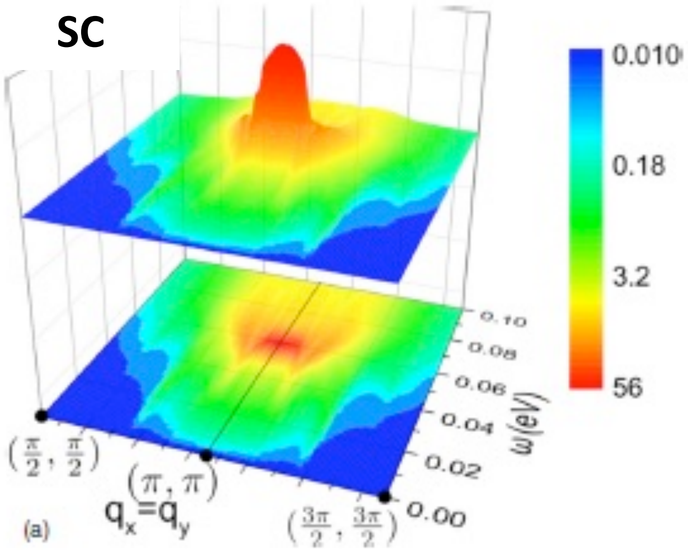

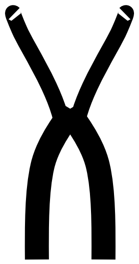

narrow S=1 mode

RES

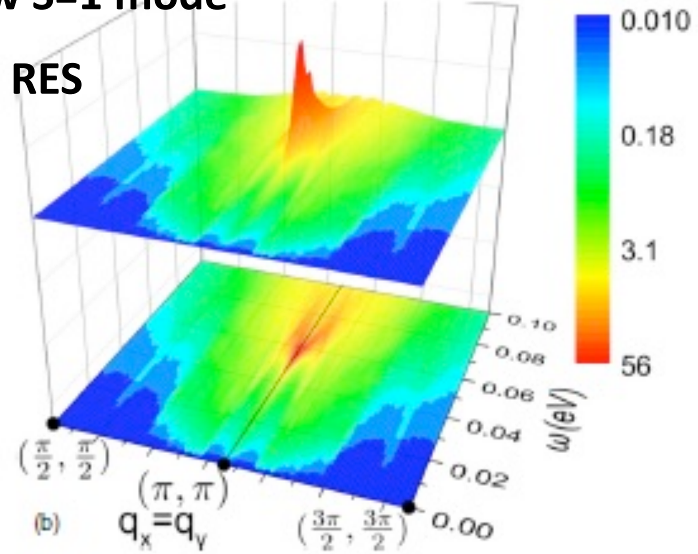

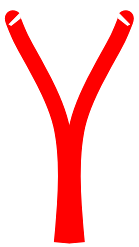

Self organization of doped holes : vertical stripes

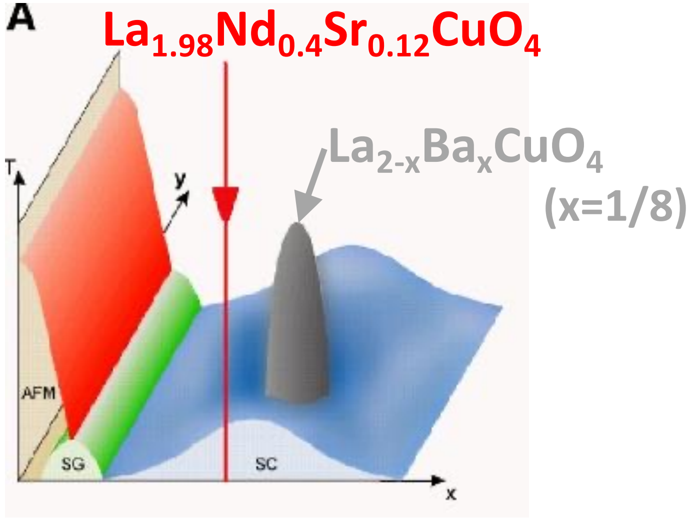

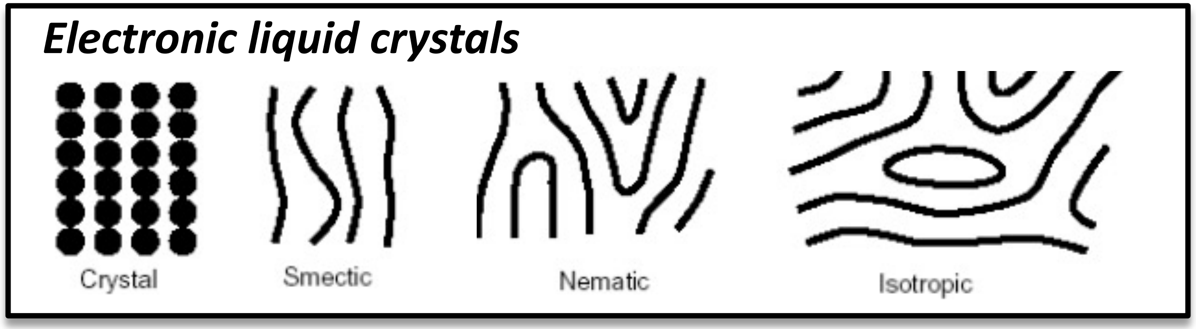

Bond centered stripes

4a = 1/2d

hole river

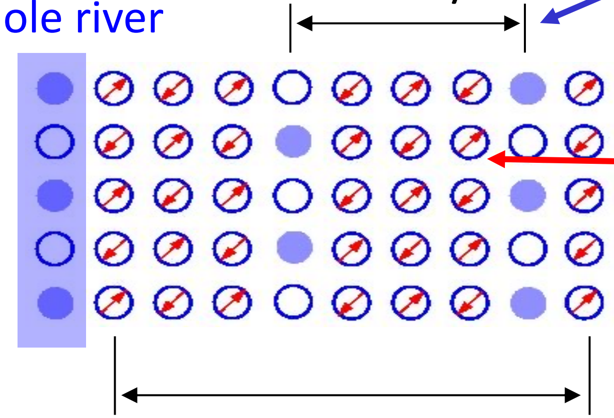

8a = the spin periodicity
= 1/d

Charge order

Spin order

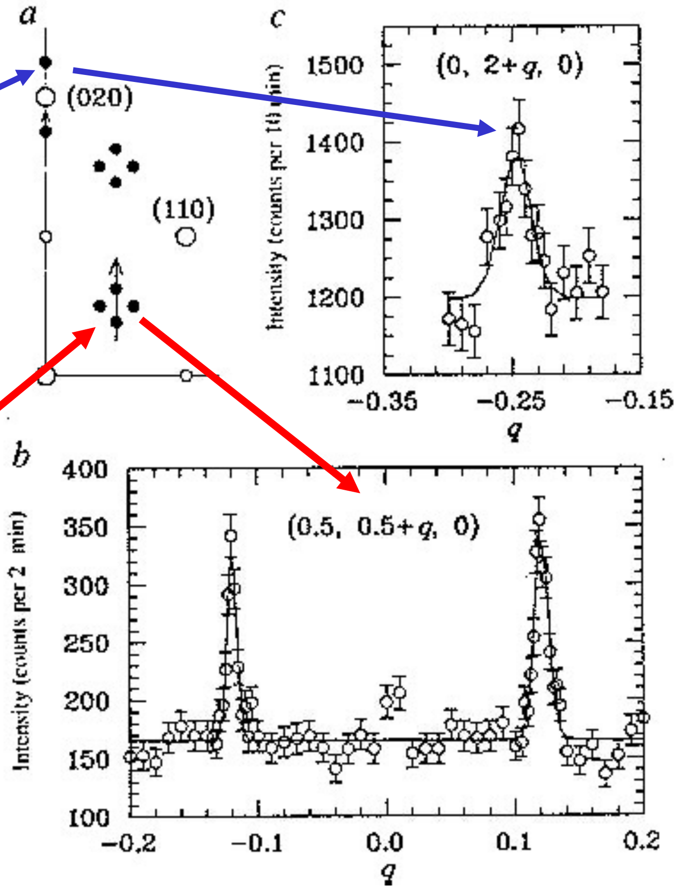

Charge
Order induces a lattice distortion which is detected by neutron scattering

J. Tranquada et al., Nature 1995

Hourglass dispersion in stripe ordered $La_{2-x}Ba_xCuO_4$ (x=1/8)

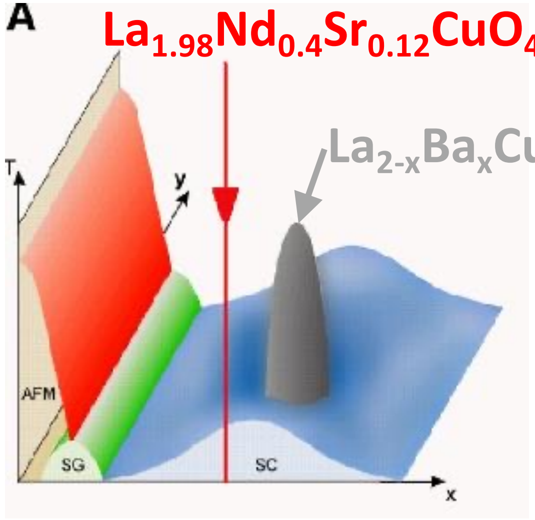

$La_{2-x}Ba_xCuO_4$ (x=1/8)

Hourglass dispersion
dynamical hallmark of stripes

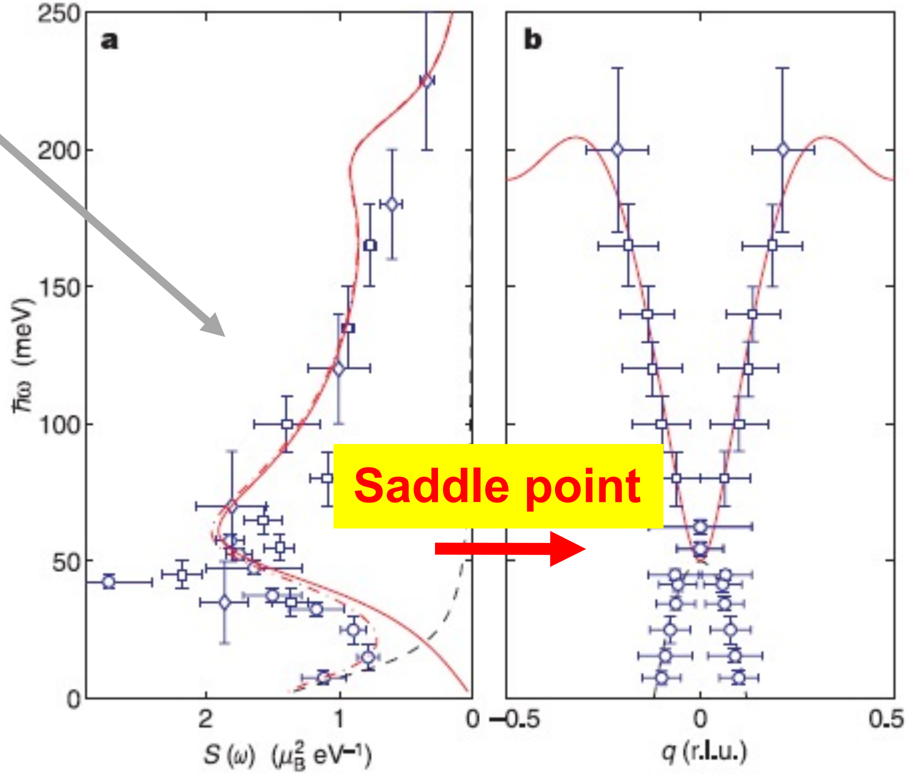

Saddle point

J. Tranquada et al., Nature 2004

2 leg ladder stripes

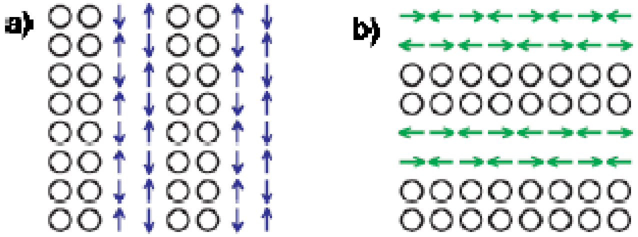

Inter- stripes

Intra- stripes

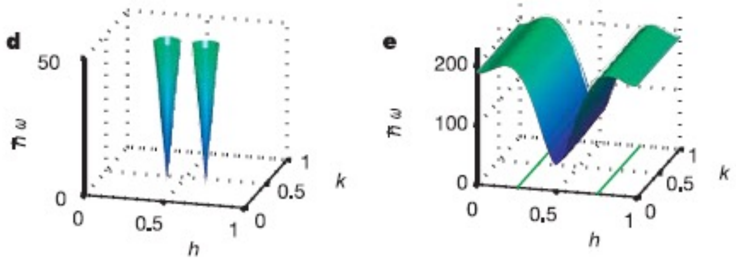

Low energy

High energy

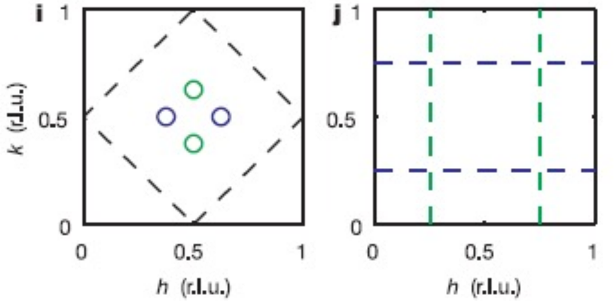

Theory *Vojta et al., PRL (2004), Uhrig et al., PRL (2004), Seibold et al., PRL (2005), Vojta et al., PRL (2006)*

Loop Current order : intra-unit-cell magnetism

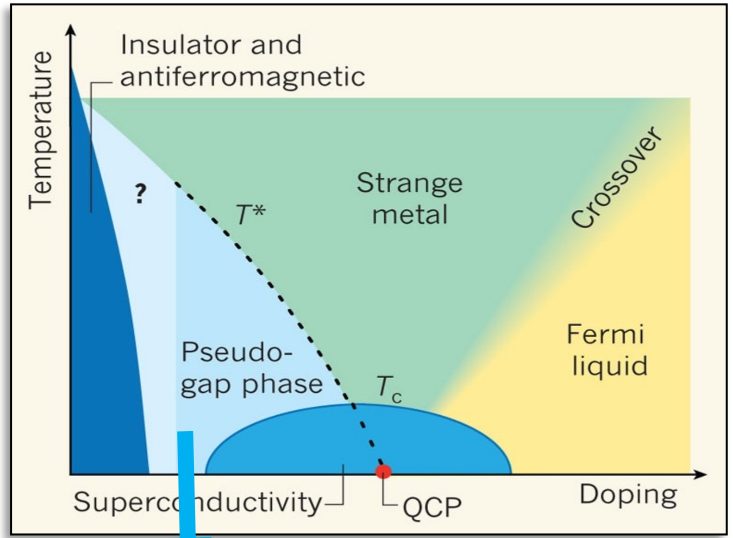

C.M. Varma, PRB 1997; PRB 2006

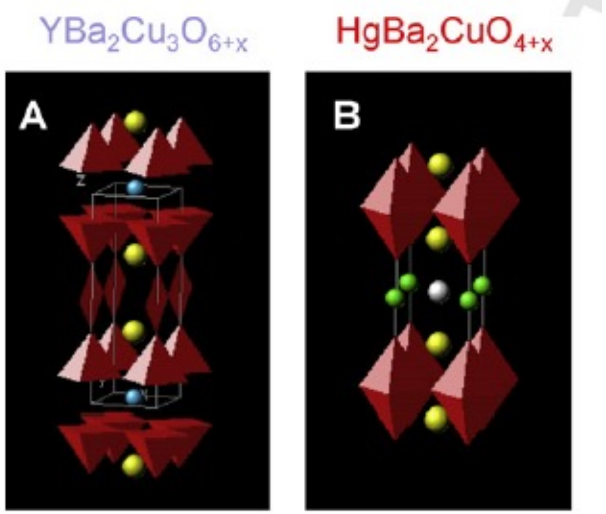

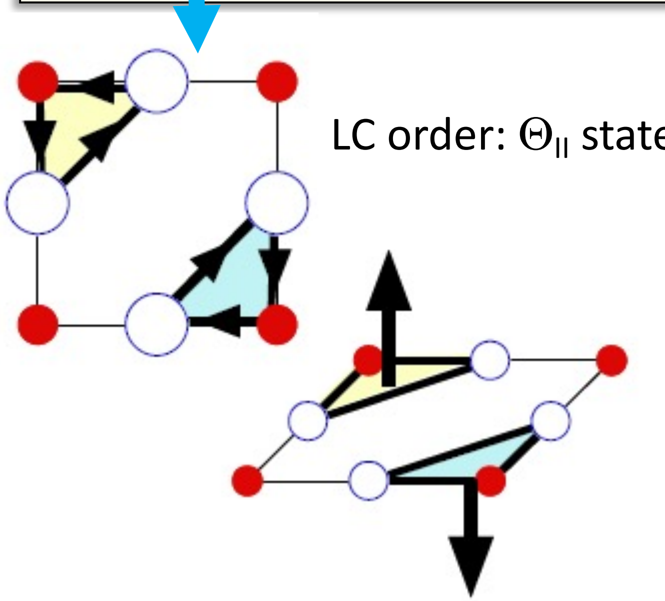

LC order: Θ_{II} state

Corresponding magnetic pattern

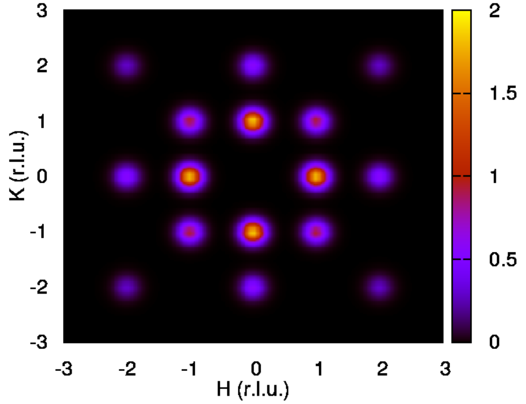

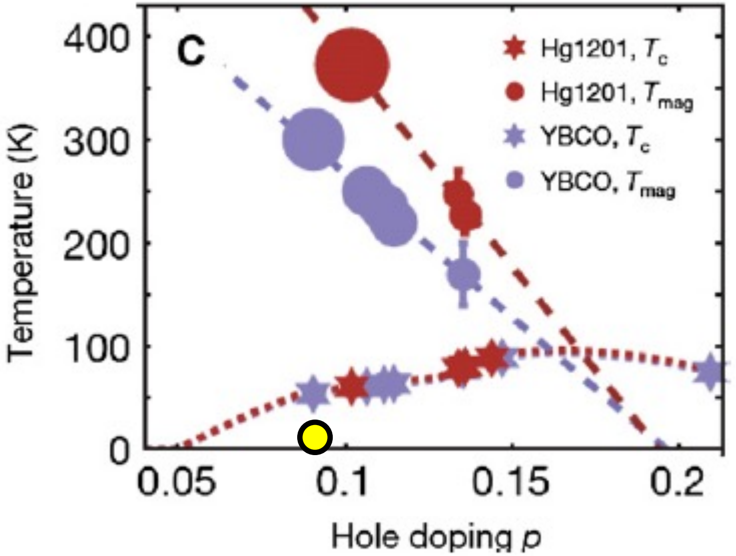

Broken symmetries
T, P, C_4

Polarized neutron diffraction data

B. Fauqué et al., PRL 2006
Y. Li et al., Nature 2008

Loop Current order : Ising-like collective modes

He & Varma, PRL 2011

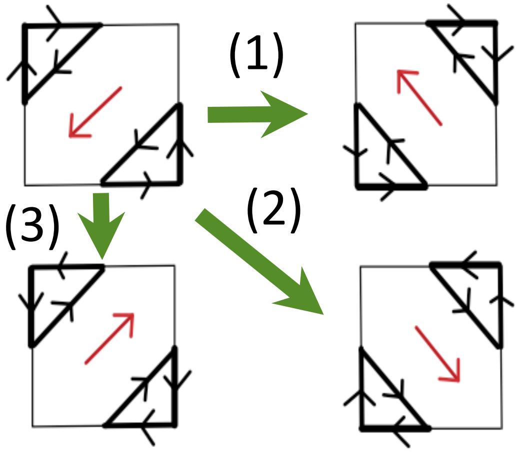

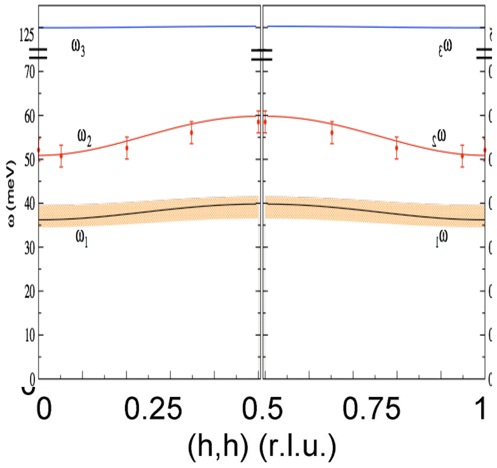

Dynamic hallmark

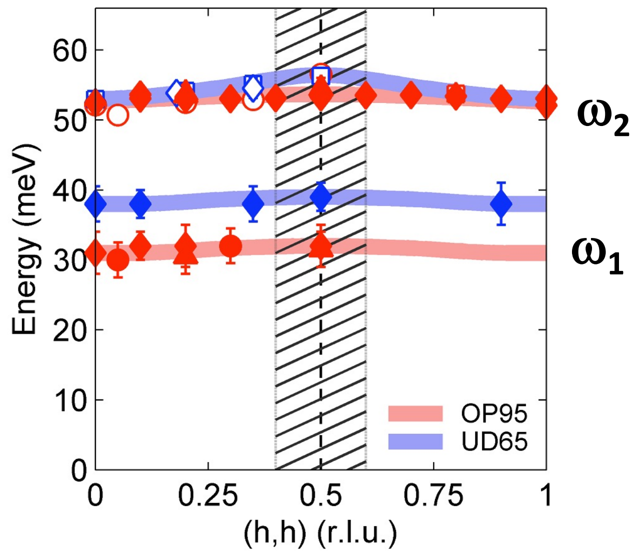

$HgBa_2CuO_{4+x}$

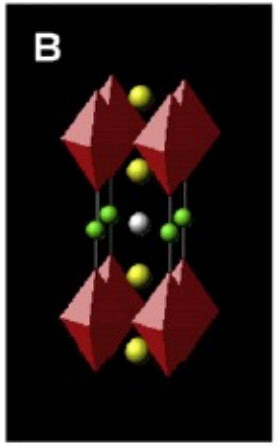

Y. Li et al, Nature 2010

Y. Li et al, Nat. Phys. 2012

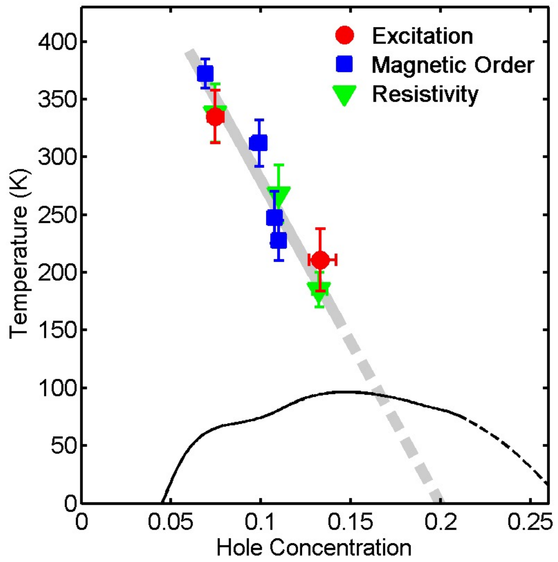

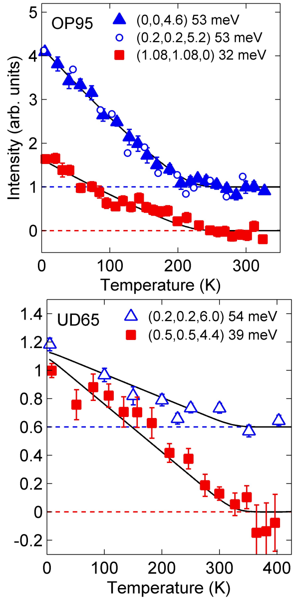

Spin dynamics in Fe-based supercondcutors

Y. Sidis

Laboratoire Léon Brillouin, CEA-CNRS

Cargèse-2022

Main bibliographical sources ….

Pencheng DAI
Rice University

Markus BRADEN
University of Cologne

REVIEWS OF MODERN PHYSICS, VOLUME 87, JULY–SEPTEMBER 2015

STATIC ANTIFERROMAGNETIC ORDER AND ITS DOPING EVOLUTION

From a crystal structure point of view, the parent compounds of iron-based superconductors can be classified into **five different families:**

$RFeAsO$ (R= La, Ce, Pr, Nd, Sm,..., the 1111 system)

AFe_2As_2 (A= Ba, Sr, Ca, K, the 122 system)

$AFeAs$ (A = Li, Na, the 111 system)

$Fe_{1+y}Te_{1-x}Se_x$ (the 11 system)

$A_xFe_{2-y}Se_2$ alkali iron selenides (A= K, Rb, Cs, Tl, ..., including the insulating 245 phase A2Fe4Se5 and the semiconducting 234 phase A2Fe3Se4)

where the 122 and 245 compounds have two FeAs(Se) layers in the unit cell and other systems have single FeAs(Se) layer. A

STATIC ANTIFERROMAGNETIC ORDER AND ITS DOPING EVOLUTION

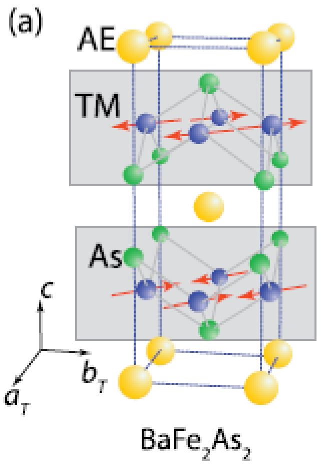

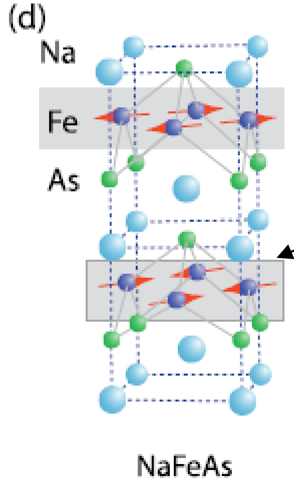

122

111

Materials	$a_T \equiv b_T$ (Å)	c (Å)
LaFeAsO[a]	4.0301	8.7368
CeFeAsO[b]	3.9959	8.6522
PrFeAsO[c]	3.997	8.6057
NdFeAsO[d]	3.9611	8.5724
$LaFeAsO_{0.5}H_{0.5}$[e]	3.975	8.67
$CaFe_2As_2$[f]	3.912	11.667
$SrFe_2As_2$[g]	3.920	12.40
$BaFe_2As_2$[h]	3.957	12.968
$Na_{0.985}FeAs$[i]	3.9448	6.9968
$Fe_{1.068}Te$[j]	3.8123	6.2517
$K_2Fe_4Se_5$[k]	8.7306	14.113
$Rb_2Fe_4Se_5$[l]	8.788	14.597
$Cs_2Fe_4Se_5$[m]	8.865	15.289
$TlFe_{1.6}Se_2$[n]	~8.71	14.02

STATIC ANTIFERROMAGNETIC ORDER AND ITS DOPING EVOLUTION

Although the field of iron-based superconductors started with the discovery of the 1111 family of materials, a majority of recent neutron scattering work has focused on the 122 family due to the availability of high quality single crystals

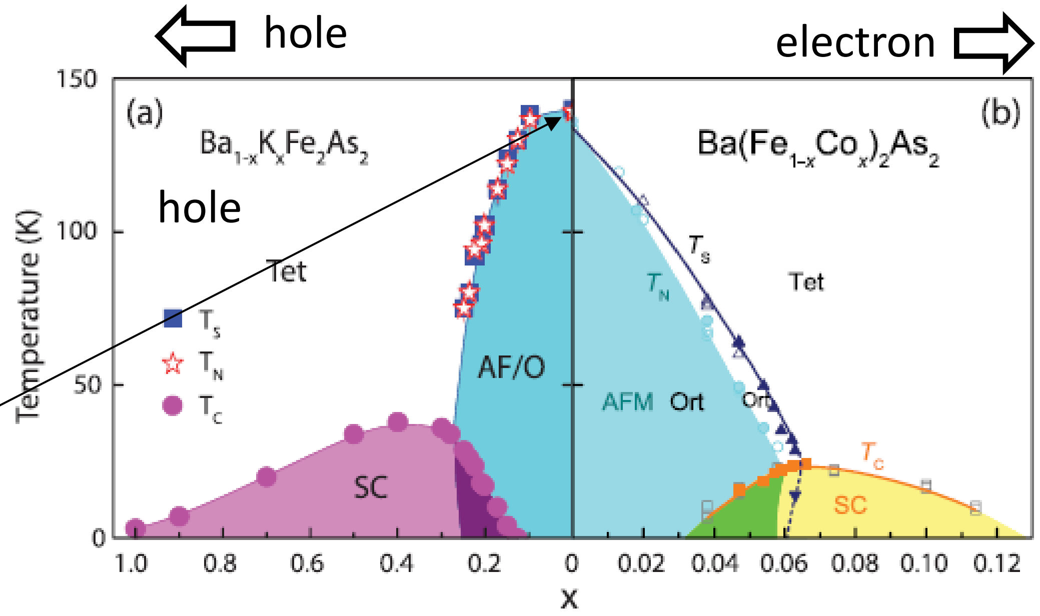

In the undoped state, a prototypical 122 compound such as $BaFe_2As_2$ exhibits tetragonal-to-orthorhombic lattice distortion and the AF order below $T_s \approx T_N \approx 138$ K

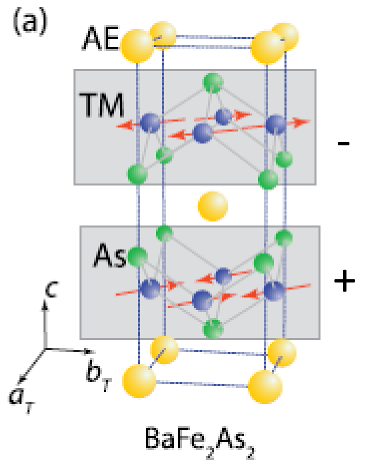

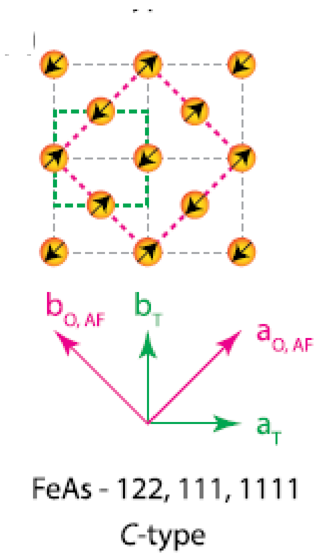

Propagation vector

$Q_T=(0,5,0,5,1)$

$Q_o=(1,0,1)$

$m=0.87\ \mu_B/Fe$

$m\ //\ a_o$

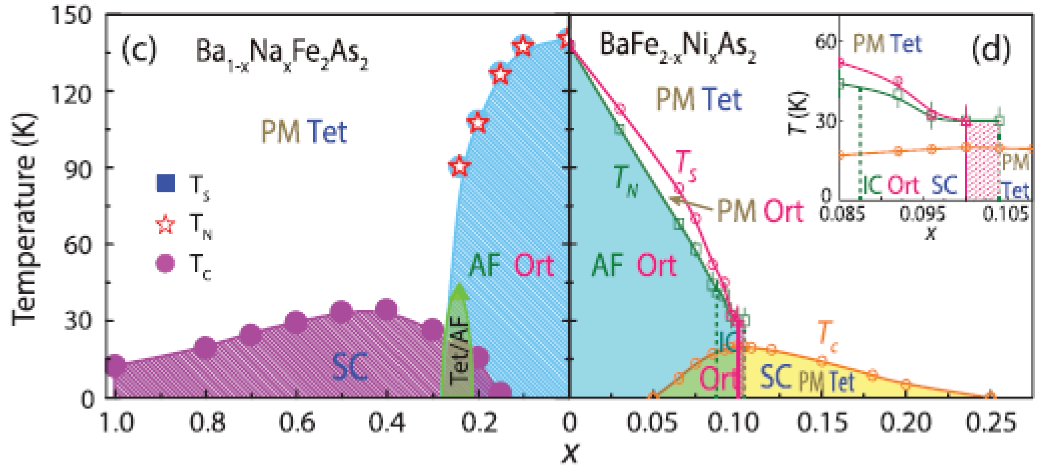

STATIC ANTIFERROMAGNETIC ORDER AND ITS DOPING EVOLUTION

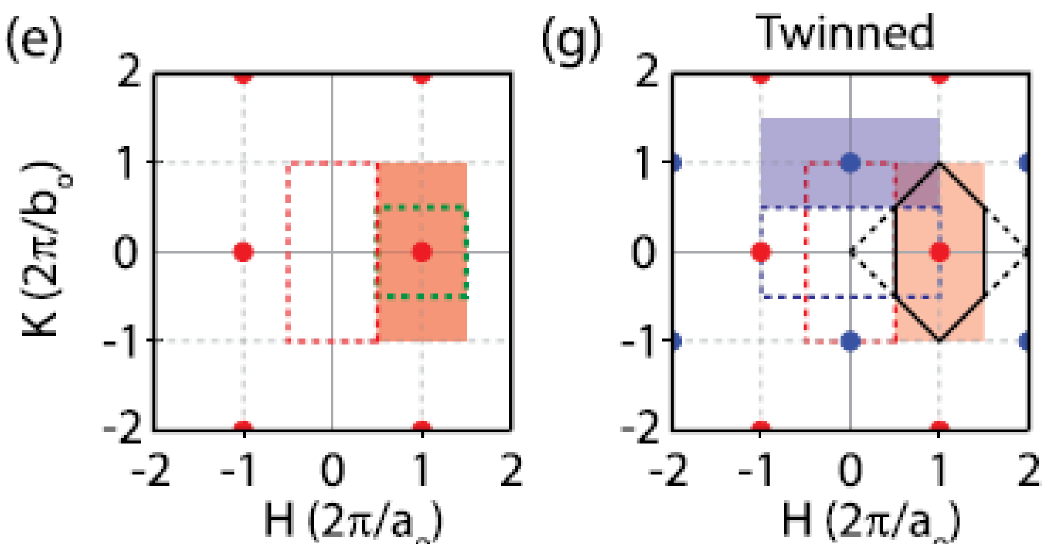

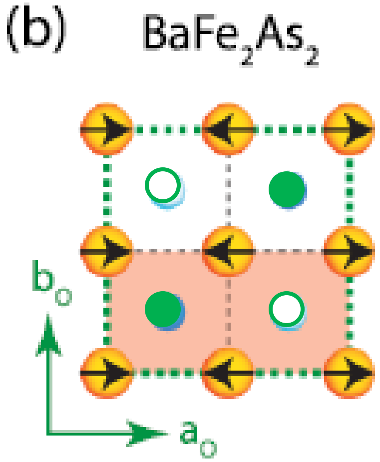

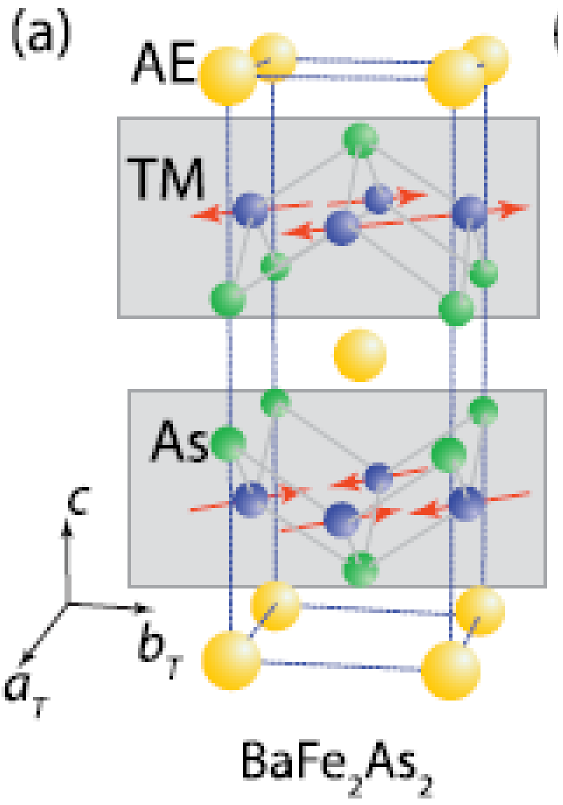

If the ordered moment is entirely on the Fe site in $BaFe_2As_2$, the chemical unit cell is twice the size of the magnetic unit cell along the b_o axis direction due to out-of-plane positions of the As atoms In a completely detwinned sample, the magnetic Brillouin zone is the shaded area

around $\mathbf{Q}_{\mathrm{AF}} = (H, K, L) = (1 \pm 2m, 0 \pm 2n, L)$, where $L = \pm 1, 3, 5, \ldots$ rlu, larger in size than the chemical Brillouin zone

STATIC ANTIFERROMAGNETIC ORDER AND ITS DOPING EVOLUTION

polarized neutrons: spin flip scattering

(1) neutron scattering: $m \perp \mathbf{Q}$
(2) neutron spin flip: $m \perp \mathbf{P}$

SF: $I_x \sim (L/Q)^2 M_a + M_b + \{1-(L/Q)^2\} M_c$
SF: $I_y \sim M_b$
SF: $I_z \sim (L/Q)^2 M_a + \{1-(L/Q)^2\} M_c = M_{ac}$

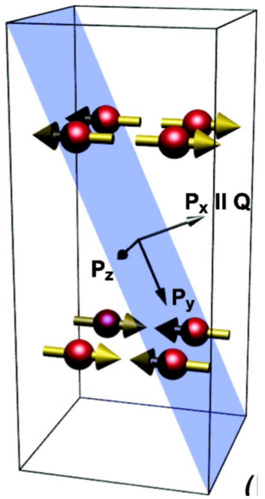

Scattering plane
[1/2,1/2,0] / [0,0,1]

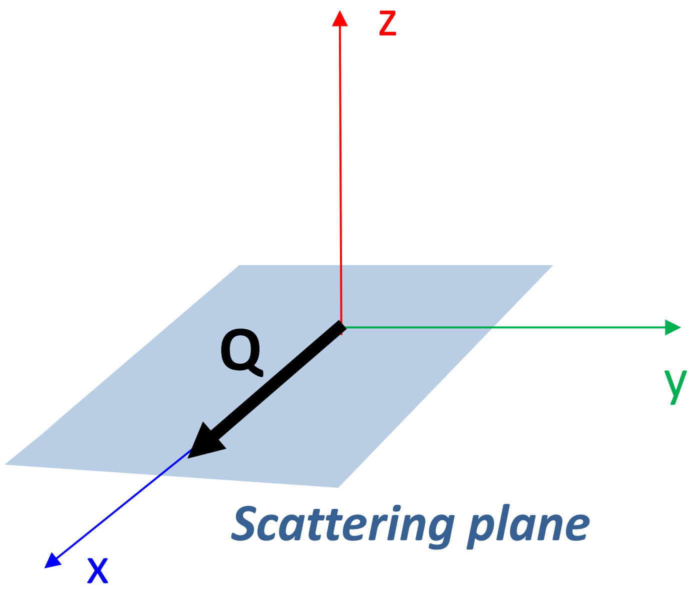

x || Q
$y \perp Q$
$z \perp$ scattering plane

STATIC ANTIFERROMAGNETIC ORDER AND ITS DOPING EVOLUTION

polarized neutrons: spin flip scattering

(1) neutron scattering: m ⊥ **Q**
(2) neutron spin flip: m ⊥ **P**

SF: $I_x \sim (L/Q)^2 M_a + M_b + \{1-(L/Q)^2\} M_c$
SF: $I_y \sim M_b$
SF: $I_z \sim (L/Q)^2 M_a + \{1-(L/Q)^2\} M_c = M_{ac}$

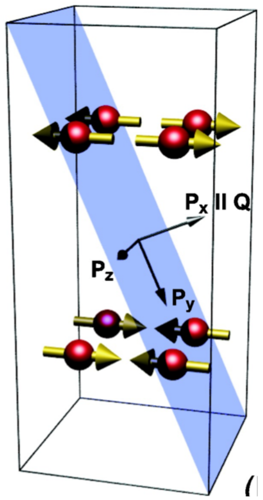

Scattering plane
[1/2,1/2,0] / [0,0,1]

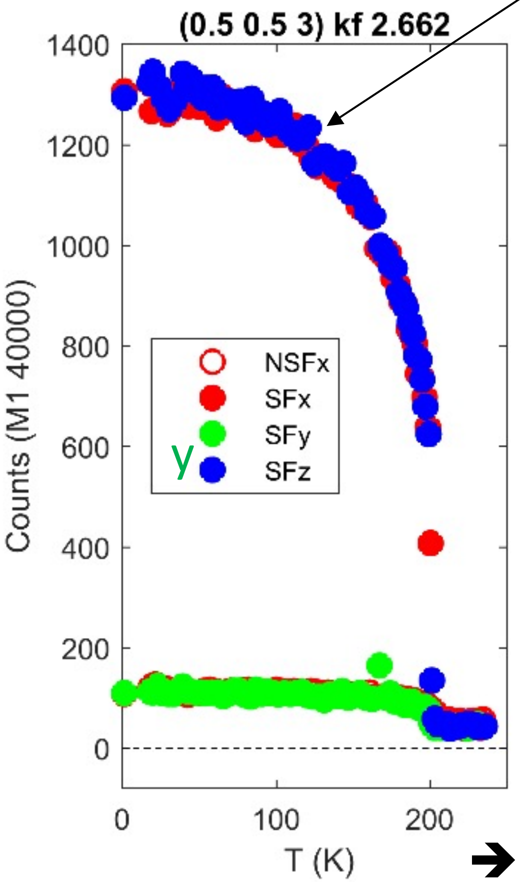

➔ separatio
moment [0.5,-0.5,0]

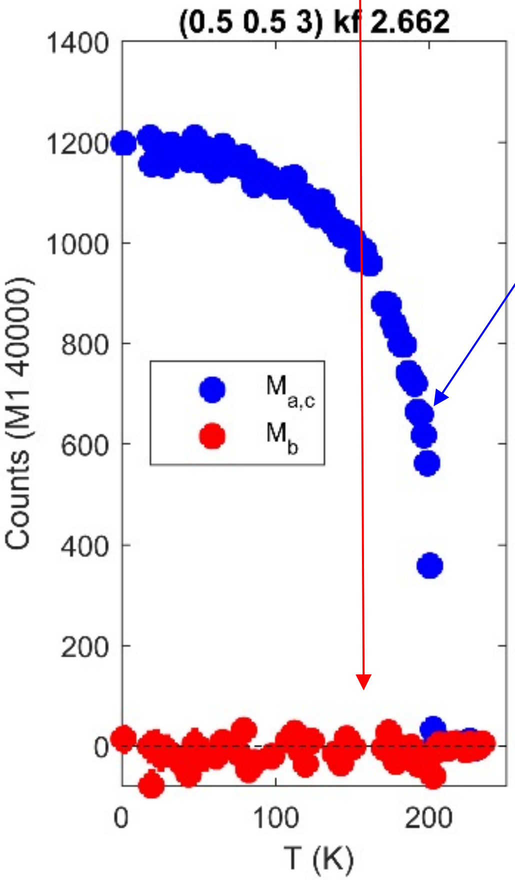

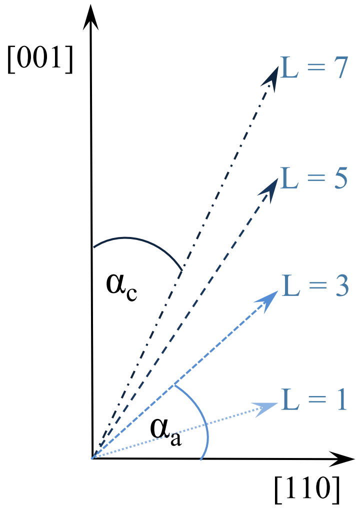

➔ distinction [0.5,0.5,0] vs. [0,0,1]
$(L/Q)^2 = \sin^2(\alpha_a)$

STATIC ANTIFERROMAGNETIC ORDER AND ITS DOPING EVOLUTION

TABLE I. Summary of the structure transition temperatures T_s, the magnetic transition temperatures T_N, and the ordered magnetic moment per iron for the AF ordered parent compounds of the iron-based superconductors. The lattice parameters in the paramagnetic tetragonal state are also listed.

Materials	$a_T \equiv b_T$ (Å)	c (Å)	T_s (K)	T_N (K)	Moment/Fe (μ_B)
$LaFeAsO$[a]	4.0301	8.7368	155	137	0.36–0.6
$CeFeAsO$[b]	3.9959	8.6522	158	140	0.8
$PrFeAsO$[c]	3.997	8.6057	153	127	0.48
$NdFeAsO$[d]	3.9611	8.5724	150	141	0.25
$LaFeAsO_{0.5}H_{0.5}$[e]	3.975	8.67	95	92	1.21
$CaFe_2As_2$[f]	3.912	11.667	173	173	0.80
$SrFe_2As_2$[g]	3.920	12.40	220	220	0.94
$BaFe_2As_2$[h]	3.957	12.968	~140	~140	0.87
$Na_{0.985}FeAs$[i]	3.9448	6.9968	49	39	0.09
$Fe_{1.068}Te$[j]	3.8123	6.2517	67	67	2.25
$K_2Fe_4Se_5$[k]	8.7306	14.113	578	559	3.31
$Rb_2Fe_4Se_5$[l]	8.788	14.597	515	502	3.3
$Cs_2Fe_4Se_5$[m]	8.865	15.289	500	471	3.4
$TlFe_{1.6}Se_2$[n]	~8.71	14.02	463	100	~3

SPIN WAVE

Spin waves in $BaFe_2As_2$ and $SrFe_2As_2$

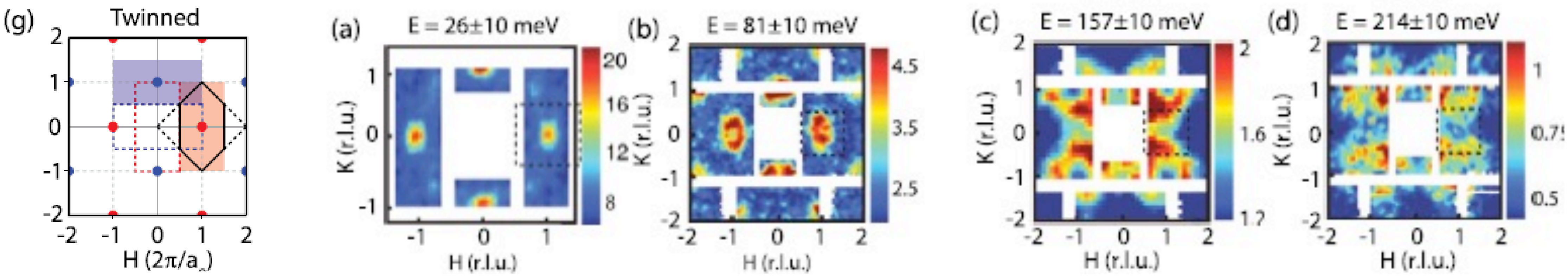

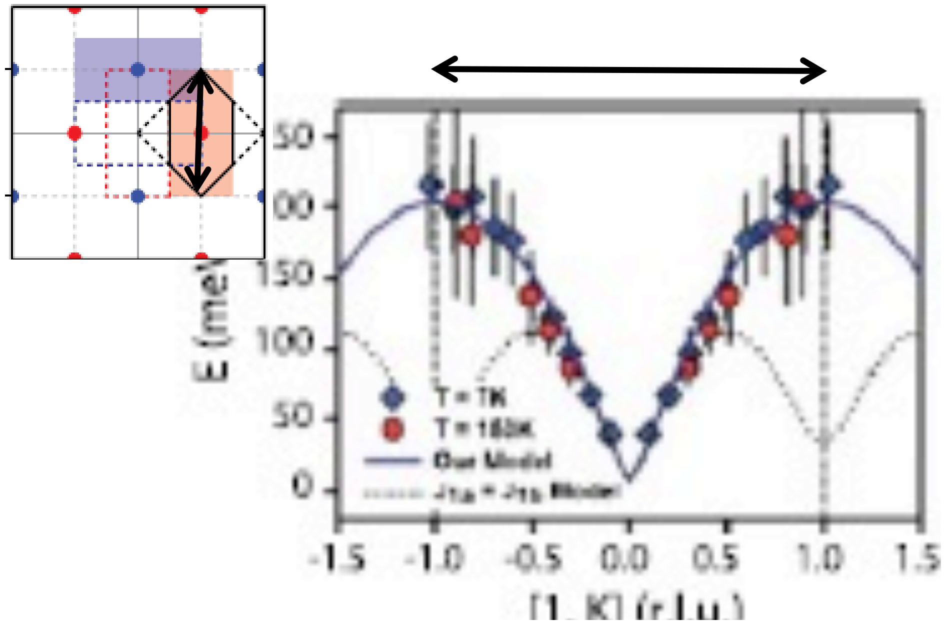

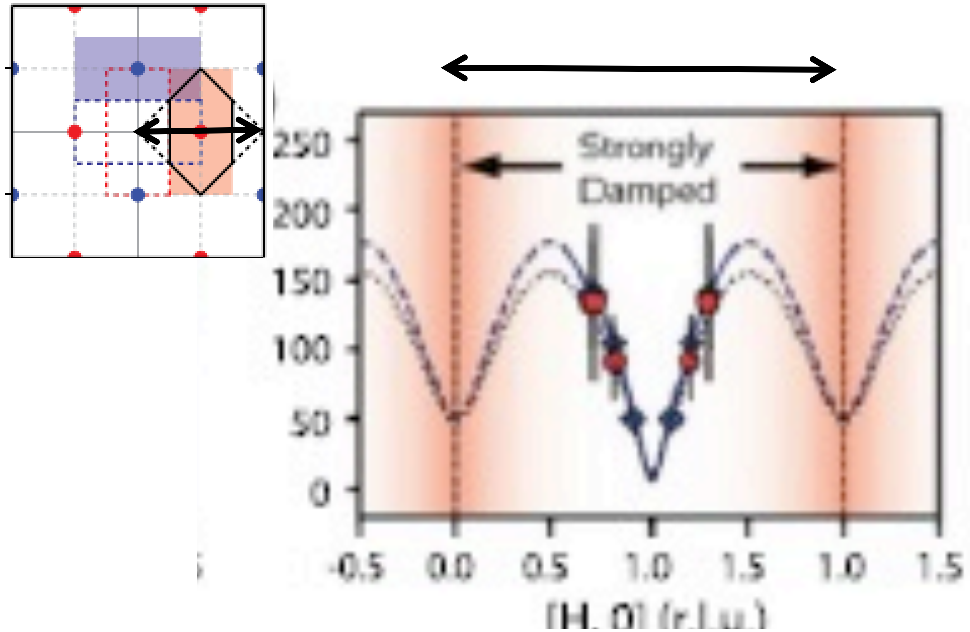

RPA

SPIN WAVE

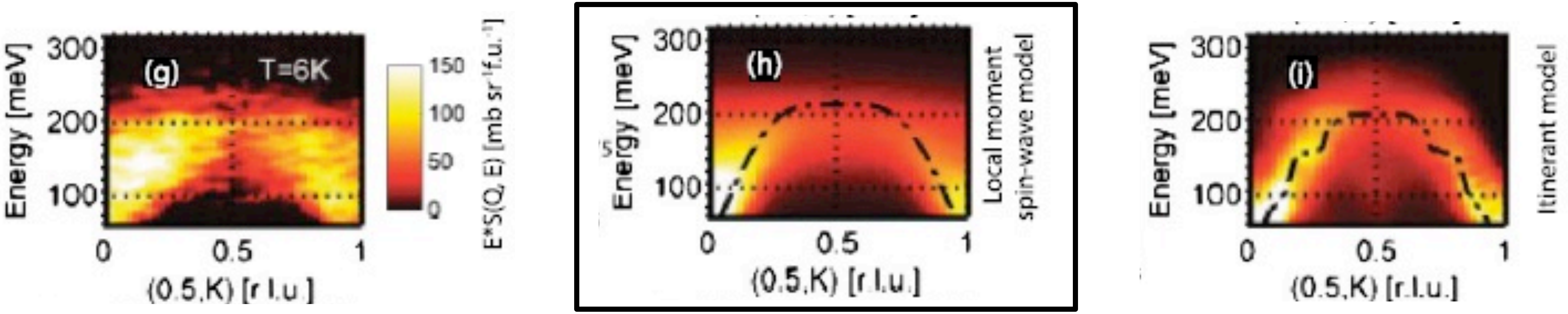

Using a **Heisenberg** Hamiltonian with anisotropic spin-wave damping, one can fit the entire spin wave spectrum with a large in-plane nearest neighbor magnetic exchange anisotropy ($J_{1a} > 0$, $J_{1b} < 0$) and finite next nearest neighbor exchange coupling ($J_2 > 0$)

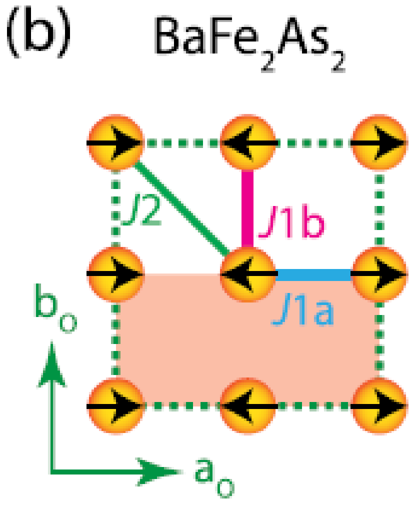

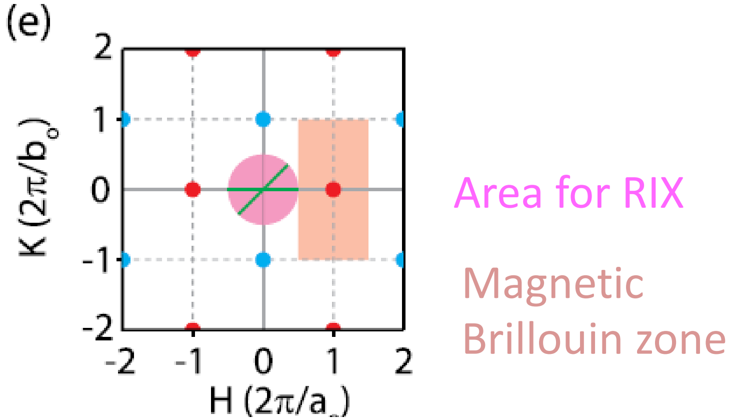

SPIN WAVE

TABLE II. Comparison of the effective magnetic exchange couplings for parent compounds of copper-based and iron-based superconductors. Here the nearest, next nearest, next next nearest neighbor, and c axis exchange couplings are SJ_{1a} (SJ_{1b}), SJ_{2a}(SJ_{2b}), SJ_3, and SJ_c, respectively, where S is the spin of the system.

Materials	SJ_{1a} (meV)	SJ_{1b} (meV)	SJ_{2a} (meV)	SJ_{2b} (meV)	SJ_3 (meV)	SJ_c (meV)
La_2CuO_4[a]	55.9 ± 2	55.9 ± 2	-5.7 ± 1.5	-5.7 ± 1.5	0	0
NaFeAs[b]	40 ± 0.8	16 ± 0.6	19 ± 0.4	19 ± 0.4	0	1.8 ± 0.1
$CaFe_2As_2$[c]	49.9 ± 9.9	-5.7 ± 4.5	18.9 ± 3.4	18.9 ± 3.4	0	5.3 ± 1.3
$BaFe_2As_2$[d]	59.2 ± 2.0	-9.2 ± 1.2	13.6 ± 1	13.6 ± 1	0	1.8 ± 0.3
$SrFe_2As_2$ (L)[e]	30.8 ± 1	-5 ± 4.5	21.7 ± 0.4	21.7 ± 0.4	0	2.3 ± 0.1
$SrFe_2As_2$ (H)[f]	38.7 ± 2	-5 ± 5	27.3 ± 0.3	27.3 ± 0.3	0	2.3 ± 0.1
$Fe_{1.05}Te$[g]	-17.5 ± 5.7	-51.0 ± 3.4	21.7 ± 3.5	21.7 ± 3.5	6.8 ± 2.8	~ 1
$Rb_{0.89}Fe_{1.58}Se_2$[h]	-36 ± 2	15 ± 8	12 ± 2	16 ± 5	9 ± 5	1.4 ± 0.2
$(Tl, Rb)_2Fe_4Se_5$[i]	-30 ± 1	31 ± 13	10 ± 2	29 ± 6	0	0.8 ± 1
$K_{0.85}Fe_{1.54}Se_2$[j]	-37.9 ± 7.3	-11.2 ± 4.8	19.0 ± 2.4	19.0 ± 2.4	0	0.29 ± 0.06

The outcomes of the fits with anisotropic in-plane magnetic exchanges are shown as solid lines while the dashed lines are calculations assuming isotropic in-plane magnetic exchange couplings.

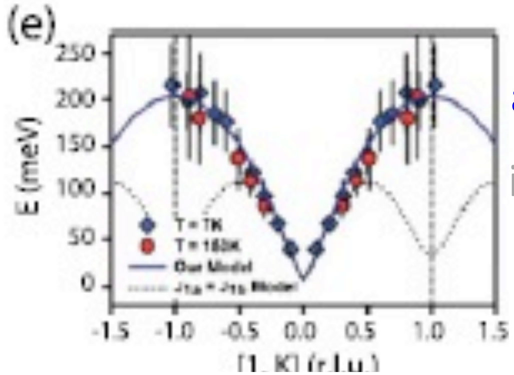

anisotropic

isotropic

SPIN WAVE

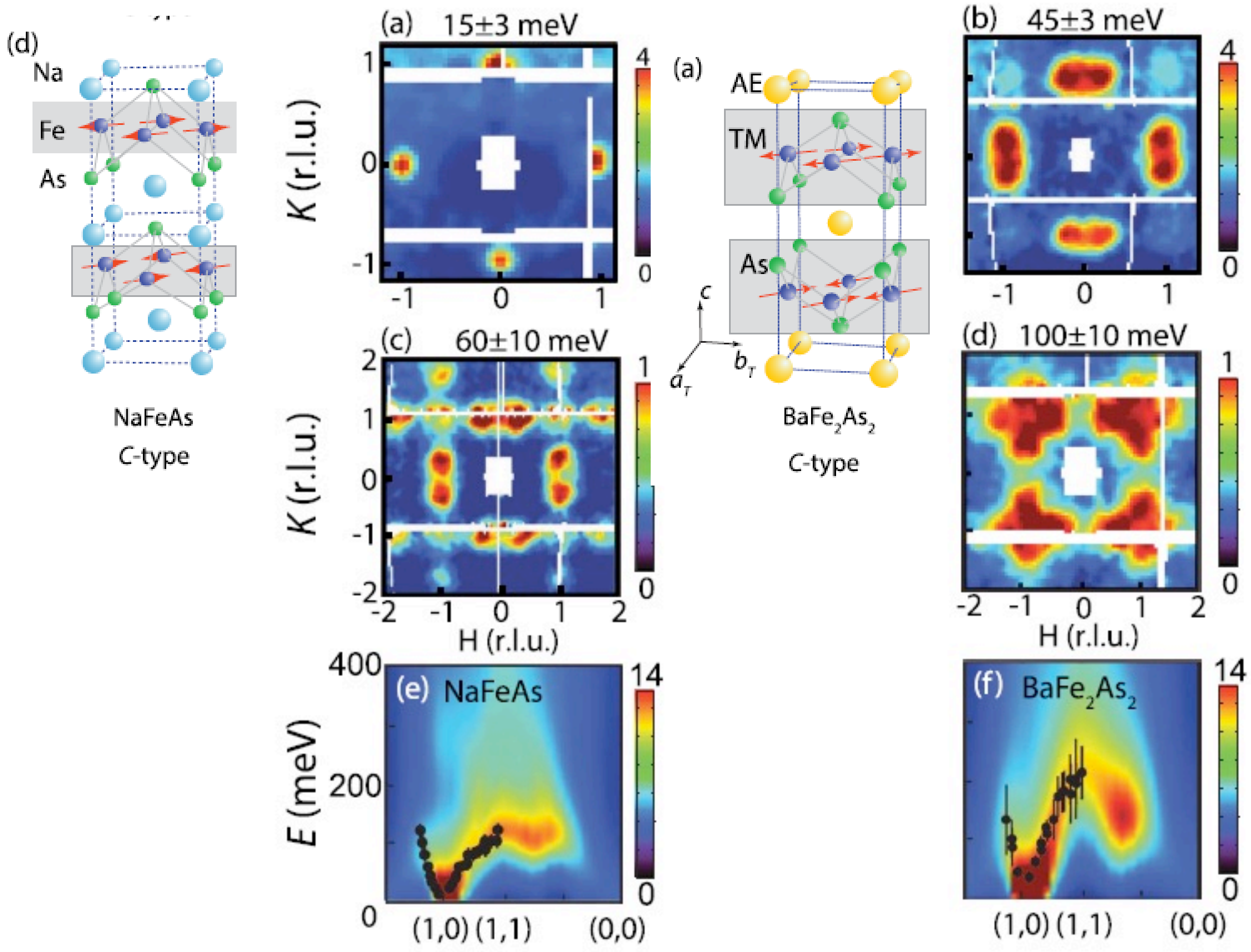

Figures compare the experimental and combined density functional theory and dynamical meanfield theory (DFT + DMFT) calculations of spin-wave dispersion of NaFeAs and $BaFe_2As_2$, respectively.

The outcome suggests that the pnictogen height is correlated with the strength of electron-electron correlations and consequently the effective bandwidth of magnetic excitations in iron pnictides

SPIN WAVE : spin-space anisotropy

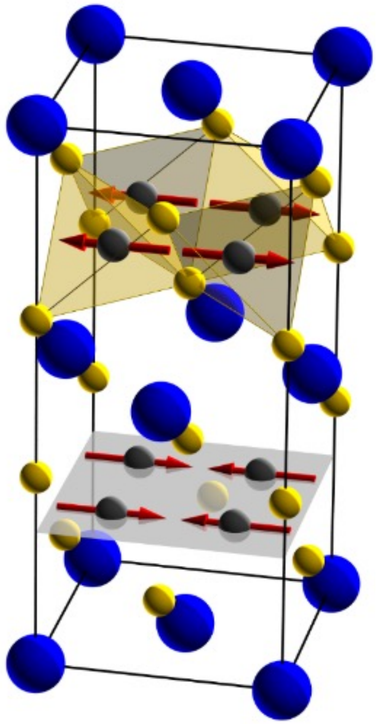

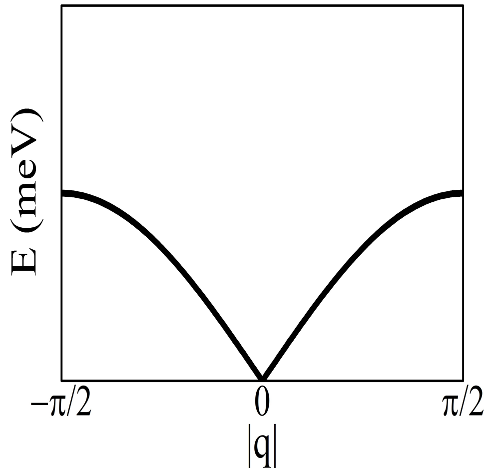

$$\mathcal{H} = \sum_{i,j} \mathrm{J}_{i,j} \mathbf{S}_i \cdot \mathbf{S}_j$$

no spin-space anisotropy

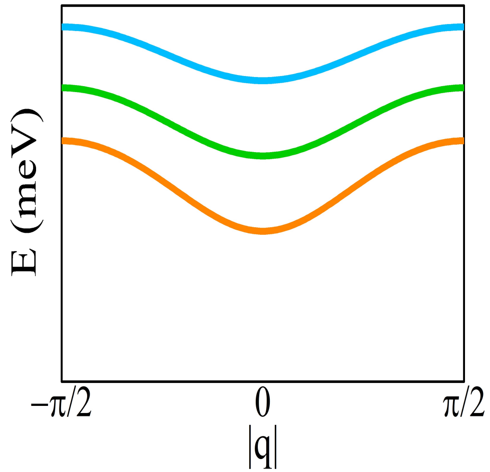

$$\mathcal{H} = \sum_{i,j} \mathrm{J}_{i,j} \mathbf{S}_i \cdot \mathbf{S}_j - \sum_{i} \Lambda (S_i^x)^2$$

with spin-space anisotropy

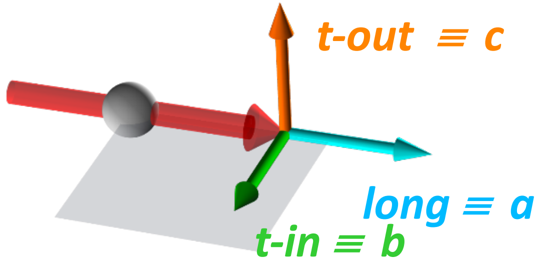

SPIN WAVE : spin-space anisotropy

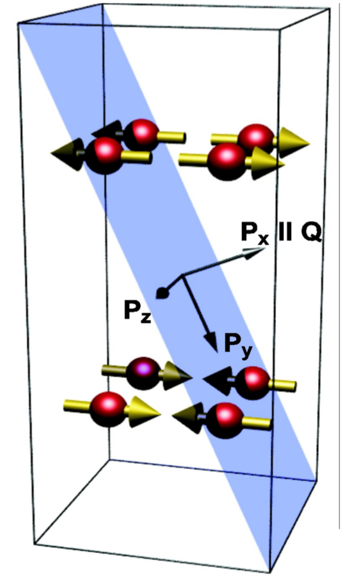

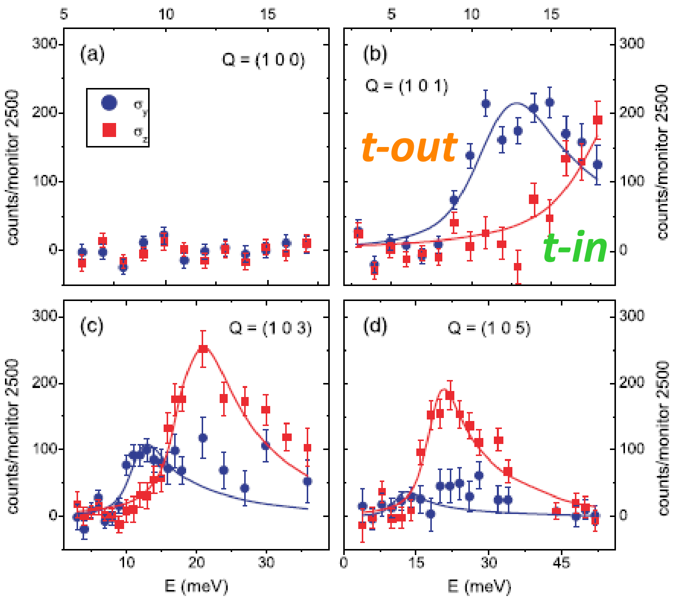

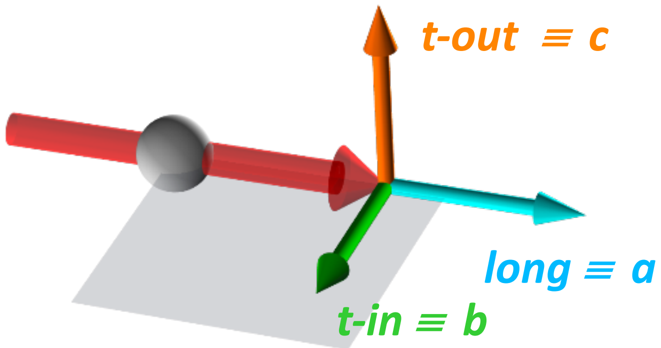

SF: $\sigma_x \sim (L/Q)^2 M_a + M_b + \{1-(L/Q)^2\} M_c$

SF: $\sigma_y \sim M_b$

SF: $\sigma_z \sim (L/Q)^2 M_a + \{1-(L/Q)^2\} M_c$

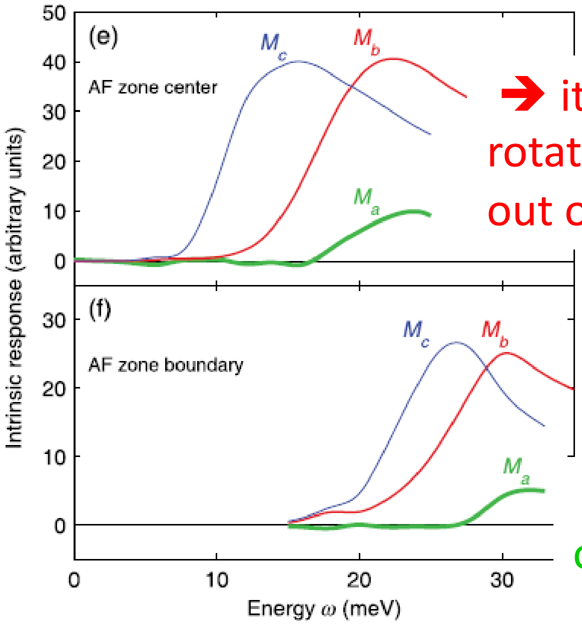

➔ it costs more energy to rotate the spin in the plane than out of it

➔ These results suggest a contribution of itinerant electrons to the magnetism

STATIC ANTIFERROMAGNETIC ORDER AND ITS DOPING EVOLUTION

F. Waßer et al., Sci. Rep. 7, 10307 (2017)

* Splitting: T_S=65K > T_N

the orthorhombic lattice distortion δ = (a-b)/(a+b) initially increases with decreasing temperature below T_N, but then decreases dramatically below T_c.

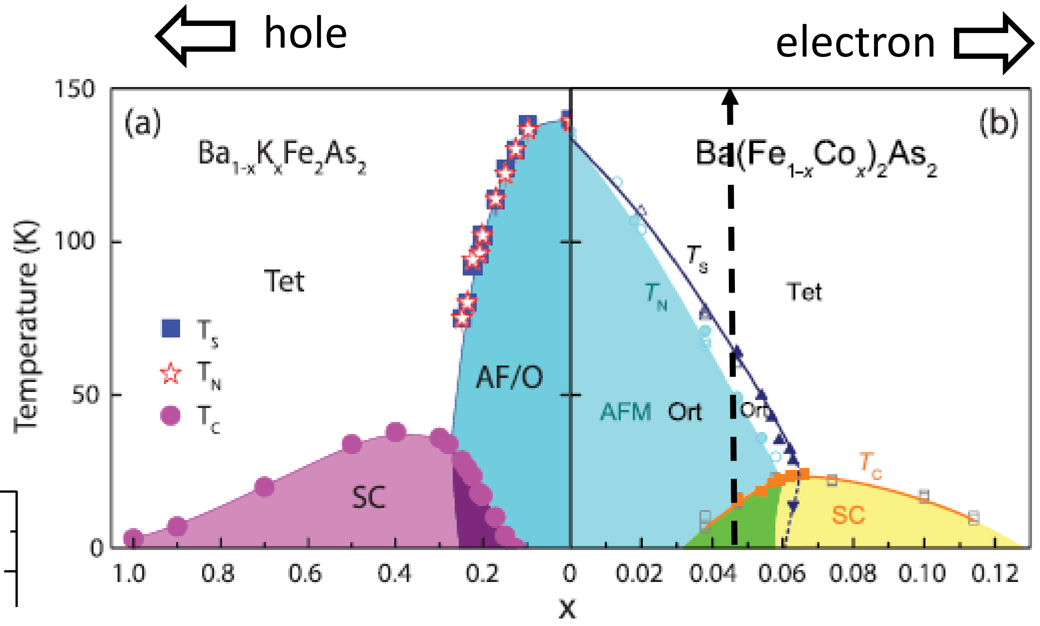

Reentrant behavior

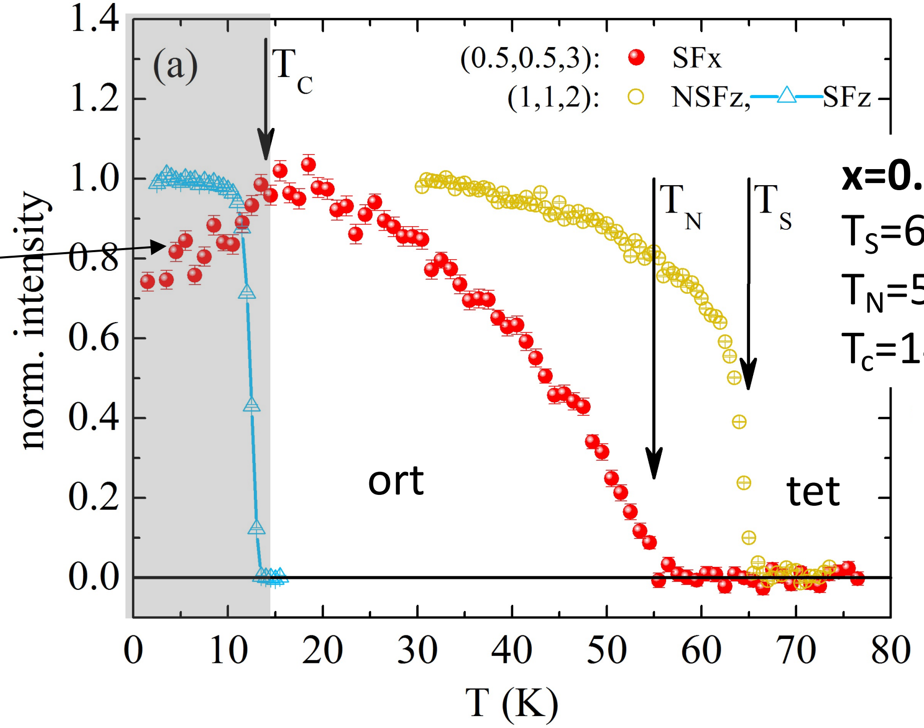

x=0.045

T_S=65K

T_N=55K

T_c=14K

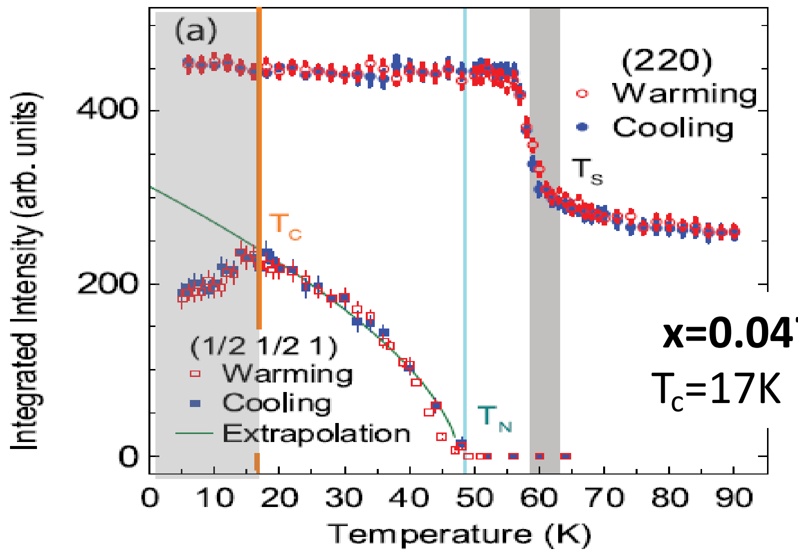

x=0.047

T_c=17K

STATIC ANTIFERROMAGNETIC ORDER AND ITS DOPING EVOLUTION

tet. AFM2 **Ort. AFM1** **tet. para**

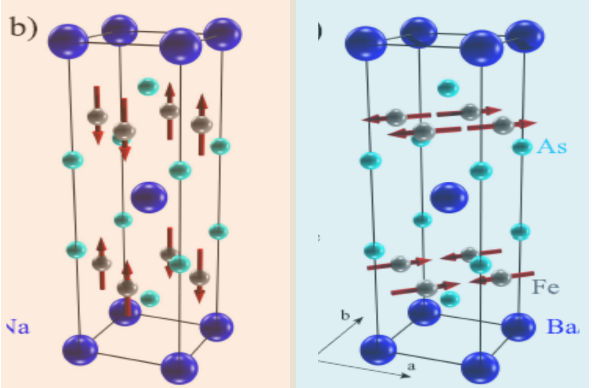

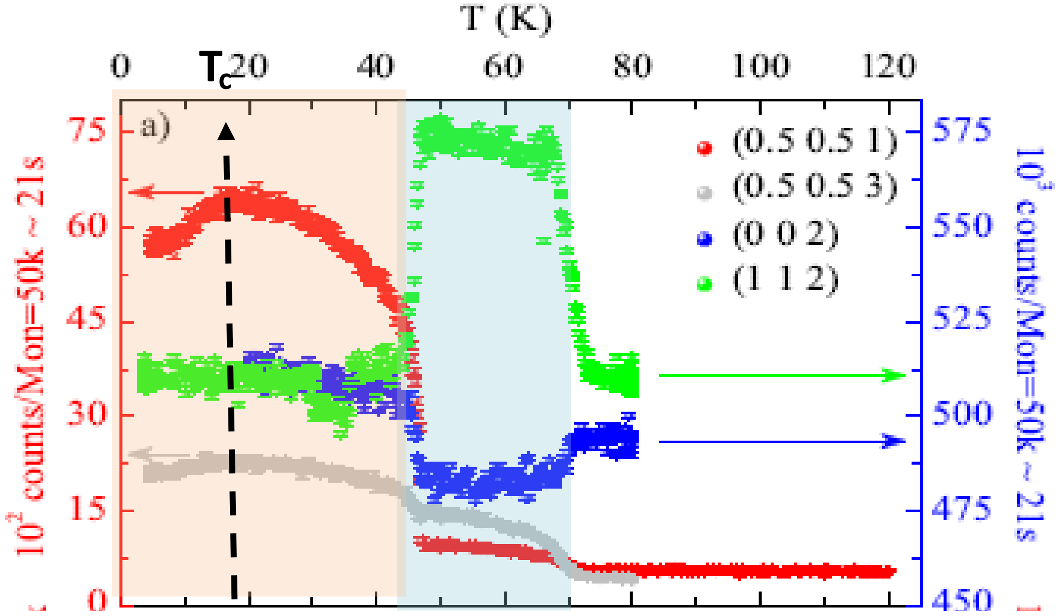

Twinned sample : $I_{mag} \sim \frac{1}{2}\,|1+(L/Q)^2|\,M_{ab} + |1-(L/Q)^2|\,M_c$

hole electron

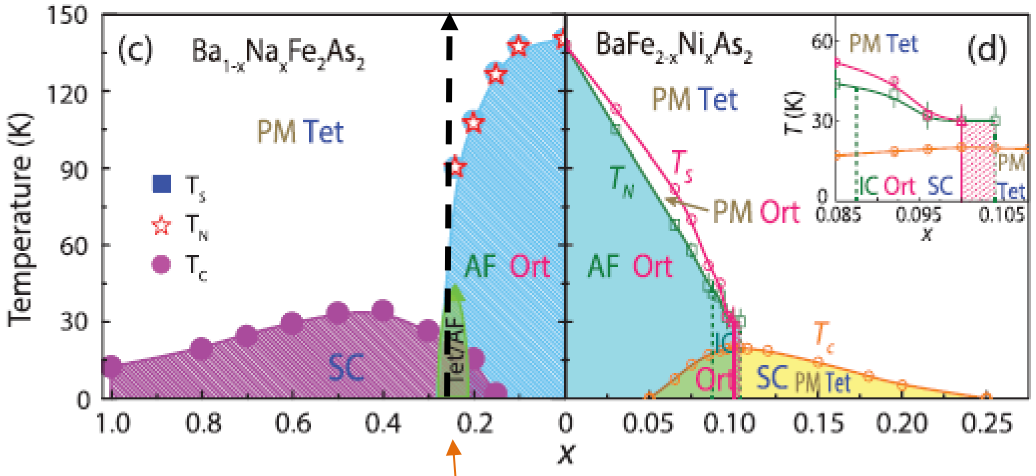

C4 tetragonal symmetry

Spin re-orientation

m // c

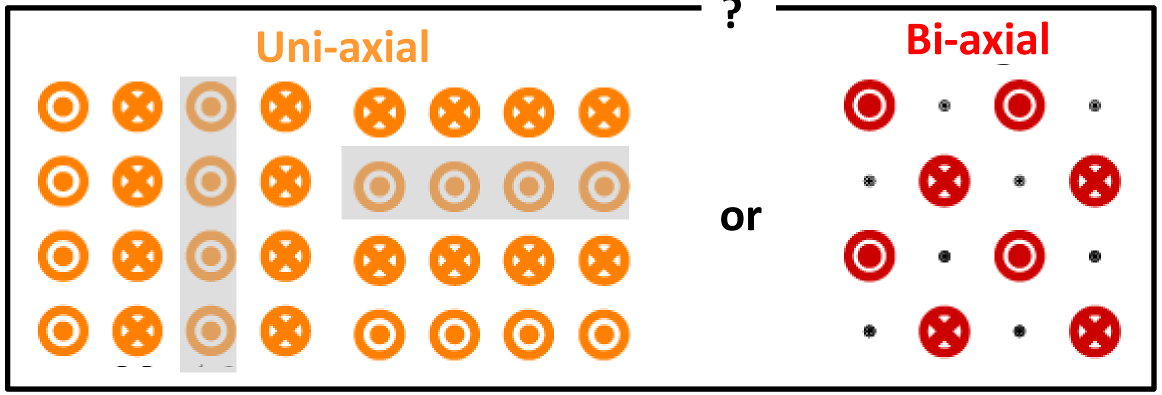

THEORETICAL CONSIDERATIONS : multi-orbital model

Multi-orbital

the direct Fe-Fe hopping along with the d-p hybridization through the pnictogen or chalcogen anions leads to a metallic groundstate

$$H_0 = \sum_{ij}\sum_{\ell n\sigma} t_{ij}^{\ell n} c_{i\ell\sigma}^{\dagger} c_{jn\sigma} + \sum_i \sum_{\ell\sigma} \varepsilon_\ell n_{i\ell\sigma}.$$

$\ell = (1, 2, \ldots, 5)$ denotes the Fe-d orbitals $(d_{xz}, d_{yz}, d_{xy}, d_{x^2-y^2}, d_{3z^2-r^2})$

$t_{ij}^{\ell n}$ describe the one-electron hopping

ε_ℓ is the site energy of the ℓth orbit

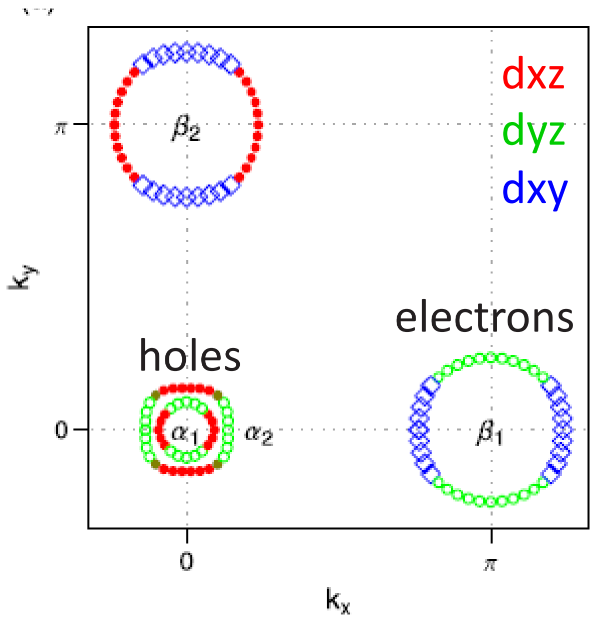

Multi-interaction

The on-site Coulomb and exchange interaction part of the Hamiltonian

$$H_1 = \sum_i \Bigg(\sum_\ell U n_{i\ell\uparrow} n_{i\ell\downarrow} + U' \sum_{\ell'<\ell} n_{i\ell} n_{i\ell'} - J \sum_{\ell \neq \ell'} \mathbf{S}_{i\ell} \cdot \mathbf{S}_{i\ell'} + J' \sum_{\ell \neq \ell'} c_{i\ell\uparrow}^{\dagger} c_{i\ell\downarrow}^{\dagger} c_{i\ell'\downarrow} c_{i\ell'\uparrow} \Bigg),$$

$U' = U - 2J$

$J' = J$

with $n_{i\ell} = n_{i\ell\uparrow} + n_{i\ell\downarrow}$ and $\mathbf{S}_{i\ell} = \frac{1}{2} c_{i\ell\sigma}^{\dagger} \boldsymbol{\sigma}_{\sigma\sigma'} c_{i\ell\sigma'}$

U and U' are the intraorbital and interorbital Coulomb interactions.
J is the Hund's rule exchange, and J' is the so-called pair hopping term

THEORETICAL CONSIDERATIONS : nesting

Shortly after the discovery of iron-based superconductors, band structure calculations predicted that the Fermi surfaces of parent compounds would consist of:
quasi-2D near-circular hole pockets centered around the zone center Γ,
2D electron pockets centered around the (1,0) and (0,1) points in the orthorhombic unfolded Brillouin zone

holes

electrons

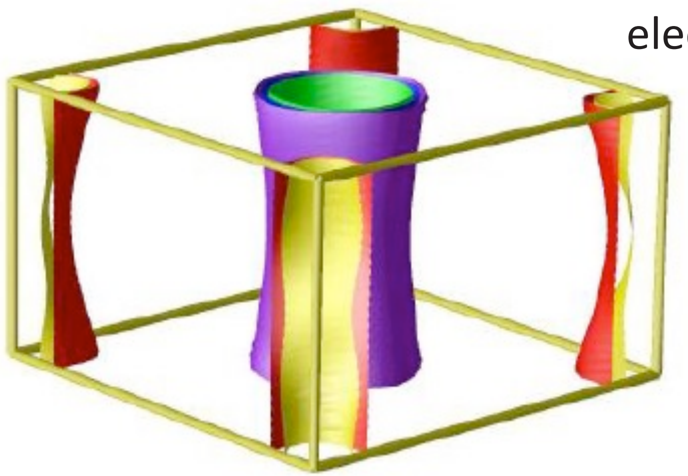

5 3d-Fe orbitales

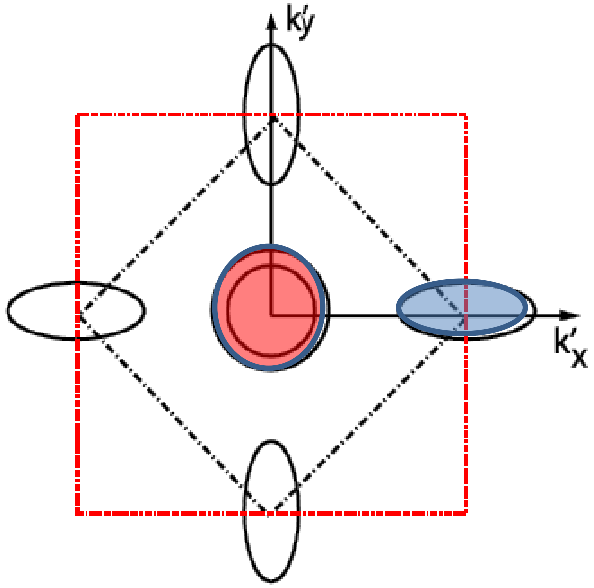

In weak-coupling analysis:

- Fe-based superconductors and their parents are assumed to be good metals made of itinerant electrons with a spin-density-wave–type AF order.

* Spin waves and spin excitations can then be calculated using RPA in a multiband Hubbard model with appropriate Fermi surfaces for hole and electron pockets

THEORETICAL CONSIDERATIONS : anisotropy and SOC

Scherer et al., PRL 2018

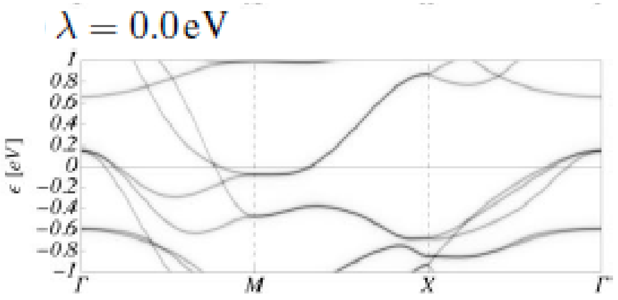

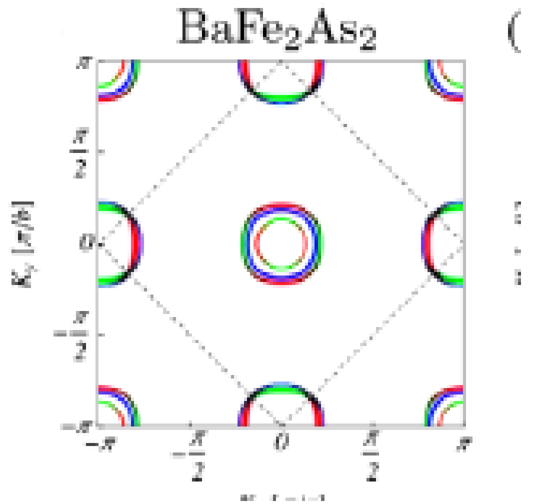

multiorbital Hubbard Hamiltonian $H = H_0 + H_{\mathrm{SOC}} + H_{\mathrm{int}}$

$$H_0 = \sum_{\sigma} \sum_{l,l',i,j} \sum_{\mu,\nu} c^{\dagger}_{li\mu\sigma}\left(t^{\mu\nu}_{li;l'j} - \mu_0 \delta_{ll'}\delta_{ij}\delta_{\mu\nu}\right) c_{l'j\nu\sigma}$$

$$\boxed{H_{\mathrm{SOC}} = \frac{\lambda}{2} \sum_{l,i} \sum_{\mu,\nu} \sum_{\sigma,\sigma'} c^{\dagger}_{li\mu\sigma} [\mathbf{L}_l]_{\mu\nu} \cdot \boldsymbol{\sigma}_{\sigma\sigma'} c_{li\nu\sigma'}}$$

unique source of anisotropy

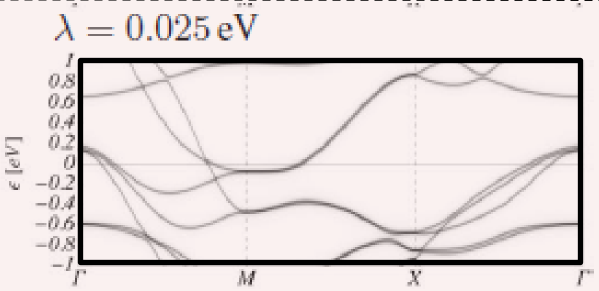

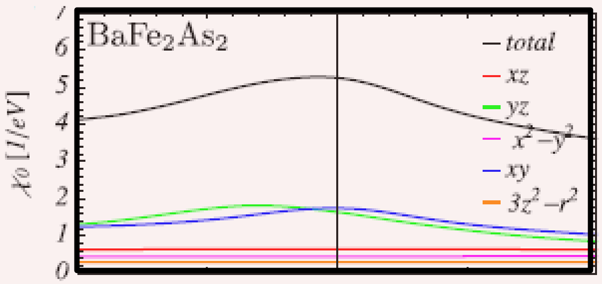

SOC modify the non interaction spin susceptibility

$$[\chi_0]^{X_1;X_2}_{X_3;X_4}(\mathrm{i}\omega_n, \mathbf{q}) = -\frac{1}{N} \sum_{\mathbf{k},n_1,n_2} [\mathcal{M}_{n_1,n_2}(\mathbf{k},\mathbf{q})]^{X_1;X_2}_{X_3;X_4} \frac{f(E_{n_1}(\mathbf{k}-\mathbf{q})) - f(E_{n_2}(\mathbf{k}))}{\mathrm{i}\omega_n + E_{n_1}(\mathbf{k}-\mathbf{q}) - E_{n_2}(\mathbf{k})},$$

$$H_{\mathrm{int}} = U \sum_{l,i,\mu} n_{li\mu\uparrow} n_{li\mu\downarrow} + \left(U' - \frac{J}{2}\right) \sum_{l,i,\mu<\nu,\sigma,\sigma'} n_{li\mu\sigma} n_{li\nu\sigma'}$$
$$-2J \sum_{l,i,\mu<\nu} \mathbf{S}_{li\mu} \cdot \mathbf{S}_{li\nu} + J' \sum_{l,i,\mu<\nu,\sigma} c^{\dagger}_{li\mu\sigma} c^{\dagger}_{li\mu\bar{\sigma}} c_{li\nu\bar{\sigma}} c_{li\nu\sigma}$$

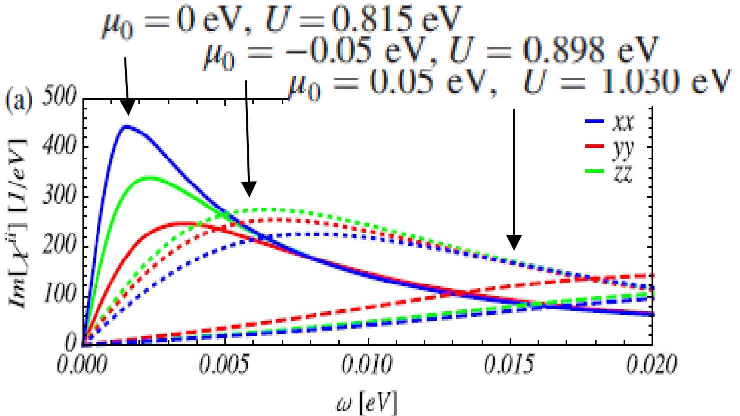

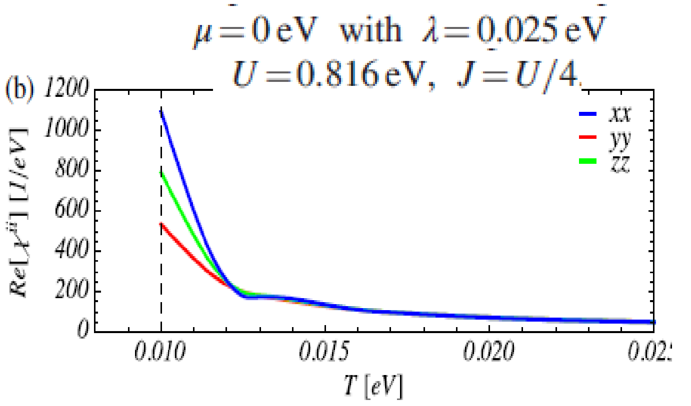

THEORETICAL CONSIDERATIONS : preemptive state

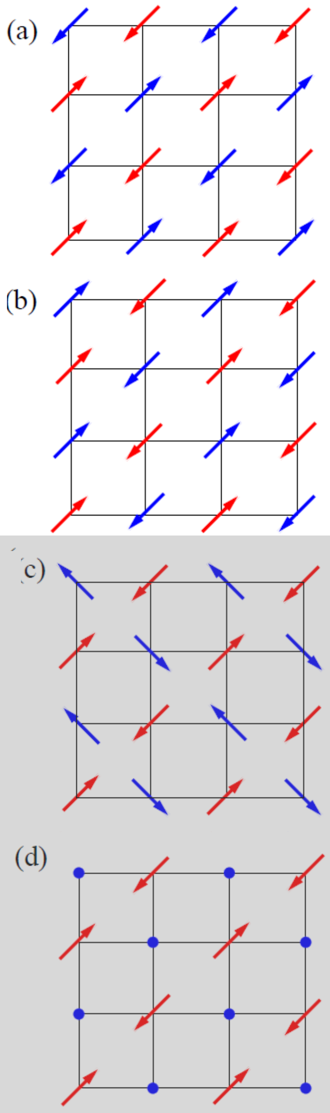

Various SDW spin configurations described by $\vec{\Delta}_1 e^{i\mathbf{Q}_1 R} + \vec{\Delta}_2 e^{i\mathbf{Q}_2 R}$

(1,2) = (x,y)

$\vec{\Delta}_y = 0$

Stripe-SDW
C_4-> C_2 + Broken O(3) spin rotation symmetry

$\vec{\Delta}_x = 0$

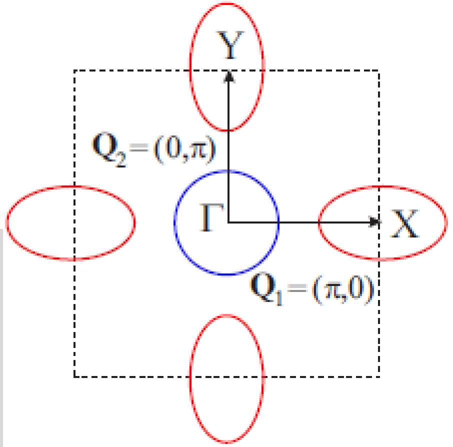

Spin-Vortex Crystal

$\vec{\Delta}_x \perp \vec{\Delta}_y$

Charge-SDW

$\vec{\Delta}_x = \vec{\Delta}_y$

C_4

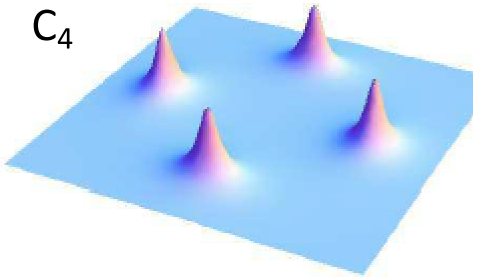

Stripe-nematic
C_4-> C_2

$\langle \Delta_X^2 \rangle = \langle \Delta_Y^2 \rangle$
$\langle \Delta_X \rangle = \langle \Delta_Y \rangle = 0$

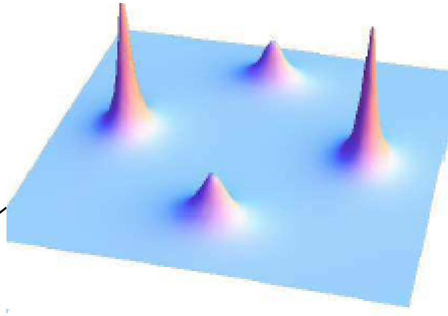

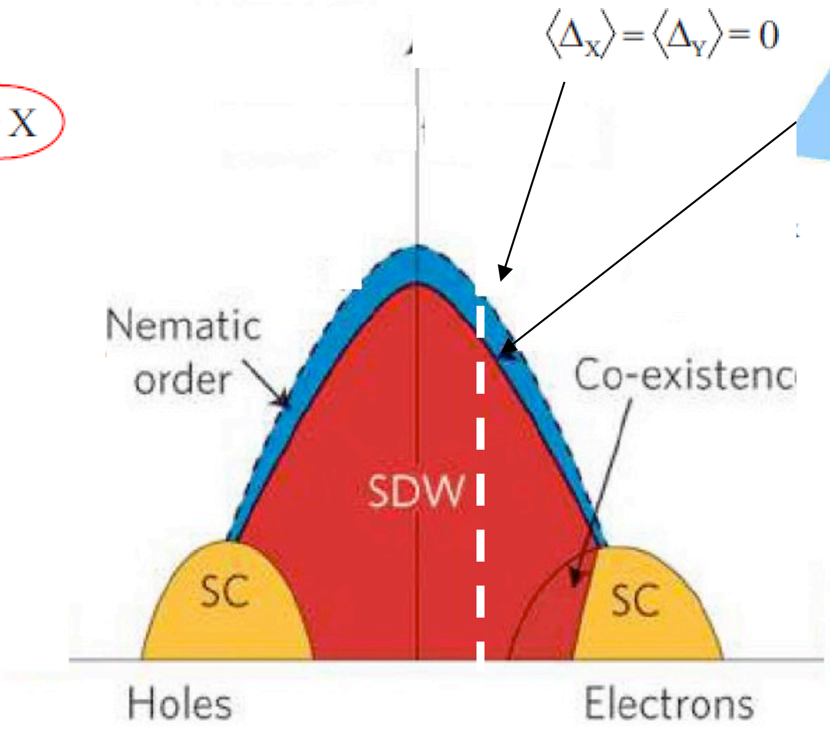

$\langle \Delta_X^2 \rangle > \langle \Delta_Y^2 \rangle$
$\langle \Delta_X \rangle = \langle \Delta_Y \rangle = 0$

THEORETICAL CONSIDERATIONS weak vs. strong coupling limit

In the **weak coupling limit**, the large in-plane effective magnetic exchange coupling anisotropy in the spin waves of Fe pnictides can be understood as due to the ellipticity of the electron pockets, which induces frustration between the (1,0) and (0,1) wave vectors connecting the hole and electron pockets

In a systematic study of spin excitations in $BaFe_{2-x}Ni_xAs_2$, the electron-doping evolution of the low-E spin excitations was found to qualitatively agree with RPA calculations of the nested Fermi surfaces

However, the high-E spin excitations are weakly electron-doping independent, and have values much different from that found by RPA calculations). These results suggest that the weak-coupling analysis based on purely itinerant electrons is insufficient to explain the entire spin-excitation spectrum and its electron- or hole-doping evolution.

In the **strong-coupling limit**, all unpaired electrons, not just itinerant electrons near the Fermi surface, participate in forming magnetic order.

The AF ordered state of Fe-based superconductors can be described by a local-moment Heisenberg Hamiltonian. In this picture, the large in-plane magnetic exchange coupling anisotropy in the parent compounds of iron pnictides is understood in terms of the presence of the biquadratic exchange coupling K between the nearest spins in the AF ordered states, which can be mapped onto the J1a-J1b model with a specific relationship between J1a-J1b and J1-K

$$H = J_1\sum_{i,\delta}\mathbf{S}_i\cdot\ \mathbf{S}_{i,\delta} + J_2\sum_{i,\delta}\mathbf{S}_i\cdot\mathbf{S}_{i+\delta} - K\sum_{i,\delta}(\mathbf{S}_i\cdot\mathbf{S}_{i,\delta})^2,$$

However, in a strict local-moment Heisenberg Hamiltonian, spin waves should have only transverse components and do not support longitudinal spin excitations in the AF ordered phase of Fe pnictides as seen in polarized INS.

Furthermore, the electron- and hole-doping evolution of the low-energy spin excitations are consistent with the Fermi surface nesting predictions, but it is unclear whether the data are also compatible with a pure local-moment Heisenberg Hamiltonian.

PARAMAGNETIC AND SUPERCONDUCTING STATE

The electron and hole-doping evolution of the spin excitations in the BaFe2As2 family of iron pnictides

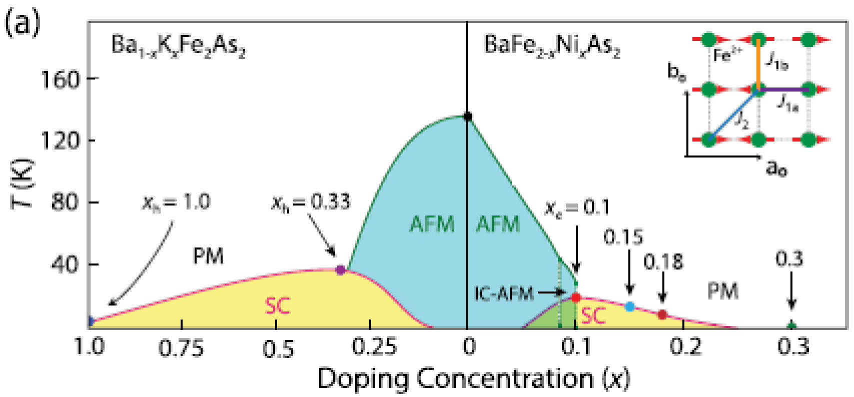

1/ High-E spin dispersive spin excitations

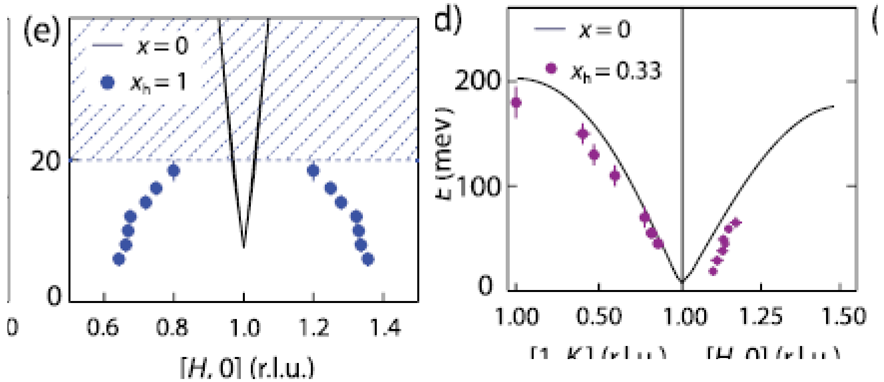

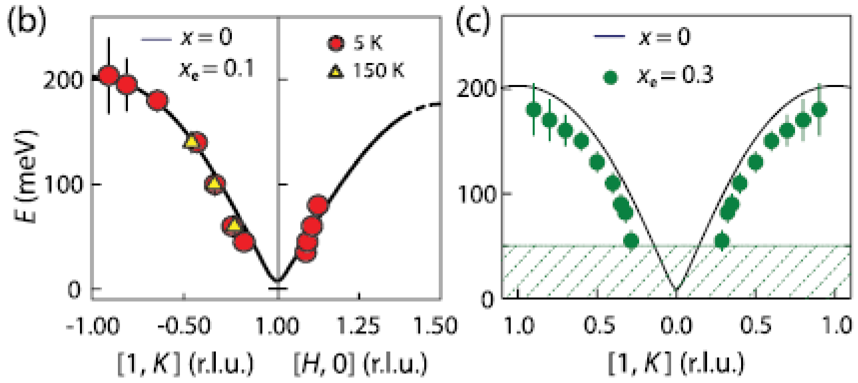

While electron doping does not much affect the high-energy spin excitations and dispersion, hole doping suppresses the high-E spin excitations.

Upon electron doping to induce optimal superconductivity, spin excitations become broader at low energies (E ≤ 80 meV) and couple to superconductivity almost unchanged at high-E(E > 80 meV)

PARAMAGNETIC AND SUPERCONDUCTING STATE

The electron and hole-doping evolution of the spin excitations in the BaFe2As2 family of iron pnictides

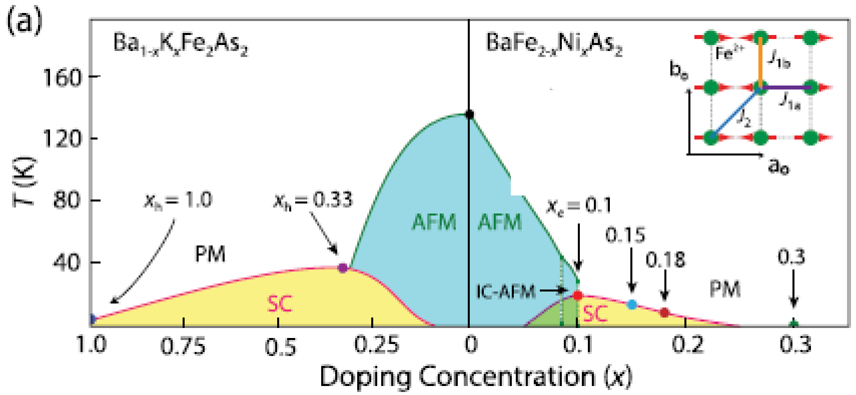

2/ E-dependence of the local dynamic susceptibility $\chi''(\omega)$

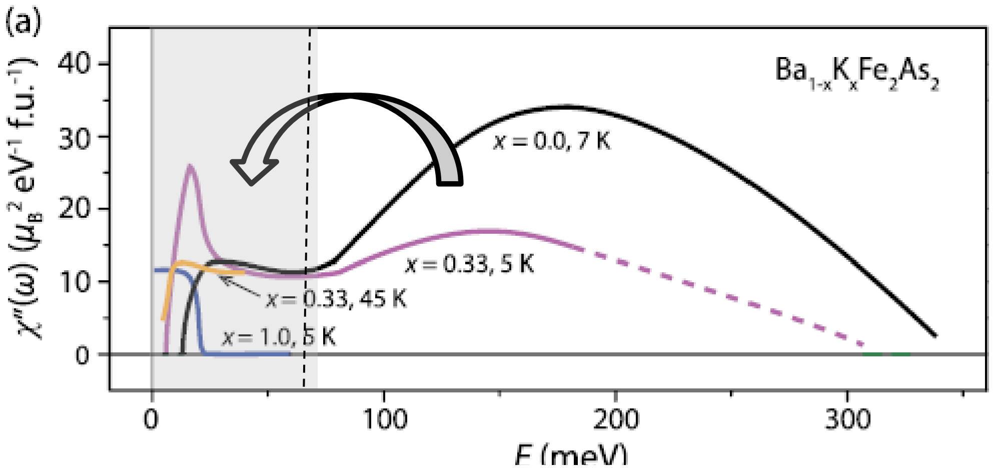

The effect of hole doping near optimal superconductivity is to suppress high-E spin excitations and transfer spectral weight to low E

The intensity changes across Tc for hole-doped Ba0.67K0.33Fe2As2 are much larger than those of the electron-doped BaFe1.9Ni0.1As2

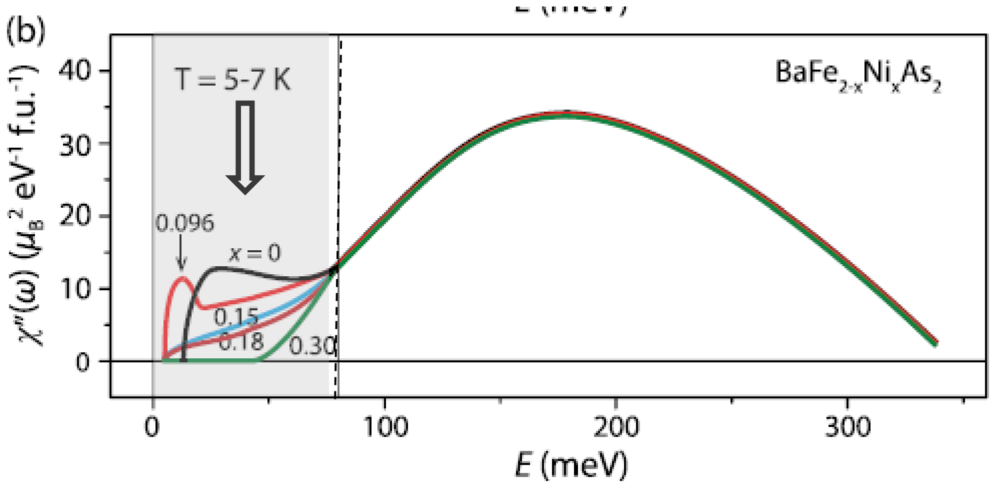

As a function of increasing electron doping, the local dynamic susceptibility at low E decreases and finally vanishes for electron overdoped non SC sample

PARAMAGNETIC AND SUPERCONDUCTING STATE

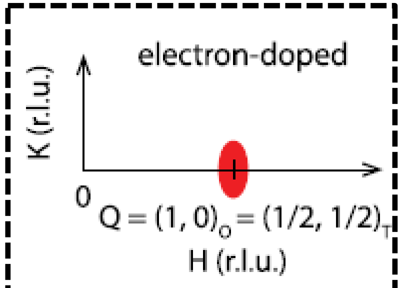

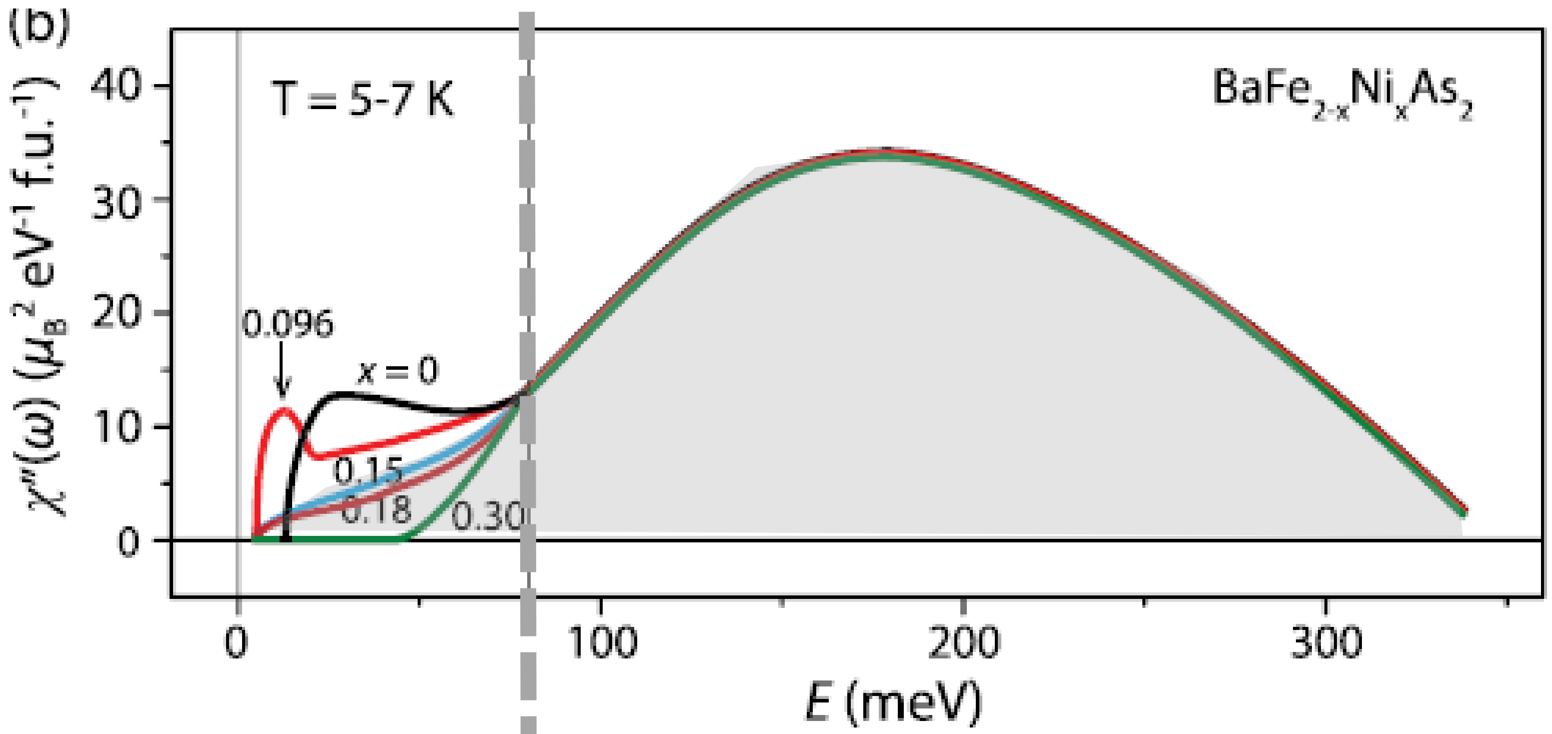

x=0.15

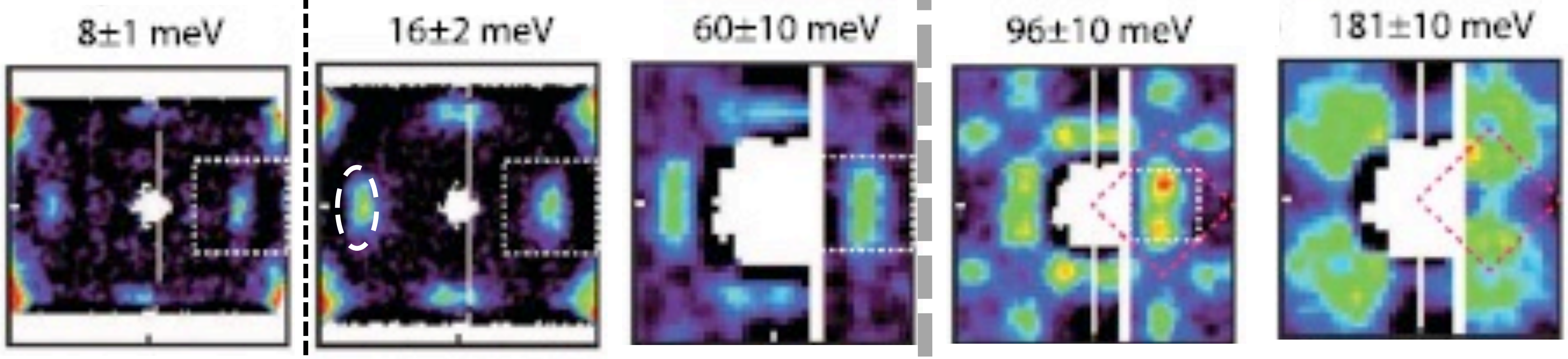

PARAMAGNETIC AND SUPERCONDUCTING STATE

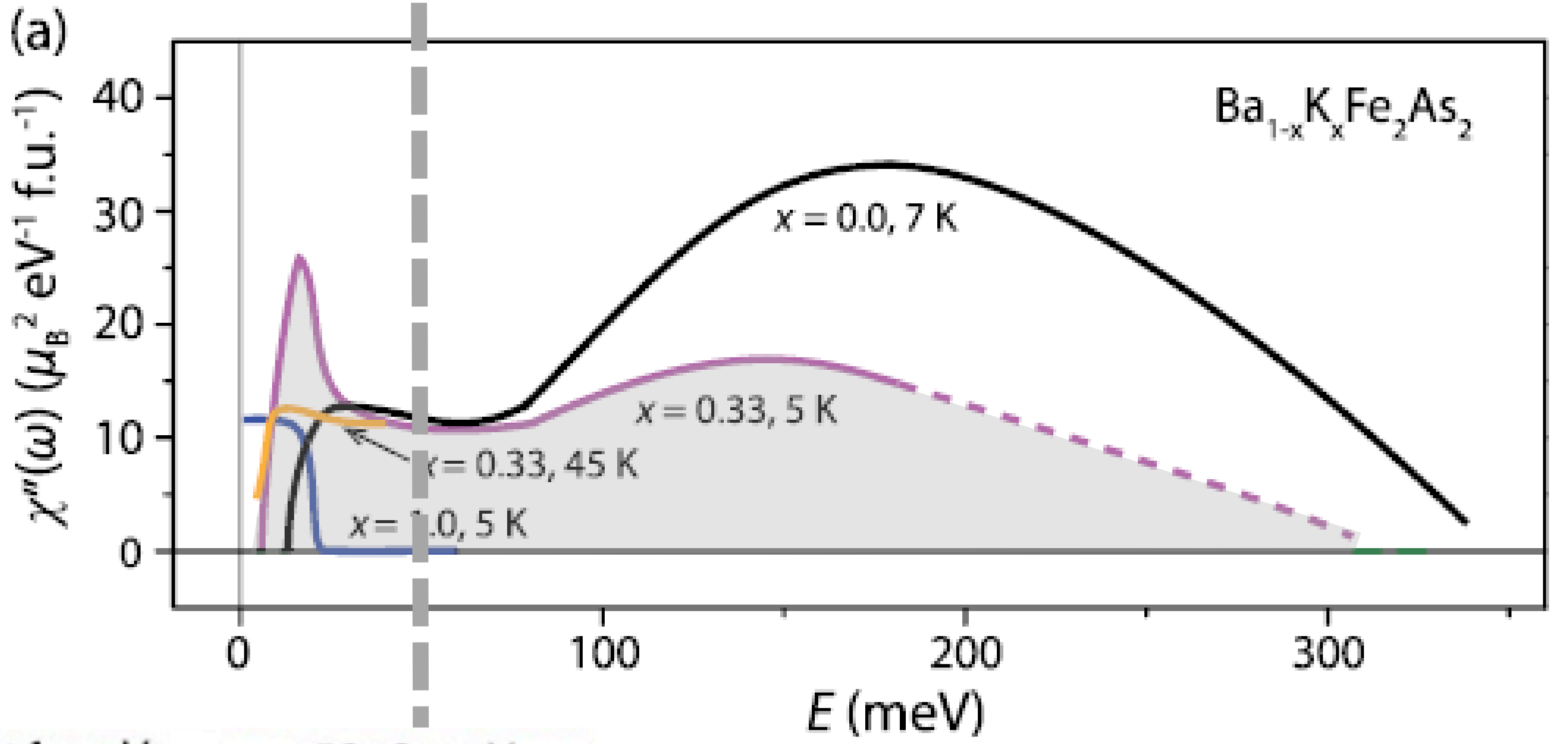

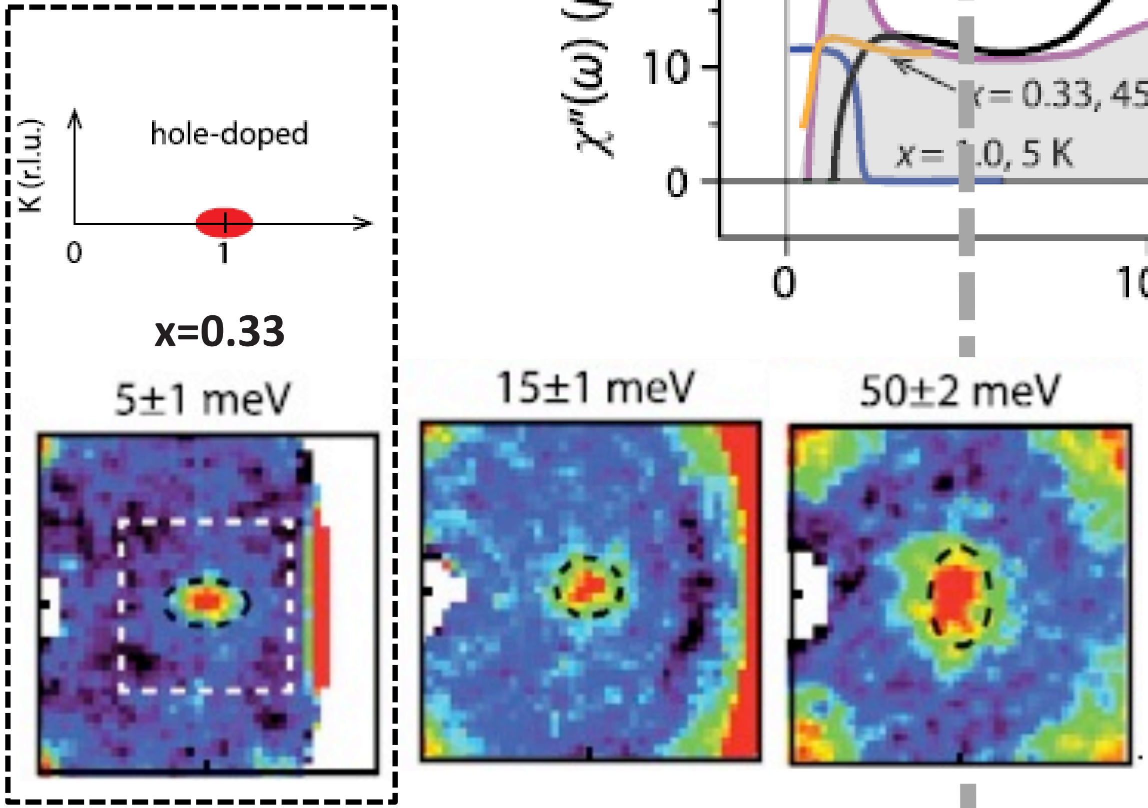

PARAMAGNETIC AND SUPERCONDUCTING STATE

The electron and hole-doping evolution of the spin excitations in the BaFe2As2 family of iron pnictides

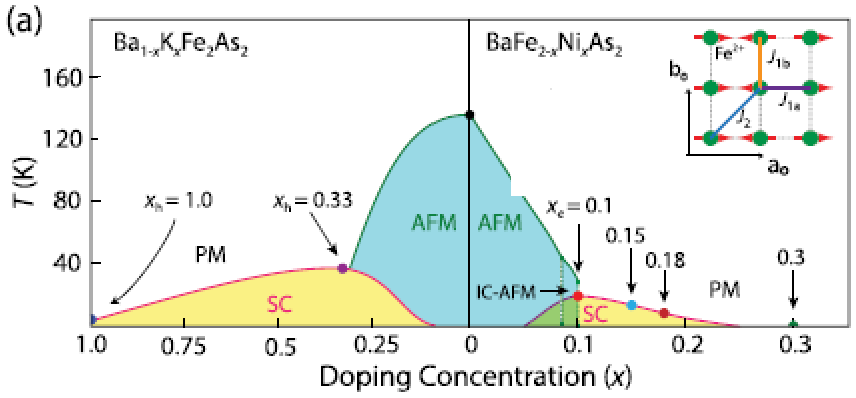

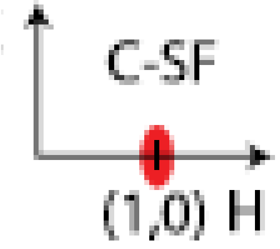

2/ low energy spin fluctuation: itinerant character

electron-doped $BaFe_2As_2$.

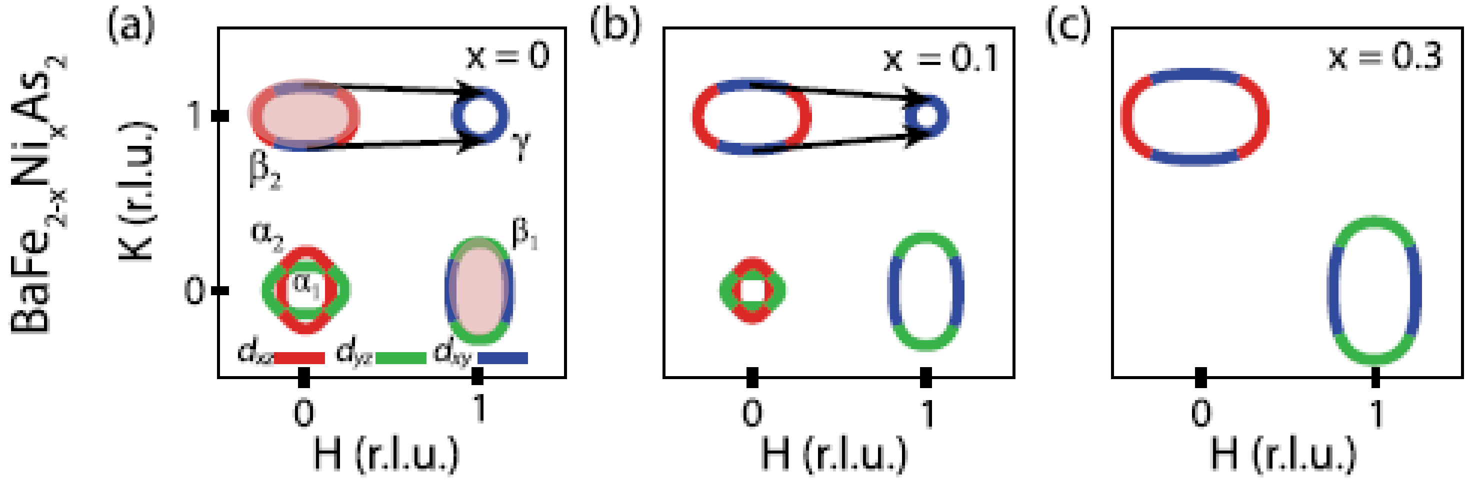

hole-like **pockets near Γ** and
electron-like pockets
near M point at Q_{AF} (1,0)

With increasing electron doping, the hole and electron Fermi surfaces decrease and increase in size

PARAMAGNETIC AND SUPERCONDUCTING STATE

The electron and hole-doping evolution of the spin excitations in the BaFe2As2 family of iron pnictides

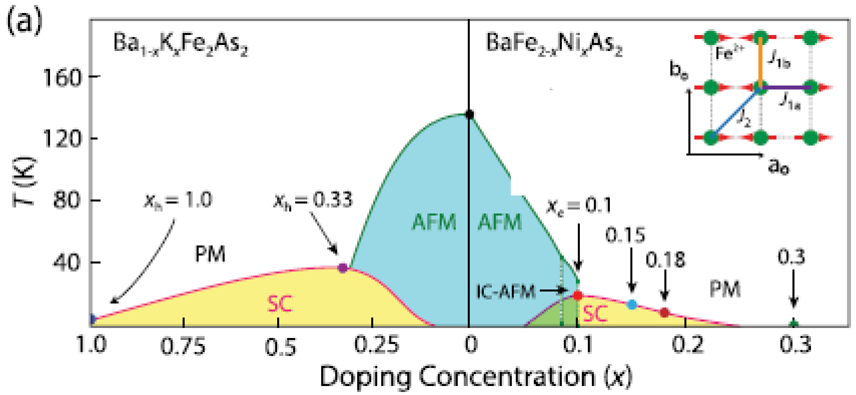

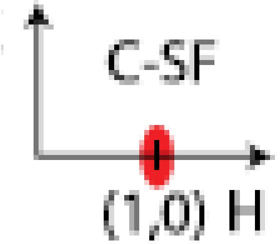

2/ low energy spin fluctuation: itinerant character

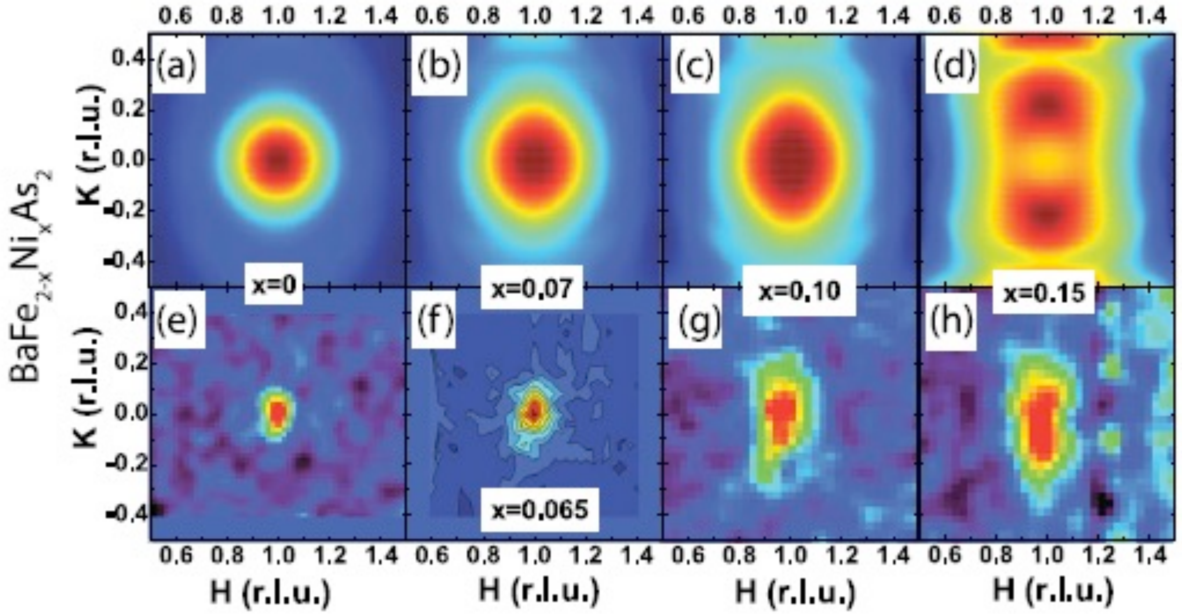

Comparison of wave vector evolution of the low-energy spin excitations in electron-doped BaFe2−xNixAs2 with the RPA calculation based on a rigid band shift model.

E = 8 meV
x = 0; 0.07; 0.1, and 0.15, respectively.

PARAMAGNETIC AND SUPERCONDUCTING STATE

The electron and hole-doping evolution of the spin excitations in the BaFe2As2 family of iron pnictides

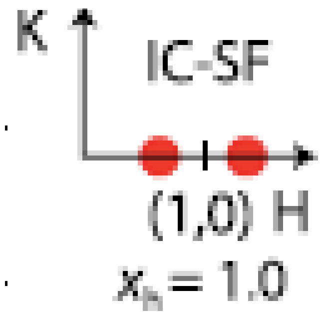

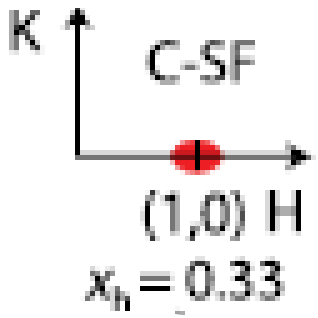

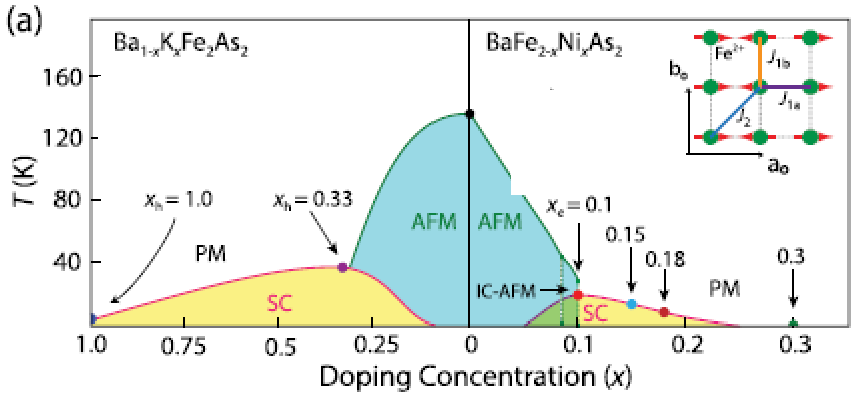

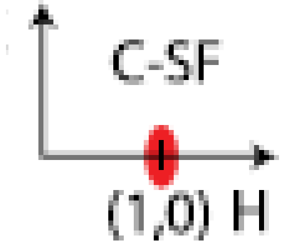

2/ low energy spin fluctuation: itinerant character

In the case of hole-doped materials, RPA calculations predicted that spin excitations should be longitudinally elongated and thus **rotated 90**° from those of the electron dopedBa$Fe_{2-x}T_xAs_2$

INS experiments on hole-doped superconducting $Ba_{0.67}Ka_{0.33}Fe_2As_2$ (T_c = 38 K) reveal longitudinally elongated spin excitations for energies near the resonance, **consistent with RPA calculations**

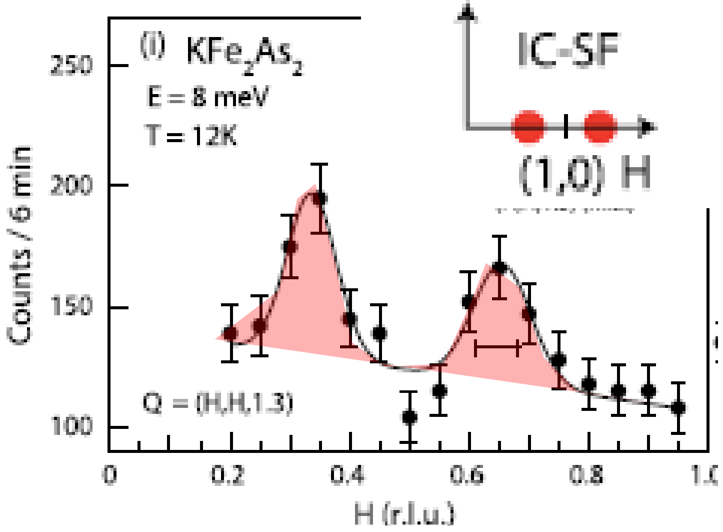

hole-overdoped KFe2As2 found
2 incommensurate spin-excitation peaks
located longitudinally away from QAF

SUPERCONDUCTING STATE : Spin Resonant Mode(s) - SRMs

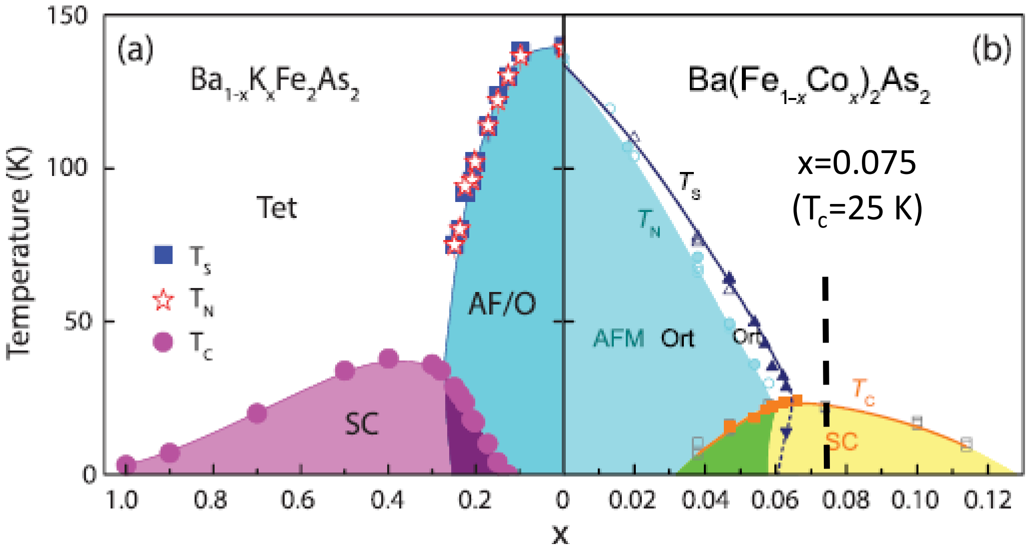

Below T_c, the spin excitation spectrum is characterized by

1/ a spin gap

2/ the enhanecment of the magnetic responce at the spin resonant mode energy

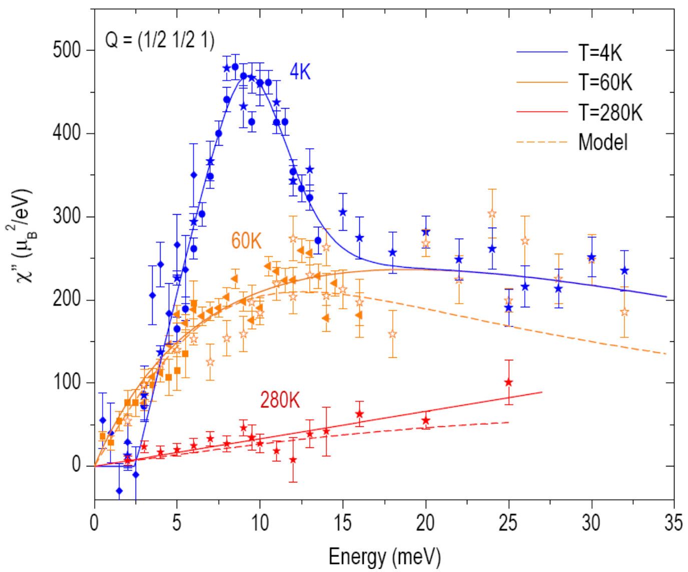

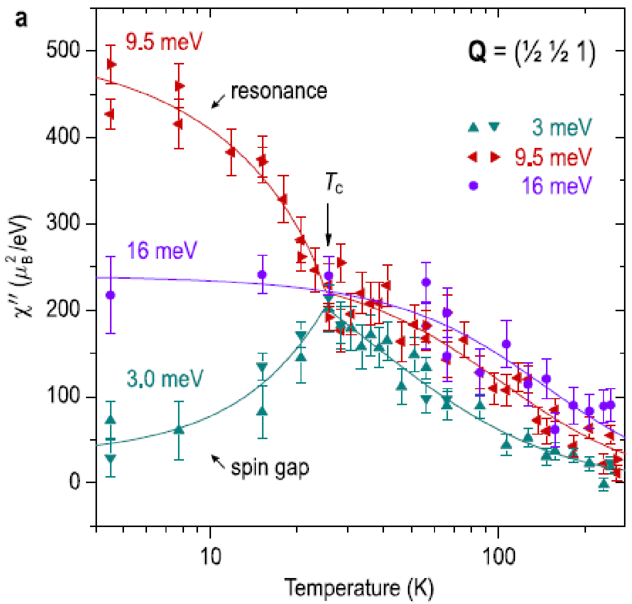

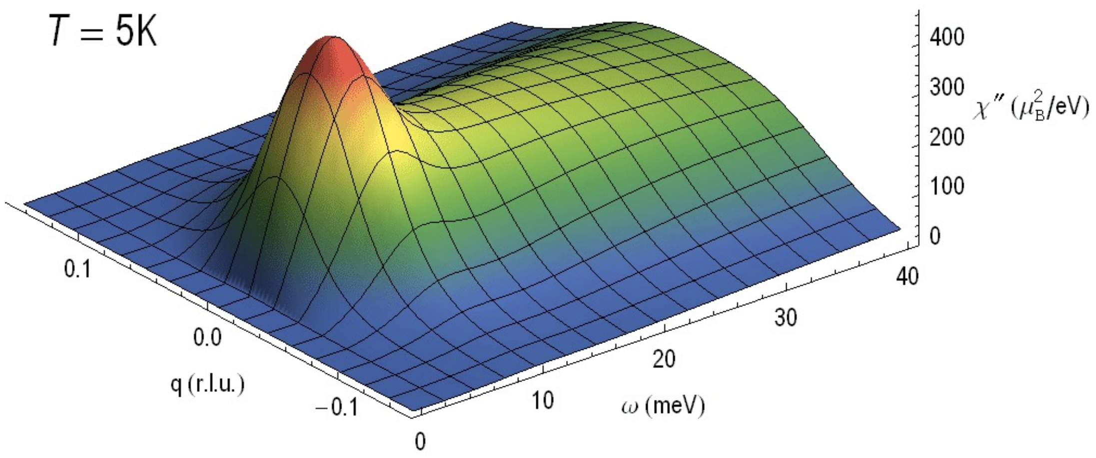

SUPERCONDUCTING STATE : Spin Resonant Mode(s) - SRMs

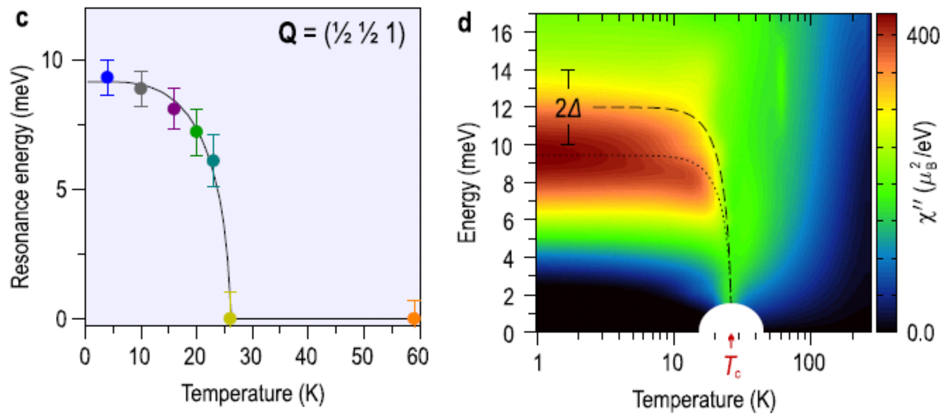

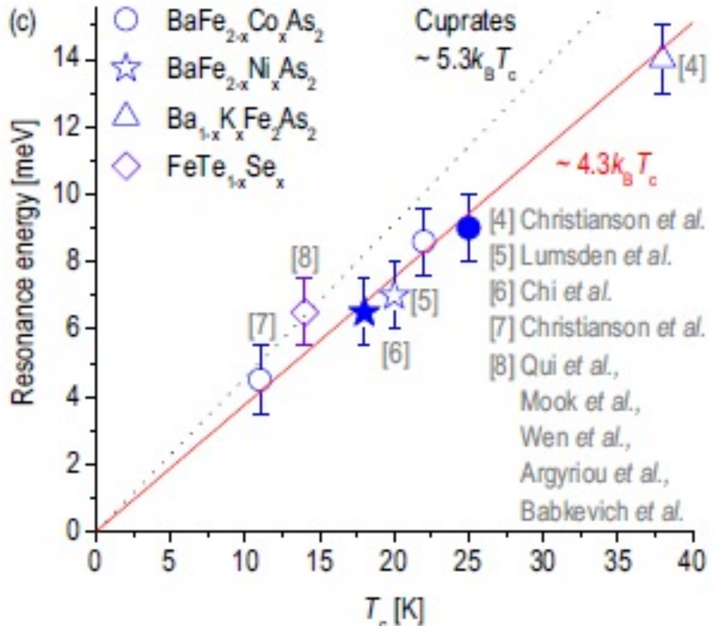

The amplitude and the characteristic energy Ω of the magnetic resonance peak show similar T dependencies to that of the superconducting order parameter.

Ω is of the same order of magnitude as the energy required to break Cooper pairs (~2 Δ ~ 12 meV)

Ω ~1.6 D ~ 4.3 k_BT_c

The observation of a magnetic resonance peak magnetic resonance peak at the AF wave vector is compatible with a superconductivity s^{+-} (coherence factor in the BCS susceptibility)

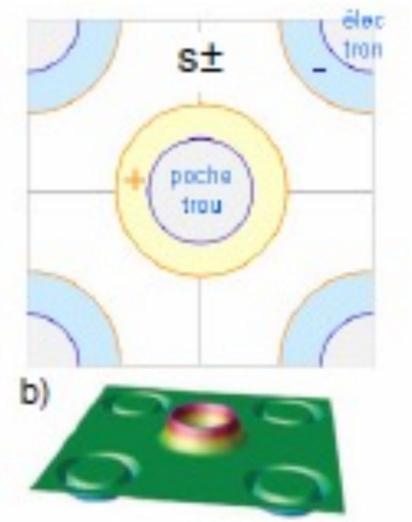

SUPERCONDUCTING STATE : Spin Resonant Mode(s) - SRMs

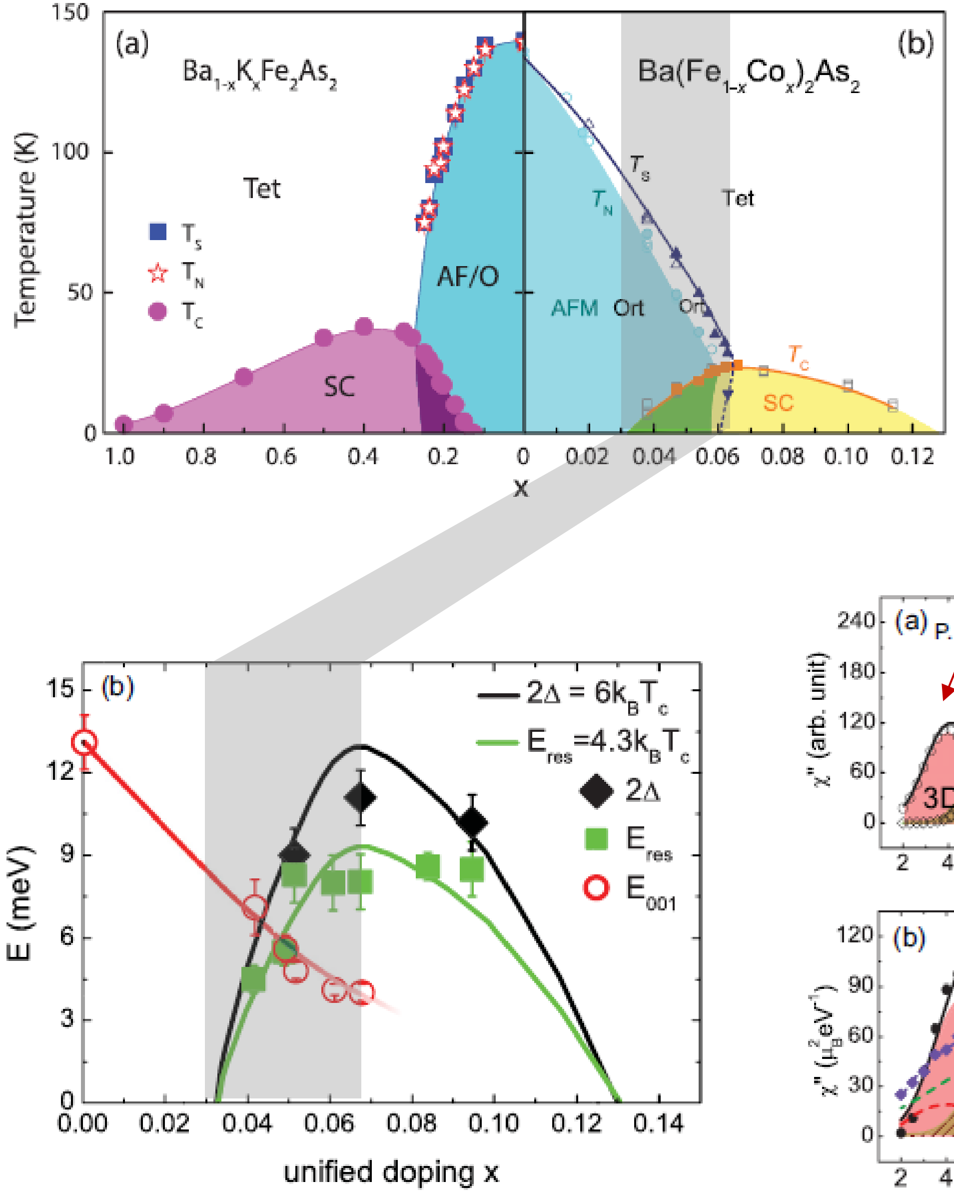

Additional low E SRM
72% // c , 28 % // a
3D

Q(0.5,0.5,1) SF channel

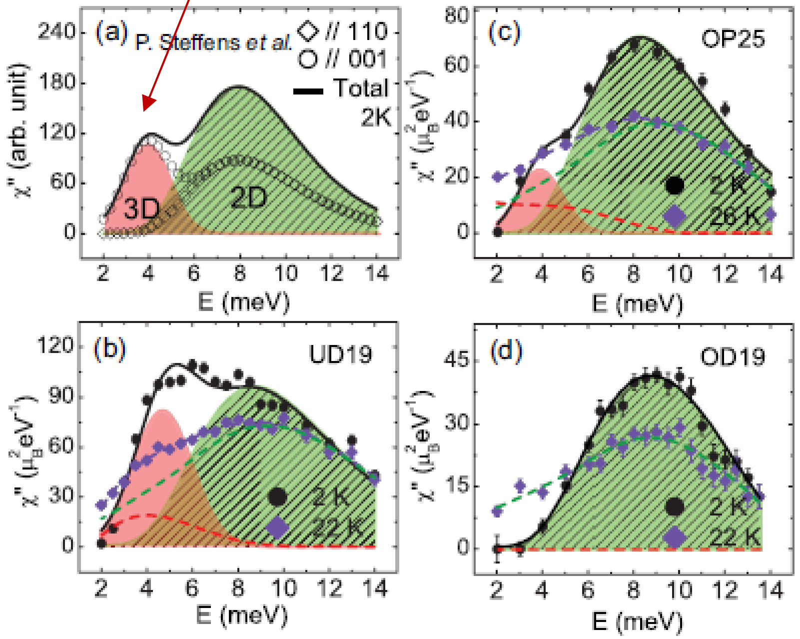

theories
⇔ spin orbit coupling

Magnetic fluctuations ⇔ ordering

Knolle, Eremin, Schmalian, & Moessner,
Magnetic resonance from the interplay of frustration and superconductivity.
Phys. Rev. B 84, 180510(R) (2011).

Lv, W., Moreo, A. & Dagotto, E.
Double magnetic resonance and spin anisotropy in Fe-based superconductors due to static and fluctuating antiferromagnetic orders.
Phys. Rev. B 89, 104510 (2014).

Wang, M. et al.
Experimental elucidation of the origin of the double spin resonances in $Ba(Fe_{1-x}Co_x)_2As_2$. Phys. Rev. B 93, 205149 (2016).

Orbital selective pairing

Yu, R., Zhu, J.-X. & Si, Q.
Orbital-selective superconductivity, gap anisotropy, and spin resonance excitations in a multiorbital t–J_1 – J_2 model for iron pnictides.
Phys. Rev. B 89, 024509 (2014).

SUPERCONDUCTING STATE : Spin Resonant Mode(s) - SRMs

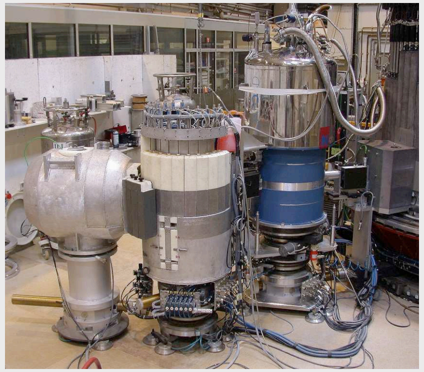

H // Q

horizontal cryomagnet @ ILL
Compatible with
neutron polarization analysis

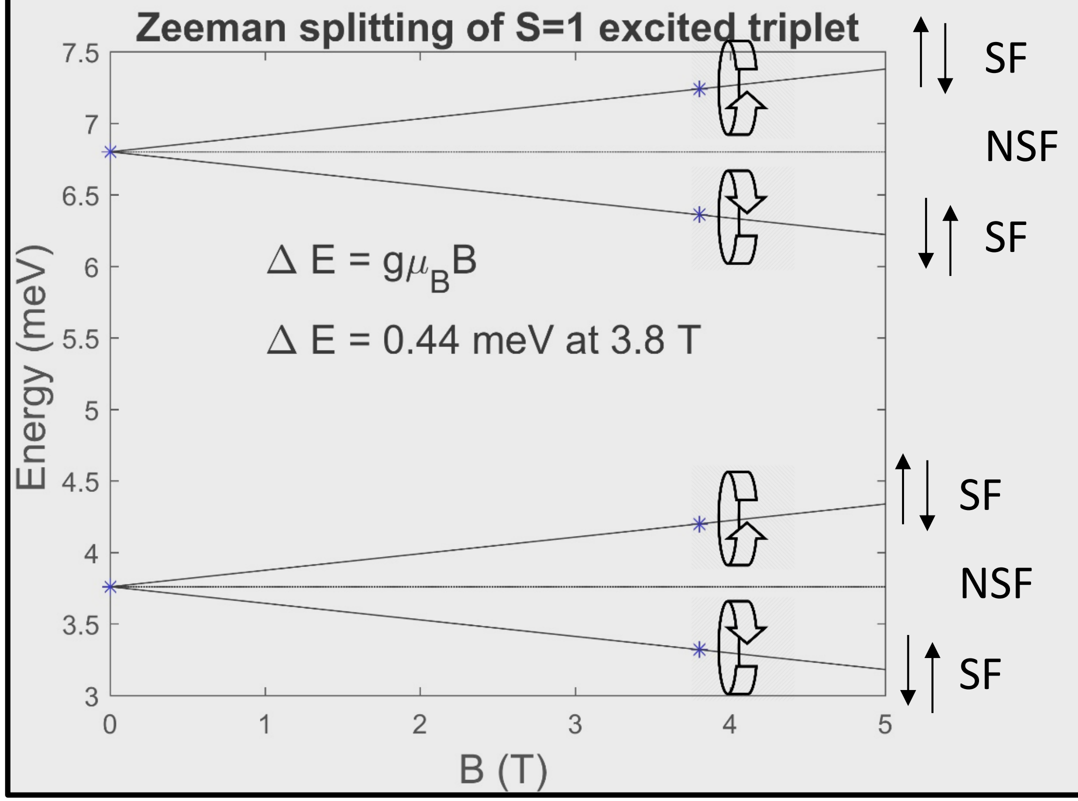

What is the character of the two SRM's?
Singlet – triplet exciton ?

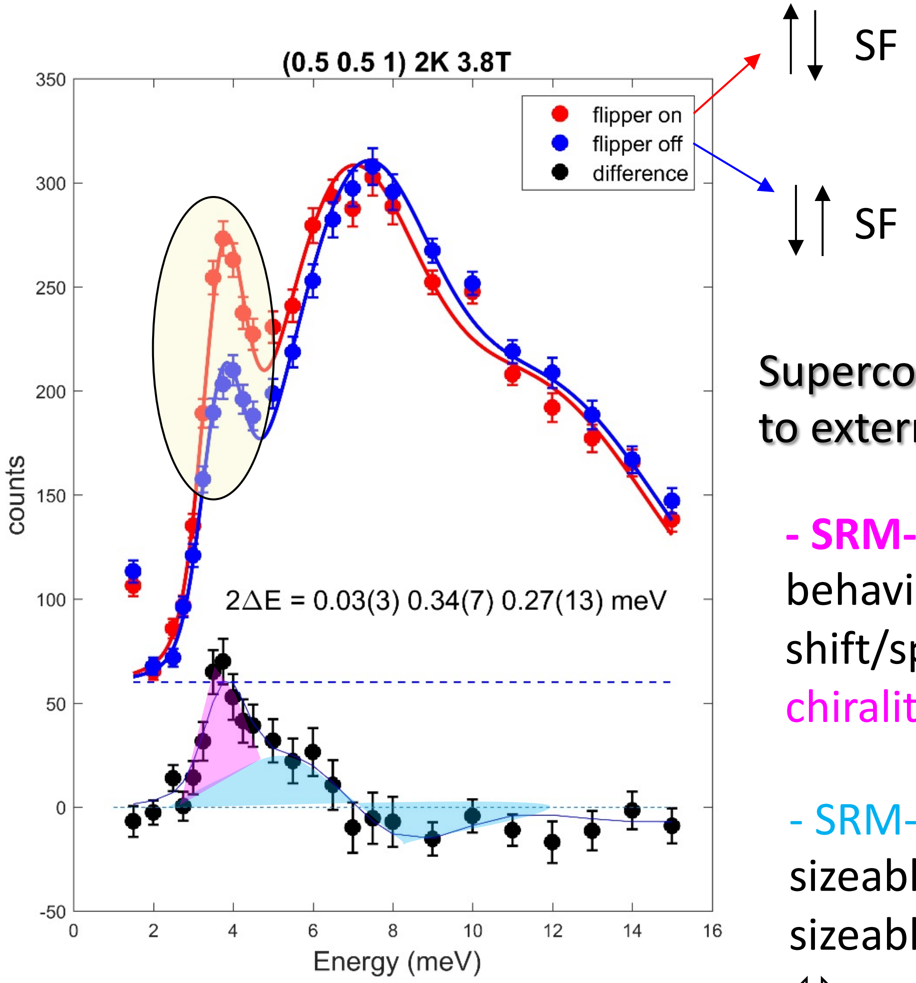

Area for RIX

Superconductivity couples to external magnetic fields

- **SRM-1:** different behavior, no very weak shift/splitting, strong chirality

- SRM-2:
sizeable chiral signal and sizeable splitting
⇔ agrees with triplet

Vortex and chirality

ξ = coherence length ~ 3 nm

λ = penetration depth ~200 nm

j= supercurrent

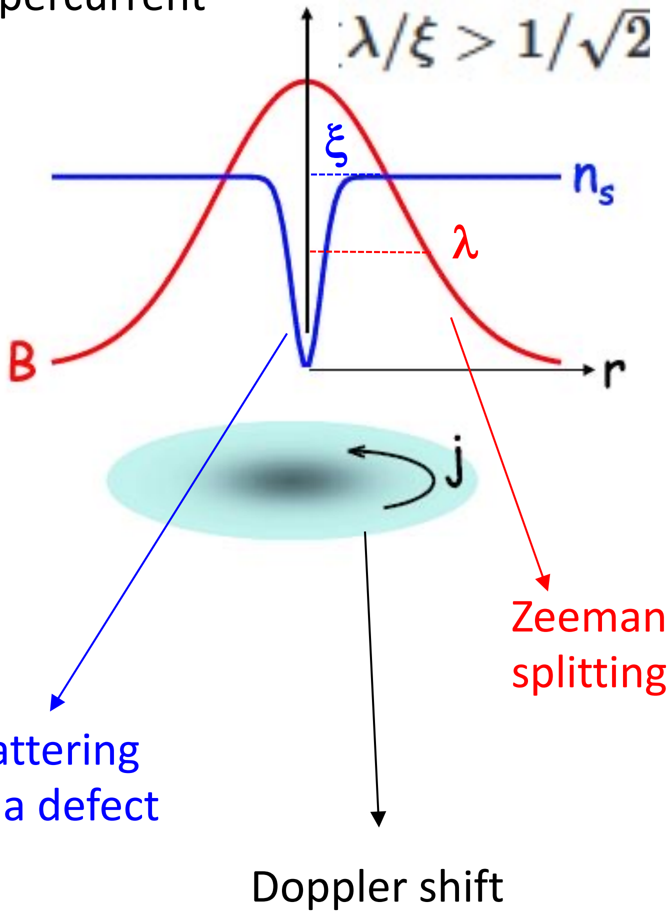

$\gamma = \lambda_c / \lambda_{ab} \sim \xi_{ab} / \xi_c$ The direction of B with respect to the ab plane matters

Example of chirality : p+ip'

Triplet pairing S_z=0

$$V^{(2)}_{\text{tr0}} = \frac{1}{2}V^{zz}_{\text{sp}} - V^{+-}_{\text{sp}} - \frac{1}{2}V_{\text{ch}}$$

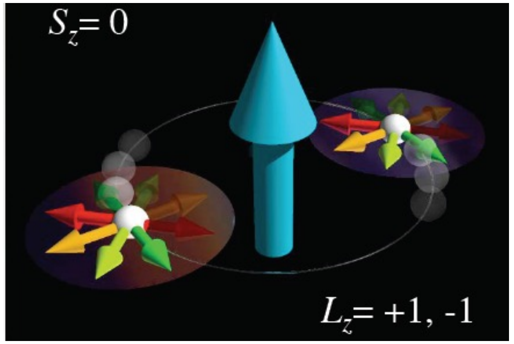

$$\vec{d} = \Delta_0 \hat{z}(k_x \pm ik_y)$$

$$\chi^{sc}_{\alpha\beta}(\mathbf{q},\omega) = -\sum_{\mathbf{k}} \frac{C_{\alpha\beta}(\mathbf{k},\mathbf{q})}{\omega + i\epsilon - E_+ - E_-}$$

$$E_\pm = \sqrt{(\xi_{\mathbf{k}\pm\mathbf{q}/2})^2 + |\Delta^\star(\mathbf{k} \pm \mathbf{q}/2|^2}$$

χ becomes spontaneously anisotropic

$$C_{xx,yy}(\mathbf{k},\mathbf{q}) = \frac{1}{4}\frac{(E_+ + \xi_+)(E_- - \xi_-) + (\Delta^\star_+\Delta_-}{E_+E_-}$$

$$C_{zz}(\mathbf{k},\mathbf{q}) = \frac{1}{4}\frac{(E_+ + \xi_+)(E_- - \xi_-) - (\Delta^\star_+\Delta_-}{E_+E_-}$$

Joynt & Rice PRB 38, 2345 (1988)

Triplet SC state

Maier-0805.0316v1

$\Delta(\mathbf{k}) = \sin k_x,\ \sin 2k_x$ and $\sin k_x + i \sin k_y$

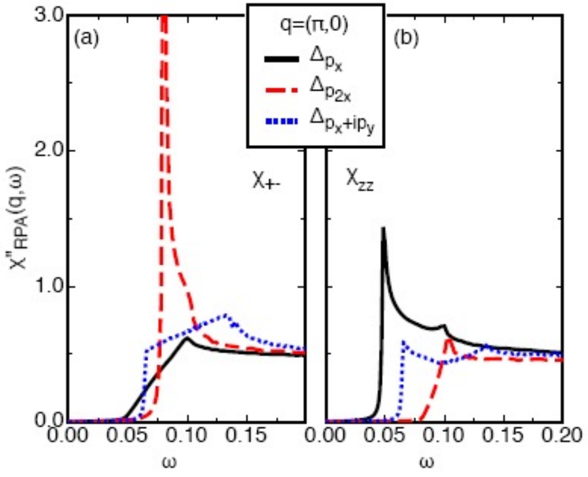

AFM + SC STATES : Spin Resonant Mode(s) - SRMs

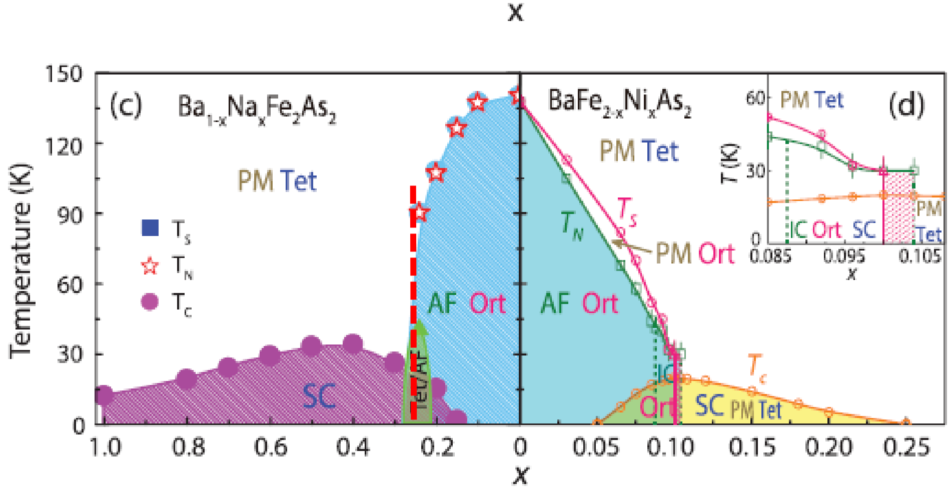

hole-doped Ba1−xNaxFe2As2 that displays a spin reorientation transition. This reorientation has little impact on the overall appearance of the resonance excitations with a high-E isotropic and a low-E anisotropic mode.

However, the strength of the anisotropic low-E mode sharply peaks at the highest doping that still exhibits magnetic ordering resulting in the strongest SRM observed in any Fe-based superconductor so far.

This remarkably strong SRM is accompanied by a loss of about half of the magnetic Bragg intensity upon entering the SC phase. Anisotropic SRMs thus can allow the system to compensate for the loss of exchange energy arising from the reduced antiferromagnetic correlations within the SC state

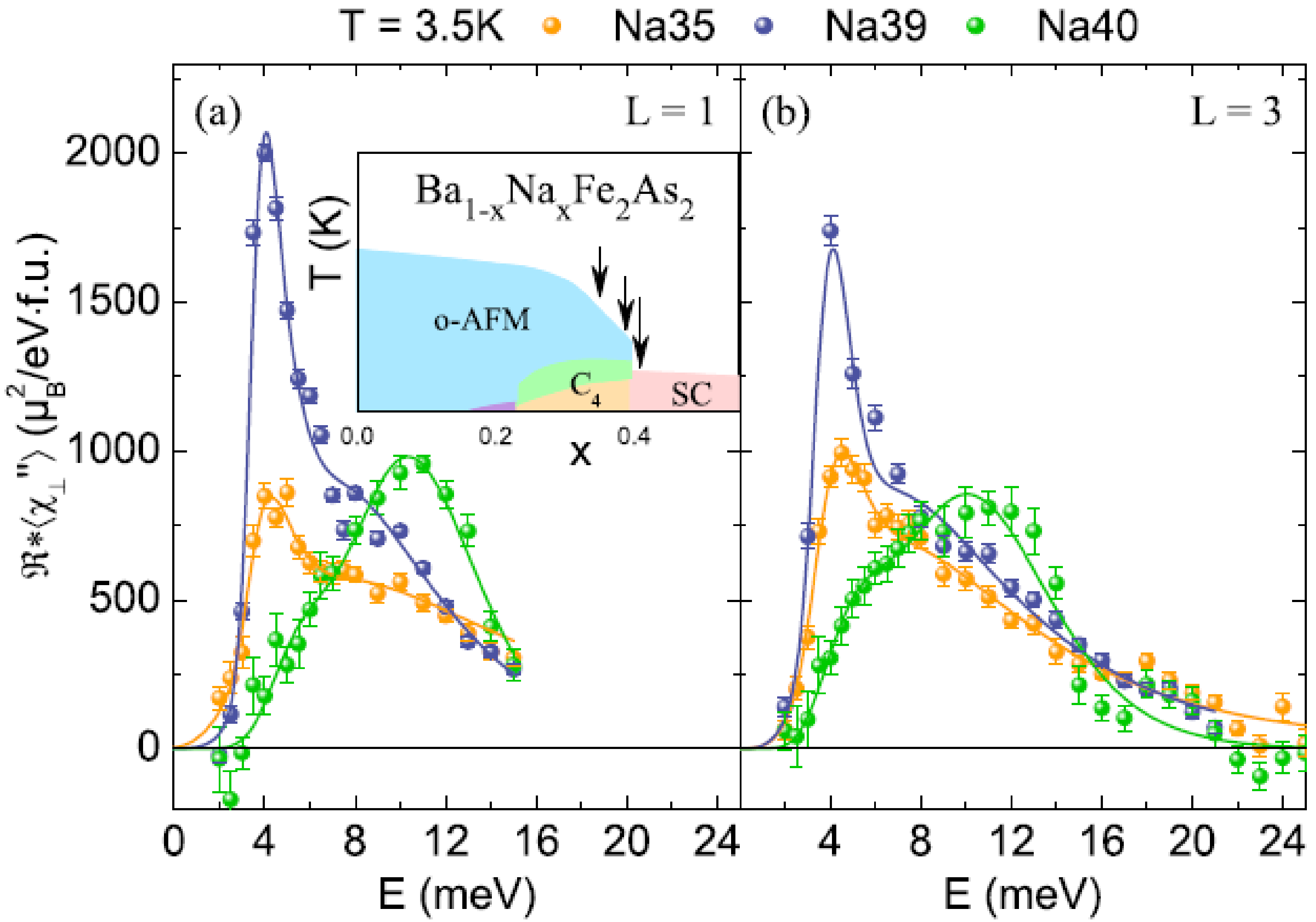

a-b ANISOTROPY

the resistivity anisotropy in transport measurements is **NOT** a consequence of the shift in T_N and Ts under uniaxial strain

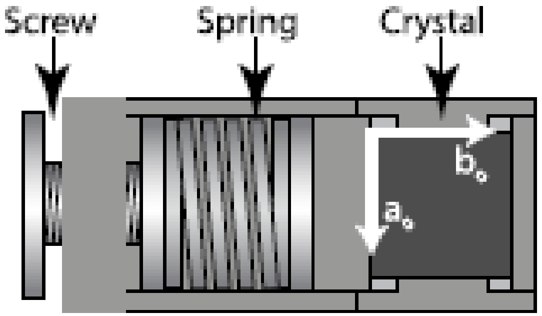

P=15 MPa

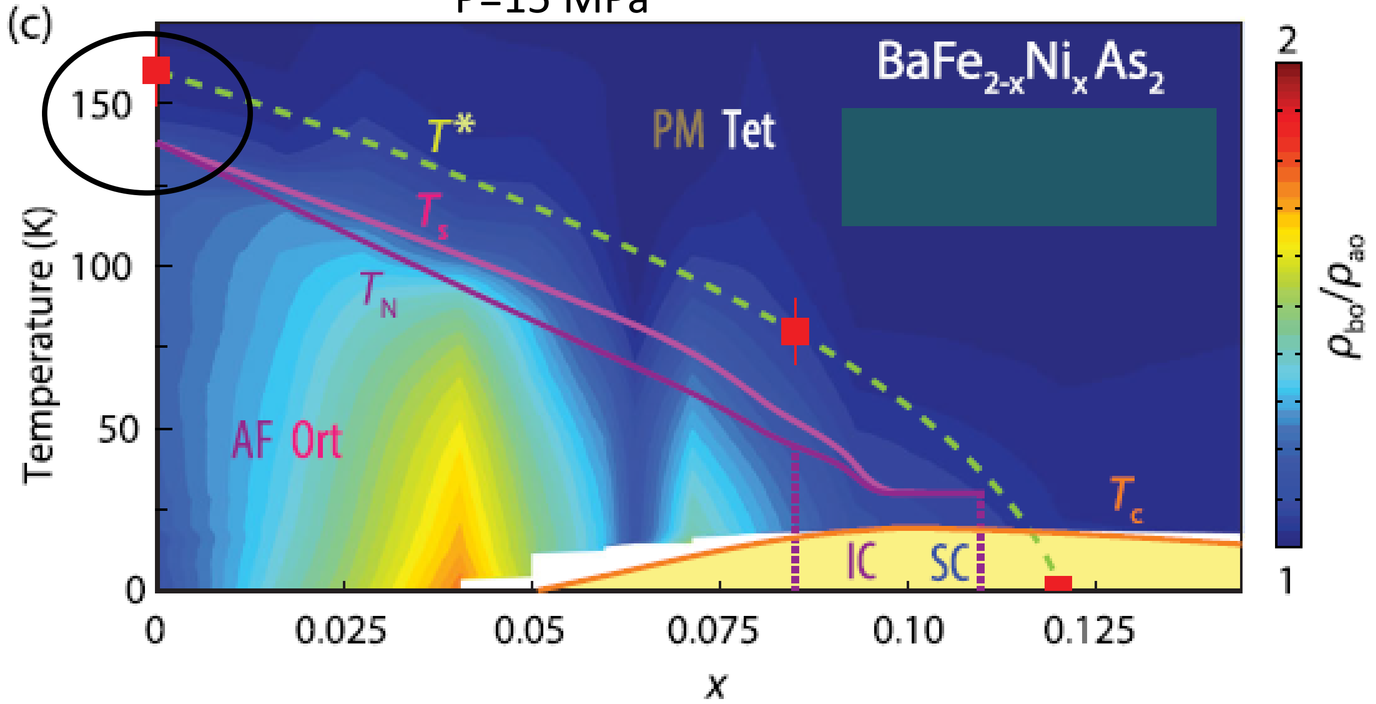

15 MPa

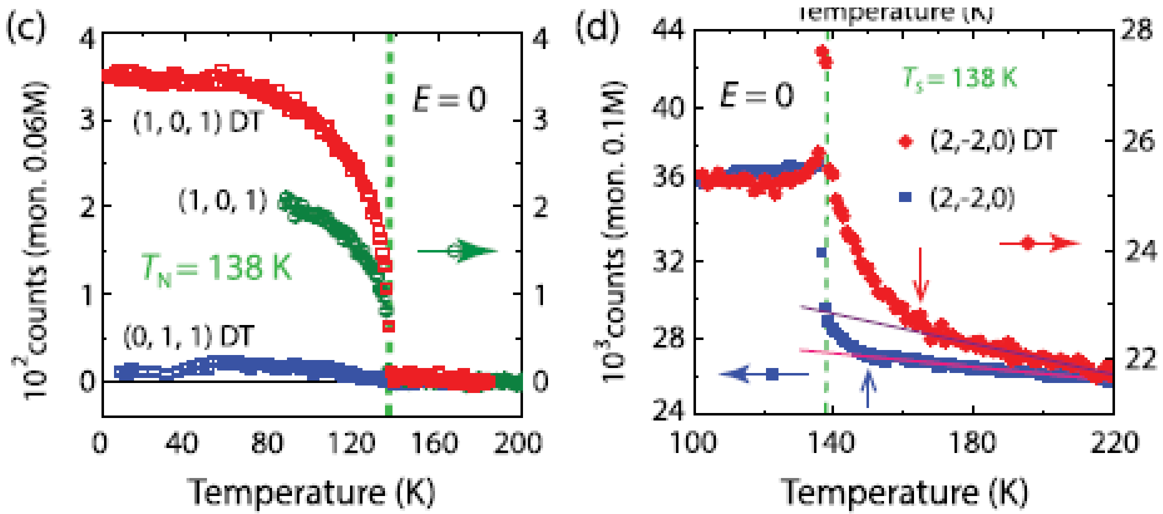

a-b ANISOTROPY

As a function of increasing electron doping, the resistivity anisotropy first increases and then vanishes near optimal superconductivity

consistent with a signature of the **spin nematic phase** that breaks the in-plane fourfold rotational symmetry (C4) of the underlying tetragonal lattice

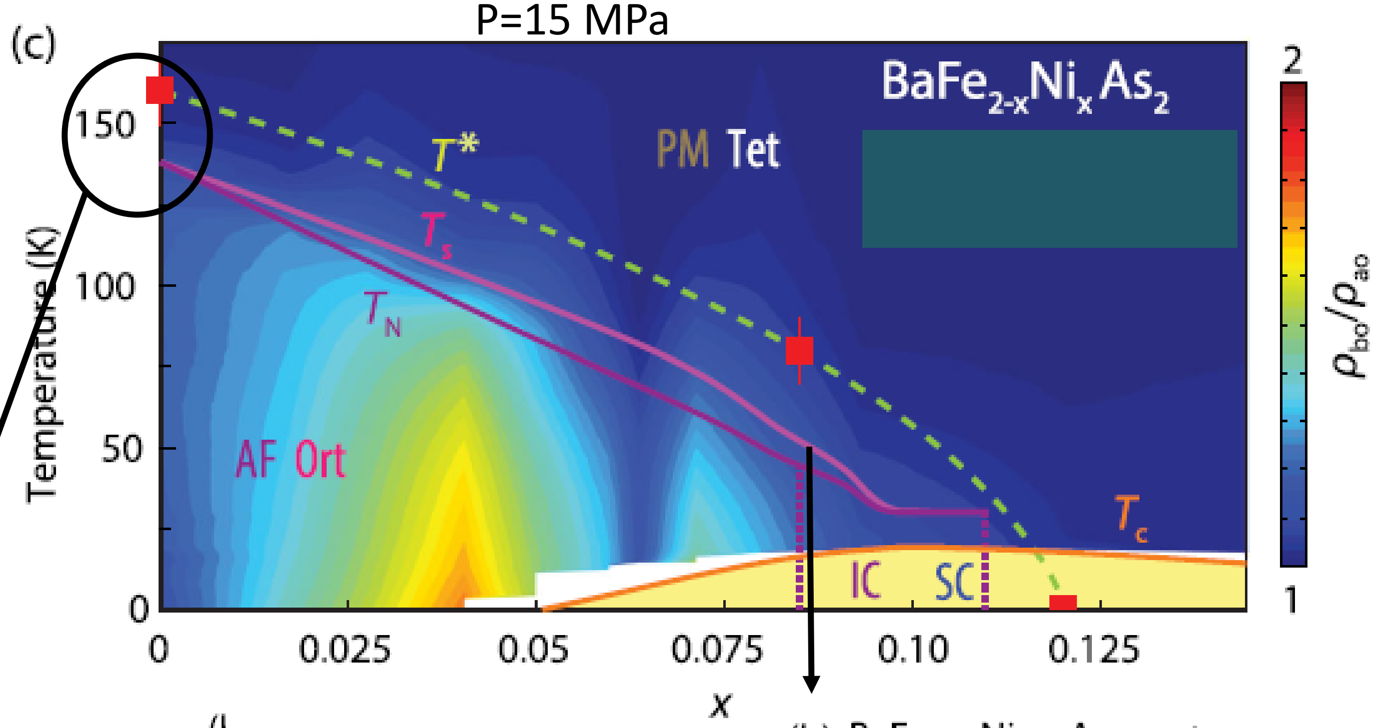

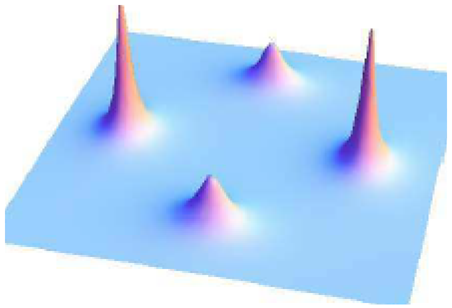

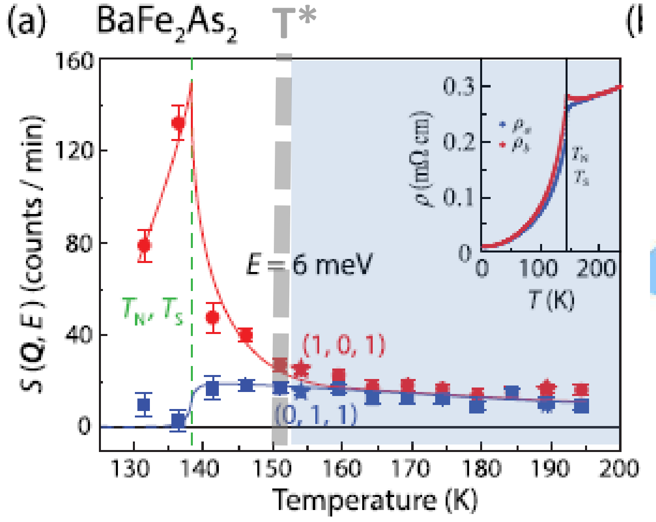

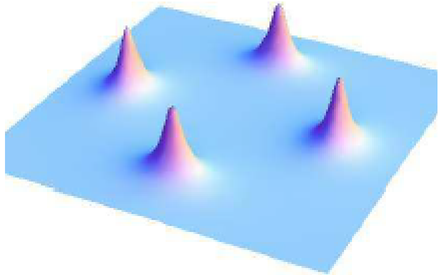

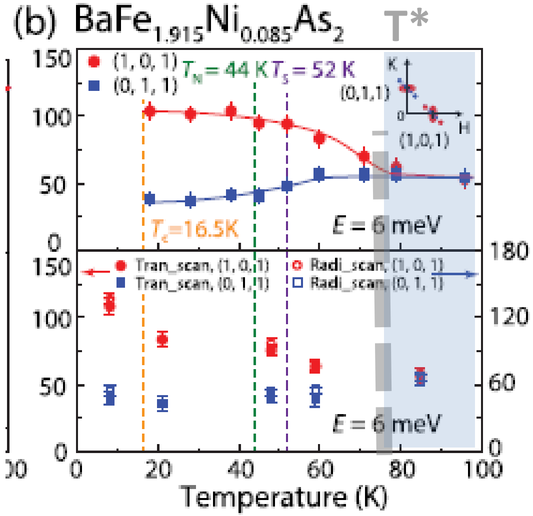

a-b ANISOTROPY

in-plane spin-excitation anisotropy is associated with resistivity anisotropy in a strain-induced sample

spin-excitation anisotropy in iron pnictides is a direct probe of the **spin-orbit coupling** in these materials

P=15 MPa

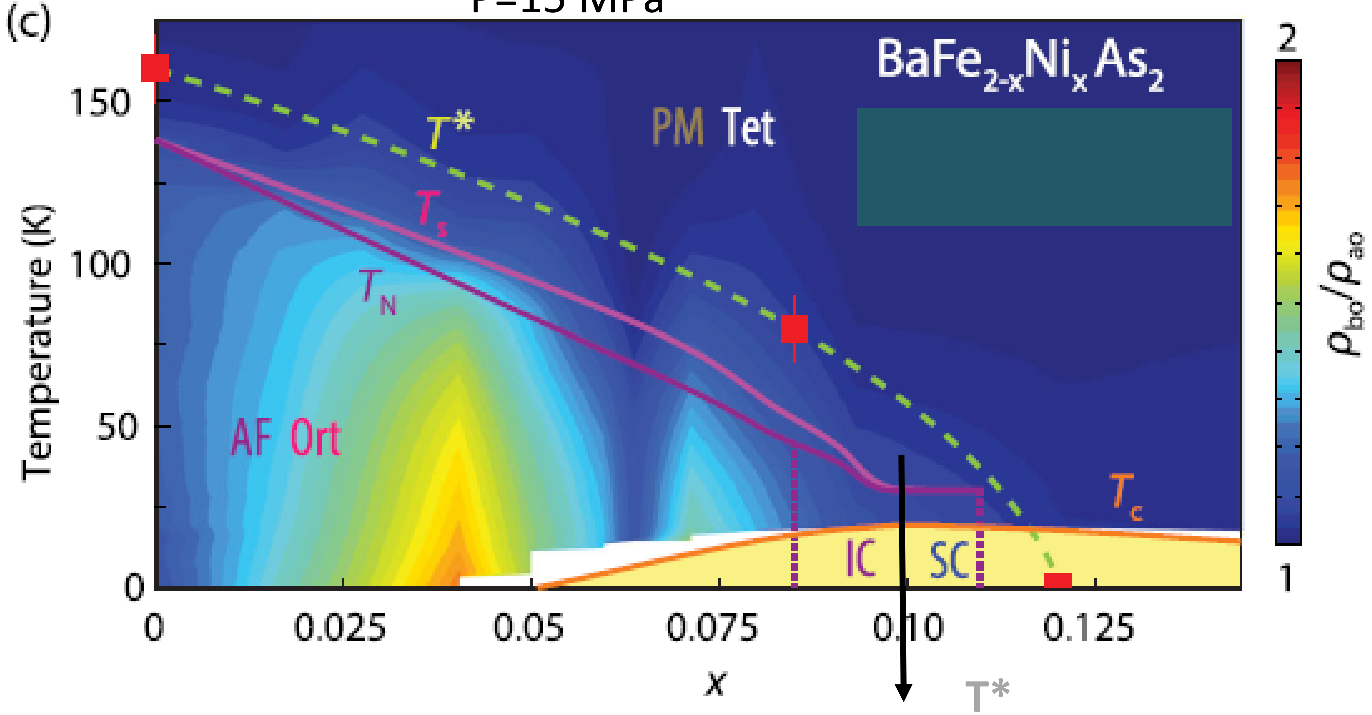

T*

My and Mz become different below T*, illustrating the fact that the magnetic anisotropy first appears below the temperature where transport measurements on uniaxial strain detwinned samples display in-plane resistivity anisotropy

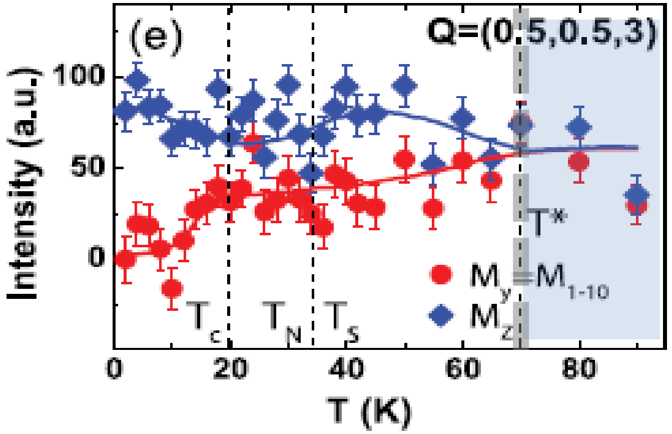

E=5 meV
X=0.10

THEORETICAL CONSIDERATIONS : Hund's metal

Instead of a strong- or weak-coupling approach, the Fe pnictides may be Hund's metals, where the interaction between the electrons is not strong enough to fully localize them to form a Mott insulator, but is sufficient so that the low E-quasiparticles have much enhanced mass.

Here the electron correlation strength would be primarily controlled by the Hund's coupling J_H, which depends on the pnictogen heights and tends to align spins of all the electrons on a given Fe atom, and hence enhances spin excitations without appreciably affecting the charge excitations.

This is different from the effect of large Coulomb repulsion U in a Mott insulator, which hampers charge excitations in order to enhance spin fluctuations.

The electronic excitations in iron-based superconductors are neither fully itinerant nor fully localized, but have a dual nature that can be realistically described by a combination of DFT and DMFT.

This idea is similar to the picture where single electron spectral function is composed of coherent and incoherent parts representing electrons near (itinerant electrons) and far away (local moments) from the Fermi surface,

THEORETICAL CONSIDERATIONS : spin fluctuation exchange pairing

In general, for the multiorbital models, the orbital structure of the pairing interaction is important and one introduces an orbital dependent pairing interaction $\Gamma_{\ell_1\ell_2\ell_3\ell_4}$ which describes the irreducible particle-particle scattering of electrons in orbitals ℓ_1, ℓ_4 with momentum k, and $-k$ into orbitals ℓ_2, ℓ_3 with momentum k' and $-k'$. In terms of this vertex, the effective pairing interaction for scattering a $(k'\uparrow, -k'\downarrow)$ pair on the ν_j Fermi surface to a $(k\uparrow, -k\downarrow)$ pair on the ν_i Fermi surface is

$$\Gamma_{ij}(k,k') = \sum_{\ell_1\ell_2\ell_3\ell_4} a_{\nu_i}^{\ell_2*}(k) a_{\nu_i}^{\ell_3*}(-k) \Gamma_{\ell_1\ell_2\ell_3\ell_4}(k,k') \times a_{\nu_j}^{\ell_1}(k') a_{\nu_j}^{\ell_4}(-k'),$$

with $a_{\nu_j}^{\ell_1}(k)$ the orbital matrix element $\langle \nu_j k | \ell_1 \rangle$

In the RPA and FLEX approaches, the orbital dependent vertex is given by

$$\begin{aligned}\Gamma_{\ell_1\ell_2\ell_3\ell_4}(\mathbf{k},\mathbf{k}',\omega) = [&\tfrac{3}{2}U^S \chi_1^{\mathrm{RPA}}(\mathbf{k}-\mathbf{k}',\omega) U^S \\ &- \tfrac{1}{2}U^C \chi_0^{\mathrm{RPA}}(\mathbf{k}-\mathbf{k}',\omega) U^C \\ &+ \tfrac{1}{2}(U^S + U^C)]_{\ell_1\ell_2\ell_3\ell_4},\end{aligned}$$

with

$$\chi_1^{\mathrm{RPA}}(q) = \chi^0(q)[1 - U^S \chi^0(q)]^{-1}$$

and

$$\chi_0^{\mathrm{RPA}}(q) = \chi^0(q)[1 + U^C \chi^0(q)]^{-1}.$$

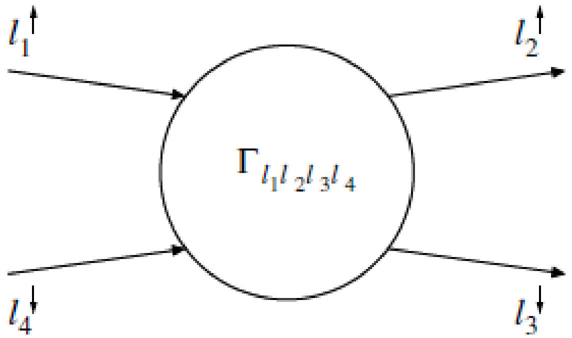

THEORETICAL CONSIDERATIONS : spin fluctuation exchange pairing

$$\Gamma_{ij}(k,k') = \sum_{\ell_1\ell_2\ell_3\ell_4} a_{\nu_i}^{\ell_2}(k)\, a_{\nu_i}^{\ell_3}(-k)\, \Gamma_{\ell_1\ell_2\ell_3\ell_4}(k, \ldots,$$
$$\times\, a_{\nu_j}^{\ell_1}(k')\, a_{\nu_j}^{\ell_4}(-k'),$$

one sees that the effective pairing interaction Γ_{ij}(k,k')for a multi-orbital system depends upon the number of Fermi surfaces and their shapes as well as the orbital matrix elements.

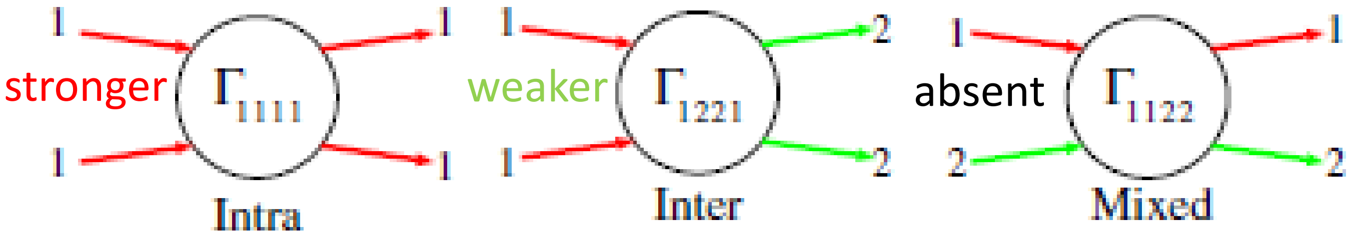

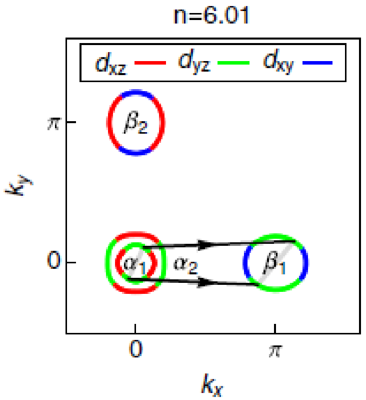

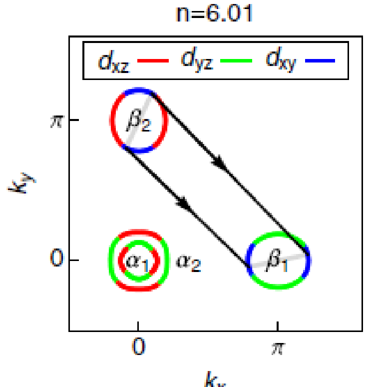

Gap eigenfunctions

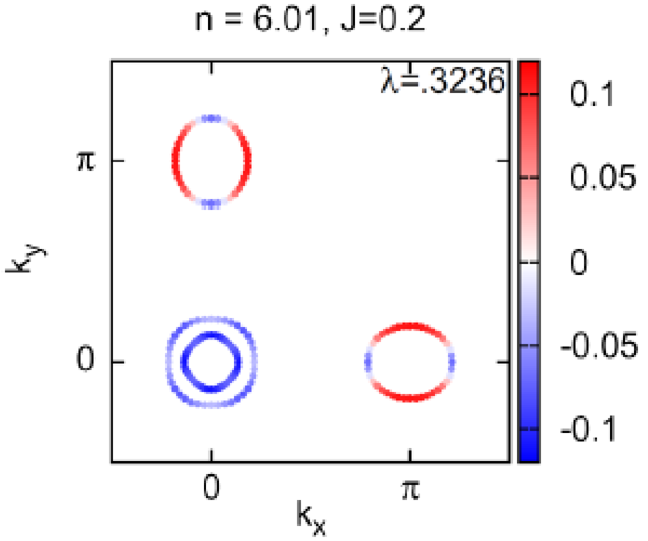

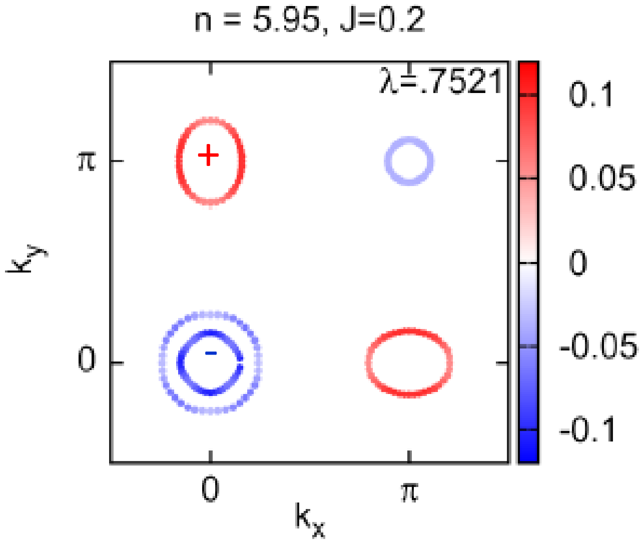

The β–γ pair scatterings stabilize s+-